รายงานวิจัยฉบับสมบูรณ์

โครงการ การศึกษากลไกการนำเข้าและการเคลื่อนที่ของไวรัสหัวเหลืองในกุ้ง

(Dissecting the cell entry and trafficking pathways of yellow head virus infection in shrimp)

รศ. ดร. เฉลิมพร องศ์วรโสภณ

หัวหน้าโครงการ

สถาบันชีววิทยาศาสตร์โมเลกุล มหาวิทยาลัยมหิดล

กรกฎาคม ๒๕๖๐

สัญญาเลขที่ BRG5780006

รายงานวิจัยฉบับสมบูรณ์

โครงการ การศึกษากลไกการนำเข้าและการเคลื่อนที่ของไวรัสหัวเหลืองในกุ้ง

(Dissecting the cell entry and trafficking pathways of yellow head virus infection in shrimp)

ผู้วิจัย รศ. ดร. เฉลิมพร องศ์วรโสภณ
สถาบันชีววิทยาศาสตร์โมเลกุล มหาวิทยาลัยมหิดล

สนับสนุนโดย สำนักงานกองทุนสนับสนุนการวิจัยและมหาวิทยาลัยมหิดล
(ความเห็นในรายงานนี้ เป็นของผู้วิจัย สกว. และมหาวิทยาลัยมหิดลไม่จำเป็นต้องเห็นด้วยเสมอไป)

บทคัดย่อ

รหัสโครงการ : BRG5780006

ชื่อโครงการ : การศึกษากลไกการนำเข้าและการเคลื่อนที่ของไวรัสหัวเหลืองในกุ้ง

(Dissecting the cell entry and trafficking pathways of yellow head virus infection in shrimp)

หัวหน้าโครงการ : รศ. ดร. เฉลิมพร องศ์วรโสภณ

สถาบันชีววิทยาศาสตร์โมเลกุล มหาวิทยาลัยมหิดล

E-mail Address: chalermporn.ong@mahidol.ac.th.

ระยะเวลาโครงการ : 31 กรกฎาคม 2557 ถึง 30 กรกฎาคม 2560

ไวรัสหัวเหลืองเป็นเชื้อก่อโรครุนแรงในกุ้งกุลาดำ ทำให้กุ้งตายอย่างรุนแรงทั้งบ่อได้ภายใน 2 -3 วันหลังติดเชื้อ เพื่อที่จะเข้าใจกลไกในระดับโมเลกุลของการติดเชื้อไวรัสหัวเหลือง งานวิจัยนี้ จึงได้ทำการโคลนโปรตีนหลักที่เกี่ยวข้องกับการเข้าเซลล์และการเคลื่อนที่ภายในเซลล์ของไวรัสหัวเหลืองและศึกษาการทำงานของโปรตีนเหล่านั้น โดยใช้เทคโนโลยีอาร์เอ็นเอไอ เพื่อที่จะศึกษากระบวนการเข้าเซลล์ของไวรัสหัวเหลือง จึงได้ทำการวิจัยโดยศึกษาผลของยาที่ยับยั้งการเข้าเซลล์ เช่น คลอโพรมาซีน อะมิโลราย และ เมธทิวเบตาไซโคลเด็กซ์ทริน ในกุ้งที่ติดไวรัส จากการศึกษาพบว่าการฉีดคลอโพรมาซีน ซึ่งทำหน้าที่ในการยับยั้งกระบวนการเอนโดไซโตซีสแบบคลาทรินก่อนการติดเชื้อไวรัสในกุ้ง พบว่าระดับไวรัสหัวเหลืองลดลงอย่างมีนัยสำคัญทางสถิติ จึงได้ทำการโคลนและศึกษาโปรตีนหลักของกระบวนการนี้ เช่น คลาทรินเฮพวีเชน (PmCHC) พบว่าไวรัสหัวเหลือง ใช้โปรตีน PmCHC ในกระบวนการเอนโดไซโตซีสแบบคลาทรินในการเข้าเซลล์กุ้ง เมื่อไวรัสหัวเหลืองเข้าเซลล์แล้ว จะใช้โปรตีน Rab ชนิดต่าง ๆ และโปรตีนที่จับกับโปรตีน Rab ในการเป็นตัวควบคุมหลักในแต่ละขั้นตอนของกระบวนการเอนโดไซโตซีส จากการศึกษาพบว่า PmRab5 ซึ่งเป็นโปรตีนที่ควบคุมเอนโดโซมส่วนต้นและยังจับกับโปรตีนเออลี่-เอนโดโซมอล- แอนติเจน-1 (PmEEA1) มีส่วนเกี่ยวข้องกับการเคลื่อนที่ของไวรัสหัวเหลืองไปยังเอนโดโซมส่วนต้น แสดงให้เห็นว่าโปรตีนเหล่านี้มีบทบาทสำคัญในขั้นตอนแรกของการติดเชื้อไวรัส เมื่อไวรัสจำลองตัวเองและสร้างโปรตีนชนิดต่างๆ เกิดการรวมตัวกันเป็นวิริออน (virion) และขนส่งไปยังพลาสม่าเมมเบรนเพื่อออกนอกเซลล์ ซึ่งกระบวนการนี้ควบคุมโดย PmRab11 องค์ความรู้ที่ได้นี้ทำให้เข้าใจกลไกในระดับโมเลกุลที่สำคัญที่เกี่ยวข้องกับการติดเชื้อไวรัสหัวเหลือง และอาจส่งผลให้ได้ยีนเป้าหมายใหม่ในการเป็นสารต้านไวรัส

คำหลัก: ไวรัสหัวเหลือง; เอนโดไซโตซีส; อาร์เอ็นเอสายคู่; อาร์เอ็นเอไอ; กุ้งกุลาดำ; เอ็กซ์โซไซโตซีส; รีไซคลิง เอนโดโซม

Abstract

Project Code: BRG5780006

Project Title: Dissecting the cell entry and trafficking pathways of yellow head virus infection in shrimp

Project Head: Chalermporn Ongvarrasopone, Ph.D., Assoc. Prof.

Institute of Molecular Biosciences,

Mahidol University (Salaya Campus), Nakhon Pathom, Thailand

E-mail Address: chalermporn.ong@mahidol.ac.th.

Project Period: 31 July 2557 – 30 July 2560

Yellow head virus (YHV) is a virulent pathogen in black tiger shrimp. It causes high mortality within a few days after infection. In order to understand the molecular mechanism of YHV infection, molecular cloning of the major protein components involved in YHV entry and intracellular trafficking of YHV were performed and their functions were characterized by RNA interference technology. To dissect the YHV internalization process, effects of drug inhibitors; chlorpromazine (CPZ), amiloride and methyl-β-cyclodextrin were used. Only the YHV-infected shrimp pretreated with CPZ (which inhibited the clathrin mediated endocytosis) showed a significant reduction of YHV levels. Characterization of the major component of clathrin, *Penaeus monodon* clathrin heavy chain (*Pm*CHC) demonstrated that YHV utilized PmCHC via clathrin dependent endocytosis as a route of entry into shrimp cells. Once YHV enters into shrimp cells, Rab proteins and their interacting proteins which are the key regulators of the endocytosis pathway were characterized. These studies indicated that PmRab5, an early endosomal marker and its interacting protein, early endosome antigen 1 (PmEEA1) were involved in YHV early endosomal trafficking, suggesting their roles in the early step of infection. In addition, the transportation of YHV to deliver the assembling virions to plasma membrane requires PmRab11. These knowledges provide insights of the key molecular mechanism underlying YHV infection and possibly uncover novel targets for antiviral agents.

Keyword: yellow head virus; endocytosis; double stranded RNA; RNAi; Black tiger shrimp; exocytosis; recycling endosome

สัญญาเลขที่ BRG5780006

โครงการ: การศึกษากลไกการนำเข้าและการเคลื่อนที่ของไวรัสหัวเหลืองในกุ้ง

Executive summary

Penaeid shrimp are one of the most economically important aquaculture species in Thailand. Viral diseases especially caused by Yellow head virus (YHV) can lead to shrimp mortality within 3 days. To date, effective methods and strategies to control the diseases have been extensively studied. However, no effective method can be employed successfully in the farm shrimp. This is possibly due to lacking knowledge of the molecular pathogenesis of YHV infection and viral-host interaction. In this study, we focused on dissecting the cell entry and trafficking pathway of YHV. To dissect the YHV internalization process, effects of drug inhibitors; chlorpromazine (CPZ), amiloride and methyl-β-cyclodextrin were used. Only the YHV-infected shrimp pretreated with CPZ (which inhibited the clathrin mediated endocytosis) showed a significant reduction of YHV levels. Characterization of the major component of clathrin, *Penaeus monodon* clathrin heavy chain (*Pm*CHC), demonstrated that the complete coding sequence of PmCHC is 5,055 bp encoding a putative protein of 1,684 amino acids. Silencing of PmCHC mRNA by dsRNA-PmCHC resulted in an inhibition of YHV replication within 48 hours and exhibited a delay in shrimp mortality. These results indicated that YHV utilized PmCHC via clathrin dependent endocytosis as a route of entry into shrimp cells. Once YHV is inside the cell, it can exploit the host cell machineries such as Rab proteins for intracellular trafficking to promote the viral life cycle and replication. Colocalization between YHV and *P. monodon* Rab5 (PmRab5) which was a small GTPase protein was visualized at 10 min to 3 h post YHV challenge under a confocal microscope. Silencing of PmRab5 by specific dsRNA reduced YHV replication inside the cells. Furthermore, lack of PmRab5 expression exhibited a delay of shrimp mortality after YHV infection. These results indicated that PmRab5 played a key role in the early stage of endocytosis and was involved in YHV trafficking process. In addition, early endosome antigen 1 (EEA1) protein that was shown to be involved in the tethering step of the vesicle and early endosome fusion was also investigated during YHV infection. Silencing of PmEEA1 by specific dsRNA followed by YHV challenge demonstrated a delay in shrimp mortality from 60 hpi to 168 hpi when compared to the control. These results demonstrated that YHV required PmEEA1 for trafficking within the infected cells, Then, the YHV is trafficked to late endosome and lysosome via PmRab7. Its genome was released for YHV replication. The

viral proteins were synthesized and transported to plasma membrane by Rab11. Suppression of PmRab11 using dsRNA-PmRab11 either before or after YHV-challenge resulted in significant inhibition of YHV levels in the hemocytes and viral release in the supernatant in both mRNA and protein levels. In addition, the silencing effect of PmRab11 in YHV-infected shrimps resulted in a delay in shrimp mortality for at least 2 days. Co-localization between PmRab11 and YHV was observed at 24-72 h post YHV-challenge. In contrast, the co-localization signals were absence in the PmRab11 knockdown hemocytes and the YHV signals accumulated at the perinuclear region at 24 h post YHV-challenge. Then, accumulation of YHV was hardly observed after 48-72 h. These results suggested that PmRab11 is required for YHV infection in shrimp. Taken together these studies provide a deeper understanding of how YHV enters to the cells via clathrin mediated endocytosis which requires PmCHC, PmRab5 and PmEEA1 for an initial step of YHV infection. In addition, the transportation of YHV to deliver the assembling virions to plasma membrane requires PmRab11. This knowledge provides an insight of the key molecular mechanism underlying YHV infection and possibly uncovers novel targets for antiviral agents.

เนื้อหางานวิจัย

Part I: Successful yellow head virus infection of *Penaeus monodon* requires clathrin heavy chain

Part II: Rab5, an early endosomal protein required for yellow head virus infection of *Penaeus monodon*

Part III: Roles of PmEEA1 in controlling endosomal trafficking of YHV

Part IV: Roles of PmRab11 in inhibiting YHV infection in *Penaeus monodon*

Part I: Successful yellow head virus infection of *Penaeus monodon* requires clathrin heavy chain.

Abstract

Yellow head virus (YHV) is one of the most causative agents for shrimp mortality worldwide. To study the mechanism of YHV entry into host cells, effect of drug inhibitors; chlorpromazine (CPZ), amiloride and methyl-β-cyclodextrin were used. Only the YHV-infected shrimp pretreated with CPZ (which inhibited the clathrin mediated endocytosis) showed a significant reduction of YHV levels. Characterization of the major component of clathrin, *Penaeus monodon* clathrin heavy chain (*Pm*CHC), demonstrated that the complete coding sequence of PmCHC is 5,055 bp encoding a putative protein of 1,684 amino acids with an estimated molecular weight of 192.5 kDa and a pI of 5.53. Phylogenetic analysis and domain structure comparison demonstrated that PmCHC was clustered in an invertebrate group. Silencing of PmCHC mRNA by dsRNA-PmCHC resulted in an inhibition of YHV replication within 48 hours and exhibited a delay in shrimp mortality. These results indicated that YHV utilized PmCHC via clathrin dependent endocytosis as a route of entry into shrimp cells.

Keywords: yellow head virus; endocytosis; double stranded RNA; RNAi; Black tiger shrimp

1. Introduction

Yellow head virus (YHV) is one of the most devastating shrimp pathogens as it causes mortality within 3 days. This virus was first identified in 1992 from moribund shrimp from southern Thailand (Boonyaratpalin et al., 1993). The virus was named from symptoms of the disease in which the moribund shrimp would present a yellowish cephalothorax and very sallow overall coloration. YHV can infect various penaeid shrimp such as *P. aztecus, P. duorarum, P. merguiensis, P. monodon, P. setiferus, P. stylirostris* and *L. vannamei* (Flegel, 1997). The infected moribund shrimp shows nuclear condensation as well as pyknosis and karyorrhexis which are signs of cell apoptosis (Khanobdee et al., 2002). YHV has a positive-sense single-stranded RNA genome of approximately 27 kb with a poly (A) tail. It belongs to the genus *Okavirus*, family *Roniviridae* in the order *Nidovirales.* The morphology of YHV reveals an enveloped bacilliform which has a particle size about 50-60 x 190-200 nm, containing the internal helical nucleocapsid which is closely surrounded by an envelope studded with prominent peplomers or spikes (Nadala et al., 1997; Sittidilokratna et al., 2008). YHV contains two major structural transmembrane glycoproteins (gp116 and gp64) and a nucleoprotein (p20) (Jitrapakdee et al., 2003). Antiserum against the gp116 but not gp64 can neutralize YHV infectivity in the primary lymphoid cells of *Penaeus monodon* (Assavalapsakul et al., 2005). In addition, injection of double-stranded RNA (dsRNA) targeting to the YHV-binding protein, YRP65, inhibited YHV replication (Assavalapsakul et al., 2006). Also, suppression of PmRab7 (a late endosomal marker involved in trafficking) resulted in inhibition of YHV replication (Ongvarrasopone et al., 2008). These results imply that for successful infection, YHV requires receptor mediated endocytosis as a route of entry and takes advantage of the host cell machineries for endosomal trafficking and replication. Therefore, better understanding of the endocytosis and trafficking pathway of YHV will shed lights on the mechanism of YHV infection and replication and thus will lead to the development of an antiviral agent or strategy to combat YHV infection.

Many viruses utilize well-characterized cellular endocytic mechanisms including clathrin-mediated endocytosis, lipid raft caveola-dependent endocytosis and macropinocytosis to internalize into host cells. For instance, several positive-sense ssRNA viruses such as severe acute respiratory syndrome virus (Inoue et al., 2007), hepatitis C, dengue and semliki forest virus use clathrin-mediated endocytosis (Marsh and Helenius, 2006; Meertens et al., 2006; Mercer et al., 2010) as a route of entry. In clathrin-mediated endocytosis, the cargo is trafficked through the cell via the coated vesicle which is surrounded by the polymerized clathrin in a basket-like structure. The formation of the endocytic clathrin-coated vesicles occurs through the

interaction of clathrin, heterotetrameric adaptor protein-2 (AP-2), and several accessory proteins such as Epsin, Eps15, AP180/CALM and dynamin. Clathrin, in which the light chain and heavy chain form a unique structure called the clathrin triskelion, as well as AP-2 are recruited by Epsin to the plasma membrane in response to receptor-mediated internalization signals. Epsin then mediates the assembly of a clathrin cage, which results in membrane curvature membrane by dynamin to form clathrin-coated vesicles which are then trafficked to endosomes (Doherty and McMahon, 2009; Mousavi et al., 2004). Whether YHV utilizes this pathway as a route of entry into shrimp cells remained to be investigated. Therefore, one purpose of this study was to characterize the YHV entry pathway by using several trafficking inhibitors. *Penaeus monodon* clathrin heavy chain (*Pm*CHC), a major protein component in the clathrin-dependent pathway was cloned and characterized. The suppression effect of PmCHC in YHV- challenged shrimp also was investigated. induced by the coated-pit formation. Once assembled, the clathrin-coated pits are pinched off from the plasma

2. Methods

2.1. Penaeus monodon (Black tiger shrimp) culture

Juvenile shrimp were obtained from Manoach's farm in Nakhon Pathom province, Thailand. Shrimp were sampled to determine that they were free from YHV and white spot syndrome virus (WSSV) infection using Diagnosis Strip Test YHV+WSSV (Pacific Biotech Co., Ltd, Thailand). In addition, shrimp were acclimatized for at least 5 days before use in experiments. They were maintained in large containers with oxygenated sea water at 5 ppt salinity before experiment and fed with commercial feed every day. Half of the water was exchanged every 2 days.

2.2. Yellow head virus preparation

Virus stock was prepared from hemolymph of YHV infected moribund shrimp. The moribund shrimp showed signs of YHV infection for example, a yellowish cephalothorax. To confirm that the hemolymph was collected from the moribund shrimp infected with YHV not other viruses, total RNA was extracted and reverse transcription-PCR analysis was performed to detect the helicase gene of YHV and other virus such as VP28 gene of WSSV. To prepare the viral stock, hemolymph was collected with AC-1 solution (27 mM Sodium citrate, 34.33 mM NaCl, 104.5 mM Glucose, 198.17 mM EDTA, pH 7.0), ratio 1:1, and the virus was obtained by ultracentrifugation (200,000 xg) for 1 hr. Viral pellet was dissolved in 150 mM NaCl and stored at -80 °C until used. The virus titer that causes 100 % mortality within 3-4 days was used in this experiment.

2.3. Screening of YHV entry pathways by using drug inhibitors

The entry pathways of YHV were screened by using drug inhibitors. Various inhibitors of clathrin-dependent endocytosis, macropinocytosis and caveolar endocytosis such as chlorpromazine (CPZ), amiloride and methyl-β-cyclodextrin (MβCD), respectively, were employed at a dose of 0.25 $mM.g^{-1}$ shrimp (9 shrimp per group). The inhibitors were injected into the hemolymph using 0.5 ml U-100 insulin syringe with 29 gauge needle. Injection of PBS was used as control. At 12 hours post-injection, shrimp were challenged with YHV. Then at 24 hours post YHV injection, gills from individual shrimp were collected to extract the total RNA and YHV levels were determined using quantitative RT-PCR.

2.4. Cloning of the full-length coding sequences of Penaeus monodon clathrin heavy chain (PmCHC)

Specific primers, cdfullCHC-F and cdfullCHC-R (Table 1), were used to amplify PmCHC from hemocytes of *Penaeus monodon* and were designed based on the nucleotide sequences obtained from *Marsupenaeus japonicus* clathrin heavy chain. The cDNA of PmCHC coding sequences was amplified by using Taq DNA polymerase (New England Biolabs). The PCR was performed by hot-start at 95°C for 5 min; 30 cycles of 95 °C for 30 s, 60 °C for 30 s, and 68 °C for 6 min; followed by 68 °C for 7 min. The cDNA was cloned into pGEM-T easy vector (Promega). The recombinant plasmid containing PmCHC was sequenced using T7, SP6, walkCHC-F1, walkCHC-F2, walkCHC-R1 as primers (Table 1) by First Base Co, Ltd. (Malaysia).

2.5. Sequence analysis

The nucleotide sequence analysis was performed with BLASTN (http://blast.ncbi.nlm.nih.gov). The deduced amino acid sequence of PmCHC was used to search the NCBI database (http://www.ncbi.nlm.nih.gov/Structure/cdd/wrpsb.cgi) to predict the conserved domains. Predictions of molecular weight and isoelectric point (pI) of the protein were performed by Expert Protein Analysis System (www.expasy.org). Sequences of proteins from several organisms were obtained from GenBank database. Multiple amino acid sequence alignments were performed by VectorNTI program (Invitrogen). Phylogenetic analysis (http://www.phylogeny.fr/version2_cgi/phylogeny.cgi) was based on the neighbor-joining method (Dereeper et al., 2008, 2010).

2.6. Construction of the recombinant plasmid expressing dsRNA-PmCHC

Recombinant plasmid containing stem-loop of dsRNA was constructed in pGEM-3Zf+ (Promega) and pET-17b (Novagen) vectors. Sense-loop region of the dsRNA was amplified from the first-strand cDNA by specific primers, sCHC-F1 and lpCHC-R1 (Table 1). The antisense region was amplified by asCHC-F2 and asCHC-R2 (Table 1). Both PCR

fragments were gel-purified and subjected to restriction enzyme digestion. The purified fragment of the sense-loop was cloned into the linearized fragment of pGEM-3Zf+ (digested by *Xba*I and *Kpn*I). Then, this recombinant plasmid containing the sense-loop region of PmCHC was digested by *Kpn*I and *Eco*RI and ligated with *Kpn*I and *Eco*RI digested antisense fragment. The recombinant plasmid containing sense-loop-antisense fragments of PmCHC (pGEM-3Zf+-PmCHC) was obtained. Then, the sense-loop-antisense fragment of PmCHC was subcloned into pET-17b vector at *Xba*I and *Eco*RI sites to construct recombinant plasmid pET17b-PmCHC which was used for dsRNA production by *in vivo* bacterial expression.

2.7. Production of dsRNA by in vivo bacterial expression

Recombinant plasmid pET17b-PmCHC was transformed into a RNase III mutant HT115 *E.coli* strain. This strain is modified to express T7 RNA polymerase from an isopropyl-β-D thiogalactopyranoside (IPTG) inducible promoter. Therefore, dsRNAs can be produced in the HT115 bacterial host after induction with IPTG. Double-stranded RNA was extracted and purified as previously described (Ongvarrasopone et al., 2007; Posiri et al., 2013). The quality of dsRNA was characterized by ribonuclease digestion assay using RNase A and RNase III. dsRNA concentration was estimated by agarose gel electrophoresis by comparing to the intensity of 100 bp DNA marker.

2.8. Suppression of PmCHC by dsRNA-PmCHC

The knockdown effect of dsRNA-PmCHC was tested by injection of dsRNA into hemolymph. Shrimp were injected with 2.5 $\mu g.g^{-1}$ shrimp of dsRNA-PmCHC or an unrelated gene of dsRNA-GFP dissolved in 150 mM NaCl. Injection of 150 mM NaCl was used as control. After twenty four hours post dsRNA injection, gills of individual shrimp were collected to extract total RNA. Suppression effect of dsRNA was analysed by reverse-transcription PCR (RT-PCR) to determine PmCHC mRNA level. To study the knockdown effect of PmCHC in YHV-challenged shrimp, shrimp were injected with dsRNA-PmCHC for twenty four hours before YHV challenge. Forty eight hours later, gills of individual shrimp were collected to extract total RNA to detect YHV (helicase gene) and PmCHC mRNA expression levels. PmActin mRNA was used as an internal control.

2.9. Shrimp mortality assay

The mortality of shrimp injected with dsRNA followed by YHV challenge was observed every 6 hours. Shrimp were about 1 g with 15 shrimp per group. Three independent experiments were performed. Shrimp were injected with 150 mM NaCl, 2.5 $\mu g.g^{-1}$ shrimp of dsRNA-PmCHC or dsRNA-GFP. After 24 hours post injection, shrimp were challenged with YHV. Mortality was plotted every 12 hours.

2.10. RNA isolation and RT-PCR analysis

Total RNA from gill tissues was isolated by Trizol® reagent (Molecular Research Center) following the manufacturer's procedure. The RNA concentration was measured by Nanodrop ND-1000 spectrophotometer (Nanodrop Technologies). Total RNA (2 µg) was used to generate first-strand cDNA by Improm-II™ reverse transcriptase (Promega) and PRT primer (Table 1). PmCHC mRNA level was amplified by primers; PmCHC-F1 and PmCHC-R1 (Table 1). PmActin mRNA expression, used as internal control, was amplified by specific primers, PmActin-F and PmActin-R1 (Table 1). Multiplex PCR for PmCHC and PmActin was performed according to this condition: 95°C for 5 min; 25 cycles of 95°C for 30 s, 60°C for 30 s, and 72°C for 45 s; followed by 72°C for 7 min. YHV mRNA level was amplified using primers, YHV(hel)-F and YHV(hel)-R (Table 1). The multiplex PCR condition for YHV and PmActin was as above except that the annealing temperature was changed to 55°C for 30 s. The PCR products were analyzed on 1.5% agarose gel. The intensity of each band after subtracting the background was quantified by using Image J analysis program (version 1.46r). The relative expression level of PmCHC and YHV was normalized with PmActin levels and expressed as an arbitrary unit.

2.11. Quantitative real time PCR (qPCR)

Total RNA 2 µg was used for the first-strand cDNA synthesis by Improm-II™ reverse transcriptase (Promega) using PRT primer. Dilution of cDNA at 1:32 was mixed with qPCR reaction using KAPA™ SYBR® Fast master mix (2X) ABI Prism™ (KAPA Biosystems) following manufacturer's protocol. qYHV-F and qYHV-R specific primers (Table 1) were used to amplify YHV mRNA; EF1- α (EF-1α-F and EF-1α-R) is used as internal control: 95°C for 3 min; 40 cycles of 95°C for 5 s, 60°C for 30 s. The qPCR was analyzed in an ABI 7500 real-time detection system (Applied Biosystems). The cycle threshold (Ct) value of YHV and EF1- α was compared and calculated by $2^{-\Delta\Delta C_T}$ method (Livak and Schmittgen, 2001).

2.12. Statistical analysis

The relative mRNA levels of PmCHC or YHV normalized with PmActin and fold change in PmCHC expression were presented as mean ± SEM. Cumulative percent mortality was plotted as mean ± SEM. In addition, significant differences of each experimental group were tested by using analysis of variance (ANOVA). A probability *(P)* value of 0.05 was used to define significant difference.

Table 1 Primer sequences used in the experiments.

Primers	Sequences (5′ ---► 3′)	Experiments
cdfullCHC-F	GGGGTACCATGACACAGGCGTTACCC	Full length PmCHC coding region
cdfullCHC-R	GGAATTCCATATGTTACATGCTGTAGCCTTG	Full length PmCHC coding region
walkCHC-F1	TGTATTCTTCCCACCAGAGGC	Sequencing primers
walkCHC-F2	ACGTCTGCCAGTTGTTGTGG	Sequencing primers
walkCHC-R1	CCTTGAAGTGTGACTCTCGCC	Sequencing primers
mjCHC-F	AGTGCTTTGCTGAAACTGGTC	Partial PmCHC cDNA region
mjCHC-R	CATGAATACGAGATTCCAGCC	Partial PmCHC cDNA region
sCHC-F1	GC*Xba*I TCTAGACGAAATGTAATGCGTGTC	dsRNA-PmCHC construction
lpCHC-R1	GG*Kpn*I GGTACCCTATCTGCACTACAATCTGTAG	dsRNA-PmCHC construction
asCHC-F2	G*Eco*RI GAATTCCGAAATGTAATGCGTGTC	dsRNA-PmCHC construction
asCHC-R2	GG*Kpn*I GGTACCGACCAACCATTCTGGGTT	dsRNA-PmCHC construction
PmCHC-F	CTTCTCCCAAGAACCAGAGGTGCAC	Detection of PmCHC mRNA
PmCHC-R	ATTCCTCTTCTCCACCTCTTCCACC	Detection of PmCHC mRNA
PRT-oligo dT	CCGGAATTCAAGCTTCTAGAGGATCCTTTTTTTTTTTTTTTT	Reverse transcription
YHV(hel)-F	CAAGGACCACCTGGTACCGGTAAGAC	Detection of YHV mRNA
YHV(hel)-R	GCGGAAACGACTGACGGCTACATTCAC	Detection of YHV mRNA
PmActin-F	GACTCGTACGTGGGCGACGAGG	Detection of PmActin mRNA
PmActin-R	AGCAGCGGTGGTCATCTCCTGCTC	Detection of PmActin mRNA
qYHV-F	ATCATCAGCTCACAGGCAAGTTCC	Real time PCR
qYHV-R	GGGTCTAAATGGAGCTGGAAGACC	Real time PCR
EF-1α-F	GAACTGCTGACCAAGATCGACAGG	Real time PCR
EF-1α-R	GAGCATACTGTTGGAAGGTCTCCA	Real time PCR

3. Results

3.1. Analysis of YHV entry pathway

To identify the pathway for YHV internalization into shrimp cell, shrimp of about 2 g were pretreated with inhibitors of clathrin-mediated endocytosis (chlorpromazine, CPZ), macropinocytosis (amiloride) or the caveolar dependent pathway (methyl-β-cyclodextrin, MβCD), and followed by YHV challenge. All shrimp receiving inhibitors survived throughout the experiment. Quantitative RT-PCR of the shrimp pretreated with chlorpromazine showed a significant reduction of YHV mRNA levels, approximately 77%, when compared to the PBS-YHV injected group. Whereas shrimp pretreated with amiloride and MβCD demonstrated no significant difference to the YHV control group (Fig. 1).

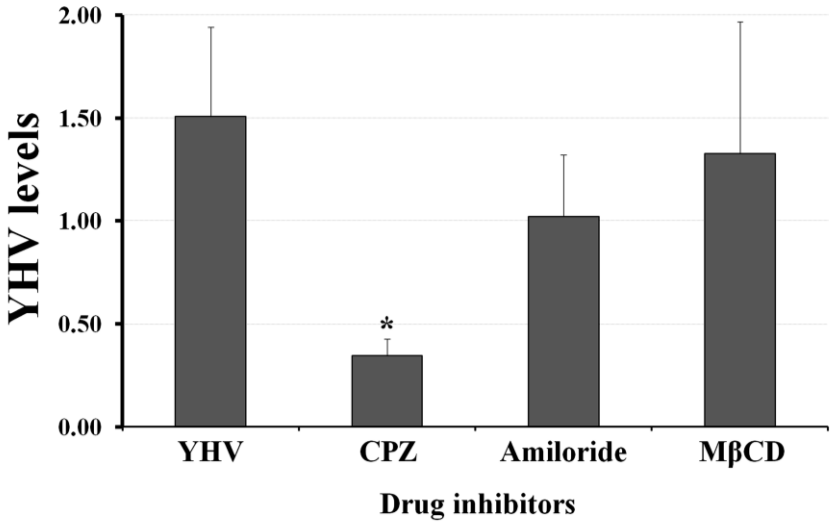

Fig. 1 Effect of drug inhibitors on YHV internalization into shrimp cell. Graphs represent the quantitative RT-PCR of YHV mRNA levels (fold change) of YHV-challenged shrimp pretreated with drug inhibitors which are chlorpromazine (CPZ), amiloride and methyl-β-cyclodextrin (MβCD). Nine shrimps per group were analyzed. (*) represents significant difference (*P< 0.05)* of YHV mRNA levels compared between the YHV- challenged groups pretreated with presence and absence of drug inhibitors.

3.2. Cloning of Penaeus monodon clathrin heavy chain (PmCHC) coding region and sequence analysis.

The sequence of *Marsupenaeus japonicus* clathrin heavy chain was used to design specific-primers to amplify the full-length coding region of *Penaeus monodon* clathrin heavy chain from hemocytes. The open reading frame of PmCHC is 5,055 bp, encoding a protein of 1,684 amino acids, with an estimated molecular weight of 192.5 kDa and a pI of 5.53. The nucleotide sequence is deposited in the GenBank database under the accession number **KJ700941**. The protein contains several conserved domains: clathrin propeller repeat (amino acid: 205-241, 259-295, 303-337), clathrin heavy chain linker (amino acid 338-361), clathrin-H-link (amino acid 363-428), and clathrin heavy chain repeat homology (amino acid: 544-682, 693-831, 844-978, 986-1127, 1139-1275, 1281-1423, 1434-1572) (Fig. 2). For most organisms (Table 2, Fig. 3), conserved domains of CHC consist of a seven CHC repeat homology, one CHC H-linker and one CHC linker. One clathrin propeller repeat is observed in plants including *Zea mays* and *Theobroma cacao*. However, three to four clathrin propeller repeats are found in both invertebrate and vertebrate species including *Penaeus monodon*, *Aedes aegypti*, *Drosophila melanogaster*, *Homo sapiens* and *Danio rerio* (Table 2). Phylogenetic tree analysis

clustered organisms in three groups which are plants, invertebrates and vertebrates. PmCHC was clustered into an invertebrate group (Fig. 4).

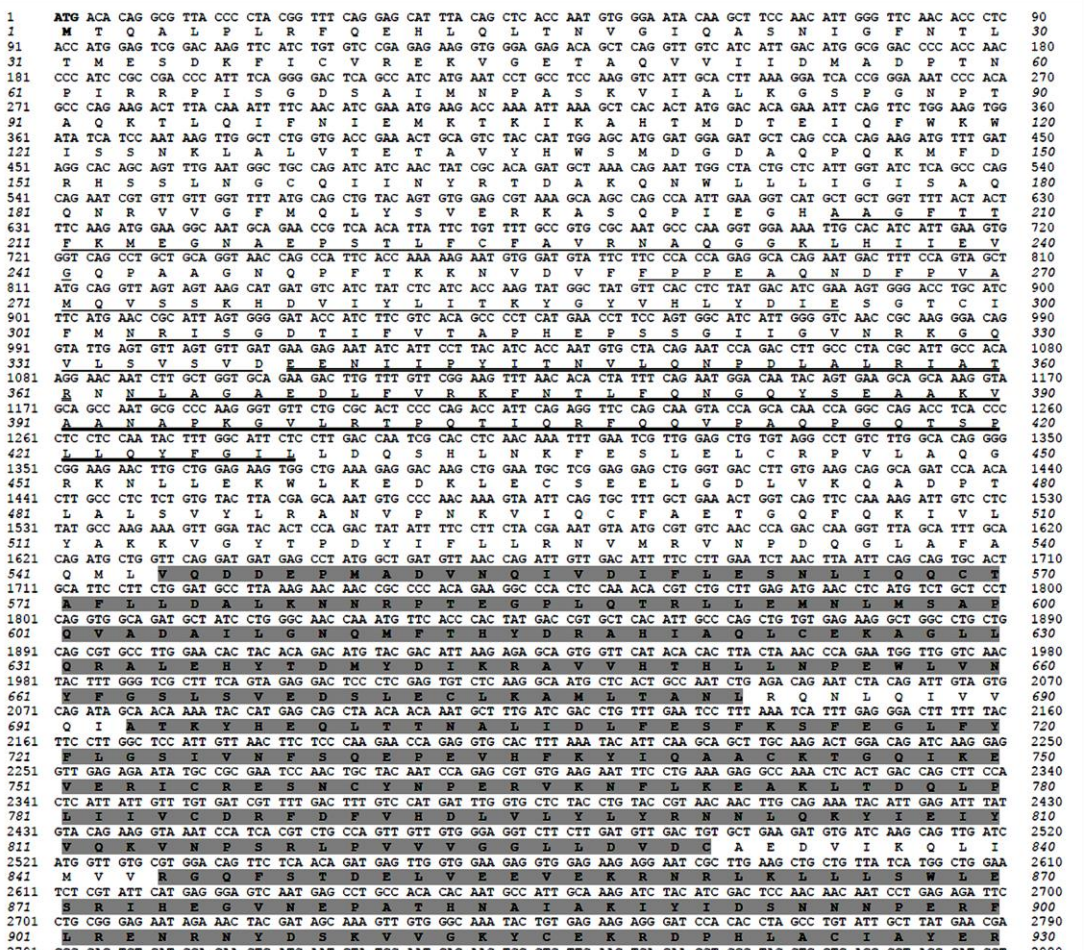

Fig. 2 The Nucleotide and amino acid sequences of *Penaeus monodon* clathrin heavy chain (*Pm*CHC). Start or stop codon is in bold letters and the asterisk demonstrates the stop codon. Underline represents clathrin propeller repeat. Double underline represents clathrin heavy chain linker. Thick line represents clathrin-H-link. Gray shade represents clathrin heavy chain repeat homology. The nucleotide sequences are deposited in the GenBank database under the accession number **KJ700941**.

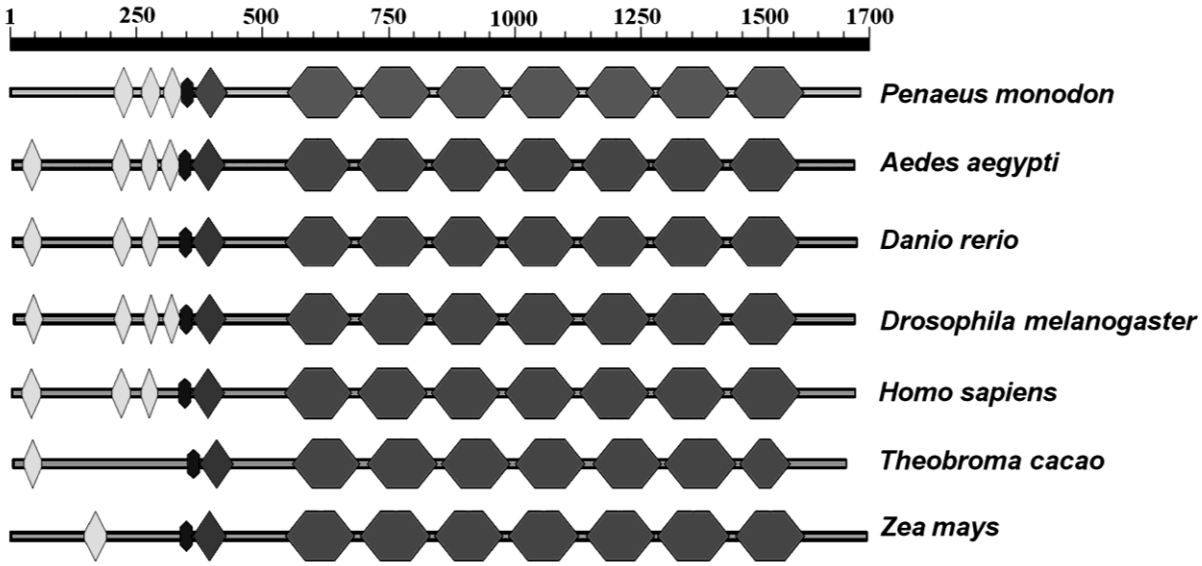

Fig. 3 Comparison of the clathrin heavy chain protein domains among several organisms. The protein domains comprising of clathrin propeller repeat (), clathrin heavy chain linker (), clathrin-H-link (), clathrin heavy chain repeat homology (). *Aedes aegypti*, *Drosophila melanogaster*, *Homo sapiens*, *Danio rerio*, *Zea mays* and *Theobroma cacao* were compared to *Penaeus monodon.*

3.3. Production of dsRNA-PmCHC and its suppression effect

Recombinant plasmid pET17b containing a stem loop of PmCHC was constructed and transformed into HT115 *E. coli* strain to be used as template for *Pm*CHC dsRNA production (dsRNA-PmCHC) by *in vivo* bacterial expression. Then, hairpin dsRNA-PmCHC was extracted using an ethanol method (Posiri et al., 2013). The quality of dsRNA-PmCHC was characterized by ribonuclease III (RNase III) and by ribonuclease A (RNase A) digestion assay. DsRNA-GFP was also produced for nonspecific dsRNA injection. The hairpin dsRNA-PmCHC and dsRNA-GFP could be cleaved by RNase III but not by RNase A, suggesting that good quality dsRNA were obtained (Fig. 5A). Injection of dsRNA-PmCHC resulted in a significant

reduction of PmCHC mRNA levels, approximately 90% when compared to the NaCl injected group (p< 0.01; n=5). In contrast, no significant difference in PmCHC expression levels was observed between dsRNA-GFP- and NaCl-injected groups (Fig. 5B and 5C).

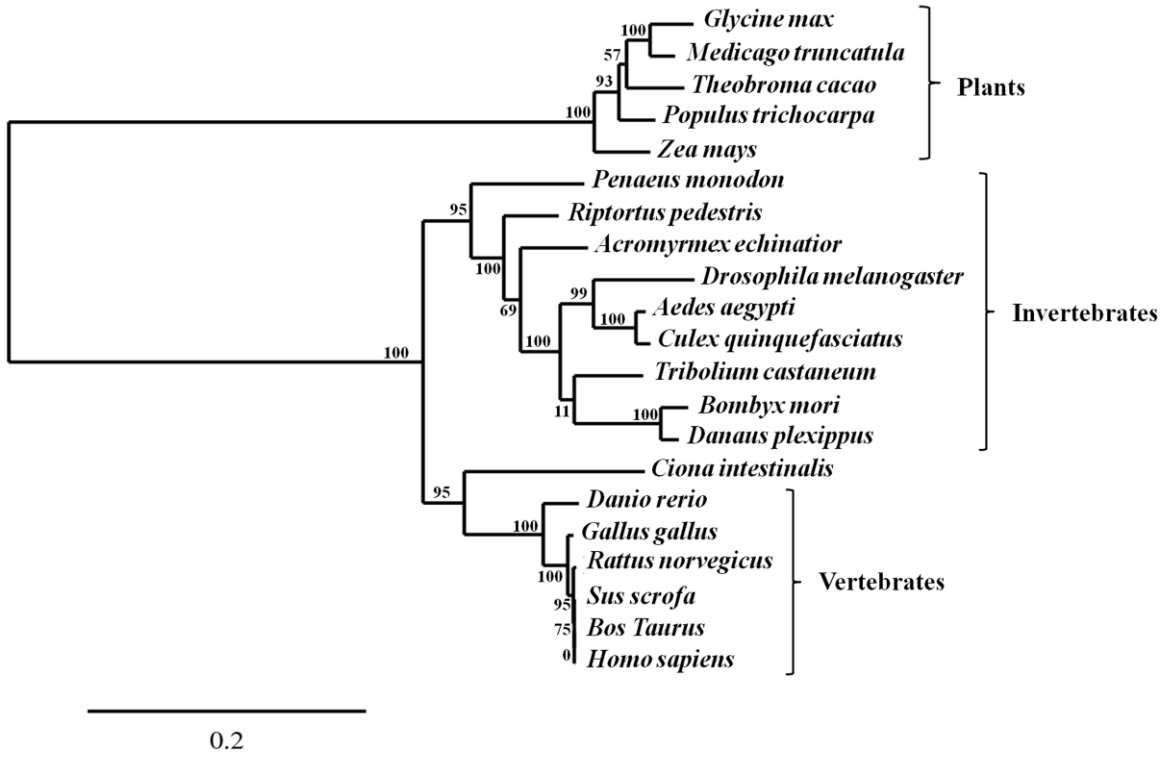

Fig. 4 Phylogenetic analysis of the clathrin heavy chain based on amino acid sequences using Neighbor-joining distance analysis. There are several organisms included in this analysis which are *Glycine max*, *Medicago truncatula*, *Theobroma cacao*, *Populus trichocarpa*, *Zea mays*, *Penaeus monodon*, *Riptortus pedestris*, *Acromyrmex echinatior*, *Drosophila melanogaster*, *Aedes aegypti*, *Culex quinquefasciatus*, *Tribolium castaneum*, *Bombyx mori*, *Danaus plexippus*, *Ciona intestinalis*, *Danio rerio*, *Gallus gallus*, *Rattus norvegicus*, *Sus scrofa*, *Bos Taurus*, *Homo sapiens* and *Penaeus monodon.* The GenBank accession number of CHC from each organism was demonstrated in Table 2. Bootstrap values from 1000 replicates are indicated at the node.

Table 2 Accession number of organisms used for phylogenetic analysis

Organisms	Accession number
Acromyrm exechinatior	EGI60613
Aedes aegypti	XP_001656878
Bombyx mori	NP_001136443
Bos taurus	AAC48524
Ciona intestinalis	XP_002130279
Culex quinquefasciatus	EDS40945
Danaus plexippus	EHJ79063
Danio rerio	NP_001005391
Drosophila melanogaster	NP_001096993
Gallus gallus	NP_001073586
Glycine max	AAC49294
Homo sapiens	NP_004850
Medicago truncatula	AES71175
Penaeus monodon	KJ700941
Populus trichocarpa	EEF02372
Rattus norvegicus	AAA40874
Riptortus pedestris	BAN20627
Sus scrofa	NP_001139599
Theobroma cacao	EOY34523
Tribolium castaneum	XP_967829
Zea mays	AGC82051

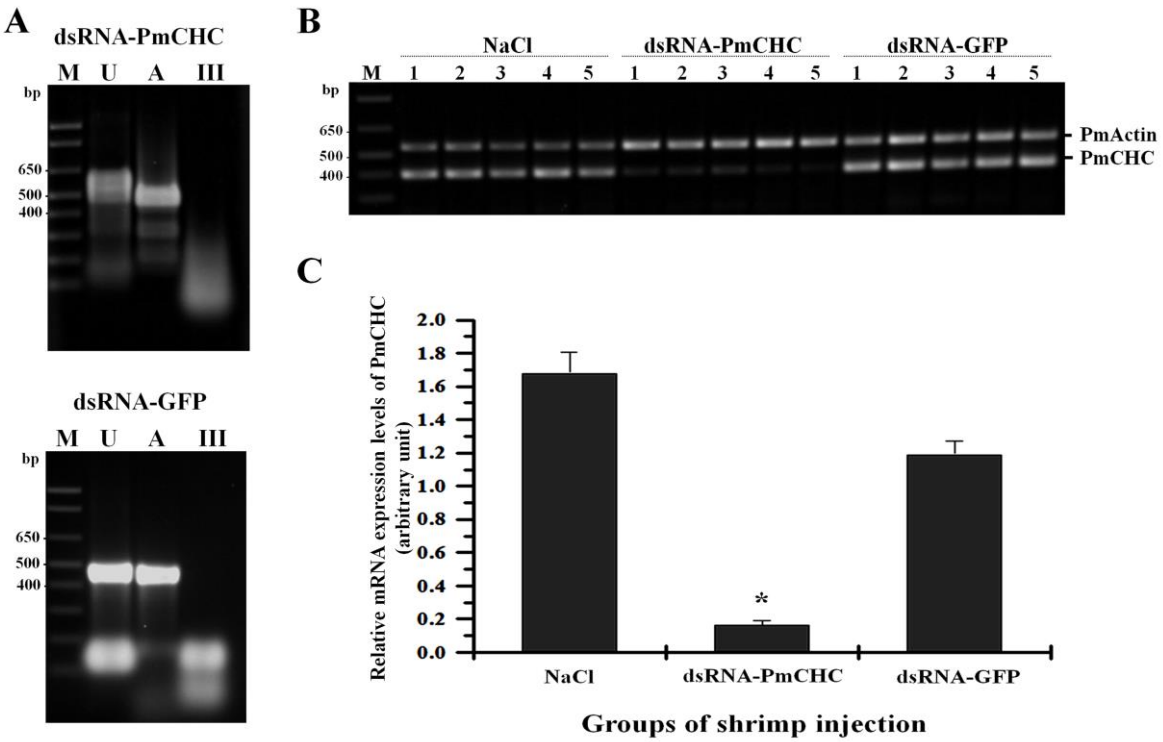

Fig. 5 Effectiveness of dsRNA-PmCHC on silencing of PmCHC mRNA. (A) Quality of dsRNA-PmCHC and dsRNA-GFP produced by *in vivo* bacterial expression; M is 1 kb plus DNA ladder whereas U, A and III are undigested dsRNA, digested dsRNA with RNase A and RNase III, respectively. (B) Representative agarose gel of RT-PCR products of PmCHC and PmActin expression of NaCl control, injected with dsRNA-PmCHC and dsRNA-GFP groups, respectively. M is 1 kb plus DNA marker. (C) Relative mRNA expression levels of PmCHC when normalized with PmActin were presented as mean±SEM (n=5). (*) Statistically significant difference between dsRNA-CHC compared with NaCl injected group ($P< 0.01$).

3.4. Suppression effect of PmCHC in YHV-challenged shrimp inhibited YHV mRNA levels

To determine whether PmCHC is required for YHV internalization into shrimp cells, the PmCHC-knockdown shrimp were challenged with YHV. After 48-hours, gills were collected for total RNA extraction and RT-PCR analysis to determine mRNA expression of YHV and PmCHC. The results demonstrated the suppression effect of PmCHC, by dsRNA-PmCHC, resulted in almost complete inhibition of YHV mRNA expression. However, high levels of YHV mRNA were still observed in both NaCl-injected and dsRNA-GFP injected groups (Fig. 6A and 6B).

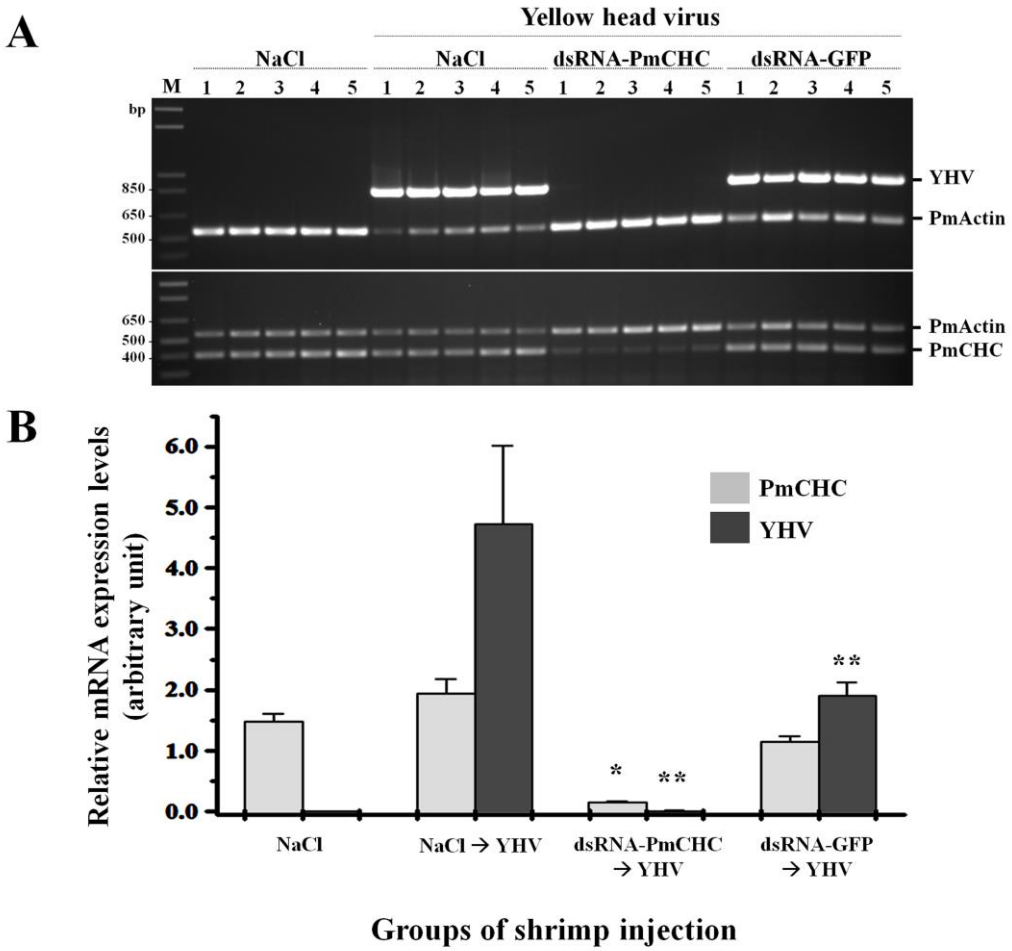

Fig. 6 Suppression effect of PmCHC inhibited YHV infection. (A) A representative gel of RT-PCR products of YHV (top panel) and PmCHC (bottom panel) mRNA levels. PmActin was used as an internal control. Shrimp were divided into 4 groups; NaCl alone and NaCl, dsRNA-PmCHC or dsRNA-GFP followed by YHV challenge (n=5 per group). M is 1 kb plus DNA marker. (B) The relative mRNA expression levels of PmCHC (gray bar) and YHV normalized with PmActin (light black bar). Data is expressed as mean±SEM in an arbitrary unit. (*) represents significant difference (*P< 0.05)* of PmCHC mRNA levels comparing between dsRNA-PmCHC→YHV and NaCl injected group. (**) represents statistically significant difference (*P< 0.05*) of YHV mRNA levels comparing between dsRNA-injected group and NaCl→YHV group.

3.5. Suppression of PmCHC in YHV-challenged shrimp delayed mortality

Shrimp receiving dsRNA-*Pm*CHC, followed by YHV challenge, reached 100% cumulative mortality at 120 hours post YHV injection (hpi) whereas NaCl- and dsRNA-GFP-injected groups gave 100% mortality at 108 hpi. Furthermore, shrimp injected with dsRNA-

PmCHC followed by YHV challenge showed significant reduction in cumulative percent mortality at 84 – 108 hpi when compared with the NaCl injection group (Fig. 7A). This result suggested that clathrin heavy chain is required for YHV infection. However, shrimp injected with dsRNA-PmCHC at 2.5 $\mu g.g^{-1}$ shrimp without YHV challenge reached 100% mortality at 156 hours post dsRNA injection whereas shrimp injected with NaCl or dsRNA-GFP showed no mortality (Fig. 7B). In addition, shrimp injected with dsRNA-PmCHC at lower dosage, 1.25 $\mu g.g^{-1}$ shrimp, without YHV challenge reached 100% mortality at a later time, 180 hours post dsRNA injection. A 75% mortality was observed in shrimp injected with dsRNA-PmCHC at 0.63 $\mu g.g^{-1}$ without YHV challenge during 144-240 hours post dsRNA injection (Fig. 8). Dead shrimp were sampled for viral load detection. The results showed that dsRNA-PmCHC →YHV group (Fig. 7C (b)) demonstrated lower YHV mRNA levels when compared to NaCl →YHV group (Fig. 7C (a)) and dsRNA-GFP →YHV group (Fig. 7C (c)). All dead shrimp except samples from lanes 2, 3, 8, 11, and 12 in the dsRNA-PmCHC →YHV group showed the presence of YHV. This suggested that the shrimps in lanes 2, 3, 8, 11, and 12 were protected from YHV infection but were dead from the PmCHC knockdown. Taken together, the results strongly suggested that clathrin heavy chain is essential for YHV infection.

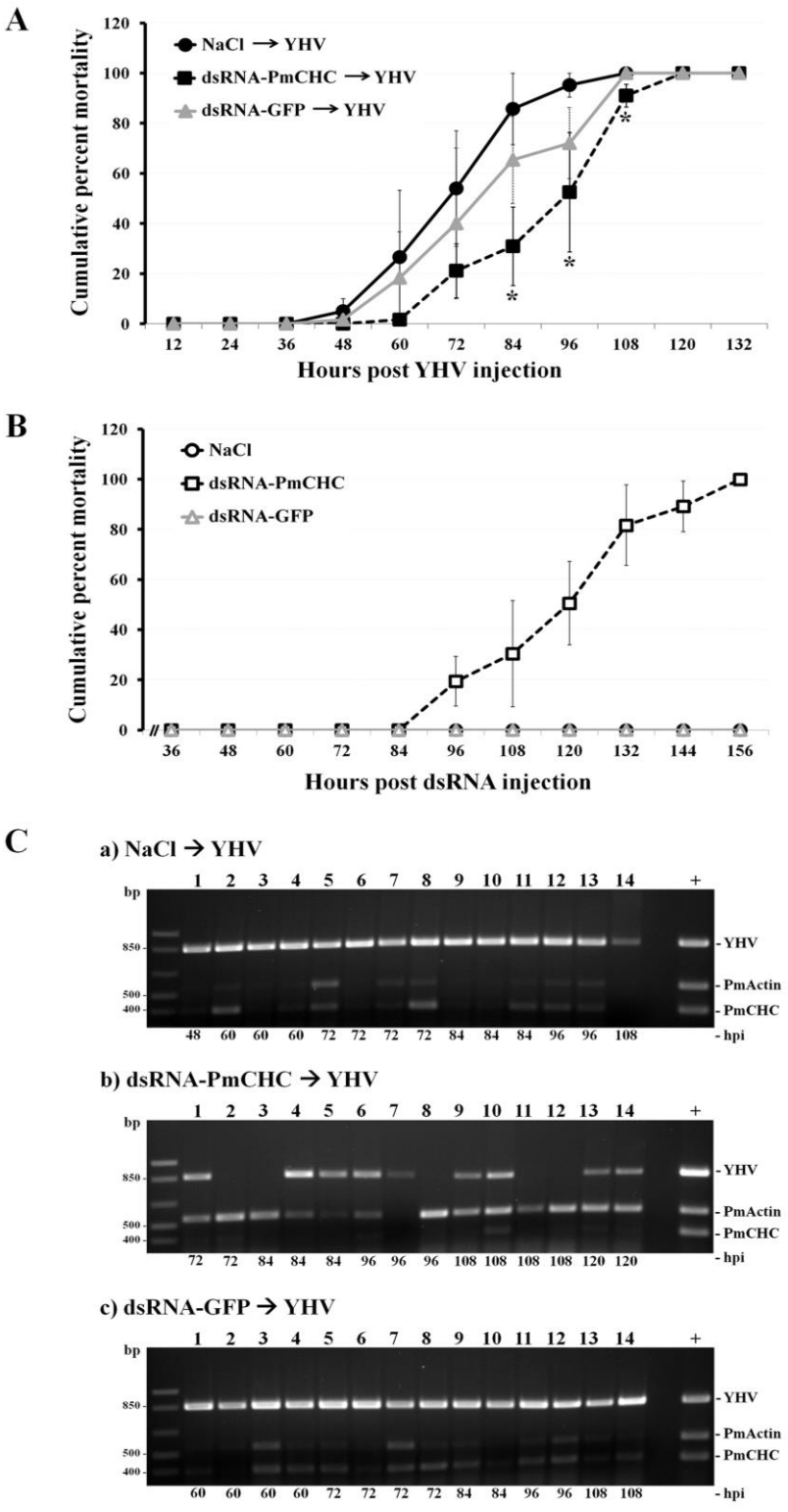

Fig. 7 The cumulative percent mortality of shrimps injected with NaCl, dsRNA-PmCHC, or dsRNA-GFP followed by YHV challenge (A) or without YHV challenge (B). * represents significantly difference between dsRNA-PmCHC→YHV and NaCl→YHV group. (C) A representative gel of RT-PCR products of YHV mRNA levels of dead as an internal control. The number on the bottom of the each lane represents the time (hours of post YHV challenge,

hpi) that the shrimp die. The expression of PmActin in dead shrimp samples that showed high expression levels of YHV were very faint. This result was also demonstrated in the previous studies (Posiri et al., 2011).

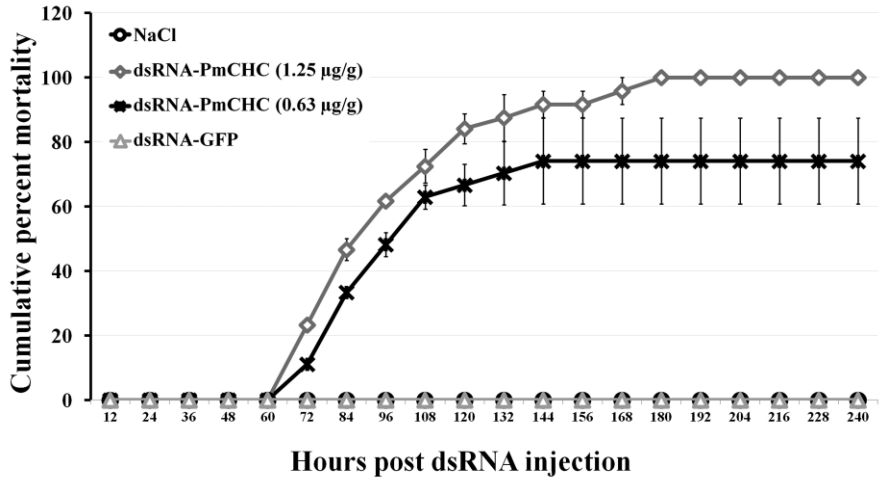

Fig. 8 The cumulative percent mortality of shrimp injected with NaCl (), varying doses of dsRNA-PmCHC at 0.63 () and 1.25 () µg.g^{-1} shrimp, or dsRNA-GFP(). Three independent experiments were performed with 9 shrimp per group. Shrimp mortality was observed every 12 hours post dsRNA injection for 10 days.

4. Discussion

Clathrin heavy chain (CHC) is a major protein in clathrin-coated pit and clathrin-coated vesicle. Clathrin heavy and light chains are assembled to form a three-legged structure, called a triskelion. Clathrin heavy chain together with adaptor and accessory proteins, including AP2, EPS15, AP-180, Epsin or dynamin (McMahon and Boucrot, 2011; Mousavi et al., 2004; Young, 2007) are involved in endocytosis. The functions of clathrin heavy chain are believed to be involved in sorting cargo protein in the membrane and membrane curvature.

In black tiger shrimp, the role of clathrin heavy chain in virus infection has not been previously investigated. In this study, we have cloned *Penaeus monodon* clathrin heavy chain (*Pm*CHC). The function of PmCHC especially for yellow head virus (YHV) infection was tested to study the major route for YHV internalization. RNA interference (RNAi) was used as a tool to study the function of PmCHC. Shrimp injected with dsRNA-PmCHC showed reduction of PmCHC mRNA levels up to 90% when compared to the NaCl-injected control group. In addition, knockdown of PmCHC mRNA in YHV-challenged shrimp exhibited low levels of YHV expression (Figs. 6 and 7C) and a delay in shrimp mortality up to 24 hours post YHV injection

(84 – 108 hpi) (Fig. 7A). These effects may be due to suppression of PmCHC gene (Fig. 7B and Fig. 8). After knocking down of PmCHC mRNA, low levels of PmCHC present may slow down the entry of YHV into the cell, thus resulting in a delay of shrimp mortality. Moreover, the shrimp death may also be due to the depletion of clathrin heavy chain (Fig. 7B and Fig. 8). This is because clathrin heavy chain has diverse cellular functions such as transportation of cargo inside the cell, cytokinesis and glucose metabolism (Brodsky, 2012). Depletion of PmCHC may inhibit some cellular functions which are essential for cell survival. Several studies have shown that some viruses required clathrin heavy chain for infection (Hong Liang and Cheng Yu, 2009; Hussain et al., 2011; Bhattacharyya et al., 2010). For instance, confocal microscopy demonstrated the colocalization between rhesus rhadinovirus and clathrin heavy chain (Zhang et al., 2010). Similar to this study, suppression of the clathrin heavy chain by small interfering RNA exhibited a reduction of viral load in the host cells, including influenza A virus, severe acute respiratory syndrome coronavirus or human enterovirus 71 (Hong Liang and Cheng Yu, 2009; Hussain et al., 2011; Inoue et al., 2007). It has been shown that the cargo molecules that can be transported via clathrin-meditated endocytosis is size dependent, approximately 200 nm (Rejman et al., 2004) which nicely fit with the YHV virion, whose size is ~50-60 × 190-200 nm (Nadala et al., 1997). In addition, a recent report showed the reduction of YHV level in clathrin coat AP17 knockdown shrimp (Jatuyosporn et al., 2014). Moreover, by using various inhibitors (CPZ, MβCD and amiloride), only the YHV-challenged shrimp pretreated with CPZ showed a significant reduction of YHV levels. These results suggested that the major route of YHV into the shrimp cells was via clathrin-mediated endocytosis pathway.

In shrimp, a previous study has identified a protein in the endocytosis pathway, *Penaeus monodon* Rab7 (PmRab7) (Sritunyalucksana et al, 2006). Rab7 is a small GTPase protein and plays a crucial role to regulate the transportation from late endosome to lysosome during endosome maturation (Huotari and Helenius, 2011). In addition, PmRab7 is required for several shrimp viruses such as white spot syndrome virus (WSSV), taura syndrome virus (TSV) Laem-Singh virus (LSNV) or YHV for intracellular trafficking inside the cell (Ongvarrasopone et al., 2008, 2010, 2011). Therefore based on the previous evidence and this study, the mechanism of YHV entry and intracellular trafficking can be proposed. YHV enters the shrimp cells by using the envelop protein gp116 to bind to YHV binding protein, PmYRP65 (Assavalapsakul et al., 2006). Then, many adaptor proteins which are involved in clathrin-coated pit formation including AP2, AP17 and PmCHC are recruited to induce membrane invagination to form clathrin-coated vesicles which then transport YHV to the early endosome which also may require Rab5 protein (Hutagalung and Novick, 2011; Stenmark, 2009). After that, YHV may be transported toward the late endosome and lysosome via the regulation by

PmRab7 for viral uncoating. The intracellular trafficking process of YHV may be similar to semliki forest virus (SFV) which is internalized via clathrin mediated endocytosis and requires Rab7 for transportation inside the cell (Vonderheit and Helenius, 2005).

5. References

Assavalapsakul, W., Tirasophon, W., Panyim, S., 2005. Antiserum to the gp116 glycoprotein of yellow head virus neutralizes infectivity in primary lymphoid organ cells of *Penaeus monodon*. Dis. Aquat. Org. 63, 85-88.

Assavalapsakul, W., Smith, D.R., Panyim, S., 2006. Identification and characterization of a *Penaeus monodon* lymphoid cell-expressed receptor for the yellow head virus. J. Virol. 80 (1), 262-269.

Bhattacharyya, S., Warfield, K.L., Ruthel, G., Bavari, S., Aman, M.J., Hope, T.J., 2010. Ebola virus uses clathrin-meditated endocytosis as and entry pathway. Virology 401, 18-28.

Boonyaratpalin, S., Supamattaya, K., Kasornchandra, J., Direkbusaracom, S., Aekpanithanpong, U., Chantanachooklin, C., 1993. Non-occluded baculo-like virus, the causative agent of yellow head disease in the black tiger shrimp (*Penaeus monodon*). Fish Pathol. 28 (3), 103-109.

Brodsky, F.M., 2012. Diversity of clathrin function: New tricks for an old protein. Annu. Rev. Cell Dev. Biol. 28, 309-336.

Dereeper, A., Audic, S., Claverie, J-M., Blanc, G., 2010. BLAST-EXPLORER helps you building datasets for phylogenetic analysis. BMC Evol. Biol. 12, 10:8.

Dereeper, A., Guignon, V., Blanc, G., Audic, S., Buffet, S., Chevenet, F., Dufayard, J-F., Guindon, S., Lefort, V., Lescot, M., Claverie, J-M., Gascuel, O., 2008. Phylogeny.fr: robust phylogenetic analysis for the non-specialist. Nucleic Acids Res. 36, W465-W469.

Doherty, G.J., McMahon, H.T., 2009. Mechanisms of endocytosis. Annu. Rev. Biochem. 78, 31.1–31.46.

Flegel, T.W., 1997. Major viral diseases of the black tiger prawn (*Penaeus monodon*) in Thailand. World J. Microbiol. Biotechnol. 13, 433-442.

Hongliang, W., Chengyu, J., 2009. Influenza A virus H5N1 entry into host cells is through clathrin-dependent endocytosis. Sci. China, C, Life Sci. 52 (5), 464-469.

Huotari, J., Helenius, A., 2011. Endosome maturation. EMBO J. 30 (17), 3481–3500.

Hussain, K.M., Leong, K.L., Ng, M.M., Chu, J.J., 2011. The essential role of clathrin-mediated endocytosis in the infectious entry of human enterovirus 71. J. Biol. Chem. 286 (1), 309-321.

Hutagalung, A.H., Novick, P.J., 2011. Role of Rab GTPases in membrane traffic and cell physiology. Physiol. Rev. 91, 119-149.

Inoue, Y., Tanaka, N., Tanaka, Y., Inoue, S., Morita, K., Zhuang, M., Hattori, T., Sugamura, K., 2007. Clathrin-dependent entry of severe acute respiratory syndrome coronavirus into target cells expressing ACE2 with the cytoplasmic tail deleted. J. Virol. 81 (16), 8722-8729.

Jatuyosporn, T., Supungul, P., Tassanakajon, A., Krusong, K., 2014. The essential role of clathrin-mediated endocytosis in yellow head virus propagation in the black tiger shrimp *Penaeus monodon*. Dev. Comp. Immunol. 44, 100–110.

Jitrapakdee, S., Unajak, S., Sittidilokratna, N., Hodgson, R.A., Cowley, J.A., Walker, P.J., Panyim, S., Boonsaeng, V., 2003. Identification and analysis of gp116 and gp64 structural glycoproteins of yellow head nidovirus of *Penaeus monodon* shrimp. J. Gen. Virol. 84, 863-873.

Khanobdee, K., Soowannayan, C., Flegel, T.W., Ubol, S., Withyachumnarnkul, B., 2002. Evidence for apoptosis correlated with mortality in the giant black tiger shrimp *Penaeus monodon* infected with yellow head virus. Dis. Aquat. Org. 48, 79-90.

Livak, K.J., Schmittgen, T.D., 2001. Analysis of relative gene expression data using real-time quantitative PCR and the $2^{-\Delta\Delta C}{}_T$ method. Methods 25, 402–408.

Marsh, M., Helenius, A., 2006. Virus entry: Open sesame. Cell 124, 729-740.

McMahon, H.T., Boucrot, E., 2011. Molecular mechanism and physiological functions of clathrin-mediated endocytosis. Nat. Rev. Mol. Cell Biol. 12, 517-533.

Meertens, L., Bertaux, C., Dragic, T., 2006. Hepatitis C Virus entry requires a critical postinternalization step and delivery to early endosomes via clathrin-coated vesicles. J. Virol. 80 (23), 11571-11578.

Mercer, J., Schelhaas, M., Helenius, A., 2010. Virus entry by endocytosis. Annu. Rev. Biochem. 79, 803-833.

Mousavi, S.A., Malerod, L., Berg, T., Kjeken, R., 2004. Clathrin-dependent endocytosis. Biochem. J. 377, 1–16.

Nadala Jr., C.B.., Tapay, L.M., Loh, P.C., 1997. Yellow-head virus: a rhabdovirus-like pathogen of penaeid shrimp. Dis. Aquat. Org. 31, 141-146.

Ongvarrasopone, C., Chanasakulniyom, M., Sritunyalucksana, K., Panyim, S., 2008. Suppression of PmRab7 by dsRNA inhibits WSSV or YHV infection in shrimp. Mar. Biotechnol. 10 (4), 374-381.

Ongvarrasopone, C., Chomchay, E., Panyim, S., 2010. Antiviral effect of PmRab7 knock-down on inhibition of Laem-Singh virus replication in black tiger shrimp. Antiviral Res. 88, 116–118.

Ongvarrasopone, C., Roshorm, Y., Panyim, S., 2007. A simple and cost effective method to generate dsRNA for RNAi studies in invertebrates. ScienceAsia 33, 35-39.

Ongvarrasopone, C., Saejia, P., Chanasakulniyom, M., Panyim, S. 2011 Inhibition of Taura syndrome virus replication in *Litopenaeus vannamei* through silencing LvRab7 gene by double-stranded RNA. Arch virol 156,1117-23.

Posiri, P., Ongvarrasopone, C., Panyim, S., 2013. A simple one-step method for producing dsRNA from *E. coli* to inhibit shrimp virus replication. J. Virol. Methods 188, 64-69.

Posiri, P., Ongvarrasopone, C., Panyim, S., 2011 Improved preventive and curative effects of YHV infection in *Penaeus monodon* by a combination of two double stranded RNAs. Aquaculture 314:34-38.

Rejman, J., Oberle, V., Zuhorn, I.S., Hoekstra, D., 2004. Size-dependent internalization of particles via the pathways of clathrin and caveolae-mediated endocytosis. Biochem. J. 377, 159–169.

Sittidilokratna, N., Dangtip, S., Cowley, J.A., Walker, P.J., 2008. RNA transcription analysis and completion of the genome sequence of yellow head nidovirus. Virus Res. 136, 157-165.

Sritunyalucksana, K., Wannapapho, W., Lo, C.F., Flegel, T.W., 2006. PmRab7 is a VP28-binding protein involved in white spot syndrome virus infection in shrimp. J. Virol. 80 (21), 10734-10742.

Stenmark, H., 2009. Rab GTPases as coordinators of vesicle traffic. Nat. Rev. Mol. Cell Biol. 10, 513-525.

Vonderheit, A., Helenius, A., 2005. Rab7 associates with early endosomes to mediate sorting and transport of semliki forest virus to late endosomes. PLoS Biol. 3 (7), 1225-1238.

Young, A., 2007. Structural insights into the clathrin coat. Semin. Cell Dev. Biol. 18, 448–458.

Zhang, W., Zhou, F., Greene, W., Gao, S-J., 2010. Rhesus rhadinovirus infection of rhesus fibroblasts occurs through clathrin-mediated endocytosis. J. Virol. 84 (22), 11709–11717.

Part II: Rab5, an early endosomal protein required for yellow head virus infection of *Penaeus monodon*

Abstract

Yellow head virus (YHV) is a virulent pathogen in black tiger shrimp. It causes high mortality within a few days after infection. In this study, colocalization between YHV and *P. monodon* Rab5 (PmRab5) which is a small GTPase protein was visualized at 10 min to 3 h post YHV challenge under a confocal microscope. The result indicated that PmRab5 plays a key role in the early stage of endocytosis, and is involved in YHV trafficking process. Molecular cloning showed that the open reading frame of PmRab5 is 633 bp encoding a putative protein of 210 amino acids with an estimated molecular weight of 23 kDa. PmRab5 contained all Rab-specific signature motifs: Rab family motif (RabF), Rab subfamily motif (RabSF), G-boxes and cysteine prenylation signal. Silencing of PmRab5 by specific dsRNA reduced YHV replication inside the cells. Furthermore, lack of PmRab5 expression exhibited a delay of shrimp mortality after YHV infection. The results demonstrated that PmRab5 is involved in YHV early endosomal trafficking, suggesting its role in the early step of infection.

Keywords: double stranded RNA; RNAi; black tiger shrimp; endocytosis; yellow head disease

1. Introduction

Enveloped yellow head virus (YHV) belongs to the genus *Okavirus*, family *Roniviridae* in the order *Nidovirales* which is a highly virulent pathogen against *Penaeus monodon* or black tiger shrimp. *P. monodon* is an economically important aquaculture shrimp in Thailand. YHV is a positive-sense ssRNA virus of approximately 27 kb, with poly-(A) tail. Morphology of YHV revealed an envelope bacilliform which has a particle size of about 50-60 x 190-200 nm. Within the YHV particle, it contains the internal helical nucleocapsid which is closely surrounded by an envelope studded with prominent peplomers or spikes (Nadala et al., 1997; Sittidilokratna et al., 2008). YHV contains three structural proteins: two major structural transmembrane glycoproteins (gp116 and gp64) and a nucleoprotein (p20) (Jitrapakdee et al., 2003).

Infection of several enveloped viruses is initiated by the viral glycoprotein binding to its cellular receptor. The conformational change in the virus particle promotes endocytic internalization into the host cell. The virus is delivered from the surface membrane toward early endosomes, maturing endosomes, late endosomes and lysosomes. The acidic condition of the endosomal compartment can trigger the penetration of the viral genome into cytosol. The low pH induces conformational changes of the fusion protein which exists in the viral membrane resulting in host-virus membrane fusion. The virus then uncoats and releases the genome into the cytoplasm (Greber et al., 1994; Marsh and Helenius, 2006; Mercer et al., 2010). Intracellular membrane traffic between these membranous organelles by vesicular transport requires tight regulation to ensure both fidelity and efficiency. The Rab GTPase family which belongs to the Ras superfamily plays a central role in regulating vesicle transports, including vesicle budding, delivery, tethering and fusion with the target membrane (Hutagalung and Novick, 2011; Stenmark, 2009). The intracellular localization and associated vesicle transport of plasma membrane to early endosome and mature endosome requires Rab5 protein. Rab5 associates with plasma membrane-derived clathrin-coated vesicles (Bucci et al., 1992) and mediates tethering with Early Endosome Antigen1 (EEA1), a Rab5 effector protein (Merithew et al., 2003). Then, the trafficking of vesicles from mature endosome to late endosome and lysosome is regulated by Rab7 (Hutagalung and Novick, 2011; Mercer et al., 2010; Stenmark, 2009).

However, molecular mechanisms of the early steps in intracellular trafficking of YHV entry into the shrimp cell are poorly defined. Recently, it has been demonstrated that YHV utilizes clathrin-mediated endocytosis to invade shrimp cells (Jatuyosporn et al., 2014, Posiri et al., 2015). In addition, silencing of *P. monodon* Rab7 (PmRab7), a late endosomal marker resulted in inhibition of YHV replication, suggesting that YHV could not move from the late endosome to the lysosome where its genome was uncoated and released into the cytoplasm

for replication (Ongvarrasopone et al., 2008). How YHV is trafficked from the plasma membrane toward late endosomal compartment has not been investigated. An increasing evidence for the requirement of Rab5 in the early entry step of several viruses including dengue virus, west nile virus and foot-and-mouth disease virus (Johns et al., 2009; Krishnan et al., 2007) could suggest a possible role of Rab5 for YHV entry into shrimp cells. Therefore, in this study, the molecular mechanism of Rab5 in YHV entry into the shrimp cells was investigated.

2. Methods

2.1. Primary hemocyte culture

Hemolymph was collected from *P. monodon* using sterile syringe and 18 gauge needle with anticoagulant AC-1 (27 mM Sodium citrate, 34.33 mM NaCl, 104.5 mM Glucose, 198.17 mM EDTA, pH 7.0) in a ratio 1:1. The mixture of hemolymph and anticoagulant was centrifuged at 550 x g for 10 min to separate the hemocyte pellet from the hemolymph. The hemocyte pellet was washed in 1 ml of L-15 culture medium washing solution (2× Leibovitz L-15 medium, 15% (v/v) fetal bovine serum, 200 IU/ml penicillin and 200 µg/ml streptomycin). Then the washing step was repeated three times. After that, the hemocytes were resuspended in 1 ml of L-15 culture medium working solution (2× Leibovitz L-15 medium, 15% (v/v) fetal bovine serum, 200 IU/ml penicillin, 200 µg/ml streptomycin, and 15% (v/v) shrimp meat extract). The hemocyte number was counted under a light microscope by using hemocytometer. The cells (10^5 cells per well) were seeded into a 24-well plate.

2.2. Yellow head virus (YHV) stock

Viral free shrimp was injected with YHV to propagate the virus. All use of 'shrimp' refers to *P. monodon*. Hemolymph was collected with AC-1 solution from YHV infected moribund shrimp. The hemolymph was centrifuged at 20,000 × g for 20 min at 4 °C to remove hemocyte debris. Then, free YHV particles were collected by ultracentrifugation (100,000 × g) for 1 h. Virus pellets were dissolved with 150 mM NaCl and stored at -80 °C until used. YHV titer was determined by using RT-PCR with YHV helicase gene.

2.3. Immunofluorescence staining of YHV and P. monodon Rab5 (PmRab5)

The primary hemocytes (10^5 cells) in 24-well plates with cover-slip were incubated at 4 °C. After 30 min, the cells were washed with ice-cold phosphate buffer saline (1 × PBS, pH 7.4) and then infected with YHV at a multiplicity of infection (MOI) of 10 for 30 min at 4 °C. The cells were then transferred to 28 °C for 10 min to allow the cells to recover (specified as time 0). Next, the cells were fixed in ice-cold 4% paraformaldehyde at different time points, 0 min, 10 min, 30 min, 1 h, 3 h, 6 h, and 12 h, followed by three washing steps with ice-cold 1 × PBS pH 7.4 for 5 min each. The fixed hemocytes were permeabilized with 0.1% Triton X-100 in 1×PBS,

pH 7.4, and then blocked with 10% fetal bovine serum. Then, the cells were incubated with rabbit anti-Rab5 primary antibody (ab94690, abcam, USA) at 1:400 dilution at room temperature, overnight. Then the cells were incubated with mouse anti-gp64, a YHV detecting antibody (kindly provided by Professor Paisarn Sithigorngul, Department of Biology, Faculty of Science, Srinakharinwirot University) at 1:200 dilution. After 2 h, the cells were washed 3 times with 0.05% Tween-20 in 1×PBS, pH 7.4, and then incubated with secondary antibody, goat anti-mouse Alexa Fluor® 488 and goat anti-rabbit Alexa Fluor® 594 (Invitrogen), (1:500 dilution) for 1 h in the dark, and washed three times with 0.05% Tween-20 in 1×PBS, pH 7.4. Subsequently, the nuclei of the hemocytes were stained with TO-PRO®-3 iodide at1:500 dilution (Invitrogen) in 1×PBS, pH 7.4, at room temperature for 1 h in the dark, and washed three times with 0.05% Tween-20 in 1 × PBS, pH 7.4. The cover slips were mounted with anti-fade permount (Invitrogen). Fluorescence signals were detected by using a confocal microscope (FluoView FV10i - Olympus).

2.4. Cloning of the full-length PmRab5 cDNA from P. monodon

Multiple sequence alignment of Rab5 proteins from several species (Table 2) was aligned and used to design degenerate primers, dRab5-F and dRab5-R (Table 1), to PCR amplify the partial sequence of PmRab5. The PCR condition was: a hot-start at 95°C for 5 min, then 30 cycles of 95 °C for 30 s, 46 °C for 30 s, and 72 °C for 45 s, followed by 72 °C for 7 min. Next, the expected PmRab5 band was cut and gel purified using Gel/PCR DNA fragments extraction kit (Geneaid). The fragment (346 bp) was cloned into pGEM-T easy vector (Promega) and sequenced (First Base Co, Ltd., Malaysia).

The 5' and 3' ends of PmRab5 were amplified by using rapid amplification of cDNA ends (RACE) approach. For 5'-RACE, the cDNA was first generated by using Superscript III® reverse transcriptase (Invitrogen) with a PmRab5-specific primer, PmRab5-R1 (Table 1). Then, the RNA template was removed by RNaseH (Promega) and the first-stranded cDNA was purified by ethanol precipitation, followed by Geneaid spin column (Geneaid). The purified cDNA was performed an polyA-tailing by terminal deoxynucleotidyl transferase (TdT) (Promega). Then, polyA-tailed cDNA was used as template to perform the first PCR with PmRab5-R1 and PRT primers. Next, the obtained PCR product was diluted at 1:100 and used as template for nested PCR with PmRab5-R2 and PM1 nested primer (Table 1). For 3' RACE, first-strand cDNA was generated by Impromp II™ reverse transcriptase (Promega) with PRT primer (Table 1). Then, cDNA was used as template for the first PCR with PmRab5-F1 (Table 1) and PRT primer. All of RACE products were purified, cloned and sequenced as described above.

The 3 partial sequences obtained from PCR using degenerate primers, 5' and 3' RACE products were *in silico* assembled to obtain the full-length PmRab5 cDNA. In order to verify that the assembled sequence is indeed corresponded to the full-length PmRab5 sequence, PCR was performed using primers targeting to the 5' and 3' ends, fullR5-F2 and fullR5-R (Table 1), and Vent® DNA polymerase (New England Biolabs). The PCR condition was as follow: denaturation at 95 °C for 5 min, 30 cycles of 95 °C for 30 s, 51 °C for 30 s, and 72 °C for 2 min 30 s, followed by 72 °C for 7 min. PCR products were purified, cloned and sequenced as described.

Table 1 Primer sequences of the experiments

Primers	Sequences (5' → 3')	Experiments
dRab5-F	AAGGGCCAGTTCCACGAGTACCA(G/A)GA	Amplify PmRab5 partial sequences
dRab5-R	AAGATGTCGTTCACGTTCATGGCGGT	
PmRab5-R1	GGTCTGGGCCTCTTCATATTCAACC	5' RACE of PmRab5
PRT	CCGGAATTCAAGCTTCTAGAGGATCCTTTTTTTTTT TTTTTT	Reverse transcription and RACE assay
PmRab5-R2	CCTTTACCCAGGTCTTAGCACGACC	5' RACE of PmRab5
PM1	CCGGAATTCAAGCTTCTAGAGGATCC	5' RACE of PmRab5
fullR5-F2	GGTTGTGTGGTTGATCCTG	Full-length of PmRab5 cDNA
fullR5-R	TTTTTTCTTAAAAATGTCTAACAC	
stPmRab5-F1-*Xba*I	GC*XbaI*TCTAGAGTCAACTATTGGAGCTGCA	Amplification of Sense-loop region of dsRNA-PmRab5
lpPmRab5-R1-*Kpn*I	GGG*KpnI*GTACCTATTGGACAGGCTGACATC	
stPmRab5-F2-*Eco*RI/*Xho*I	G*EcoRI*GAATTC*XhoI*CGAGGTCAACTATTGGAGCTGCA	Amplification of Antisense region of dsRNA-PmRab5
stPmRab5-R2-*Kpn*I	GGG*KpnI*GTACCCTTAGCAGAGGTCTCCATAA	
PmRab5-F1	GGAGCTGCATTTCTGACACAGACAG	3' RACE of PmRab5 and Detection of PmRab5 mRNA
PmRab5-R1	GGTCTGGGCCTCTTCATATTCAACC	Detection of PmRab5 mRNA
PmActin-F	GACTCGTACGTGGGCGACGAGG	Detection of PmActin mRNA
PmActin-R	AGCAGCGGTGGTCATCTCCTGCTC	
YHV(hel)-F	CAAGGACCACCTGGTACCGGTAAGAC	Detection of YHV mRNA
YHV(hel)-R	GCGGAAACGACTGACGGCTACATTCAC	

2.5. Sequence analysis of PmRab5 cDNA

Sequence analysis was performed with BLASTN (http://blast.ncbi.nlm.nih.gov). The conserved domain of the deduced amino acid sequences were predicted using NCBI database (Zhu et al., 2004). Molecular weight and isoelectric point (pI) of the protein were performed with Expert Protein Analysis System (www.expasy.org). Rab5 protein sequences from several

organisms were obtained from GenBank database. Multiple alignments were performed using VectorNTI program (Invitrogen). Molecular Evolutionary Genetics Analysis (MEGA) 4.1 program was used for phylogenetic analysis based on the neighbor-joining method (Kumar et al., 2008).

2.6. Construction of the recombinant plasmid for production of dsRNA-PmRab5

Recombinant plasmid containing stem-loop of dsRNA-PmRab5 was constructed in pGEM-3Zf+ (Promega) and pET-17b (Novagen) vectors. Sense-loop region of the dsRNA, size 494 bp, was amplified from the first-strand cDNA by stPmRab5-F1-*Xba*I and lpPmRab5-R1-*Kpn*I specific primers (Table 1). Antisense region, size 394 bp, was amplified by stPmRab5-F2-*EcoR*I/*Xho*I and stPmRab5-R2-*Kpn*I primers (Table 1). The PCR fragment of sense-loop was cloned into pGEM-3Zf+ followed by the antisense fragment in the sense and antisense orientation, respectively. Then, this stem-loop fragment of size about 888 bp was subcloned into *Xba*I and *Xho*I sites of pET-17b vector for construction of recombinant plasmid, named pET17b-PmRab5, which was used for *in vivo* bacterial expression of dsRNA-PmRab5. In addition, recombinant plasmid containing stem-loop of dsRNA-GFP (kindly provided by Asst. Prof. Witoon Tirasophon) was used to express dsRNA-GFP which was used as an unrelated dsRNA (Ongvarrasopone, et al., 2007).

2.7. Production of dsRNA-PmRab5 by in vivo bacterial expression

Recombinant plasmid pET17b-PmRab5 was transformed into a ribonuclease (RNase) III mutant HT115 *Escherichia coli* strain. This strain is modified to express T7 RNA polymerase from an isopropyl-β-D thiogalactopyranoside (IPTG) inducible promoter. Therefore, dsRNAs can be produced in the HT115 bacterial host after induction with 0.1 mM IPTG. Double stranded RNA was extracted and purified as previously described (Ongvarrasopone et al., 2007; Posiri et al., 2013). The quality of dsRNA was characterized by ribonuclease digestion assay using RNase A and RNase III. dsRNA concentration was estimated by agarose gel electrophoresis and compared to the intensity of 100 bp DNA marker.

2.8. Black tiger shrimp culture

Juvenile shrimp, sizes about 10 g, were obtained from commercial shrimp farms in Thailand. The shrimp were maintained in large boxes with oxygenated sea water at 20 ppt salinity for 1 day before experiment and fed with commercial diet every day. Half of the water was exchanged every 2 days.

2.9. Suppression of PmRab5 mRNA by dsRNA-PmRab5 in P. monodon

The knockdown effect of PmRab5 mRNA using dsRNA-PmRab5 was tested by injection of dsRNA into hemolymph. Shrimp were injected with 2.5 $\mu g.g^{-1}$ shrimp of dsRNA-PmRab5 dissolved in 150 mM NaCl. Then, hemolymph was collected at time 0, 3, 6, 12, 18 and 24 h post-dsRNA injection to extract total RNA. Suppression effect of the PmRab5 was

analyzed by RT-PCR to determine mRNA level. In addition, hemocytes of shrimp injected with 2.5 μg.g^{-1} shrimp of dsRNA-PmRab5, unrelated dsRNA-GFP and NaCl were collected to observe PmRab5 mRNA by using RT-PCR and protein level by western blot analysis and an immunofluorescence assay.

2.10. Effect of dsRNA-PmRab5 during YHV infection

To study the function of PmRab5 on YHV infection, shrimp was injected into hemocoel with dsRNA-PmRab5 or dsRNA-GFP at 2.5 μg.g^{-1} shrimp. After 24-h post-injection (hpi), YHV was injected. Then, gill was collected at 48 h post-YHV challenge to detect PmRab5 and YHV mRNA expressions. Hemocytes of each group were collected to investigate PmRab5 and YHV protein levels by an immunofluorescence assay. Injection of 150 mM NaCl alone or prior to YHV challenge was used as experimental controls.

2.11. Shrimp mortality assay

The mortality of shrimp injected with dsRNA-Rab5 with YHV challenge was observed every 12 h. Shrimp size about 1 g and 15 shrimps per group were tested. Four independent experiments were performed. Shrimp were injected with 150 mM NaCl, 2.5 μg.g^{-1} shrimp of dsRNA-PmRab5 or unrelated dsRNA-GFP. After 24-h post-injection, YHV was injected. Dead shrimp were recorded every 12 h.

2.12. RNA isolation and RT-PCR

Total RNA from gill tissues or hemolymph was isolated by Trizol® reagent (Molecular Research Center) following the manufacturer's procedure. The RNA concentration was measured by Nanodrop ND-1000 spectrophotometer (Nanodrop Technologies). RNA (2 μg) was used as template to generate the first-strand cDNA by Improm-II™ reverse transcriptase (Promega) using PRT primer (Table 1). PmRab5 was amplified by PCR using primers PmRab5-F1 and PmRab5-R1. PmActin mRNA expression, used for internal control, was amplified by PmActin-F and PmActin-R1 specific primers (Table 1). Multiplex PCR for PmRab5 and PmActin was amplified according to this condition: 95°C for 5 min, 25 cycles of 95°C for 30 s, 60°C for 30 s, and 72°C for 45 s, followed by 72°C for 7 min. YHV expression was amplified by using YHV(hel)-F and YHV(hel)-R primers (Table 1). PCR products were electrophoresed on 1.5% agarose gel. The intensity of each band after subtracting the background was quantified by using ImageJ (version 1.46r) program. The relative expression level of PmRab5 was normalized with PmActin level and expressed as an arbitrary unit.

2.13. Western blot analysis

Hemocyte proteins were extracted by using Buffer T (8 M Urea, 2 M Thiourea, 0.4% Triton X-100, 60 mM DTT, 1 mM PMSF, 1 x Protease inhibitor cocktail (Sigma)). The protein lysate of each shrimp was electrophoresed in 10% SDS-polyacrylamide gel (SDS-

PAGE). The proteins in SDS-PAGE were transferred from gel onto a PVDF membrane (Bio-Rad) by electrophoresis with 1 X transfer buffer [0.025 M Tris-HCl pH 8.3, 0.192 M glycine, and 20% (v/v) methanol]. The membrane was blocked in 5% skimmed milk in 1 X PBS containing 0.05% Tween-20 (PBST). PmRab5 and β-tubulin were detected by incubating the membrane with rabbit anti-Rab5 (ab94690, abcam, USA) and anti-β-tubulin (kindly provided by Dr. Phattara-Orn Havanapan) antibody, respectively. Then, the membrane was washed with PBST for 10 min at least 3 times. After that, it was incubated with horseradish peroxidase conjugated to goat anti-rabbit polyclonal antibodies (Sigma), followed by washing as described above. The signal was detected by Luminata™ Forte Western HRP Substrate (Millipore Corporation). PmRab5 and β-tubulin have sizes about 23 and 50 kDa, respectively.

2.14. Statistical analysis

The relative mRNA levels of PmRab5 normalized with PmActin were presented as mean ± SEM. Cumulative percent mortality was plotted as mean ± SEM. Moreover, significant differences of each experimental group were tested by analysis of variance (ANOVA). A probability *(P)* value less than 0.05 was used to define significant difference.

3. Results

3.1. Full-length cDNA and amino acid sequences of PmRab5

The conserved domains from the alignment of Rab5 proteins from several organisms were used to design primers to amplify the partial sequence of Rab5 from gill tissue of *P. monodon* by PCR. A partial sequence of 346 nucleotides of the putative PmRab5 showed more than 90% sequence identity to Rab5 protein of other species (data not shown). The 5’ and 3’ ends of PmRab5 were obtained by using RACE approach. The full-length cDNA of PmRab5 was confirmed by using specific primers targeting the 5' and 3' ends. It comprised of 1,293 bp with a 113 bp 5' untranslated region (UTR), a 633 bp of open reading frame (ORF) (nucleotide 114-746), a 547 bp 3' UTR with polyadenylation (poly-A) signal. The Kozak’s consensus sequence (*AXXATGG*) was present at nucleotide 111-117 (*ATTATGG*). Moreover, a typical poly-A signal (*AATATTA*) was found at nucleotide 1252-1258 (Supplementary Fig. 1). The sequence of PmRab5 cDNA was submitted into the GenBank database under the accession number KT896540.

The deduced amino acid sequence of PmRab5 is 210 amino acids with an estimated molecular weight of 22.97 kDa and a pI of 8.29. Blastp search of NCBI database showed high sequence homology of PmRab5 protein with other known Rab5 proteins in the database (Table 2). Moreover, the alignment of PmRab5 to Rab5 proteins from several organisms such as mosquito (*Aedes aegypti*), dog (*Canis lupus*), human (*Homo sapiens*),

mouse (*Mus musculus*), frog (*Xenopus tropicalis*), sea anemone (*Aiptasia pulchella*) and butterfly (*Danaus plexippus*) demonstrated the conserved motifs of Rab protein family, including five Rab family motifs (RabF1-5), four Rab subfamily motifs (RabSF1-4) which defined Rab5 protein, five signature domains for GTP-binding sites (G1-G5) and a putative prenylation signal (*XCCX*) at the C-terminal of the invertebrates sequence (Stenmark and Olkkonen, 2001; Zhu et al., 2004) (Fig. 1A). Phylogenetic tree analysis separated Rab5 protein into 3 clusters, including vertebrate, invertebrate and plant. The tree revealed that PmRab5 is in the invertebrates group (Fig. 1B). The expression of PmRab5 in *P. monodon* was examined by multiplex RT-PCR. The results demonstrated that PmRab5 was expressed at similar levels in several tissues including brain, thoracic ganglia, nerve cord, gill, lymphoid organ, hepatopancreas, ovary and hemocytes (Supplementary Fig. 2).

Table 2. Percent amino acid sequence identity of PmRab5 compared with each organism. Accession number of organisms used for Rab5 protein domain and phylogenetic analysis are listed.

Organisms	Accession number	Rab5 isoforms	Percent identity of PmRab5 compared with each organism
Aedes aegypti	XP_001658691	AaRab5	77
Aiptasia pulchella	AAV34202	ApRab5	85
Apis mellifera	XP_003251474	AmRab5B	76
Ascaris suum	ADY48161	AsRab5B	79
Bombyx mori	NP_001037614	BmRab5	78
Canis lupus	NP_001003317	ClRab5A	75
	XP_531627	ClRab5B	81
	CAA81626	ClRab5C	81
Danaus plexippus	EHJ77299	DpRab5	81
Danio rerio	NP_957264	DrRab5A	75
	AAI65047	DrRab5C	77
Homo sapiens	CAG38731	HsRab5A	75
	CAG46491	HsRab5B	81
	CAG46699	HsRab5C	81
Litopenaeus vannamei	AFK08607	LvRab5	100
Loa loa	XP_003136717	LlRab5	77
Medicago truncatula	AES68021	MtRab5C	48
Mus musculus	BAF02855	MmRab5A	75
	CAA59016	MmRab5B	81
	BAF02857	MmRab5C	80
Oryza sativa	AAK38149	OsRab5	60
Penaeus monodon	**KT896540**	**PmRab5**	-
Physcomitrella patens	BAG09234	PpRab5	48
Suberites domuncula	ABD65432	SdRab5	76
Tribolium castaneum	EFA04701	TcRab5	84
Xenopus tropicalis	NP_001008068	XtRab5A	76
	AAH75323	XtRab5B	80
	CAJ81259	XtRab5C	76

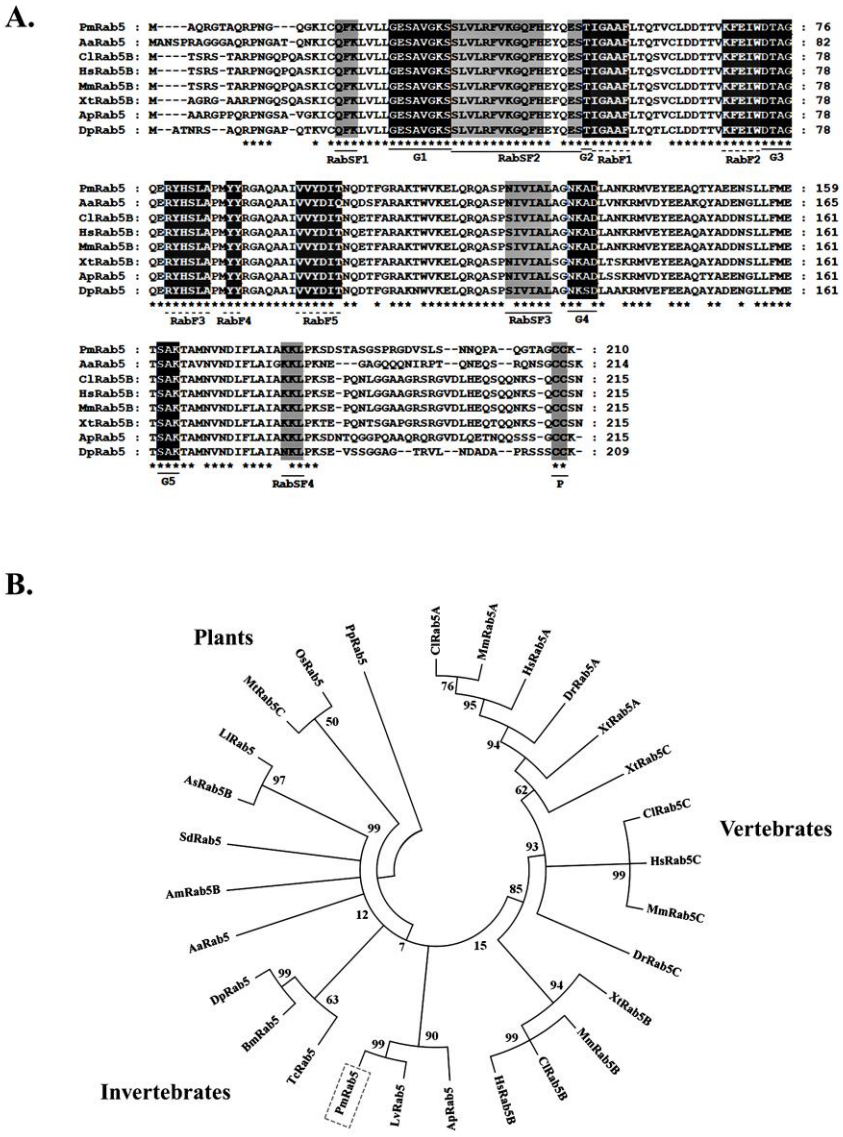

Fig. 1 PmRab5 domains and phylogenetic tree analysis. (A) Amino acid sequence alignment of Rab5 proteins from selected organisms demonstrated a signature of five Rab family motifs (RabF1-RabF5) (light gray shade), four Rab subfamily domains (RabSF1-RabSF4) (heavy gray), five G-boxes (G1-G5) (black) and a prenylation site (P). Star (*) represents the consensus amino acid sequence. (B) Phylogenetics tree analysis of Rab5 based on amino acid sequences. Molecular Evolutionary Genetics Analysis (MEGA) 4.1 program was used for phylogenetic tree construction from several species: *Aedes aegypti* (Aa), *Aiptasia pulchella* (Ap), *Apis mellifera* (Am), *Ascaris suum* (As), *Bombyx mori* (Bm), *Canis lupus* (Cl), *Danaus plexippus* (Dp), *Danio rerio* (Dr), *Homo sapiens* (Hs), *Litopenaeus vannamei* (Lv), *Loa loa* (Ll), *Medicago truncatula* (Mt), *Mus musculus* (Mm), *Oryza sativa* (Os), *Penaeus monodon* (Pm), *Physcomitrella patens* (Pp), *Suberites domuncula* (Sd), *Tribolium castaneum* (Tc), and *Xenopus tropicalis* (Xt).

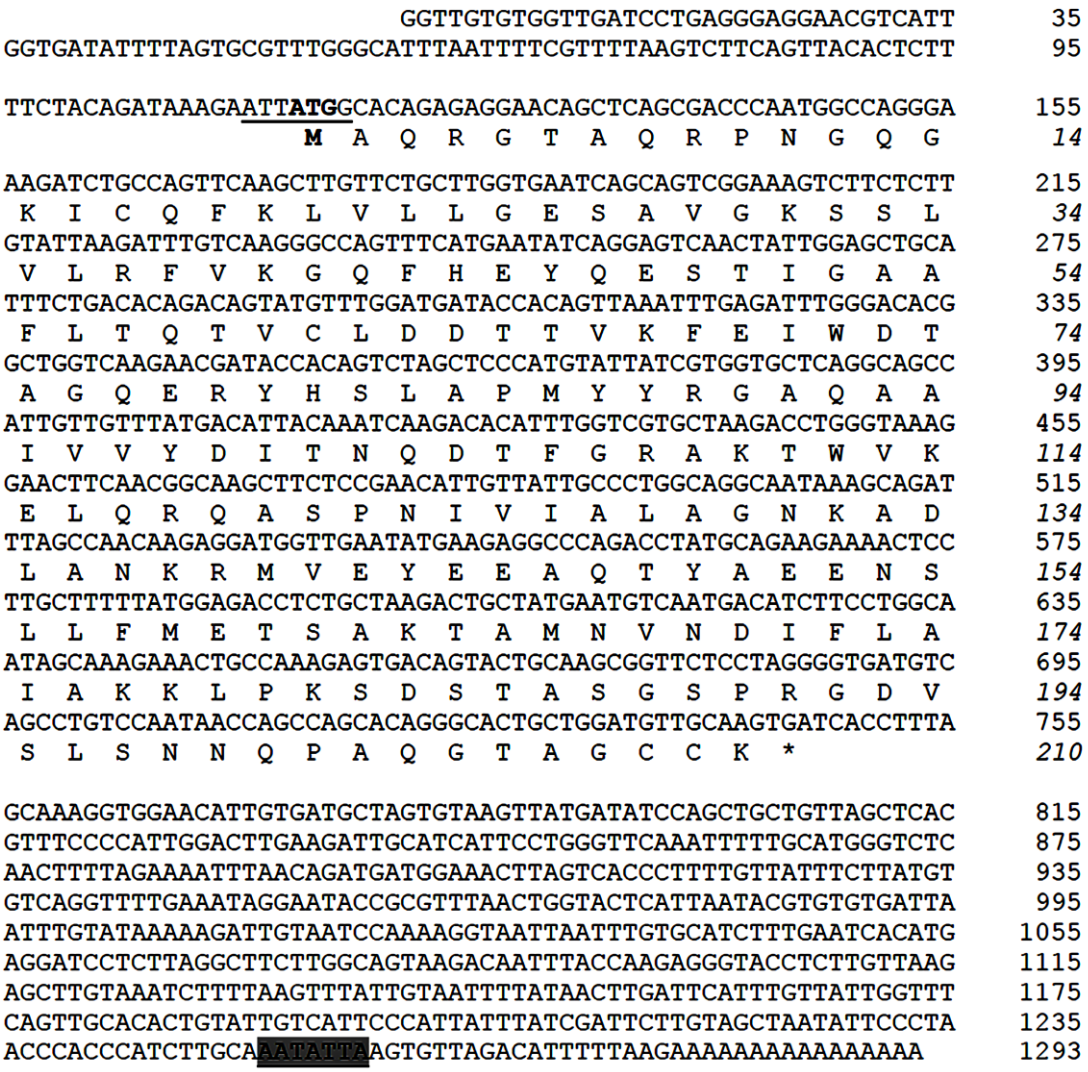

Supplementary Fig. 1 Full-length cDNA and the deduced amino acid sequences of *P. monodon* Rab5 (PmRab5). The start codon (ATG) showed in bold letter and is located within Kozak's consensus sequence, underlined. Polyadenylation (poly-A) signal was predicted in gray shaded sequences. The deduced amino acid is shown as a single letter under the respective codon. The nucleotide sequences are deposited in GenBank NCBI database under accession number KT896540.

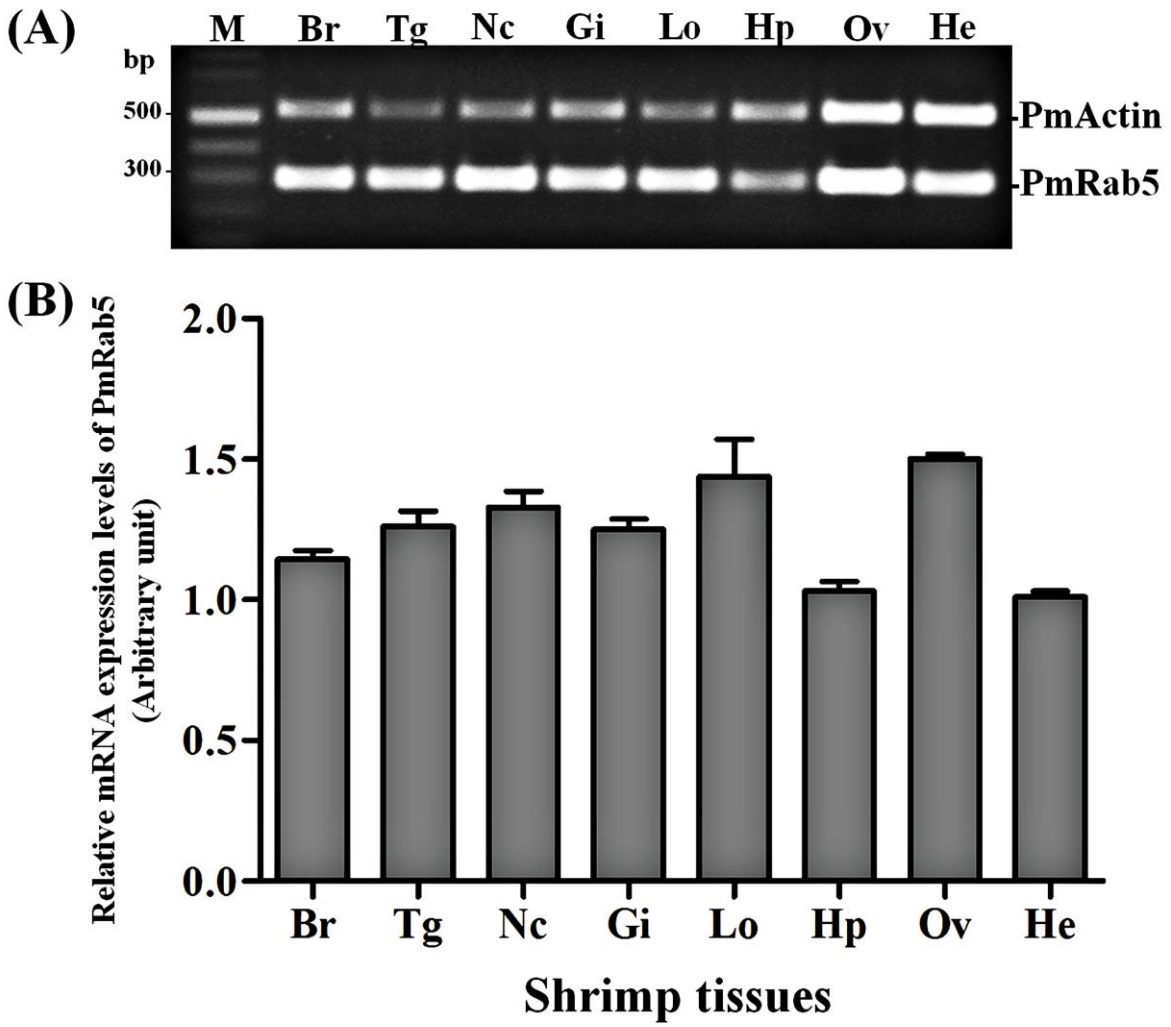

Supplementary Fig. 2 Tissue distribution of PmRab5 expression. (A) A representative gel demonstrating RT-PCR products of PmRab5 and PmActin mRNA expression in tissues: brain, Br; thoracic ganglia, Th;, nerve cord, Nc;, gill, Gi;, lymphoid organ, Lo; hepatopancreas, Hp; ovary, Ov; hemocytes, He. M is 2-log DNA marker. (B) Relative mRNA expression levels (mean ± SEM, n=3) of PmRab5 normalized with PmActin in an arbitrary unit.

3.2. YHV and PmRab5 are colocalized in the hemocytes during YHV infection.

Rab5 protein regulates endocytic vesicle membrane that transports the cargo from plasma membrane to the early endosome (Bucci et al., 1992). This process is an early step for many viruses to enter into the cells (Cheng et al., 2012; Clemente and de la Torre, 2009; Johns et al., 2009; Macovei et al., 2013). To elucidate the function of PmRab5 that is possibly involved in the molecular trafficking process of YHV entry into hemocytes, colocalization of YHV and PmRab5 was investigated. Primary hemocyte culture was infected with YHV. Localization

of YHV and PmRab5 were investigated at 0 min, 10 min, 30 min, 1 h, 3 h, 6 h and 12 h post-infection (pi.). The signal of YHV was detected around the cell surface and no colocalization of YHV particles and PmRab5 was observed at 0 min. From 10 to 30 min, strong colocalized signals of YHV and PmRab5 were detected. The signals were strongest at time 1 to 3 hpi. Interestingly, the colocalization signal was faint at 6 hpi and completely absent at 12 hpi (Fig. 2).

3.3. PmRab5 was suppressed by specific dsRNA in shrimp.

In order to study the function of PmRab5 in shrimp, RNA interference (RNAi) was used as a tool to investigate its role. First, dsRNA targeting PmRab5 (dsRNA-PmRab5) was constructed and tested for its suppression of endogenous PmRab5 transcript. Shrimps received dsRNA-PmRab5 injection showed significant reduction of PmRab5 transcript at more than 85% from 3 hpi to 24 hpi (Fig. 3A and 3B). Moreover, specificity of the knockdown effect by dsRNA-PmRab5 was also tested. Shrimps received dsRNA-PmRab5 demonstrated reduction of PmRab5 at both the mRNA and protein levels. In contrast, the knockdown effect of PmRab5 was not seen in shrimp injected with unrelated dsRNA-GFP or NaCl-injected groups (Fig. 3C and 3D). In addition, immunofluorescence staining of the hemocytes obtained from shrimps injected with dsRNA-PmRab5 demonstrated faint PmRab5 signal when compared to that of the NaCl and dsRNA-GFP groups (Fig. 3E).

3.4. YHV requires PmRab5 for entry into shrimp cells.

To study the suppression effect of PmRab5 during YHV challenge, shrimps were injected with dsRNA-PmRab5 at 2.5 $\mu g.g^{-1}$ shrimp 24 h prior to YHV challenge. Injection of dsRNA-GFP was used as an unrelated control group. Then, gills were collected for total RNA extraction after 48 h post-YHV challenge. Injection of dsRNA-PmRab5 demonstrated approximately 97% reduction of PmRab5 transcript when compared to the NaCl and dsRNA-GFP groups, resulting in hardly observable YHV mRNA level. On the other hand, injection of NaCl or dsRNA-GFP prior to YHV challenge showed high levels of YHV (Fig. 4A). Moreover, immunofluorescence staining of hemocytes collected 48 h post-YHV challenge in dsRNA-PmRab5 injected group showed faint signal of PmRab5 protein when compared to the hemocytes from NaCl or dsRNA-GFP group. Interestingly, the depleted PmRab5 cells hardly showed any YHV particles inside the cells. Colocalization between YHV particles with PmRab5 could be barely detected in the PmRab5-knockdown cells. However, a clear colocalization signal of PmRab5 and YHV could be clearly observed in the hemocytes from NaCl and dsRNA-GFP injected group (Fig. 4B).

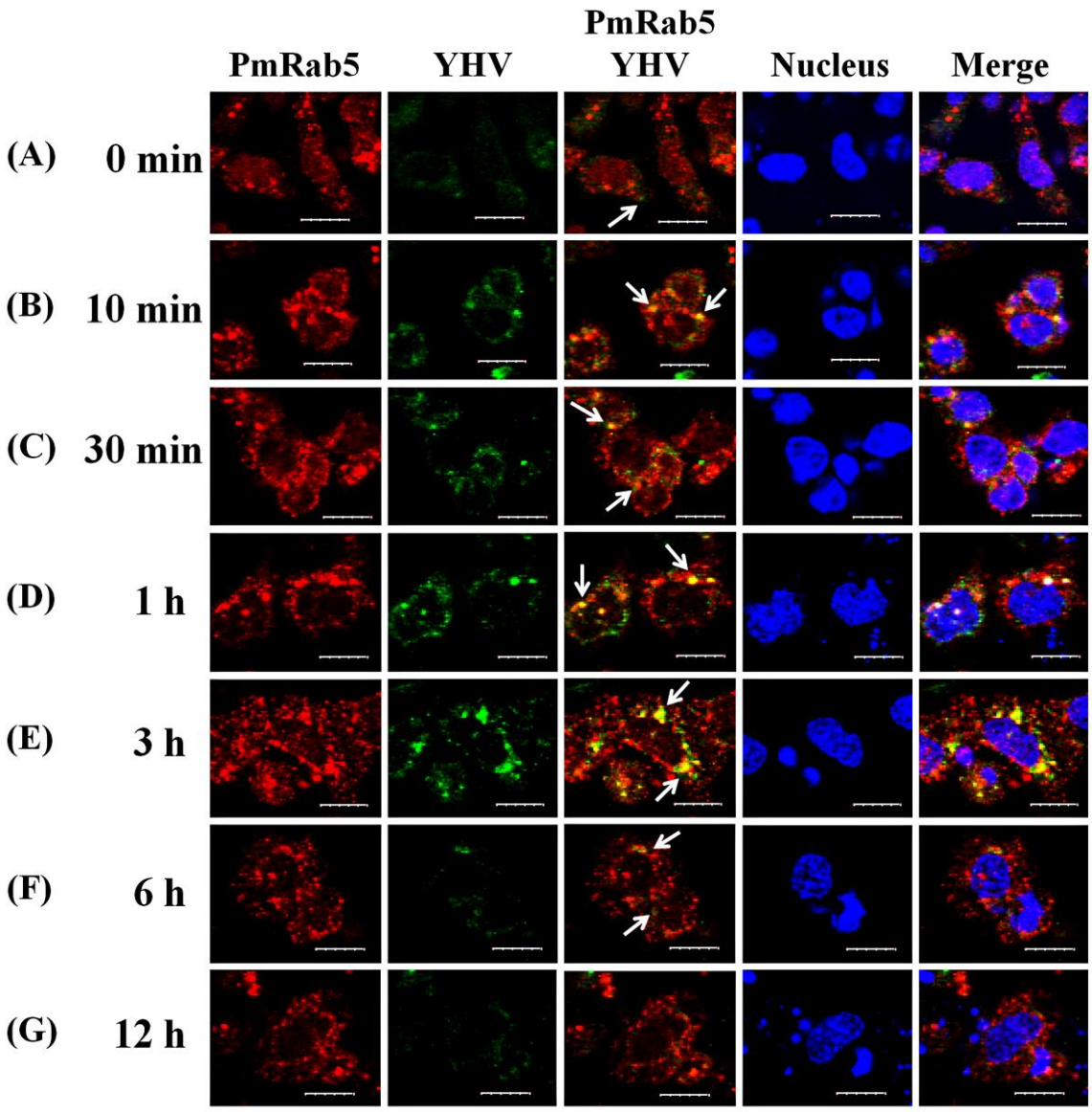

Fig. 2 Visualization of the interaction between PmRab5 protein and YHV particles. The primary hemocytes were first incubated with YHV and then the infected cells were fixed at various time points. (A) At time point 0 min post-infection, no colocalization between YHV and PmRab5 was observed. YHV particles could be detected around the cell (arrow). (B and C) YHV particles demonstrated colocalizing with PmRab5 (arrow) at 10 and 30 min post-infection. (D and E) Increased intensity of the colocalization signal (arrow) was observed at 1 to 3 h post-infection. (F) The signal of YHV particles at time 6 hpi showed inside the cells without colocalization with PmRab5 (arrow). (G) At 12 hpi, YHV signal was hardly detected. PmRab5 signal was detected by anti-Rab5 antibody and showed in red. YHV particle was detected by anti-gp64 antibody and showed in green. Colocalization of PmRab5 and YHV was shown as yellow. Cell nuclei were stained blue with TOPRO®-3 iodide. Scale bar is 10 μm.

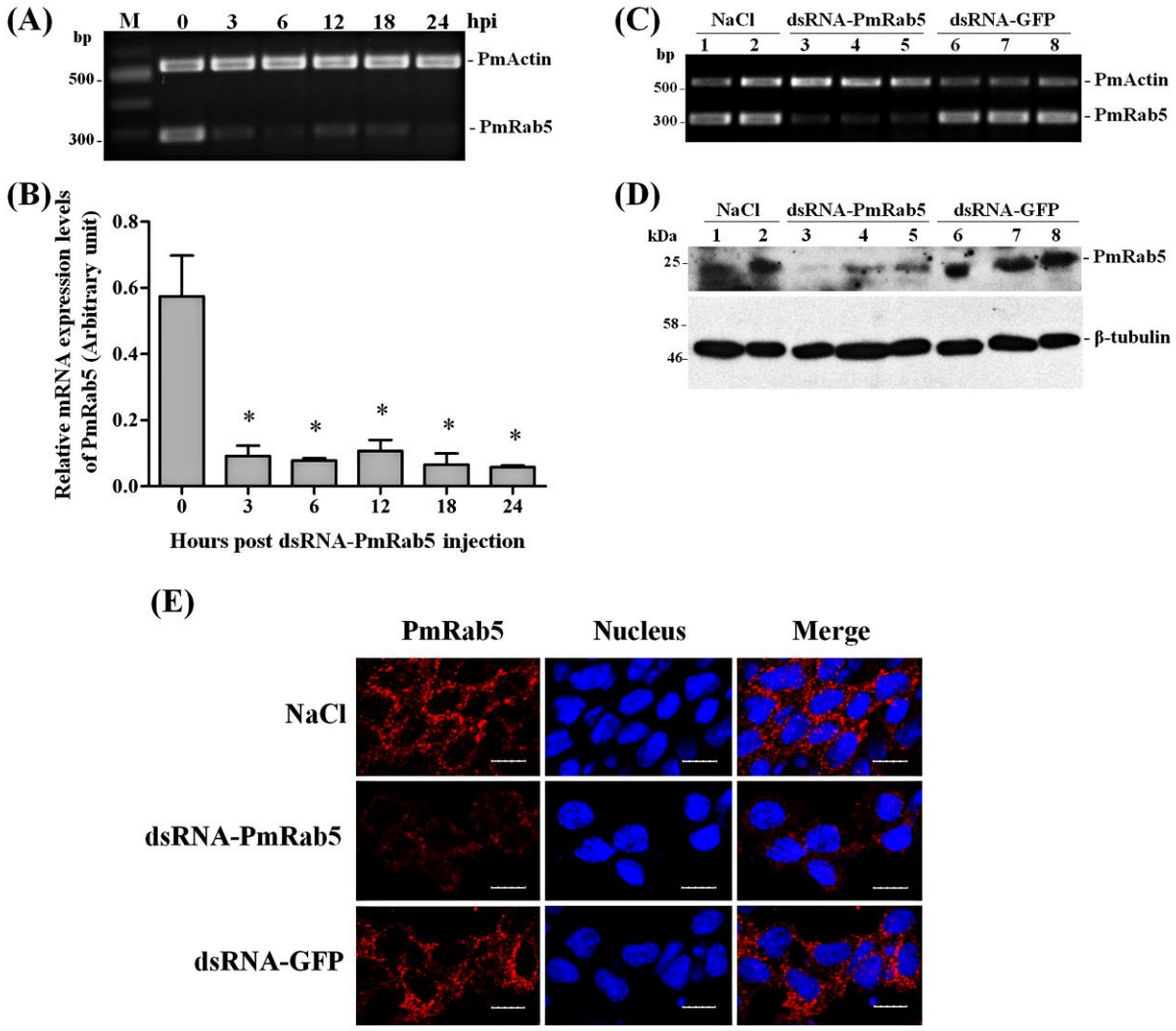

Fig. 3 Knockdown effect of PmRab5 by dsRNA-PmRab5. (A) A representative gel of RT-PCR products of PmRab5 and PmActin expression of shrimp injected with dsRNA-PmRab5. The hemolymph were collected at 0, 3, 6, 12, 18 and 24 h post-dsRNA injection. M is 1 kb+ DNA marker. (B) The relative mRNA expression levels (mean ± SEM) of PmRab5 normalized with PmActin and expressed as arbitrary unit (n=3 for each time course of post dsRNA injection). (*) represents statistically significant difference between before (time 0) and after dsRNA-PmRab5 injection at various time courses ($p < 0.05$). The mRNA level of PmRab5 and PmActin (C); and, protein level of PmRab5 and β-tubulin (D) of shrimp injected with NaCl (lanes 1-2), dsRNA-PmRab5 (lanes 3-5) and dsRNA-GFP (lanes 6-8) at 24-h post-dsRNAs injection. (E) Confocal immunofluorescence study of the hemocytes collected at 24-h post-dsRNAs injection compared to the NaCl and unrelated dsRNA-GFP control groups. The localization of PmRab5 was represented in red. Cell nuclei were stained blue with TOPRO®-3 iodide. Scale bar is 10 μm.

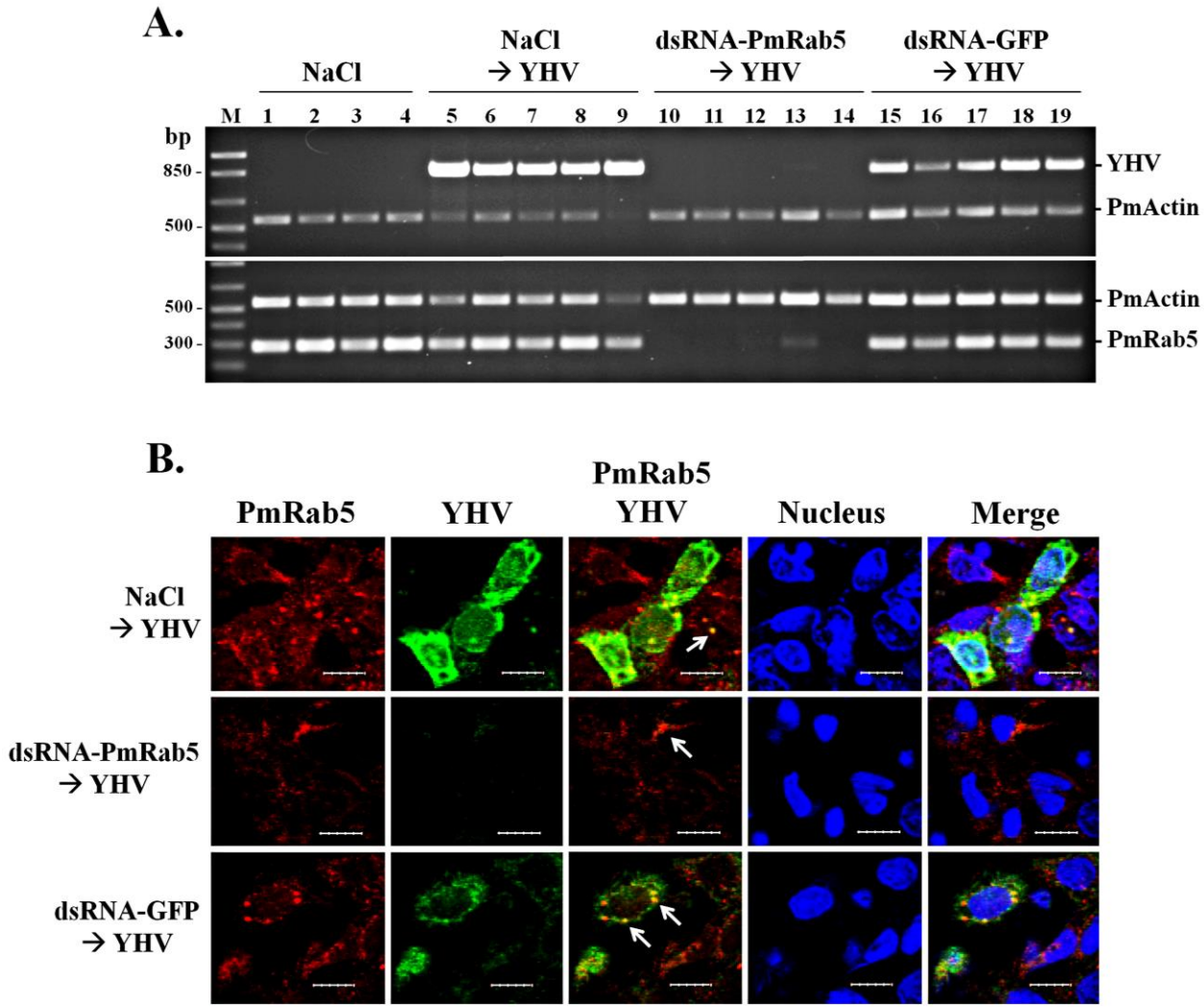

Fig. 4 Depletion of PmRab5 during YHV infection. (A) A representative gel of RT-PCR products of YHV (top panel), PmRab5 (bottom panel) and PmActin from gill tissues of shrimp injected with NaCl only (lanes 1-4) and challenged with YHV (lanes 5-9) and shrimp injected with dsRNA-PmRab5 (lanes 10-14) or dsRNA-GFP (lanes 15-19) prior to YHV challenge. M is 1 kb+ DNA marker. (B) Confocal immunofluorescence study demonstrated that knockdown of PmRab5 by dsRNA-PmRab5 disrupted YHV trafficking during the early-stage of YHV infection. The hemocytes were collected at 48 h post-YHV injection from shrimp injected with NaCl, 2.5 $\mu g.g^{-1}$ shrimp of dsRNA-PmRab5 or 2.5 $\mu g.g^{-1}$ shrimp of dsRNA-GFP prior to YHV challenge. The PmRab5 signal is represented in red. YHV is represented in green. The colocalization between YHV particles and PmRab5 are shown by arrows. Cell nuclei were stained blue with TOPRO®-3 iodide. Scale bar is 10 μm.

3.5. Silencing of PmRab5 levels delayed YHV replication and shrimp mortality in infected shrimp.

To further investigate the suppression effect of PmRab5 in YHV infected shrimp, shrimp mortality assay was performed. Shrimp injected with dsRNA-PmRab5 followed by YHV challenge exhibited 97.5% cumulative mortality at 132 hpi. Rate of shrimp death in this group still unchanged after 240 hpi. On the other hand, shrimp challenged with YHV alone or injected with unrelated dsRNA-GFP followed by YHV challenge that used as the control groups demonstrated 100 % mortality at 168 and 108 hpi, respectively. A significant decrease of cumulative percent mortality in YHV infected shrimp could be observed at 72-120 hpi in the PmRab5 knockdown group when compared to the control groups (Fig. 5). To check YHV levels, shrimp died at various time points were sampled. YHV mRNA levels could not be detected during 60-108 hpi in dead shrimp that the PmRab5 expression was suppressed. However, YHV mRNA levels could be observed after 120 hpi (Fig. 5B (b)). In contrast, high levels of YHV expression can be detected in all dead shrimps from the control groups (Fig. 5B (a and c)).

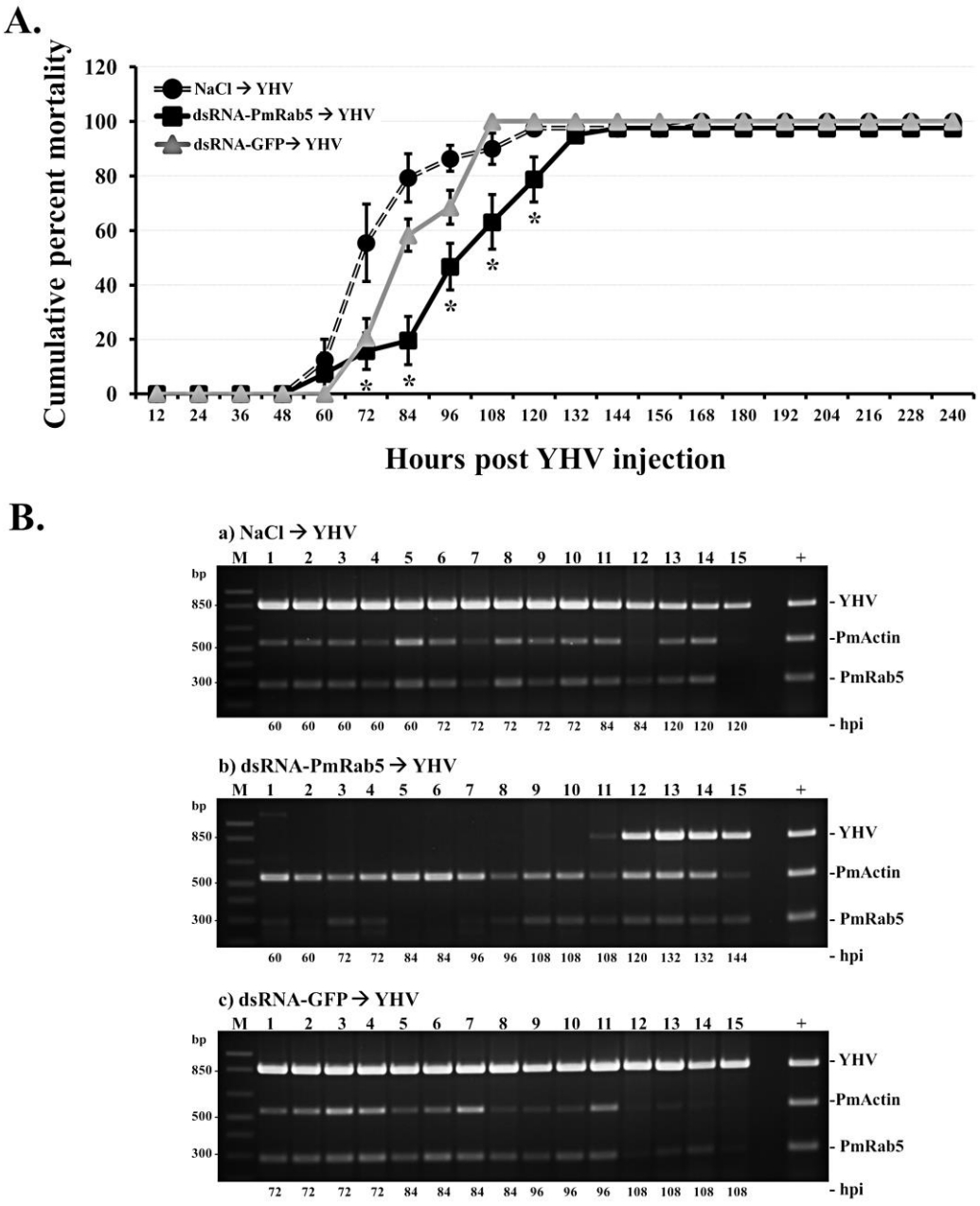

Fig. 5 Cumulative mortality assay in the PmRab5 knockdown shrimp upon YHV infection. (A) The cumulative percent mortality of shrimp injected with NaCl, 2.5 μg.g^{-1} shrimp of dsRNA-PmRab5, or 2.5 μg.g^{-1} shrimp of dsRNA-GFP 24 h before YHV challenge. Dead shrimp were recorded every 12 h post-YHV injection. (*) represents statistically significant difference between NaCl → YHV and dsRNA-PmRab5 → YHV injection ($p< 0.05$). (B) A representative gel of RT-PCR products for YHV and PmRab5 mRNA levels of dead shrimp. PmActin was used as internal control. (a) NaCl →YHV group, (b) dsRNA-PmRab5 →YHV group and (c) dsRNA-GFP →YHV group. The number on the bottom of each lane demonstrated the time (hours of post YHV challenge, hpi) of dead shrimp. M is 1 kb+ DNA marker.

4. Discussion

Yellow head virus is a serious causative agent that led to high mortality rate in *P. monodon*. Understanding of the virus trafficking pathway especially the mechanism of YHV infection is still poorly understood. Knowledge of the virus life cycles needs to be examined to shed light on providing useful information and to develop approaches for prevention and cure of shrimp from YHV infection. The endocytosis pathway of YHV has been characterized. Specifically, YHV utilized clathrin-mediated endocytosis which required clathrin coated vesicle protein including *P. monodon* clathrin heavy chain (PmCHC) and clathrin coat assembly protein 17 (AP17) to invade shrimp cells (Jatuyosporn et al., 2014; Posiri et al., 2015). Moreover, Rab5, a small GTPase protein formed complex with guanine-nucleotide dissociation inhibitor (GDI) and then associated into clathrin-coated vesicle membrane. After the association, GDI is released and Rab5 is converted into GTP-bound form to regulate downstream processing (Horiuchi et al., 1995; McLauchlan et al., 1997). Rab5 protein regulates the transportation of the vesicle from plasma membrane to early endosome of the endocytic pathway (Bucci et al., 1992). Therefore, YHV possibly utilizes the Rab5 protein to invade the host cells. In addition, previous study in *P. monodon* has identified a small GTPase Rab7 protein as a WSSV-VP28 binding protein in shrimp (Sritunyalucksana et al., 2006). The protein plays a crucial role in regulation of vesicle formation and membrane trafficking from late endosome to lysosome which is a sequential process from early endosome (Hutagalung and Novick, 2011; Stenmark, 2009). Interestingly, the *P. monodon* Rab7 (PmRab7) was involved in YHV replication in shrimp (Ongvarrasopone et al., 2008). However, this is the first report demonstrating that Rab5 protein is involved in YHV infection in *P. monodon*.

In this study, PmRab5 demonstrated conserved regions of Rab family and Rab5 subfamily which were similar to other organisms including *Aiptasia pulchella* (Chen et al., 2004) and many other vertebrates (Fig. 2). In shrimp, its amino acid sequence identity is highly conserved to human Rab5B (81.1%). Differences in the three isoforms of Rab5 proteins (Rab5A, 5B, and 5C) have no effect in the regulation of trafficking pathway from plasma membrane to early endosome but they are differentially recognized by different specific kinases (Bucci et al., 1995; Chiariello et al., 1999). In addition, colocalization between YHV and PmRab5 was observed in the hemocytes from 10 min to 3 h and rarely observed from 6 to 12 hpi. These results suggested that YHV and PmRab5 were transported together until 3 hpi. Then, YHV may be uncoated and released into the cytoplasm for replication process. Previously, semliki forest virus (SFV) and dengue virus (DENV) demonstrated colocalization with early endosome antigen 1 (EEA1), an effector protein of Rab5, at early time of infection and then later associated with Rab7. After that the viruses which were in hybrid organelles

would separate from Rab5 and colocalize with only Rab7 (van der Schaar et al., 2008; Vonderheit and Helenius, 2005). The colocalization of YHV and Rab7 has not been reported but this event may be similar to SFV and DENV.

The function of PmRab5 on YHV replication was also investigated by using RNA interference technique. Levels of PmRab5 mRNA were suppressed at more than 85% by specific dsRNA after 3 hpi and showed partial recovery after 3 dpi (data not shown). Depletion of Rab5 protein causes accumulation of small vesicles around the cytoplasm due to the vesicles could not be fused with early endosome (Bucci et al., 1992). The fusion of the vesicles from plasma membrane with early endosome occurred from specific interaction of Rab5 and EEA1 protein. Rab5 protein could bind to both $C_2H_2Zn^{2+}$ finger and FYVE domain of EEA1 protein (Lawe et al., 2000; Merithew et al., 2003). Inhibition of the membrane fusion might block the transportation of many essential cargo proteins and might lead to cell death. Moreover, Rab5 protein is involved in the internalization of integrin which is critical for caspase-8 functions to regulate cell motility, metastasis and survival (Torres et al., 2010). Therefore, silencing of PmRab5 may cause a loss of cell equilibrium and induces death in shrimps. Furthermore, depletion of PmRab5 by using dsRNA could silence YHV mRNA levels and suppressed YHV infection in shrimp cells. These results suggested that YHV required PmRab5 for transportation into the cell similar to other envelope positive-sense single-stranded RNA viruses such as dengue virus (DENV), west nile virus (WNV) or hepatitis C virus (HCV). Knockdown of Rab5 by siRNA showed the reduction of both DENV and WNV (Krishnan et al., 2007) while a dominant negative mutant of Rab5 could be used to decrease RNA progeny of HCV (Stone et al., 2007). Moreover, Rab5 protein is required for many viruses such as borna disease virus (BDV), bovine ephemeral fever virus (BEFV), hepatitis B virus, and foot and mouth disease virus (FMDV) to transport within the host cell (Cheng et al., 2012; Clemente and de la Torre, 2009; Johns et al., 2009; Macovei et al., 2013). Taken together, the model of YHV entry into shrimp cell is proposed (Fig. 6). First, YHV glycoprotein 116 binds with PmYRP65, a shrimp cell receptor. Then, it utilizes clathrin dependent endocytosis to enter into the cells. The virus requires PmRab5 and PmRab7 to regulate the transportation from plasma membrane to early endosome and from early endosome to late endosome, respectively (Assavalapsakul et al., 2006; Jatuyosporn et al., 2014; Ongvarrasopone et al., 2008; Posiri et al., 2015). When the pH was lowered, YHV genome may be released into the cytoplasm for replication process which is similar to other enveloped RNA viruses, such as SFV and sindbis virus (Glomb-Reinmund and Kielian, 1998; Helenius et al., 1980). In conclusion, YHV requires PmRab5 transport within the shrimp cell.

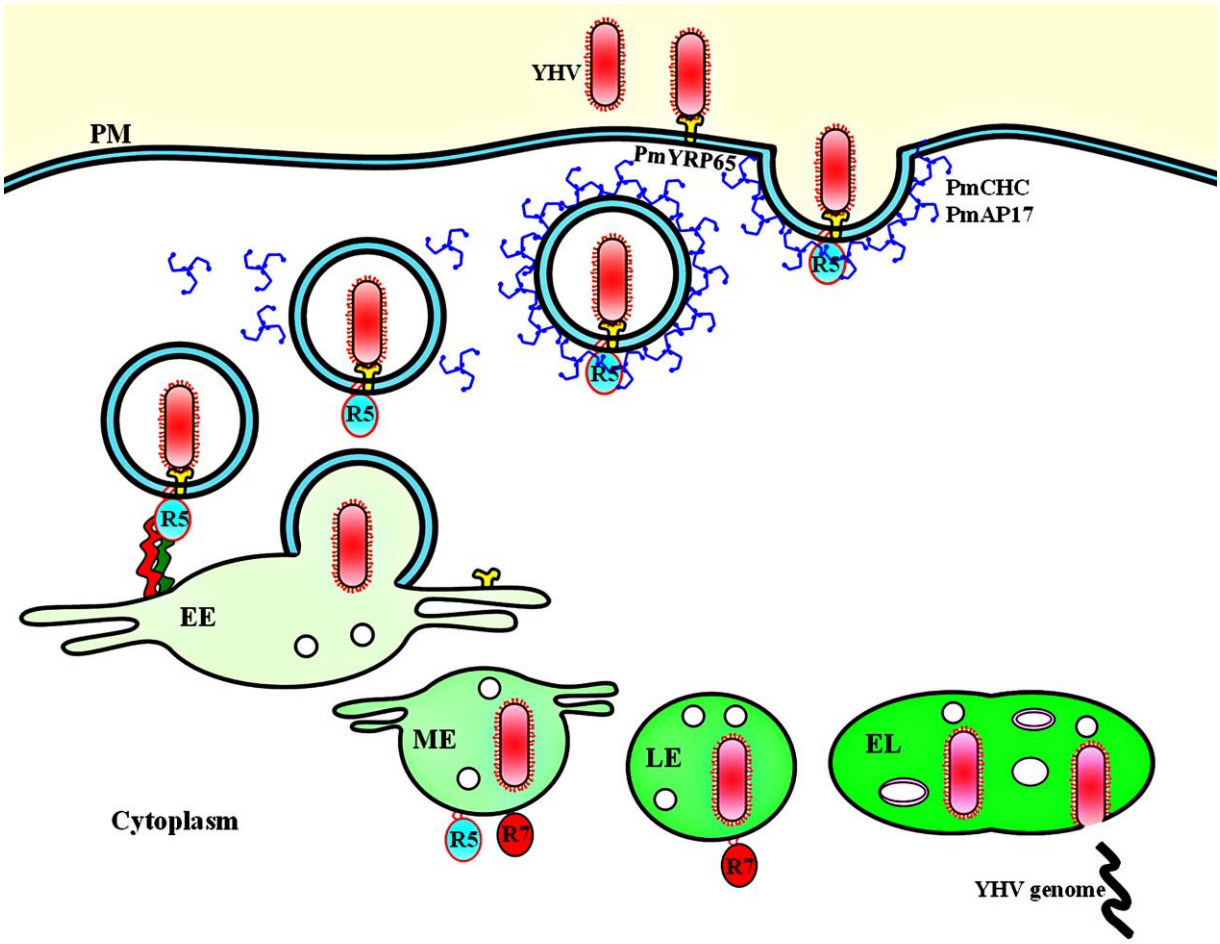

Fig. 6 Schematic model of YHV trafficking into shrimp cell. YHV binds with its receptor (PmYRP65) and internalizes into the cells via clathrin-mediated endocytosis which required PmCHC and PmAP17 proteins. Vesicle containing the virus is transported from plasma membrane (PM) to early endosome (EE) and then moved toward maturing endosome (ME), late endosome (LE) and endolysosome (EL). These processes, PM to EE and to ME are regulated by PmRab5 (R5) whereas ME to LE and to EL are regulated by PmRab7 (R7) protein. YHV genome may be released by acidic condition in endolysosome into the cytoplasm where the replication process begins.

5. References

Assavalapsakul, W., Smith, D.R., Panyim, S., 2006. Identification and characterization of a *Penaeus monodon* lymphoid cell-expressed receptor for the yellow head virus. J. Virol. 80 (1), 262-269.

Bucci, C., Lütcke, A., Steele-Mortimer, O., Olkkonen, V. M., Dupree, P., Chiariello, M., Bruni, C. B., Simons, K., Zerial, M., 1995. Co-operative regulation of endocytosis by three Rab5 isoforms. FEBS Lett. 366, 65-71.

Bucci, C., Parton, R. G., Mather, I. H., Stunnenberg, H., Simons, K., Hoflack, B., Zerial, M., 1992. The small GTPase rab5 functions as a regulatory factor in the early endocytic pathway. Cell 70, 715-728.

Chen, M. C., Cheng, Y. M., Hong, M. C., Fang, L. S., 2004. Molecular cloning of Rab5 (ApRab5) in *Aiptasia pulchella* and its retention in phagosomes harboring live zooxanthellae. Biochem. Biophys. Res. Commun. 324, 1024–1033.

Cheng, C. Y., Shih, W. L., Huang, W. R., Chi, P. I., Wu, M. H., Liu, H. J., 2012. Bovine ephemeral fever virus uses a clathrin-mediated and dynamin 2-dependent endocytosis pathway that requires Rab5 and Rab7 as well as microtubules. J. Virol. 86, 13653–13661.

Chiariello, M., Bruni, C. B., Bucci, C., 1999. The small GTPases Rab5a, Rab5b and Rab5c are differentially phosphorylated *in vitro*. FEBS Lett. 453, 20-24.

Clemente, R., de la Torre, J. C., 2009. Cell entry of borna disease virus follows a clathrin-mediated endocytosis pathway that requires Rab5 and microtubules. J. Virol. 83, 10406–10416.

Greber, U. F, Singh, I., Helenius, A., 1994. Mechanisms of virus uncoating. Trends Microbiol. 2, 52-56.

Glomb-Reinmund, S., Kielian, M., 1998. The role of low pH and disulfide shuffling in the entry and fusion of semliki forest virus and sindbis virus. Virology 248, 372–381.

Helenius, A., Kartenbeck, J., Simons, K., Fries, E., 1980. On the entry of semliki forest virus into BHK-21 cells. J. Cell Biol. 84, 404-420.

Horiuchi, H., Giner, A., Hoflack, B., Zerial, M., 1995. A GDP/GTP exchange-stimulatory activity for the Rab5-RabGDI complex on clathrin-coated vesicles from bovine brain. J. Biol. Chem. 270, 11257-11262.

Hutagalung, A. H., Novick, P. J., 2011. Role of Rab GTPases in membrane traffic and cell physiology. Physiol. Rev. 91, 119-149.

Jatuyosporn, T., Supungul, P., Tassanakajon, A., Krusong, K., 2014. The essential role of clathrin-mediated endocytosis in yellow head virus propagation in the black tiger shrimp *Penaeus monodon*. Dev. Comp. Immunol. 44, 100–110.

Jitrapakdee, S., Unajak, S., Sittidilokratna, N., Hodgson, R. A., Cowley, J. A., Walker, P. J., Panyim, S., Boonsaeng, V., 2003. Identification and analysis of gp116 and gp64 structural glycoproteins of yellow head nidovirus of *Penaeus monodon* shrimp. J. Gen. Virol. 84, 863–873.

Johns, H. L., Berryman, S., Monaghan, P., Belsham, G. J., Jackson, T., 2009. A dominant-negative mutant of Rab5 inhibits infection of cells by foot-and-mouth disease virus: implications for virus entry. J. Virol. 83, 6247–6256.

Krishnan, M. N., Sukumaran, B., Pal, U., Agaisse, H., Murray, J. L., Hodge, T. W., Fikrig, E., 2007. Rab 5 is required for the cellular entry of dengue and west nile viruses. J. Virol. 81, 4881–4885.

Kumar, S., Nei, M., Dudley, J., Tamura, K., 2008. MEGA: A biologist-centric software for evolutionary analysis of DNA and protein sequences. Brief. Bioinform. 9, 299-306.

Lawe, D. C., Patki, V., Heller-Harrison, R., Lambright, D., Corvera, S., 2000. The FYVE domain of early endosome antigen 1 is required for both phosphatidylinositol 3-phosphate and Rab5 binding. J. Biol. Chem. 275, 3699–3705.

Macovei, A., Petrareanu, C., Lazar, C., Florian, P., Branza-Nichita, N., 2013. Regulation of hepatitis B virus infection by Rab5, Rab7, and the endolysosomal compartment. J. Virol. 87, 6415–6427.

Marsh, M., Helenius, A., 2006. Virus entry: open sesame. Cell 124, 729-740.

Mercer, J., Schelhaas, M., Helenius, A., 2010. Virus entry by endocytosis. Annu. Rev. Biochem. 79, 803-833.

Merithew, E., Stone, C., Eathiraj, S., Lambright, D. G., 2003. Determinants of Rab5 interaction with the N terminus of early endosome antigen 1. J. Biol. Chem. 278, 8494–8500.

McLauchlan, H., Newell, J., Morrice, N., Osborne, A., West, M., Smythe, E., 1997. A novel role for Rab5–GDI in ligand sequestration into clathrin-coated pits. Curr. Biol. 8, 34–45.

Nadala, E. C. B., Tapay, L. M., Loh, P. C., 1997. Yellow-head virus: a rhabdovirus-like pathogen of penaeid shrimp. Dis. Aquat. Org. 31, 141-146.

Ongvarrasopone, C., Chanasakulniyom, M., Sritunyalucksana, K., Panyim, S., 2008. Suppression of PmRab7 by dsRNA inhibits WSSV or YHV infection in shrimp. Mar. Biotechnol. 10, 374-381.

Ongvarrasopone, C., Roshorm, Y., Panyim, S., 2007. A simple and cost effective method to generate dsRNA for RNAi studies in invertebrates. Sci. Asia. 33, 35-39.

Posiri, P., Kondo, H., Hirono, I., Panyim, S., Ongvarrasopone, C., 2015. Successful yellow head virus infection of *Penaeus monodon* requires clathrin heavy chain. Aquaculture 435, 480–487.

Posiri, P., Ongvarrasopone, C., Panyim, S., 2013. A simple one-step method for producing dsRNA from *E. coli* to inhibit shrimp virus replication. J. Virol. Methods 188, 64-69.

Sittidilokratna, N., Dangtip, S., Cowley, J. A., Walker, P. J., 2008. RNA transcription analysis and completion of the genome sequence of yellow head nidovirus. Virus Res. 136, 157-165.

Sritunyalucksana, K., Wannapapho, W., Lo, C. F., Flegel, T. W., 2006. PmRab7 is a VP28-binding protein involved in white spot syndrome virus infection in shrimp. J. Virol. 80, 10734-10742.

Stenmark, H., 2009. Rab GTPases as coordinators of vesicle traffic. Nat. Rev. Mol. Cell Biol. 10, 513-525.

Stenmark, H., Olkkonen, V. M., 2001. The Rab GTPase family. Genome Biol. 2, 3007.1–3007.7.

Stone, M., Jia, S., Heo, W. D., Meyer, T., Konan, K. V., 2007. Participation of Rab5, an early endosome protein, in hepatitis C virus RNA replication machinery. J. Virol. 81, 4551–4563.

Torres, V. A., Mielgo, A., Barbero, S., Hsiao, R., Wilkins, J. A., Stupack, D. G., 2010. Rab5 mediates caspase-8–promoted cell motility and metastasis. Mol. Biol. Cell. 21, 369–376.

van der Schaar, H. M., Rust, M. J., Chen, C., van der Ende-Metselaar, H., Wilschut, J., Zhuang, X., Smit, J. M., 2008. Dissecting the cell entry pathway of dengue virus by single-particle tracking in living cells. PLoS Pathog . 4, e1000244.

Vonderheit, A., Helenius, A., 2005. Rab7 associates with early endosomes to mediate sorting and transport of semliki forest virus to late endosomes. PLoS Biol. 3, 1225-1238.

Zhu, G., Zhai, P., Liu, J., Terzyan, S., Li, G., Zhang, X. C., 2004. Structural basis of Rab5-Rabaptin5 interaction in endocytosis. Nat. Struct. Mol. Biol. 11, 975 – 983.

Part III: Roles of PmEEA1 in controlling endosomal trafficking of YHV

Abstract

Yellow head disease (YHD) is an infectious disease of *Penaeus monodon* which is caused by the yellow head virus (YHV). YHV infection invariably leads to 100% shrimp mortality within 3-5 days. Currently, an effective method to prevent or cure shrimp from YHV infection has not been elucidated. Therefore, the molecular mechanism underlying YHV infection should be examined. In this study, early endosome antigen 1 (EEA1) protein that was involved in the tethering step of the vesicle and early endosome fusion was investigated during YHV infection. The open reading frame of *Penaeus monodon* EEA1 (PmEEA1) was cloned and sequenced (3,000 bp). It encoded a putative protein of 999 amino acids and contained the zinc finger C2H2 domain signature at the N-terminus and the FYVE domain at the C-terminus. Suppression of PmEEA1 by specific dsRNA in shrimp showed inhibition of YHV replication after 48 hours post YHV injection (hpi). On the other hand, shrimp received only NaCl without any dsRNA showed high YHV levels at approximately one hundred thousand times at 24 hpi and 48 hpi. Moreover, silencing of PmEEA1 by specific dsRNA followed by YHV challenge demonstrated a delay in shrimp mortality from 60 hpi to 168 hpi when compared to the control. These results indicated that YHV required PmEEA1 for trafficking within the infected cells, strongly suggesting that PmEEA1 may be a potential target to control and prevent YHV infection in *P. monodon.*

Keywords: Rab5-interacting protein; endocytosis; RNAi; dsRNA; black tiger shrimp

1. Introduction

YHD outbreaks have been reported since 1990 as epizootic events in the eastern, central and southern parts of Thailand, and resulted in shrimp production loss worldwide. A causative agent of this disease is the Yellow head virus (YHV) (Boonyaratpalin, et al., 1993). YHV is a positive-sense single stranded RNA virus that is classified into genus *Okavirus*, family *Roniviridae*, in the order *Nidovirales* (Mayo, 2002, Walker, et al., 2005) and is closely related to gill-associated virus (GAV) from Australia particularly in terms of the nucleotide and amino acid sequences, histological, and morphological observations (Cowley, et al, 1999, Spann, et al., 2000). YHV is approximately 50-60 × 190-200 nm in size, with enveloped bacilliform surrounded by prominent peplomers or spikes (Nadala, et al., 1997). The genome of the virus is approximately 27 kb in length and consists of ORF1a, ORF1b, ORF2 and ORF3. The enveloped glycoprotein, gp116, which is involved in the entry process of YHV into the cells is encoded from ORF3 (Sittidilokratna, et al., 2008).

Currently, it is believed that the major route of YHV entry into the cells of *Penaeus monodon* is by clathrin-mediated endocytosis via clathrin heavy chain and AP17 protein (Jatuyosporn, et al., 2014, Posiri, et al., 2015). The clathrin-coated vesicle containing YHV requires a small GTPase Rab5 protein to traffic it from the plasma membrane towards the first sorting station, the early endosome. *P. monodon* Rab5 was identified and showed to colocalize with YHV particles (Chavrier, et al., 1990, Posiri, Panyim, and Ongvarrasopone, 2016). At the early endosomal compartment, Rab5 protein binds to the Rab5 effector protein, the early endosome antigen 1 (EEA1), to promote the fusion between the vesicular and early ndosomal membranes, causing the cargo proteins including the virus to be transported inside of the early endosome (Christoforidis, et al., 1999).

Rab5 effector EEA1 works with SNAREs complexes to promote the transported vesicle-endosome membrane tethering and fusion (Christoforidis, et al., 1999). EEA1 location is associated with the early endosome and showed colocalization with Rab5 protein (Mu, et al., 1995). The EEA1 structure is a long parallel coiled coil homodimer that contains C_2H_2 zinc finger (ZF) domain at the N-terminus and FYVE domain at the C-terminus (Callaghan, et al., 1999). Interactions between the N-terminal ZF domain of EEA1 with Rab5 protein and the SNAREs complexes facilitate the docking and fusion processes. Furthermore, the fusion step of the vesicle and the early endosome requires phosphatidylinositol-4-5-bisphosphate 3-kinase (PI(3)K) activity whereby the C-terminal FYVE domain of EEA1 can bind directly to the product of PI(3)K, phosphatidylinositol-3-phosphate (PtdIns3P). Taken together, the specific binding of Rab5-GTP bound form, together with PI(3)K activity are needed in the vesicle-early endosome membrane fusion (Simonsen, et al., 1998, Callaghan, et al., 1999, Lawe, et al., 2000, Merithew,

et al., 2003). Furthermore, EEA1 has been shown to colocalize with Semliki forest virus (SFV) (Vonderheit and Helenius, 2005) and hepatitis C virus (HCV) (Lai, et al., 2010). In addition, EEA1 protein also demonstrated colocalization with YHV (data not shown), suggesting that the protein may be involved in YHV infection process. Our previous study found that YHV utilized clathrin heavy chain, Rab5 and Rab7 proteins to get into the shrimp cells (Posiri, et al., 2015, Posiri, Panyim and Ongvarrasopone, 2016, Ongvarrasopone, et al., 2008). It is thus possible that YHV also requires Rab5 effector early endosome antigen 1 (EEA1) protein during infection. Therefore, in this study, the roles of EEA1 during YHV infection and shrimp mortality in *P. monodon* was investigated.

2. Methods

2.1. The black tiger shrimp

Penaeus monodon or the black tiger shrimps were obtained from Choochai farm in Chonburi province and also from the Shrimp Genetic Improvement Center (SGIC, BIOTEC) in Surat Thani province, Thailand. Shrimps were acclimatized for at least 2 days and maintained in large containers with oxygenated sea water at 10-30 ppt salinity before used. They were fed with commercial feed every day. The water was changed every 2 days.

2.2. Cloning of the full-length PmEEA1

Coding region of EEA1 from *Marsupenaeus japonicus* kindly provided by Dr. Hidehiro Kondo was used to design specific primers to amplify a region of PmEEA1. First, total RNA from ovary was extracted using Tri Reagent (Molecular Research Center) and cDNA was synthesized using Improm-II reverse transcriptase (Promega) according to the manufacturer's protocol. The full-length open reading frame of EEA1 was amplified using Q5 DNA polymerase (New England Biolabs) wtih cdEEA1-F and cdEEA1-R primers (Table 1), with an expected size of approximately 3,000 bp. The PCR condition was: denaturation at 98°C for 30 sec, then 35 cycles of 98°C for 10 sec, 55°C for 20 sec, and 72°C for 3 min. The PCR product was purified and cloned into pGEMT-easy vector and sequenced using T7, SP6, EEA1-Fseq, EEA1-Rseq and asEEA1-R2 primers (Table 1) by First Base Co, Ltd. (Malaysia).

2.3. PmEEA1 Nucleotide and protein sequence analysis

The nucleotide sequence of PmEEA1 was confirmed and analyzed by BLASTN program using search under nucleotide database. Predictions of molecular weight and isoelectric point (pI) of the protein were performed by Expert Protein Analysis System (www.expasy.org). Conserved motifs of the deduced amino acids were scanned using ScanProsite tool (http://prosite.expasy.org/scanprosite). EEA1 protein sequences from several organisms were obtained from GenBank database. Phylogenetic analysis was performed using

Phylogeny.fr with “A la Carte” mode (http://www.phylogeny.fr) based on neighbor-joining method and 1000 replicates of bootstrap with distance methods (Dereeper, et al., 2008, Dereeper, et al., 2010).

2.4. Construction of two dsRNAs targeting PmEEA1 mRNA

Recombinant plasmid containing stem-loop of dsRNA of PmEEA1 was constructed in pET-17b (Novagen) vectors. Two plasmids containing dsRNA-Cter and dsRNA-Nter whose targets were close to the stop and start codons of *PmEEA1* gene, respectively, were constructed. Sense-loop regions of the dsRNAs located near stop and start codons were amplified from the first-strand cDNA using specific primers, sEEA1-F1 and lEEA1-R1 for dsRNA-Cter, and nSLEEA1-F1 and nSLEEA1-R1 for dsRNA-Nter (Table 1). In addition, antisense regions were amplified using asEEA1-F2 and asEEA1-R2 for dsRNA-Cter, and nASEEA1-F2 and nASEEA1-R2 for dsRNA-Nter (Table 1). All PCR fragments were gel-purified and verified by restriction enzyme digestion. The purified fragments of the sense-loop and antisense of the Cter region were digested with *Eco*RI and ligated together using T4 DNA ligase (NEB). Then, the sense fragment was digested by *Xba*I whereas the antisense fragment was cut by *Xho*I. The ligated fragment of the sense and antisense of PmEEA1 was cloned into pET-17b to obtain pET-17b-dsRNA-Cter. In addition, the PCR fragment of sense-loop of the Nter region was cloned into pGEM-3Zf+ at *Xba*I and *Kpn*I sites and then the antisense fragment of the Nter region was subsequently cloned into *Kpn*I and *Eco*RI site of this recombinant plasmid. Then, the sense-loop and antisense fragments of the Nter region in pGEM-3Zf+ was cut and subcloned into pET-17b vector to construct recombinant plasmid named pET-17b-dsRNA-Nter. Both of the recombinant plasmids were used for dsRNA production by *in vivo* bacterial expression.

2.5. Production of dsRNAs by in vivo bacterial expression

The recombinant plasmids, pET-17b-dsRNA-Cter and –Nter, were transformed into a RNase III mutant HT115 *E.coli* strain. DsRNAs expressions were induced by 0.1 mM IPTG. Then, they were extracted by using ethanol method (Ongvarrasopone, Roshorm and Panyim, 2007, Posiri, Ongvarrasopone and Panyim, 2013). The quality of the dsRNAs was characterized by ribonuclease digestion assay using RNase A and RNase III digestions. Concentration of dsRNA was estimated visually using agarose gel electrophoresis by comparing the target band intensity to that of the 100 bp DNA marker.

2.6. Yellow head virus (YHV) preparation

YHV stock was prepared using the hemolymph of YHV-infected moribund black tiger shrimp. The hemolymph was drawn and mixed with AC-1 solution (27 mM Sodium citrate, 34.33 mMNaCl, 104.5 mM Glucose, 198.17 mM EDTA, pH 7.0), at ratio 1:1, and centrifuged at

20,000 ×g for 20 minute at 4 °C to remove hemocyte debris. YHV was separated from the hemolymph by ultracentrifugation at 100,000 ×g for 1 h. YHV pellet was then dissolved with 150 mM NaCl and stored at -80 °C until used. The viral titer that caused 100% mortality within 3-4 days was used in this study.

2.7. Injection of P. monodon with dsRNAs

The efficiency of dsRNA-Cter and dsRNA-Nter were examined by injection of dsRNAs into shrimp hemocoel. Shrimps were injected with 2.5 µg. g^{-1} shrimp of dsRNA-Cter, -Nter, C+Nter or unrelated dsRNA-GFP dissolved in 150 mM NaCl. Injection of 150 mM NaCl was used as control. After 24 h post dsRNA injection, gills of the individual shrimp were collected for total RNA extraction. Suppression effect of dsRNAs was analyzed by reverse-transcription PCR (RT-PCR) to determine PmEEA1 mRNA level.

2.8. Study of the knock down effect by dsRNAs upon YHV infection and shrimp mortality assay

In order to investigate the silencing effect of PmEEA1 upon YHV infection, shrimp were injected with 2.5 µg. g^{-1} shrimp of the combination of dsRNA-C and dsRNA-Nter (1.25 µg. g^{-1} shrimp each) or unrelated dsRNA-GFP, followed by YHV challenged after 24 h post dsRNA injection. For each group, 5 shrimp were used. Twenty-four and forty-eight hours post YHV injection (hpi), gills of individual shrimp were collected and analyzed for PmEEA1 and YHV levels. Moreover, shrimp mortality was also recorded every 12 h post YHV injection (hpi) for 144 hpi. Three replicates of the experiment were performed.

2.9. Total RNA extraction and RT-PCR analysis

Total RNA from gill tissue was isolated using Tri Reagent® (Molecular Research Center) following the manufacturer's protocol. Two microgram of the total RNA was used to produce first-strand cDNA using Improm-II™ reverse transcriptase (Promega) with PRT primer (Table 1). PCR products were amplified by using Taq DNA polymerase (New England Biolabs). Multiplex PCR of PmEEA1 (PmEEA1-F and PmEEA1-R1 primers, and PmActin (PmActin-F and PmActin-R1) (Table 1) were amplified under this condition: 95°C for 5 min, then 30 cycles of 95°C for 30 s, 61°C for 30 s, and 68°C for 45 s, followed by 68°C for 7 min. The PCR products were analyzed on 1.5% agarose gel. The intensity of each band was quantitated using Scion Image program. Relative mRNA transcript levels of PmEEA1 was normalized with PmActin intensity and recorded as arbitrary unit.

2.10. Detection of YHV mRNA levels by quantitative real time PCR (qPCR)

For qPCR analysis, cDNA template was diluted at 1:4 and mixed with qPCR reaction using KAPA™ SYBR® Fast qPCR master mix (2X) ABI Prism™ (KAPA Biosystems) following manufacturer's protocol. The qPCR was analyzed using Mastercycler RealPlex4

(Eppendorf). qYHV-F and qYHV-R primers (Table 1) were used to amplify YHV mRNA. For internal control, EF1-α, was used (EF1 α -F and EF1 α -R primers) (Table 1). The qPCR condition was as followed: 95°C for 3 min; 40 cycles of 95°C for 5 s, 60°C for 30 s. The cycle threshold (C_t) values of YHV and EF1- α were compared and calculated using $2^{-\Delta\Delta C_T}$ method (Livak and Schmittgen, 2001).

2.11. Statistical analysis

The relative transcription levels of PmEEA1 and YHV that were normalized with PmActin or EF1-α were presented as mean ± SD. In addition, cumulative percent shrimp mortality was plotted as mean ± SD. A significant difference of the experiment groups was examined by analysis of variance (ANOVA). A probability *(P)* value less than 0.05 was accepted as significant difference.

Table 1 Primer sequences used in this study.

Name	Sequence (5'--> 3')	Purposes
cdEEA1-F	ATGTCAGAGAGAGGAATG	Amplification of full-length cDNA coding region of PmEEA1
cdEEA1-R	TCACATTTTTGAAGTGAG	
T7	TAATACGACTCACTATAGGG	Sequencing of PmEEA1 nucleotides
SP6	ATTTAGGTGACACTATAG	
EEA1-Fseq	GCAGGGTTGAAGGAAGAGATG	
EEA1-Rseq	CCCTTAGCAGCTTCTCTCTCC	
PRT	CCGGAATTCAAGCTTCTAGAGGATCCTT TTTTTTTTTTTTT	The first strand cDNA synthesis
sEEA1-F1	*Xba*I GCTCTAGAACAAAATGAAGCCAAGCAGC	Construction of the recombinant plasmid expressing dsRNA-Cter targeting PmEEA1 mRNA
lEEA1-R1	*Eco*RI GGAATTCTAGCAACCTCAGCCTCCAG	
asEEA1-F2	*Xho*I CCGCTCGAGACAAAATGAAGCCAAGCAGC	
asEEA1-R2	*Eco*RI GGAATTCGGCATCAATTTCAAGCTGG	
nSLEEA1-F1	*Xba*I GCTCTAGAGGGCTTCTTGTGTCCAAC	Construction of the recombinant plasmid expressing dsRNA-Nter targeting PmEEA1 mRNA
nSLEEA1-R1	*Kpn*I GGGGTACCACCTTTTCAGCTTGTAGGG	
nASEEA1-F2	*Eco*RI GGAATTCGGGCTTCTTGTGTCCAAC	
nASEEA1-R2	*Kpn*I GGGGTACCCGCAAGGAACTGTTCAAC	
PmEEA1-F	AGCTTGAAATTGATGCCCAGAAG	Detection of PmEEA1 mRNA level
PmEEA1-R	TTGTTGCAGCTGTGGCAATTTAG	
PmActin-F	GACTCGTACGTGGGCGACGAGG	Detection of PmActin mRNA level
PmActin-R1	AGCAGCGGTGGTCATCTCCTGCTC	
qYHV-F	ATCATCAGCTCACAGGCAAGTTCC	Detection of YHV mRNA level by realtime PCR
qYHV-R	GGGTCTAAATGGAGCTGGAAGACC	
EF-1α-F	GAACTGCTGACCAAGATCGACAGG	Detection of EF-1α mRNA level by realtime PCR
EF-1α-R	GAGCATACTGTTGGAAGGTCTCCA	

3. Results

3.1. Cloning and sequence analysis of PmEEA1 coding region

The sequence of early endosome antigen 1 from *Marsupenaeus japonicus* (MjEEA1) (kindly provided by Dr. Hidehiro Kondo) was used to design primers to amplify the coding region of PmEEA1 from the ovary of *Penaeus monodon*. The full-length sequence of PmEEA1 is 3,000 bp, including the stop codon (TGA), thus encoded a protein of 999 amino acids (GenBank accession #xxxxxxx; Supplementary Fig.1). The predicted molecular weight and pI of PmEEA1 protein are 112.6 kDa and 5.04, respectively. Sequence analysis revealed that PmEEA1 protein contains conserved domains of EEA1 which are Zinc finger C_2H_2 type domain at the amino acids 43-64 and 73-94, and the FYVE domain at the amino acids 938-996. These domains are conserved in both invertebrates and vertebrates including CeEEA1, DrEEA1, HsEEA1, LaEEA1, LpEEA1, and RnEEA1 (Fig. 1 and Table 2). Phylogenetic tree analysis revealed that PmEEA1 was closely related to the invertebrate group (Fig. 2).

3.2. Production of dsRNA-Cter and dsRNA-Nter targeting PmEEA1 mRNA region

In order to investigate the function of PmEEA1, RNAi technology was employed. Two dsRNAs, dsRNA-Cter and dsRNA-Nter, targeting the PmEEA1 mRNA were constructed and produced by *in vivo* bacterial expression (see materials and methods section). In addition, dsRNA-GFP was produced and used as unrelated dsRNA control. Then, the hairpin dsRNAs were extracted by ethanol method and verified by RNase digestion assay. All dsRNAs (dsRNA-Cter, -Nter, and –GFP) produced could be cleaved by RNase III but not by RNase A, suggesting that they were of good quality. The expected sizes of these dsRNAs were approximately 400 bp (Supplementary Fig. 2).

3.3. Silencing of PmEEA1 mRNA levels by two dsRNAs

The effectiveness of dsRNA-Cter and dsRNA-Nter on silencing of PmEEA1 mRNA were investigated. Shrimp were injected with dsRNAs targeting PmEEA1 or unrelated dsRNA-GFP for 24 hours. NaCl injection was employed as an experimental control. The result found that shrimp received either dsRNA-Cter or dsRNA-Nter showed a significant reduction of PmEEEA1 mRNA levels at 81% and 76%, respectively. Moreover, in shrimp injected with dsRNA-Cter and dsRNA-Nter (dsRNA-C+Nter), the level of PmEEA1 mRNA could hardly be detected (91% suppression).. Interestingly, PmEEA1 mRNA level could be silenced at about 33% in dsRNA-GFP injected shrimp (Fig. 3).

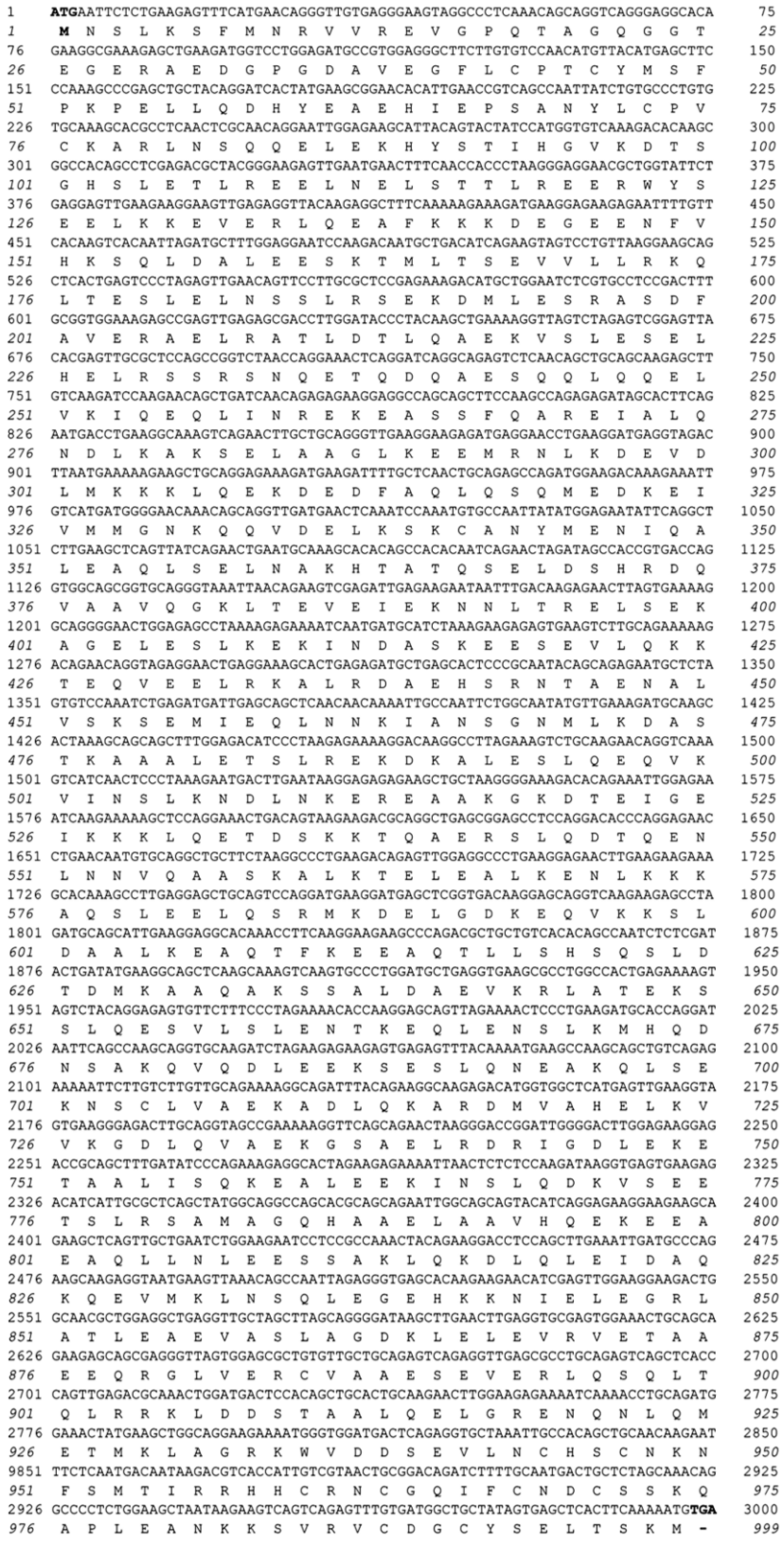

Supplementary Fig. 1 The nucleotide and deduced amino acid sequences of *Penaeus monodon* Early endosome antigen 1 (PmEEA1). The coding region of PmEEA1 is 3,000 bp encoding the protein of 999 amino acids. Start and stop codons are in bold letters; the

dash represents the stop codon. The nucleotide sequences were deposited in the GenBank database under the accession number XXXX.

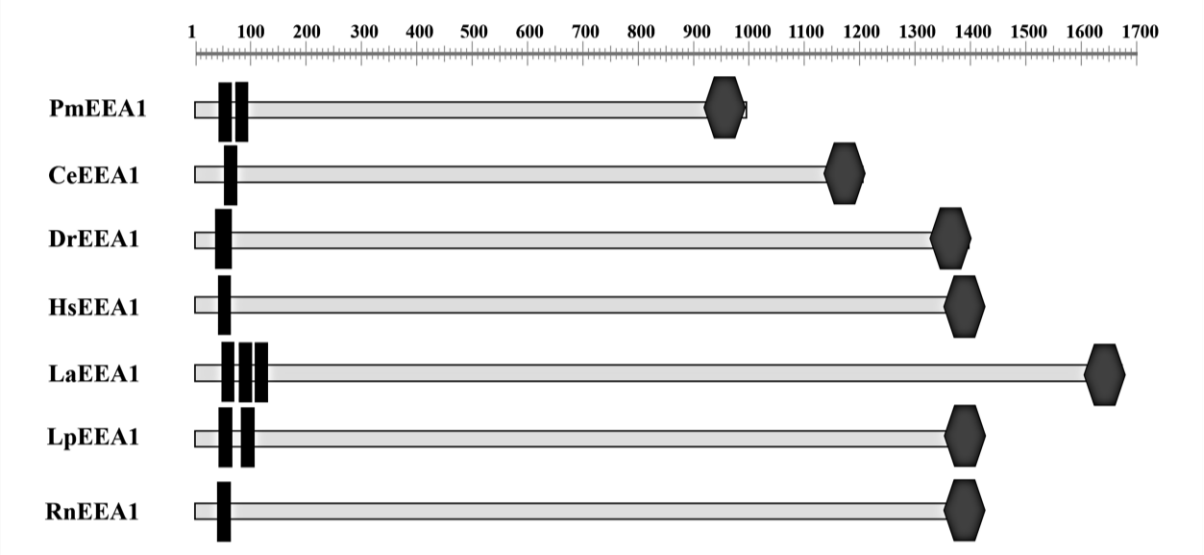

Fig. 1 Schematic of the predicted protein domains of the early endosome antigen 1 (EEA1) from *P. monodon* and other species. The size of EEA1 protein varied among organisms but all contain the signature motifs of Zinc finger C_2H_2 type domain (▮) at the N-terminus and the FYVE domain (⬮) at the C-terminus. *Penaeus monodon* EEA1 (PmEEA1) possess 999 amino acids which compose of two domains of Zinc finger C_2H_2 signature motifs at the position aa 43-64 and aa 73-94 and one FYVE domain at aa 938-996. EEA1 protein from several species including *Penaeus monodon* (PmEEA1; accession number xxxxxx), *Caenorhabditis elegans* (CeEEA1; accession number xxxxxx), *Danio rerio* (DrEEA1), *Homo sapiens* (HsEEA1), *Lingula anatine* (LaEEA1), *Limulus Polyphemus* (LpEEA1), *and Rattus norvegicus* (RnEEA1) were used for domain analysis.

Table 2 Early endosome antigen 1 (EEA1) proteins used for multiple sequence alignment and phylogenetic analysis

Abbreviations	Species	Accession number
AcEEA1	*Aplysia californica*	XP_005095892.2
BaEEA1	*Balaenoptera acutorostrata scammoni*	XP_007166165.1
BgEEA1	*Biomphalaria glabrata*	XP_013093515.1
CeEEA1	*Caenorhabditis elegans*	NP_001024127.1
DrEEA1	*Danio rerio*	XP_003200485.1
FhEEA1	*Fundulus heteroclitus*	XP_012731526.1
HsEEA1	*Homo sapiens*	NP_003557.2
LaEEA1	*Lingula anatina*	XP_013419201.1
LpEEA1	*Limulus polyphemus*	XP_013777228.1
NgEEA1	*Nannospalax galili*	XP_008822059.1
ObEEA1	*Octopus bimaculoides*	XP_014782058.1
PmEEA1	*Penaeus monodon*	
TcEEA1	*Tupaia chinensis*	ELW61492.1
TrEEA1	*Takifugu rubripes*	XP_003967354.1
RnEEA1	*Rattus norvegicus*	NP_001101556.1
XtEEA1	*Xenopus tropicalis*	XP_002935361.1

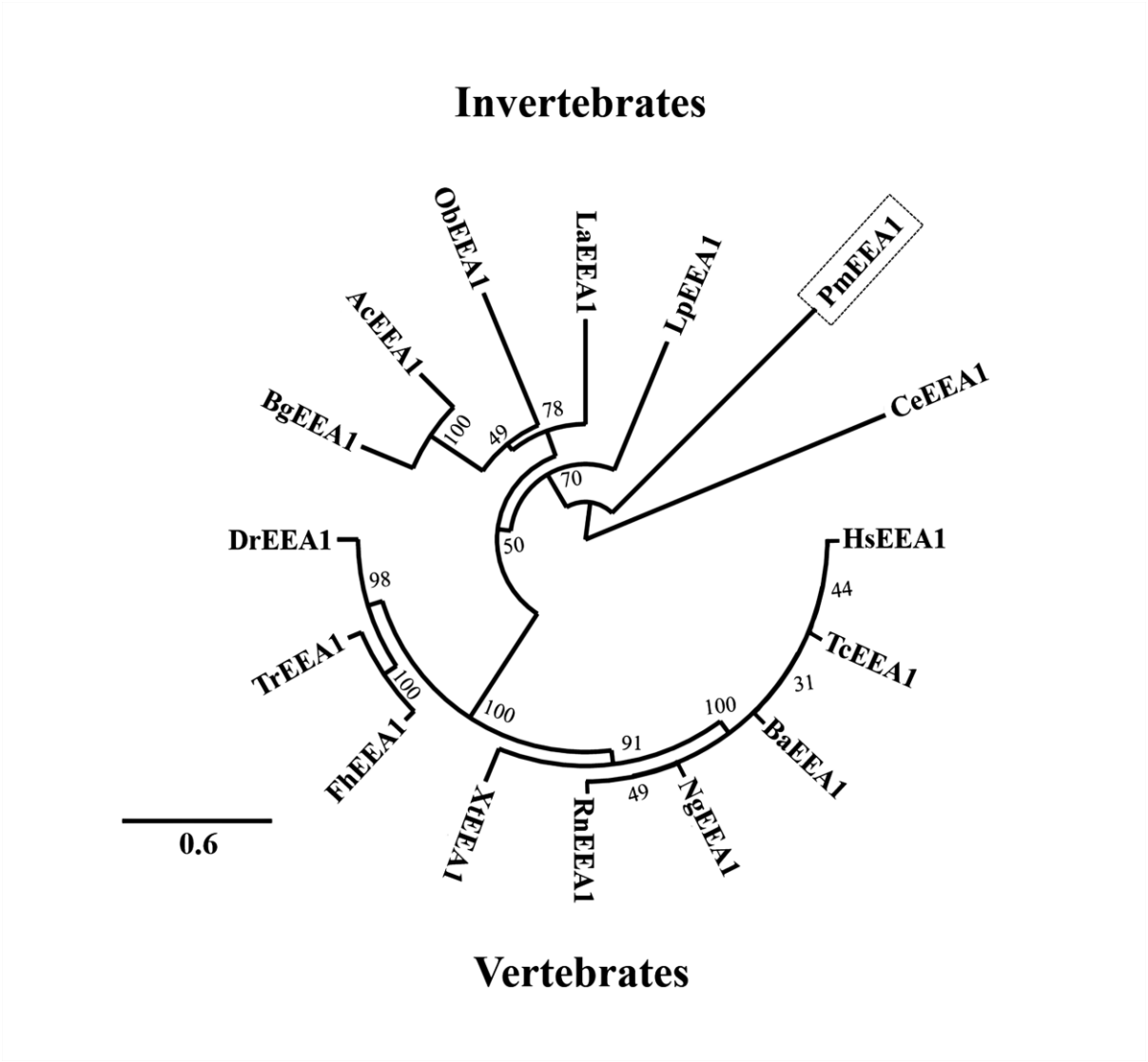

Fig. 2 Phylogenetic analysis of EEA1 protein. The phylogenetic tree was reconstructed using the Neighbor-joining method based on the full amino acid sequences of EEA1 with bootstrap value of 1,000. Organisms used for the tree reconstruction were *Aplysia californica* (AcEEA1), *Balaenoptera acutorostrata scammoni* (BaEEA1), *Biomphalaria glabrata* (BgEEA1), *Caenorhabditis elegans* (CeEEA1), *Danio rerio* (DrEEA1), *Fundulus heteroclitus* (FhEEA1), *Homo sapiens* (HsEEA1), *Lingula anatine* (LaEEA1), *Limulus Polyphemus* (LpEEA1), *Nannospalax galili* (NgEEA1), *Octopus bimaculoides* (ObEEA1), *Penaeus monodon* (PmEEA1), *Tupaia chinensis* (TcEEA1), *Takifugu rubripes* (TrEEA1), *Rattus norvegicus* (RnEEA1), *and Xenopus tropicalis* (XtEEA1).

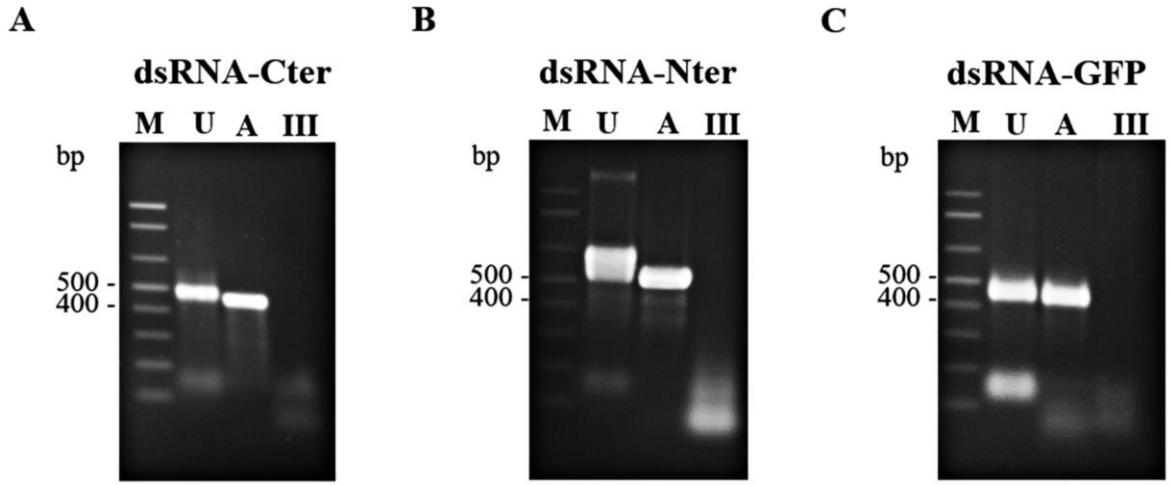

Supplementary Fig. 2 Quality of targeting PmEEA1 including dsRNA-Cter, dsRNA-Nter and dsRNA-GFP produced by *in vivo* bacterial expression. The dsRNAs were produced by *in vivo* bacterial expression and then extracted by ethanol. The dsRNAs were verified by RNase digestion assay. Lane M, U, A, and III represent 1 kb+ DNA ladder, undigested dsRNAs, dsRNA treated with RNase A and dsRNA treated with RNase III, respectively.

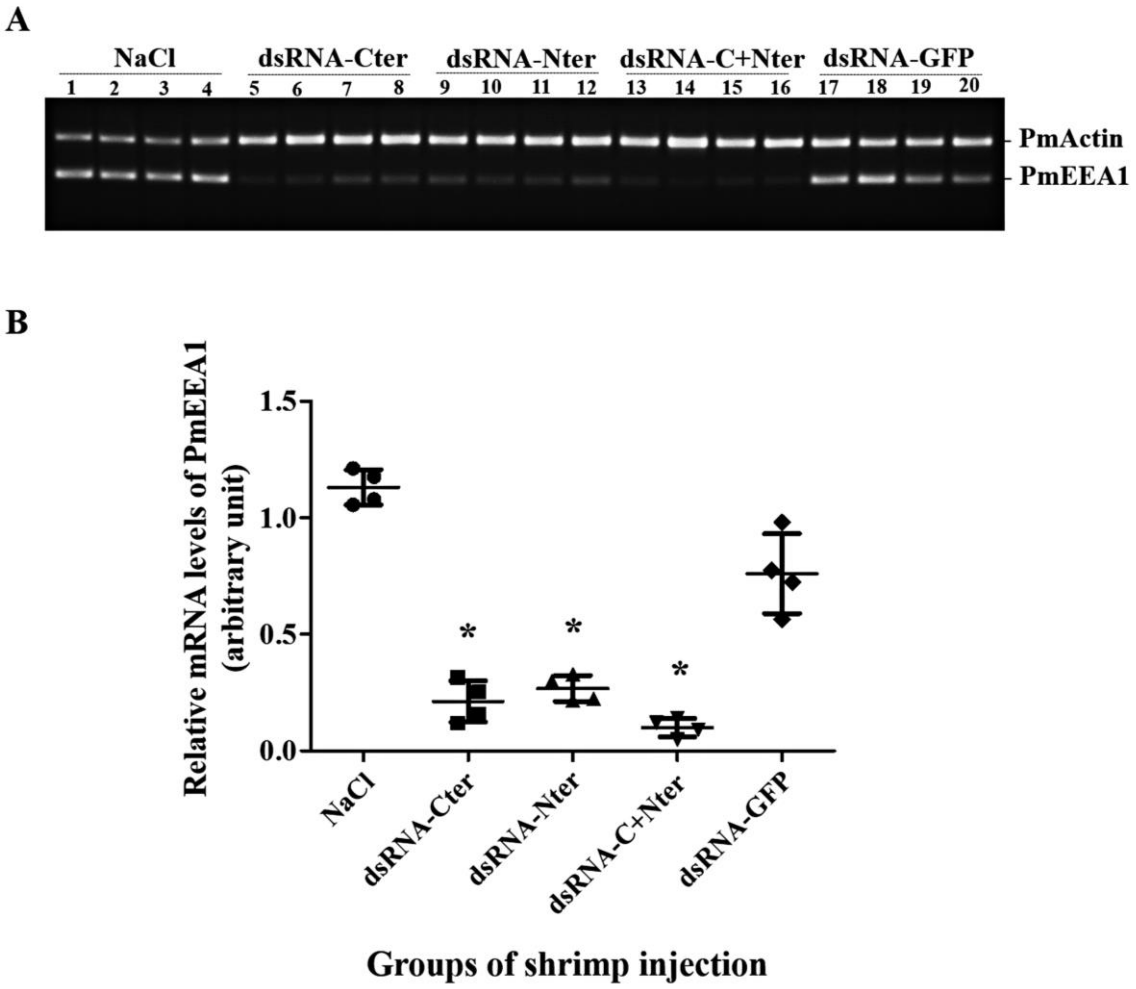

Fig. 3 Effectiveness of two type of dsRNAs targeting PmEEA1 mRNA. A representative gel of RT-PCR products was presented as expression levels of PmEEA1 and PmActin of shrimp injected with NaCl control (lanes 1-4), each dsRNA targeting PmEEA1 which are dsRNA-Cter (lanes 5-8) and dsRNA-Nter (lanes 9-12), the combination between dsRNA-Cter and -Nter (dsRNA-C+Nter) (lanes 13-16) and unrelated dsRNA-GFP (lanes 17-20) at 2.5 $\mu g.g^{-1}$ shrimp at 24 h post dsRNA injection (n=4) (A). The relative mRNA expression levels of PmEEA1 normalized with PmActin are shown as mean ± SD (n= 4) (B). (*) Statistically significant difference between dsRNA injected shrimp as compared to NaCl injected group ($P < 0.05$).

3.4. Knockdown effect of PmEEA1 reduced YHV replication levels

The role of PmEEA1 on YHV level was next investigated during YHV replication. The combination dsRNA-C+Nter were used to silence PmEEA1 mRNA. Shrimp received the dsRNA after 24 h were challenged with YHV. After 24 and 48 hours post YHV injection (hpi), the level of PmEEA1 and YHV mRNAs were determined from the gills. Injected shrimp with dsRNA-C+Nter following YHV challenge showed significant reduction of PmEEA1 at 24 and 48 hpi about 82% and 78% when compared to NaCl→YHV control group, respectively. Moreover, shrimp injected with unrelated dsRNA-GFP → YHV showed no difference in PmEEA1 mRNA levels at both 24 and 48 hpi when compared to the control (Fig. 4A).

The level of YHV mRNAs were determined by real time PCR and expressed as mean ± SD of the fold change of YHV mRNA levels compared to the NaCl injected group at 24 hpi. At 24 hpi, the fold change of YHV mRNA level in the PmEEA1 knock down group injected with dsRNA-C+Nter showed no significant difference when compared to the control groups injected with NaCl or dsRNA-GFP. At 48 hpi, the fold change of the YHV level was increase more than 100,000 and 25,000 times for NaCl- and dsRNA-GFP- injected groups, respectively. However, the fold change of the YHV level at 48 hpi (1.28 ± 1.31 fold) remained at very low level and showed no significant difference when compared at 24 hpi (1.16 ± 0.53 fold) of the PmEEA1 knock down group (Fig. 4B). These results indicated that PmEEA1 was essential for YHV replication.

3.5. Silencing of PmEEA1in YHV-infected shrimp decreased shrimp mortality

The shrimp mortality was further observed to investigate the involvement of PmEEA1 on YHV infection. There were 10-15 shrimp per group and the experiments were performed three times. Shrimp received dsRNA-C+Nter followed by YHV challenge showed a significant delay in shrimp mortality as observed in 60 hpi to 168 hpi when compared to NaCl→YHV and unrelated dsRNA-GFP→YHV groups (*P* value = 0.05). At 60 hpi, no shrimp in dsRNA-C+Nter→YHV group died whereas shrimp in the control groups of NaCl→YHV and unrelated dsRNA-GFP→YHV had 80% and 50% shrimp mortality, respectively. In addition, at 84 hpi, shrimp in both control groups showed 100% mortality while the dsRNA-C+Nter→YHV group demonstrated only 40% mortality (Fig. 5). Altogether, these results suggested that YHV required PmEEA1 for successful infection.

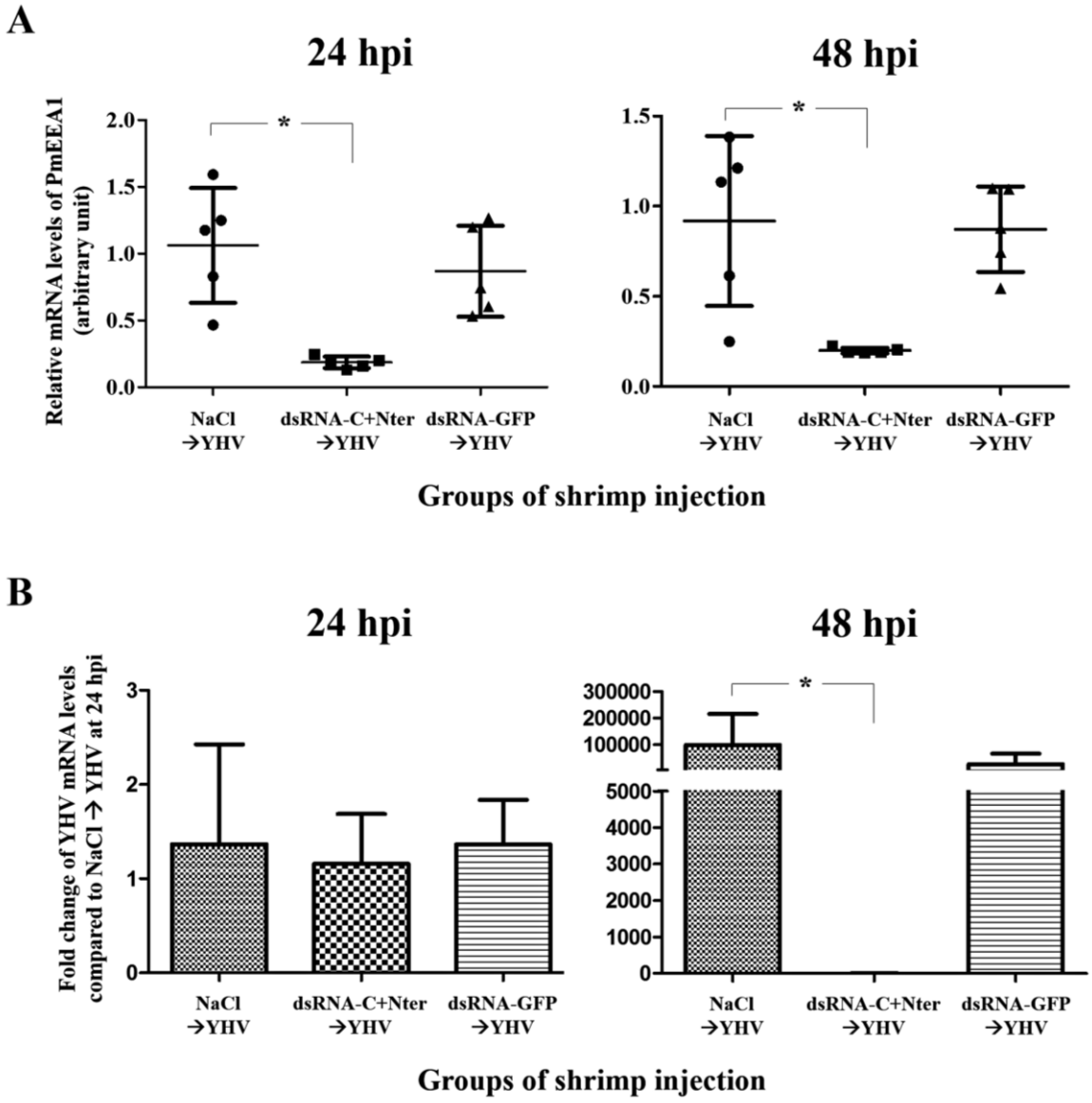

Fig. 4 Effect of PmEEA1 depletion during YHV infection. Shrimp were injected with NaCl alone, dsRNA-C+Nter, and dsRNA-GFP at 2.5 μg.g^{-1} shrimp for 24 h followed by YHV challenge and detection at 24 and 48 hpi from gill tissues (n=5). The relative mRNA levels of PmEEA1 normalized with PmActin are presented as dot graphs of arbitrary unit of mean ± SD (A). Bar graphs represent the quantitative RT-PCR of fold change of YHV mRNA levels compared to NaCl → YHV at 24 hpi. The result was demonstrated as mean ± SD (B). Asterisks indicate significant differences between experimental group and the control group ($P < 0.05$).

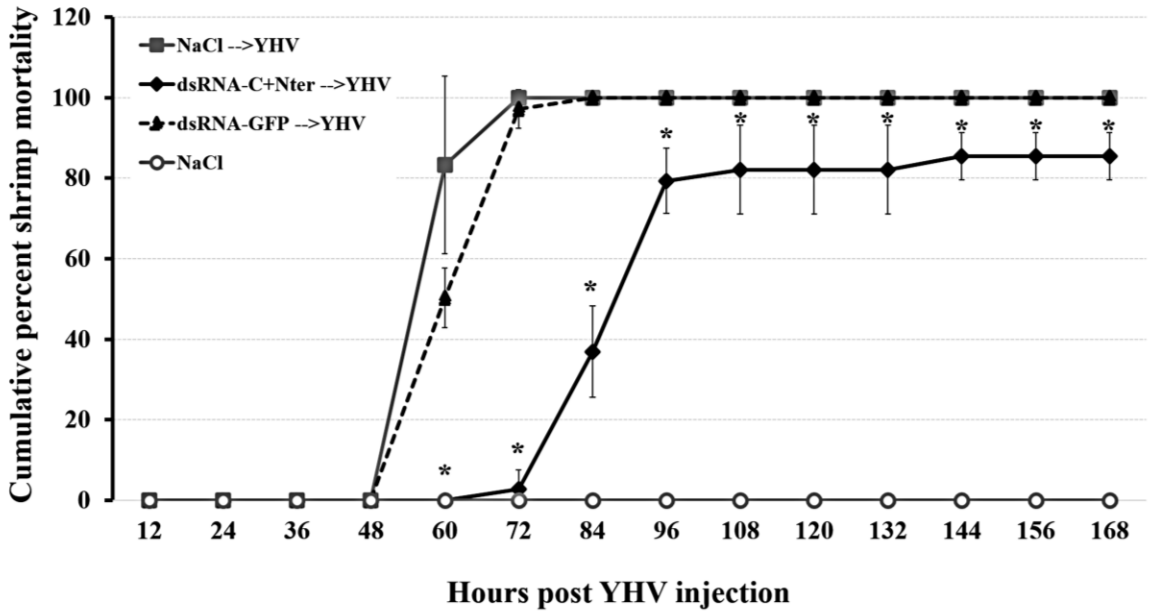

Fig. 5 Silencing of PmEEA1 by the combination dsRNA-C+Nter on YHV infection delayed shrimp mortality. The cumulative percent mortality of shrimp injected with NaCl, dsRNA targeting PmEEA1 (dsRNA-C+Nter), or unrelated dsRNA-GFP at 2.5 μg.g^{-1} shrimp followed by YHV injection were observed. Dead shrimp were recorded every 12 hpi. The graph was plotted as mean ± SD from three replicates per group (n=12-15 shrimp per group). Asterisks represent statistically significant difference between NaCl→YHV and dsRNA-C+Nter→YHV group (P < 0.05).

4. Discussion

Clathrin-mediated endocytosis is the major route of YHV penetration inside the shrimp host cell (Jatuyosporn, et al., 2014, Posiri, et al., 2015). After internalization, YHV requires a small GTPase Rab5 protein to regulate the transportation from plasma membrane to early endosome. Colocalization between YHV and *Penaeus monodon* Rab5 (PmRab5) was observed in the hemocytes from 10 min to 3 h post YHV infection (Posiri, Panyim and Ongvarrasopone, 2016). Rab5 proteins on vesicle membrane are tethered with Rab5 effector early endosome antigen 1 (EEA1) that appeared on the surface of the early endosome to promote the fusion of the two membranes (Christoforidis, et al., 1999, Lawe, et al., 2000, Merithew, et al., 2003). Previously under transmission electron microscopy, it was found that YHV particles are inside the early endosomes of shrimp cells (Duangsuwan, et al., 2011). PmEEA1 protein contains 999 amino acids, while other species including CeEEA1, DrEEA1, HsEEA1, LaEEA1, LpEEA1, and RnEEA1 have more than 1,200 amino acids (Fig. 1). Although the size of the protein from different species present a wide range of sizes, but they all showed signature characteristics of

EEA1, two Zinc finger C_2H_2 domains and FYVE domain of N- and C-terminal sites (Callaghan, et al., 1999). Moreover, the function of EEA1 during YHV infection in *P. monodon* was examined. Two dsRNAs targeting N- and C-terminus of PmEEA1 were produced and used to knockdown PmEEA1 transcripts. A combination of two dsRNAs were used to improve the inhibition of YHV infection in shrimp (Posiri, Ongvarrasopone and Panyim, 2011). Since, dsRNA targeting C-terminus of PmEEA1 region (the first construction) was located near 3' end of the open reading frame (dsRNA-Cter). This dsRNA was first injected into shrimp resulting in inhibition of PmEEA1 mRNA levels only 50-80% compared to the control (data not shown). Local protein factors involving in termination of protein synthesis may cause the positional effect that interrupts the accessibility of RISC-siRNA complex to the local target (Holen, et al., 2002). After obtaining the full-length coding region of PmEEA1, another dsRNA targeting PmEEA1 mRNA was constructed. This dsRNA was located near the 5' end of the open reading frame (dsRNA-Nter). The result demonstrated that injection of the combined two types of dsRNA targeting PmEEA1 could silence the mRNA levels more than using only one type of the dsRNA (Fig. 3). This is probably due to a variety of siRNA population generated from the combined two dsRNAs. It could increase the efficiency of siRNA to bind to the mRNA target. The siRNA could bind with the secondary structure of mRNA as stem and loop structure better than the hairpin structure (Luo and Chang, 2004, Pascut, Bedogni and Tiribelli, 2015).

After testing the effectiveness of the dsRNA, the role of PmEEA1 during YHV infection was investigated. Shrimp that were injected with NaCl→YHV at 48 hpi showed increased YHV replication at about 100,000 times when compared to 24 hpi. On the other hand, injected shrimp with dsRNA targeting PmEEA1 (using the combination between dsRNA-Cter and –Nter (dsRNA-C+Nter)) followed by YHV challenge demonstrated no significant difference of YHV levels at 24 and 48 hpi (Fig.4B). In addition, dsRNA-C+Nter→YHV group showed a delay in shrimp mortality when compared to the control NaCl→YHV group (Fig.5). Injection of dsRNA targeting PmEEA1 alone has no effect on shrimp mortality (Supplementary Fig.3). Shrimp started dying after receiving dsRNA-C+Nter followed by YHV challenge at 84 to 96 hpi (about 108 to 120 h post dsRNA injection) is probably caused by the loss of the effectiveness of its dsRNA and the increasing number of virus progenies. Longevity of dsRNA inside the shrimp cells is about five days (120 h) after dsRNA injection and YHV challenge (Yodmuang, et al., 2006). Therefore, to improve the effectiveness of dsRNA-C+Nter targeting PmEEA1 during YHV infection, multiple injections of dsRNA every 72 h may be performed in order to reduce shrimp mortality. Based on this study, silencing of PmEEA1 which is not lethal is possibly used as an alternative approach to prevent YHV replication. Taken together, this study demonstrated the crucial role of PmEEA1 during YHV transportation inside the cells.

Acknowledgement

We would like to thank Asst. Prof. Dr. Kusol Pootanakit for critically reading the manuscript, and Ms. Chaweewan Chimawei and Ms. Punnee Tongboonsong for technical assistance on culturing shrimp. We also would like to thank Mr. Wichai Boonsai from Choochai farm in Chonburi province and shrimp genetic improvement center in Surat Thani province, Thailand for providing shrimp samples. This work was supported by grants from Mahidol University and Thailand Research Fund (BRG5780006 to C.O., and DBG6180011 to S.P.). PP is supported by the grant DBG6180011.

References

Boonyaratpalin S, Supamattaya K, Kasornchandra J, Direkbusaracom S, Aekpanithanpong U, Chantanachooklin C. Non-occluded baculo-like virus, the causative agent of yellow head disease in the black tiger shrimp (*Penaeus monodon*). Fish Pathol. 1993;28(3):103-9.

Callaghan JSA, Gaullier JM, Toh BH, Stenmark H. The endosome fusion regulator early-endosomal autoantigen 1 (EEA1) is a dimer. Biochem J. 1999;338:539-43.

Callaghan J, Nixon S, Bucci C, Toh BH, Stenmark H. Direct interaction of EEA1 with Rab5b. Eur J Biochem. 1999;265(1):361-6.

Chavrier P, Parton RG, Hauri HP, Simons K, Zerial M. Localization of low molecular weight GTP binding proteins to exocytic and endocytic compartments. Cell. 1990;62: 317-29.

Christoforidis S, McBride HM, Burgoyne RD, Zerial M. The Rab5 effector EEA1 is a core component of endosome docking. Nature. 1999;397(6720):621-5.

Cowley JA, Dimmock CM, Wongteerasupaya C, Boonsaeng V, Panyim S, Walker PJ. Yellow head virus from Thailand and gill-associated virus from Australia are closely related but distinct prawn viruses. Dis Aquat Org. 1999;36(2):153-7.

Dereeper A, Audic S, Claverie J-M, Blanc G. BLAST-EXPLORER helps you building datasets for phylogenetic analysis. BMC Evol Biol. 2010;12:10:8.

Dereeper A, Guignon V, Blanc G, Audic S, Buffet S, Chevenet F, Dufayard JF, Guindon S, Lefort V, Lescot M, Claverie JM, Gascuel O. Phylogeny.fr: robust phylogenetic analysis for the non-specialist. Nucleic Acids Res 2008;36:465-9.

Duangsuwan P, Tinikul Y, Withyachumnarnkul B, Chotwiwatthanakun C, Sobhon P. Cellular targets and pathways of yellow head virus infection in lymphoid organ of *Penaeus monodon* as studied by transmission electron microscopy. Songklanakarin J Sci Technol. 2011;33(2):121-7.

Holen T, Amarzguioui M, Wiiger MT, Babaie E, Prydz H. Positional effects of short interfering RNAs targeting the human coagulation trigger tissue factor. Nucleic Acids Res. 2002;30(8):1757-66.

Jatuyosporn T, Supungul P, Tassanakajon A, Krusong K. The essential role of clathrin-mediated endocytosis in yellow head virus propagation in the black tiger shrimp *Penaeus monodon*. Dev Comp Immunol. 2014;44:100–10.

Lai CK, Jeng KS, Machida K, Lai MM. Hepatitis C virus egress and release depend on endosomal trafficking of core protein. J Virol. 2010;84(21):11590-8.

Lawe DC, Patki V, Heller-Harrison R, Lambright D, Corvera S. The FYVE domain of early endosome antigen 1 is required for both phosphatidylinositol 3-phosphate and Rab5 binding. J Biol Chem. 2000;275(5):3699–705.

Livak KJ, Schmittgen TD. Analysis of relative gene expression data using real-time quantitative PCR and the $2^{-\Delta\Delta CT}$ method. Methods. 2001;25:402–8.

Luo KQ, Chang DC. The gene-silencing efficiency of siRNA is strongly dependent on the local structure of mRNA at the targeted region. Biochem Biophys Res Commun. 2004;318(1):303-10.

Mayo MA. A summary of taxonomic changes recently approved by ICTV. Arch Virol. 2002;147:1655-6.

Merithew E, Stone C, Eathiraj S, Lambright DG. Determinants of Rab5 interaction with the N terminus of early endosome antigen 1. J Biol Chem. 2003;278(10):8494-500.

Mu FT, Callaghan JM, Steele-Mortimer O, Stenmark H, Parton RG, Campbell PL, McCluskey J, Yeo JP, Tock EP, Toh BH. EEA1, an early endosome-associated protein. EEA1 is a conserved alpha-helical peripheral membrane protein flanked by cysteine "fingers" and contains a calmodulin-binding IQ motif. J Biol Chem. 1995;270(22):13503-11.

Nadala ECB, Tapay LM, Cao S, Loh PC. Yellow-head virus: a rhabdovirus-like pathogen of penaeid shrimp. Dis Aquat Org. 1997;31:141-6.

Ongvarrasopone C, Chanasakulniyom M, Sritunyalucksana K, Panyim S. Suppression of PmRab7 by dsRNA inhibits WSSV or YHV infection in shrimp. Mar Biotechnol. 2008;10(4):374-81.

Ongvarrasopone C. Roshorm Y, Panyim S. A simple and cost effective method to generate dsRNA for RNAi studies in invertebrates. ScienceAsia. 2007;33:35-9.

Pascut D, Bedogni G, Tiribelli C. Silencing efficacy prediction: a retrospective study on target mRNA features. Biosci Rep. 2015;35(2) e00185.

Posiri P, Ongvarrasopone C, Panyim S. A simple one-step method for producing dsRNA from *E. coli* to inhibit shrimp virus replication. J Virol Methods. 2013;188:64-9.

Posiri P, Ongvarrasopone C, Panyim S. Improved preventive and curative effects of YHV infection in *Penaeus monodon* by a combination of two double stranded RNAs. Aquaculture 2011;314:34-8.

Posiri P, Kondo H, Hirono I, Panyim S, Ongvarrasopone C. Successful yellow head virus infection of *Penaeus monodon* requires clathrin heavy chain. Aquaculture. 2015;435:480–7.

Posiri P, Panyim S, Ongvarrasopone C. Rab5, an early endosomal protein required for yellow head virus infection of *Penaeus monodon*. Aquaculture 2016;459:43-53.

Simonsen A, Lippé R, Christoforidis S, Gaullier JM, Brech A, Callaghan J, Toh BH, Murphy C, Zerial M, Stenmark H. EEA1 links PI(3)K function to Rab5 regulation of endosome fusion. Nature. 1998;394(6692):494-8.

Sittidilokratna N, Dangtip S, Cowley JA, Walker PJ. RNA transcription analysis and completion of the genome sequence of yellow head nidovirus. Virus Res. 2008;136(1-2):157-65.

Spann KM, Donaldson RA, Cowley JA, Walker PJ. Differences in the susceptibility of some penaeid prawn species to gill-associated virus (GAV) infection. Dis Aquat Org. 2000;42:221-5.

Vonderheit A, Helenius A. Rab7 associates with early endosomes to mediate sorting and transport of semliki forest virus to late endosomes. PLoS Biol. 2005;3(7):1225-38.

Walker PJ, Bonami JR, Boonsaeng V, Chang PS, Cowley JA, Enjuanes L, Flegel TW, Lightner DV, Loh PC, Snijder EJ, Tang K. Virus taxonomy: classification and nomenclature of viruses: eighth report of the international committee on the taxonomy of viruses. Elsevier. 2005:975-9.

Yodmuang S, Tirasophon W, Roshorm Y, Chinnirunvong W, Panyim S. YHV-protease dsRNA inhibits YHV replication in *Penaeus monodon* and prevents mortality. Biochem Biophys Res Commun 2006;341(2):351-6.

Part IV: Roles of PmRab11 in controlling endosomal trafficking of YHV

Abstract

Yellow head virus (YHV) is one of the most serious pathogens that causes worldwide shrimp production loss. It enters the cells via clathrin-mediated endocytosis and utilizes small GTPase Rab proteins such as PmRab5 and PmRab7 for intracellular trafficking. In this study, molecular cloning and functional analysis of Rab11 during YHV infection were investigated. PmRab11 cDNA was cloned by Rapid amplification of cDNA ends (RACEs). It contained two forms of sizes 1200 and 1050 bp distinct at the 5' UTR. The coding region of PmRab11 was 645 bp, encoding 214 amino acids. It also demonstrated the characteristics of Rab11 proteins containing five GTP-binding domains, five Rab family domains, four Rab subfamily domains and a prenylation site at the C-terminus. Suppression of PmRab11 using dsRNA-PmRab11 either before or after YHV-challenge resulted in significant inhibition of YHV levels in the hemocytes and viral release in the supernatant in both mRNA and protein levels. In addition, the silencing effect of PmRab11 in YHV-infected shrimps resulted in a delay in shrimp mortality for at least 2 days. Immunofluorescence study showed co-localization between PmRab11 and YHV at 24-72 h post YHV-challenge. In contrast, the co-localization signals were absence in the PmRab11 knockdown hemocytes and the YHV signals accumulated at the perinuclear region at 24 h post YHV-challenge. Then, accumulation of YHV was hardly observed after 48-72 h. These results suggested that PmRab11 is required for YHV infection in shrimp.

Keyword: Exocytosis / Recycling Endosome / Viral budding / Black tiger shrimp / Viral transportation

1. Introduction

Thailand is the world's important exporter of shrimp products, especially the black tiger shrimp, *Penaeus monodon*. At present, losses of shrimp production are caused by various viral diseases. One of the major causative agents is the yellow head virus (YHV) which causes extensive and rapid mortality in black tiger shrimp [1, 2]. YHV is a positive sense, single-stranded RNA virus that is classified as a member of Gill-associated virus, belonging to the genus Okavirus, family Roniviridae in the order Nidovirales [3]. YHV genome is approximately 26 kb, containing four long open reading frames (ORF1a, ORF1b, ORF2, and ORF3) [4-6]. The enveloped rod-shaped YHV particles are 150-200 nm in length and 40-50 nm in diameter [1, 7]. The virion has prominent surface spikes and contains internal helical nucleocapsid [8, 9]. It contains three structural proteins, the transmembrane glycoproteins gp116 and gp64 are found in the viral envelope, and the nucleoprotein p20 [6, 10].

Recently, the mechanism of YHV transportation has been proposed. After YHV enters into the cell, it is transported via endosomal compartments [11, 12] and released its genome into the cytoplasm for replication. Then, the nucleocapsid is synthesized and transported to the ER-Golgi compartment where the envelope is formed [2, 13]. Finally, the enveloped viral particle is exocytosed at the plasma membrane. However, this exocytosis process of YHV out of the cells is not well understood. Normally, enveloped viruses are budded at the membrane in order to generate the envelope that surrounded the nucleocapsid [14]. In this process, the nucleocapsid is wrapped in a cellular membrane containing virus-specific envelope proteins. The viral envelope protein serves to target the host cell receptor [15]. Some viruses bud at the plasma membrane (PM), whereas others are assembled and budded at intracellular membranes along the secretory pathway such as the nuclear envelope, rough and smooth endoplasmic reticulum (ER), endosomes, intermediate or pre-Golgi compartment, Golgi cisternae and the trans-Golgi-network (TGN) [16]. However, the cytoplasmic transportation of viral genome or viral particle to plasma membrane requires the host proteins.

One of the cellular proteins that is involved in intracellular trafficking process is Rab11. Rab11 is a small GTPase protein belongs to the Ras superfamily, whose function is in transportation of the vesicles through the TGN [17], apical recycling of endosomes [18] and the perinuclear recycling of endosomal compartments before redirecting the vesicular cargo back to the apical plasma membrane. The Rab GTPase protein acts as molecular switches that shuffle between two conformational states, the GTP bound ‘active’ form and the GDP-bound ‘inactive’ form. In the active form, Rab protein is associated with membranes by hydrophobic geranylgeranyl groups at the C-terminal and recruited the specific effector molecules such as sorting adaptors, tethering factors, kinases, phosphatases and motor proteins in vesicle

transport process [18]. Our previous studies found that several Rab proteins are hijacked by YHV [11,12]. Specifically, the transportation of YHV particles required PmRab5 which is a key protein in vesicles transport to early endosome; whereas, PmRab7 is involved in YHV transportation from early endosome to late endosome and lysosome. The silencing effects of PmRab5 or PmRab7 in YHV-infected *P. monodon* inhibited YHV expression, suggesting that PmRab5 and PmRab7 are involved in intracellular trafficking of YHV [11,12].

Recently, several evidence revealed that some RNA viruses such as vesicular stomatitis virus, sendai virus, influenza A, measles virus, mumps virus, and hantavirus use Rab11-dependent pathway to assemble and release out of the cells [19-25]. Whether YHV which is also an RNA virus requires Rab11 for its transport out of the cell remains to be elucidated. Furthermore, subtractive hybridization study found that *RAB11* is one of the responsive genes that is upregulated after YHV infection [26]. Therefore, here, molecular cloning of the full-length cDNA in *P. monodon* Rab11 (PmRab11) and its probable function during YHV infection were performed.

2. Methods

2.1. Black tiger shrimp culture

Juvenile viral-free pathogen black tiger shrimps (*P. monodon*) of about 10-30 g were obtained from commercial shrimp farms in Thailand. Before use, shrimps were tested for YHV and white spot syndrome virus infection by using diagnostic strip test (Pacific Biotech Co. Ltd., Thailand). Shrimps were grown in a plastic box containing oxygenated seawater at 10 ppt salinity and were acclimatized for 2 days before the experiment was carried out. They were fed with commercial shrimp feed every day. The salt water was changed every 2 days.

2.2 Yellow head virus (YHV) stock

The infectious YHV was propagated by injection of YHV to viral-free shrimp. Then, hemolymph was collected from YHV-infected moribund shrimp and mixed with AC-1 solution (27 mM Sodium citrate, 34.33 mM NaCl, 104.5 mM Glucose, 198.17 mM EDTA, pH 7.0). Next, the hemolymph was centrifuged at 20,000 ×g for 20 min at 4 °C to remove hemocyte debris. Free YHV particles were collected by ultracentrifugation (100,000 ×g) for 1 h. Virus pellets were suspended with 150 mM NaCl and stored at -80 °C until used. The viral nucleic acid was purified from the YHV stock using high pure viral nucleic acid kit (Roache Diagnostics, Germany) and subjected to RT-PCR to determine viral titer using primers YHV_F: 5'-CAAGGACCACCTGGTACCGGTTAAGAC-3' and YHV_R: 5'-GCGGAAACGACTGACGGCTA CATTCAC-3' [11].

2.3 Molecular cloning of the full length PmRab11cDNA

The partial sequence of PmRab11 served as template to design primers for 5' and 3' RACE. 5' and 3' RACE were performed as previously described [11]. Briefly, 5' RACE method was performed by using 5Rab11_R1 specific primer (Table 1) to generate the first-strand cDNAs by Superscript III® reverse transcriptase (Invitrogen). Then, 5Rab11_R1 and PRT primers (Table 1) were used to synthesize the first PCR product which was diluted to 1:100 for used as template in the nested PCR with 5Rab11_R2 and PM1 primers (Table 1). To obtain the 3' end of PmRab11 cDNA, 3' RACE PCR was performed by PRT primer to generate the first-strand cDNAs. Then, the PCR reaction containing 3Rab11_F1 and PM-1 primers was performed. Next, two nested PCRs were performed using 3Rab11_F2 and PM-1 primers and 3Rab11_F3 and PM-1 primers (Table 1). Then, all expected bands of the 5' and 3' RACE PCR products were purified by Gel/PCR fragments extraction kit (Geneaid), cloned into pGEM-T-easy vector (Promega) and sequenced (First Base Co. Ltd, Malaysia).

The sequences of the 5' and 3' ends obtained from RACE-RCR were assembled together with the partial sequence of PmRab11 in order to obtain the full-length cDNA by using ContigExpress tool from Vector NTI Advance 11.5.1 program. Finally, a PCR was performed to amplify the full-length PmRab11 cDNA using *Taq* DNA polymerase (New England Biolabs) with primers that were designed based on the 5' and 3' end sequences, fullRab11_F and fullRab11_R primers (Table 1). PCR condition was: 95 °C for 5 min, followed by 30 cycles of 95 °C for 30 sec, 51 °C for 30 sec, 72 °C for 1.30 min. and 72 °C for 7 min. in the final step. Finally, the PCR product was purified, cloned and subjected to sequence following the protocol that was described earlier.

2.4 Sequence analysis of PmRab11

The full-length cDNA sequence of PmRab11 was analyzed against the NCBI's blastn database (http://blast.ncbi.nlm.nih.gov/Blast.cgi). The coding sequences were translated to amino acid sequence by using Expasy's tool (http://web.expasy.org/translate/). Amino acid sequence identity between PmRab11 and Rab11 proteins of other species was performed by using alignX of Vector NTI. In addition, the initiation codon and poly-A signal were identified by using ATGpr (http://atgpr.dbcls.jp/) and Poly (A) signal miner (http://dnafsminer.bic.nus.edu.sg/PolyA.html). Multiple sequence alignment of PmRab11 was performed to identify the conserved domains of Rab11 protein by using the conserved domain database of NCBI (http://www.ncbi.nlm.nih.gov/Structurecdd/ wrpsb.cgi). Prenylation site was identified by using Prenylation Prediction Suite (http://mendel.imp.ac.at/PrePS/)., Phylogenetic tree analysis of PmRab11 was performed based on the neighbor-joining methods (http://www.phylogeny.fr/)

[27]. The phylogeny was constructed by phylogeny.fr under “One Click” mode. The pipeline is already set up to run and connect well recognized programs: MUSCLE for multiple alignment, Gblocks for automatic alignment curation, PhyML for tree building and TreeDyn for tree drawing.

2.5 Construction of recombinant plasmid expressing dsRNA-PmRab11

A recombinant plasmid containing sense-loop and antisense fragment of PmRab11 was constructed using pGEM®-3zf(+) vector (Promega) as a plasmid backbone. A sense-loop fragment of size 494 bp was amplified from PmRab11 cDNA using slRab11_F and slRab11_R primers containing *Xba*I and *Kpn*I sites, respectively (Table 1). The amplification of the antisense fragment of size 404 bp was performed using asRab11_F and asRab11_R primers containing *Eco*RI/*Xho*I and *Kpn*I, respectively (Table 1). Then, the sense and antisense fragments were cloned into pGEM®-3zf(+) vector to obtain a recombinant clone containing the stem-loop fragment of PmRab11. Then, the stem-loop fragment, size 898 bp, was digested by *Hin*dIII and *Xho*I and subcloned to an expression vector, pET-17b to produce dsRNA-PmRab11 by *in vivo* bacterial expression. The region of dsRNA-PmRab11 is located at the nucleotides 124-510 from the start codon. In addition, a recombinant plasmid containing a stem-loop fragment of GFP (kindly provided by Asst. Prof. Witoon Tirasophon) was used to express dsRNA-GFP which served as an unrelated dsRNA [28].

2.6 Expression and extraction of dsRNA-PmRab11

A recombinant plasmid pET-17b containing a stem-loop of PmRab11 was transformed into *E. coli* HT115 which is a ribonuclease III mutant strain to produce dsRNA-PmRab11 [28]. dsRNA-PmRab11 expression was induced by 0.1 mM IPTG. dsRNA-PmRab11 was extracted and purified by ethanol method [29]. The quality of dsRNA was characterized by ribonuclease digestion assay using RNase A and RNase III (New England Biolab, USA). Yield of dsRNA-PmRab11 was determined by agarose gel electrophoresis and compared to the intensity of 2-log DNA marker. The intensity was measured by an ImageJ program.

2.7 Suppression of PmRab11 expression by dsRNA-PmRab11

In order to determine specific inhibition of PmRab11 expression, injection of dsRNA-PmRab11 was performed. Shrimps were injected in the muscle with 1.25 or 2.5 μg/g shrimp of dsRNA-PmRab11. Injection of unrelated dsRNA-GFP and 150 mM NaCl were used as controls. Then, hemolymph from individual shrimp was collected at 24, 48 and 72 h post-dsRNA or NaCl injection and mixed with anticoagulants I (27 mM sodium citrate, 34.33 mM NaCl, 104.5 mM glucose, 198.17 mM EDTA, pH 7.0) in a ratio 1:1. Total RNAs was extracted from hemolymph by TRI REAGENT® LS (Molecular Research Center). Semi-quantitative RT-PCR was performed to monitor the levels of PmRab11 expression using PmRab11 specific

primers. In addition, to examine the specificity of the knockdown effect of PmRab11, these cDNAs were used as templates for detection of other Rab genes expression using PmRab5 and PmRab7 specific primers (Table 1) [11, 12].

Table 1 List of synthetic oligonucleotide primers

Name	Sequences (5' → 3')	Experiments
PRT	CCGGAATTCAAGCTTCTAGAGGATCCTTTT TTTTTTTTTTTT	Reverse transcription
5Rab11_R1 5Rab11_R2	GGCCGTCTCTACATTAGTGGAGCC ATTCTGATCTGCATGATCTCTGAGC	5'RACE
3Rab11_F1 3Rab11_F2 3Rab11_F3 PM1	CACTTACACTAATGTAGAACGTTGGC GCTGATGTTAAGGCTATTCACGTGG AAGGCATTTGCAGAAAAGGAGGGAC CCGGAATTCAAGCTTCTAGAGGATCC	3'RACE
FullRab11_F FullRab11_R	GGA GAG GCG TAA CGG TTC GC TTTTTTTTTTAGAGAACAGGACAAACAGAG	Full-length
slRab11_F slRab11_R	GCTCTAGATCCACCATTGGTGTTGAG GGGGTACCGCATTTACAGTTGGTTCCAC	Sense-loop of dsRNA
asRab11_F asRab11_R	GGAATTCCCCTCGAGTCCACCATTGGTGT TGAG GGGGTACCACAATGCGGTAGATTTCTG	Antisense of dsRNA
PmRab11_F PmRab11_R	ATGGGGAACAGGGACGACGAGTATG GGCCTCTTCTGTGGGAACTGACCGC	Detection of PmRab11
PmRab5_F PmRab5_R	GGAGCTGCATTTCTGACACAGACAG GGTCTGGGCCTCTTCATATTCAACC	Detection of PmRab5
PmRab7_F PmRab7_R	ATGGCATCTCGCAAGAAGATT TTAGCAAGAGCATGCATCCTG	Detection of PmRab7
PmActin_F PmActin_R1 PmActin_R2	GACTCGTACGTCGGGCGACGA AGCAGCGGTGGTCATCACCTG CGTAGATGGGCACGGTGTGGG	Detection of PmActin
YHV_F YHV_R	CAAGGACCACCTGGTACCGGTTAAGAC GCGGAAACGACTGACGGCTACATTCAC	Detection of YHV

2.8 Suppression effect of PmRab11 during YHV infection.

To investigate the function of PmRab11 on YHV infection, shrimps were intramuscularly injected with dsRNA-PmRab11 at 1.25 µg/g shrimp. Injection of 150 mM NaCl and unrelated dsRNA-GFP were used as control groups. After 24 h, shrimps were challenged with 10^{-2} dilution of YHV (dose of YHV that leads to 100% mortality within 3 days). The hemolymph was collected at 24, 48, 72 and 96 h post YHV-challenge. Then, the hemocytes and supernatant were fractionated by centrifugation at 650 x g for 15 min. Total RNAs in hemocytes and supernatant were extracted by TRI REAGENT® and TRI REAGENT® LS (Molecular Research Center), respectively. The levels of PmRab11 and YHV expression were monitored by semi-quantitative RT-PCR using PmRab11 and YHV specific primers (Table 1), respectively. PmActin was used as an internal control. Finally, the relative expressions of PmRab11 and YHV in hemocytes were normalized by PmActin. However, PmActin cannot be amplified from the supernatant fraction, thus the YHV levels was analysed from equal amount of the total RNAs.

2.9 RNA isolation and RT-PCR

Total RNA from hemocytes or supernatant was isolated by Trizol® reagent (Molecular Research Center) following the manufacturer's procedure. The RNA concentration was measured by Nanodrop ND-1000 spectrophotometer (Nanodrop Technologies). Total RNAs (2 µg) was used as template to generate the first-strand cDNA by Improm-II™reverse transcriptase (Promega) using PRT primer (Table 1). PmRab11 expression was monitored by multiplex PCR using PmRab11-F and PmRab11-R primers and PmActin-F and PmActin-R1 primers for PmActin detection which served as an internal control. The PCR was carried out according to this condition: 95 °C for 5 min, followed by 30 cycles of 95 °C for 30 s, 61 °C for 30 s, 72 °C for 45 s and 72 °C for 7 min in the final step. Expressions of PmRab5, PmRab7 and YHV were determined according to the previous methods [11, 12]. PCR products were analyzed on 1.5% agarose gel electrophoresis. The intensity of each band after subtracting the background was quantified by using ImageJ program (Version 1.50b). The relative expression level of the gene of interest was normalized against PmActin level and expressed as an arbitrary unit.

2.10 Investigation of protein levels of YHV in hemocytes and supernatant

In order to investigate YHV protein levels in hemocytes and supernatant of the complete PmRab11 knockdown shrimp, shrimps were injected with dsRNA-PmRab11 at 1.8 µg/g shrimp by intramuscular injection. Injection of NaCl and unrelated dsRNA-GFP were used as control groups. After 24 h, shrimps were challenged with 10^{-2} dilution of YHV by intramuscular injection. The hemolymph was collected at 24, 48, 72 and 96 h post-YHV

injection. The hemolymph from 3 shrimps in the same group at the same time was pooled. Then, total RNA from 200 µl of the pooled hemolymph was extracted by TRI REAGENT® LS method and RT-PCR was performed in order to detect PmRab11 and YHV expression at mRNA level. To extract total protein for Western blot analysis, 2 ml of the pooled hemolymph was fractionated to separate hemocytes and supernatant by centrifugation at 650 x g. Total proteins from hemocytes were extracted by using 100 µl buffer T (8M urea, 2 M thiourea, 0.4% Triton X-100, 60 mM DTT, 1 mM PMSF, 1× Protease inhibitor cocktail (Sigma)). Whereas, total proteins from 100 µl of supernatant were precipitated by 10% TCA at final concentration and dissolved in 100 µl of buffer T. Then, Western blot was performed to detect YHV level in both fractions.

2.11 Western blot analysis

Hemocyte and supernatant proteins were extracted by using buffer T. The protein lysate (50 µg) was electrophoresed in 12% SDS-polyacrylamide gel (SDS-PAGE). Then, proteins were transferred from gel onto a nitrocellulose membrane (Bio-Rad) by electrophoresis with 1X transfer buffer [0.025 M Tris–HCl pH 8.3, 0.192 M glycine, and 20% (v/v) methanol]. Then the membrane was blocked with blocking solution [5% skimmed milk in 0.2 % PBST (0.2% (v/v) Tween-20 in 1X PBS)] for 2h. Next,, the membrane was soaked with 0.05% PBST (0.2% (v/v) Tween-20 in 1X PBS) containing primary antibody for 2 h. To detect YHV levels, the mouse anti-gp64 antibody was used as primary antibody at the dilution 1: 1000 in 0.2% PBST. In addition, dilution 1: 1000 in 0.2% PBST of the rabbit anti- β-tubulin primary antibody was used to detect β-tubulin which is an internal control. Then, the primary antibody was removed. The membrane was washed with 0.2 % PBST for 10 min, 3 times and incubated with blocking solution containing horseradish peroxidase-conjugated secondary antibody (Sigma) in dilution 1:5000. Then, the membrane was washed 1 time with 0.2% PBST and 3 times with 1X PBST. Finally, the signal was detected by adding the Luminata™ Forte Western HRP Substrate (Millipore Corporation) for 5 min and exposed to X-ray film. PmRab11 and β-tubulin have sizes of about 23 and 60 kDa, respectively.

2.12 Shrimp mortality assay

Suppression effects of PmRab11 with or without YHV challenge on shrimp mortality were investigated. Shrimps size about 1 g (n=15 shrimps per group) were injected with 1.25 or 2.5 µg/g shrimp of dsRNA-PmRab11 24 h with or without YHV challenge. Injection of 150 mM NaCl and unrelated dsRNA-GFP were used as controls. The experiment was performed in triplicates and the number of dead shrimps was recorded every day for 10 days.

2.13 Immunofluorescence assay of YHV and PmRab11 in YHV-infected hemocytes

Shrimp was injected with 1.8 µg/g shrimp of dsRNA-PmRab11 24 h prior to YHV challenge. The injection of 150 mM NaCl and unrelated dsRNA-GFP were used as control groups. Then, 250 µl of hemolymph was collected at 24, 48 and 72 h after YHV challenge. The hemocytes were separated by centrifugation at 550 x g for 10 min at 4 ºC. Cell pellet was resuspended in 500 µl of L-15 medium. Then, hemocytes mixture was seeded in 24 wells plate containing a coverslip and incubated at room temperature. After for 2 h., culture media was discarded and 500 µl of ice cold 4% (w/v) paraformaldehyde was added into each wells. After incubation at room temperature for 20 min, the supernatant was removed and fixed hemocytes were washed with 1X PBS for 5 min, 3 times. Then, they were permeabilized by adding 350 µl of 0.1 % (v/v) Triton X-100 in 1X PBS for 5 min. After the supernatant was discarded and the permeabilized hemocytes were proceeded to immunofluorescence staining according to the previous method [10]. Except that the rabbit polyclonal anti-Rab11 antibody (ab3612, Abcam, USA) and mouse monoclonal anti-gp64 of YHV antibody (kindly provided by Professor Paisarn Sithigorngul, Department of Biology, Faculty of Science, Srinakharinwirot University) were used. After washing, the secondary antibodies which are goat anti-rabbit IgG, Alexa Fluor® 596 and goat anti-mouse IgG, Alexa Fluor® 488 (Invitrogen) were used for detection of PmRab11 and YHV. The nuclei were stained by TO-PRO®-3 iodide (Invitrogen). Finally, a cover slip was mounted with 8 µl of ProLong antifade (Invitrogen). The slide was kept at 4 ºC until visualized under confocal microscope (Fluoview FV10i – DOC, Olympus).

2.14 Statistical analysis

The relative mRNA levels of PmRab11 normalized with PmActin were presented as mean ± standard error of mean (SEM). The statistical analysis of the relative mRNA expression levels was tested by using analysis of variance (ANOVA). A probability (P) value at less than 0.05 was used to define significant difference. Cumulative percent mortality was plotted as mean ± SEM.

3. Results

3.1. Full-length cDNA cloning and sequences analysis of PmRab11

The full-length cDNA was obtained from 5' and 3' RACE protocol. It has 2 forms of sizes 1217 and 1065 bp with the same coding sequences of 645 bp. The 5' and 3' untranslated region (UTR) have sizes 247 bp and 324 bp, respectively (Fig. 1). The sequence of PmRab11 cDNA of 2 variants were submitted into the GenBank database under the

accession number **KY241479** and **KY241480**, respectively. PmRab11 protein has size of 214 aa. The theoretical pI and molecular weight are 5.22 and 23.85 kDa, respectively. In addition, this protein shared the characteristics of Rab11 protein family when compared to others species such as five GTP biding domains (G1-G5), five Rab family domains (RabF1-5), four Rab subfamily domains (RabSF1-4) and a prenylation site that usually terminated in CC or CXC motif at the C-terminus (Fig. 2). The amino acid sequence identity showed that PmRab11 protein shared 100% amino sequence identity with Rab11 of Pacific white shrimp (*Litopenaeus vannamei*) and shared approximately 80% with Rab11 of vertebrates such as zebrafish (*Danio rerio*). In addition, the phylogenetic tree revealed that PmRab11 protein was closely related to Rab11 of vertebrate and arthropods (Fig. 3). It was not clustered with other Rab proteins including Rab5, Rab6 and Rab7. These results indicate that PmRab11 is a highly conserved protein.

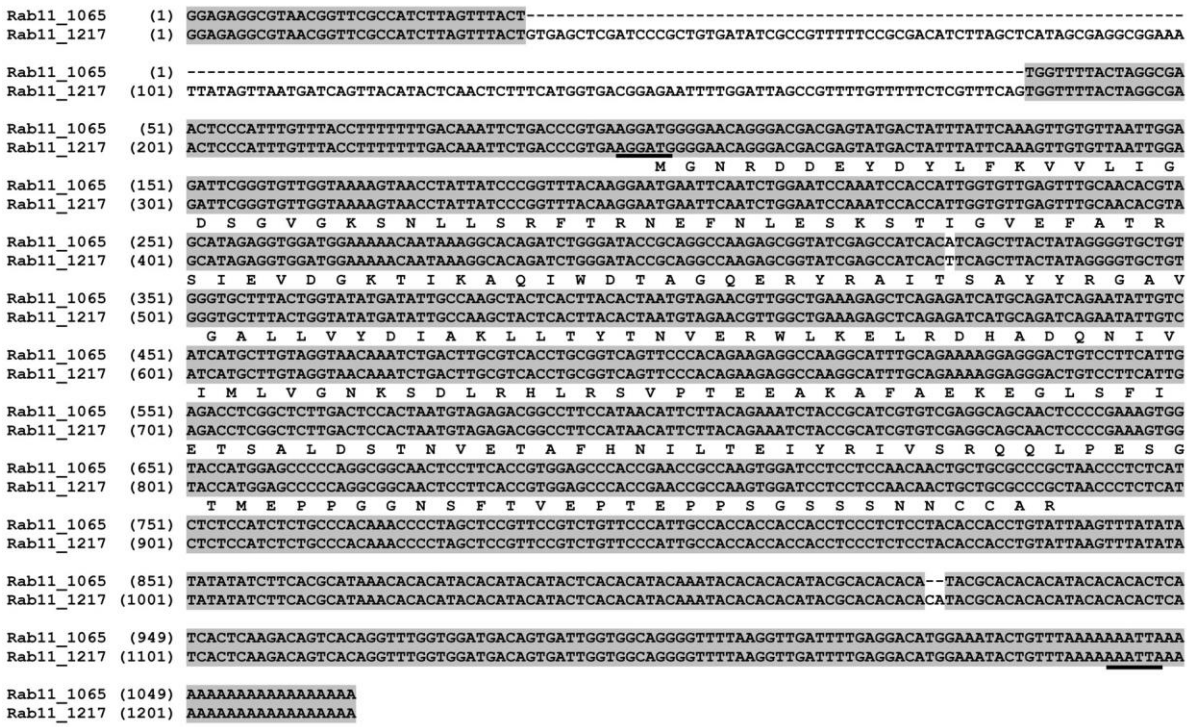

Fig. 1 Two forms of the full-length cDNAs and their deduced amino acid sequences of PmRab11. The full-length cDNA of PmRab11 has 2 forms of sizes 1217 and 1065 bp containing the open reading frame of size 645 bp. The deduced amino acid sequences of PmRab11 are represented in the capital letter under the respective codon. Kozak consensus sequences (AGGATG) and poly A signal (AAATTA) are indicated in underline.

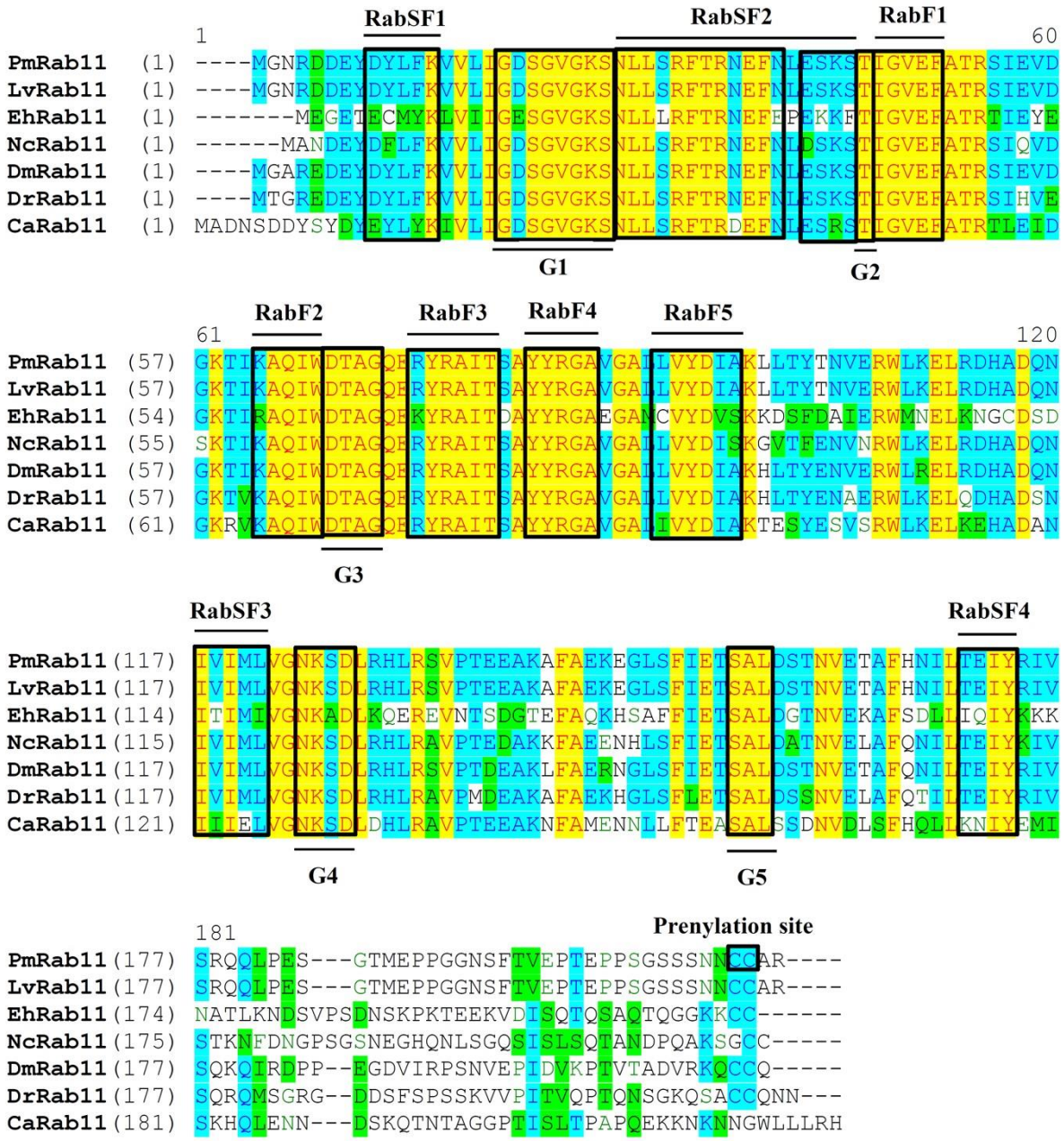

Fig. 2 Multiple sequence alignment showing conserved domains of PmRab11 compared to Rab11 proteins from other species. The conserved domains of PmRab11 shared characteristics of Rab11 among other species such as five GTP binding domains (G1-G5), five Rab family (RabF1-5) domains, four Rab subfamily (RabSF1-4) domains and a prenylation site (CCXX motif) at the C-terminus.

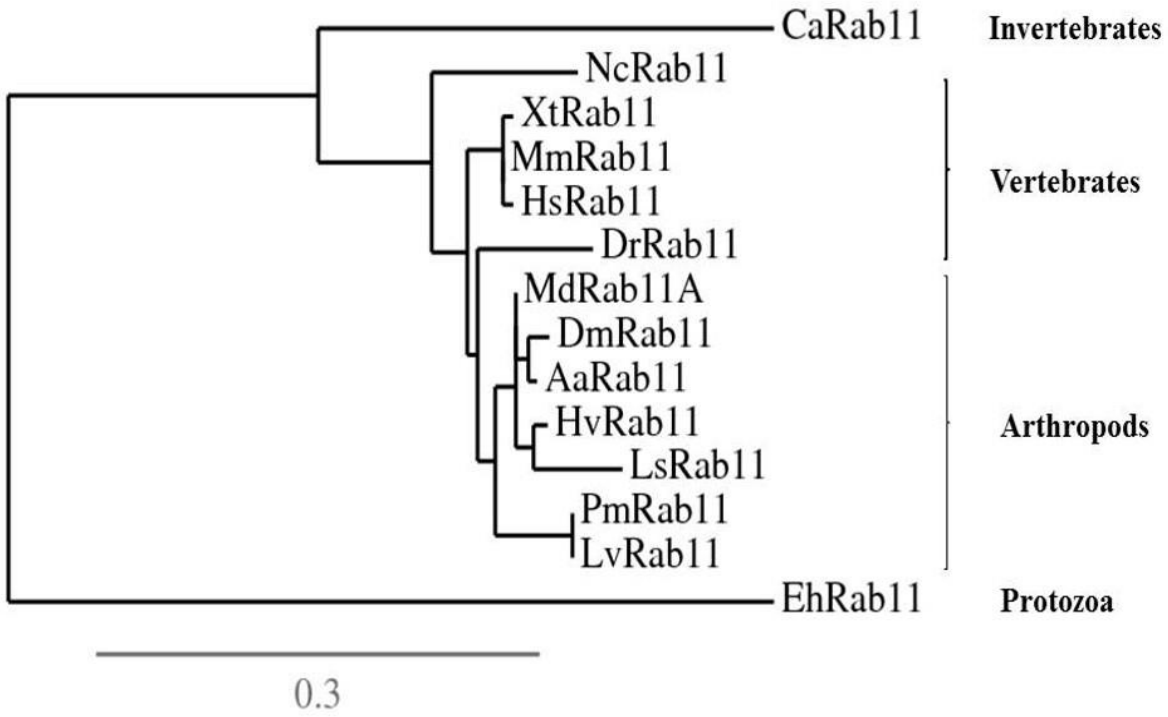

Fig. 3 Phylogenetic analysis of Rab11 of *P. monodon* compared with Rab11 of other species. The amino acid sequences of the coding region of Rab proteins of *P. monodon* and of other species were used to perform phylogenetic tree analysis based on the neighbor-joining methods by using the program from (http://www.phylogeny.fr/). The abbreviation of species is as follows: *Candida albicans (Ca), Neurospora crassa (Nc), Xenopus tropicalis (Xt), Mus musculus (Mm), Homo sapiens (Hs), Danio rerio (Dr), Microplitis demolitor (Md), Drosophila melanogaster (Dm), Aedes aegypti (Aa), Homalodisca vitripennis (Hv), Lepeophtheirus salmonis (Ls), Penaeus monodon (Pm), Litopenaeus vannamei (Lv)*, *and Entamoeba histolytica (Eh).* The accession number is in the parenthesis. PmRab11 cDNA of 2 variants were submitted into the GenBank database under the accession number KY241479 and KY241480, respectively. The abbreviation of species refers to Table 2.

Table 2 The organisms and accession number used for PmRab11 protein domain and phylogenetic analysis.

Organisms	Accession number
Candida albicans (Ca)	XP_710387
Neurospora crassa (Nc)	CAD21237
Xenopus tropicalis (Xt)	AAH41250
Mus musculus (Mm)	NP_033023.1
Homo sapiens (Hs)	CAG38733.1
Danio rerio (Dr)	AAH55141
Microplitis demolitor (Md)	EZA45322.1
Drosophila melanogaster (Dm)	NP_477170
Aedes aegypti (Aa)	XP_001659918.1
Homalodisca vitripennis (Hv)	AAT01087.1
Lepeophtheirus salmonis (Ls)	ACO11934.1
Penaeus monodon (Pm)	KY241479 and KY241480
Litopenaeus vannamei (Lv)	JN082706.1
Entamoeba histolytica (Eh)	XP_649609

*3.2 Sup*pression of PmRab11 expression by dsRNA-PmRab11

To investigate whether the PmRab11 expression can be suppressed by using RNAi approach. Double-strands RNA targeting PmRab11 was produced and injected into shrimp muscle. The expression levels of PmRab11 in dsRNA-PmRab11 injected shrimp were significantly reduced at more than 90%, 24 h post-dsRNA-PmRab11 injection at both dosages (1.25 and 2.5 μg/g shrimp) when compared to 0 h. The suppression effect of PmRab11 was maintained for at least 72 h post-dsRNA injection ($P<0.001$, n=4/time point) (Fig. 4A). As the nucleotide sequences of dsRNA-PmRab11 contained many conserved domains such as Rab family domains, Rab subfamily domains and GTP binding domains, it is possible that some of the regions of dsRNA-PmRab11 are similar to other Rab genes. Therefore, a specific inhibition to PmRab11 expression was investigated. The results showed that suppression of PmRab11 by injection of dsRNA-PmRab11 has no effect on the levels of PmRab5 and PmRab7 expression from 24-72 h post-dsRNA injection (Fig. 4B). Large standard deviation of PmRab7 after 24 h dsRNA injection may be due to varying expression of PmRab7 among shrimp samples.

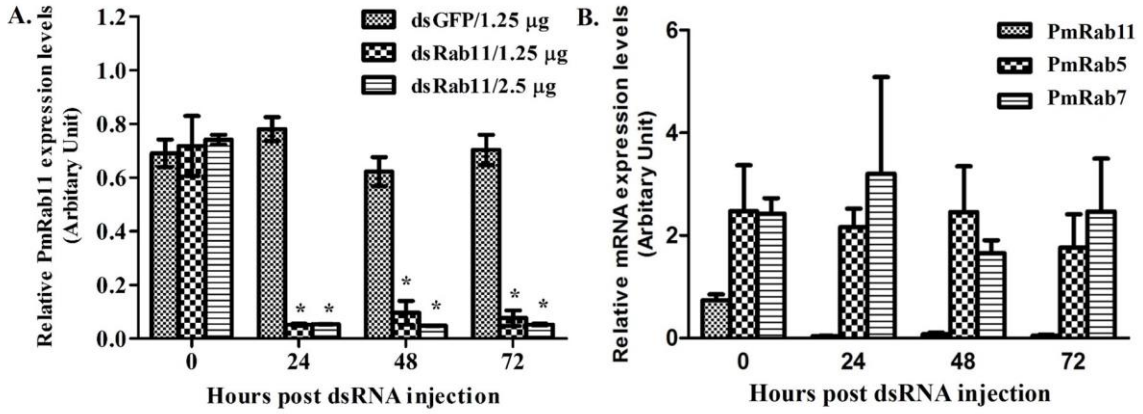

Fig. 4 Suppression of PmRab11 gene by dsRNA-PmRab11. (A) Relative mRNA expression levels of PmRab11 in shrimps injected with dsRNA-PmRab11 at 1.25 and 2.5 µg/g shrimp compared with 1.25 µg/g shrimp of dsRNA-GFP injection are presented as mean ± SEM, n=4/time point. (B) Relative mRNA expression levels of PmRab11, PmRab5 and PmRab7 are presented as mean ± SEM, n=3-4/time point. The relative mRNA expression levels of these genes were normalized with PmActin. (*) statistically significant difference between dsRNA-PmRab11 and dsRNA-GFP injected groups at each time point.

3.3 Suppression *effect of PmRab11 during YHV infection*

To investigate whether PmRab11 protein is essential for YHV transport out of the cell, suppression of PmRab11 was performed 24 h prior to YHV challenge. PmRab11 expression level in hemocytes was significantly decreased approximately 50% in shrimp injected with dsRNA-PmRab11 within 48 h post-dsRNA-PmRab11 injection. The knockdown effect of PmRab11 was increased to 75% at 72 and 96 h post-dsRNA injection ($P<0.001$, n=4/time point) (Fig. 5A). In addition, YHV levels in hemocytes and supernatant of PmRab11 knockdown group were significantly decreased from 48 to 72 h post-YHV infection when compared to NaCl injected group ($P<0.01$ for hemocytes and $P<0.001$ for supernatant, n=4/time point) (Fig. 5B, C). Notably, shrimps in 2 control groups died at 96 h while shrimp in PmRab11 knockdown group still alive at this time point.

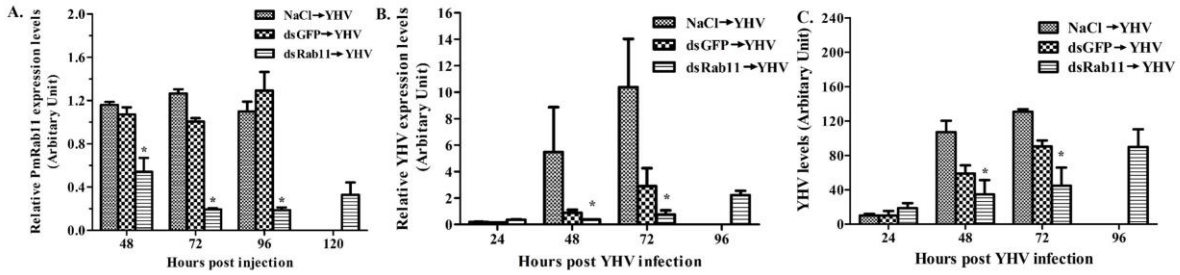

Fig. 5. Suppression of PmRab11 during YHV infection. (A) Relative expression of PmRab11 was detected from hemocytes of shrimps injected with 1.25 µg/g shrimp of dsRNA-PmRab11 followed by YHV, compared with dsRNA-GFP and NaCl injected shrimps at various time courses. Relative mRNA expression levels of YHV in hemocytes (B) and YHV levels in supernatant (C) was monitored. The data are presented as mean ± SEM, n=4/time point. (*) statistically significant difference between dsRNA-PmRab11 and NaCl injected groups at each time point.

Protein analysis revealed that an envelope glycoprotein gp64 of YHV cannot be detected in the hemocytes and supernatant of the PmRab11 knockdown group from 24-72 h post-YHV challenge. At 96 h post-YHV challenge, low levels of YHV can be detected in both hemocytes and supernatant while shrimp in both control groups died at this time point. On the other hand, high YHV level can be detected in hemocytes and supernatant of NaCl-injected groups at 48 and 72 h. However, low level of YHV expression can still be observed in dsRNA-GFP injected group at 48 h and even increased at 72 h post-YHV infection (Fig. 6A, B, Supplementary Fig. 1).

3.4 Shrimp mortality assay

To investigate the suppression effect of PmRab11 on shrimp mortality, shrimp was injected with 1.25 µg/g shrimp of dsRNA-PmRab11. Then, shrimp mortality was recorded for 10 days. The results showed that injection of dsRNA-PmRab11 caused 100% shrimp death at day 7. In contrast, injection of 1.25 µg/g shrimp dsRNA-GFP and NaCl resulted in less than 10 % shrimp mortality within 10 days (Fig. 7A). In addition, the cumulative mortalities of shrimp that injected with dsRNA-PmRab11 at 1.25 µg/g shrimp followed by YHV challenge was delayed at least 2 days when compared to the control groups (Fig. 7B).

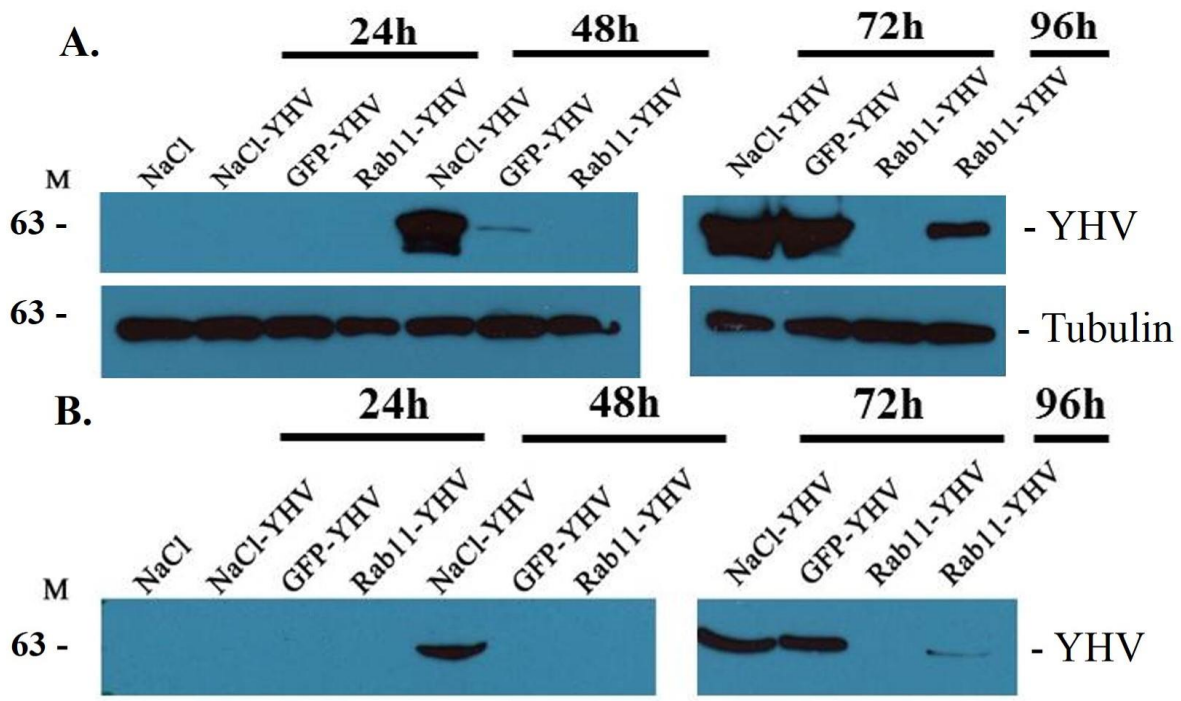

Fig. 6 Suppression effect of PmRab11 on YHV protein levels. Western blot analysis showed protein levels of YHV in hemocytes (A) and supernatant (B) of shrimps injected with 1.8 µg/g shrimp of dsRNA-PmRab11 followed by YHV, compared with dsRNA-GFP and NaCl injected shrimps at various times. Monoclonal antibody to YHV-gp64 was used to detect YHV while tubulin was used as a control.

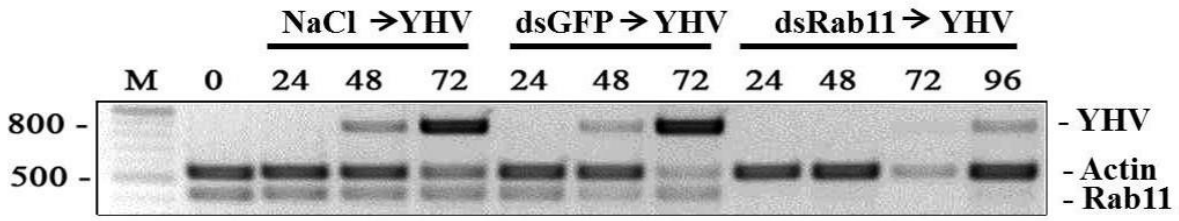

Supplementary Fig. 1 Suppression effect of PmRab11 on YHV mRNA levels. Gel electrophoresis showed the expression levels of PmRab11, YHV and PmActin of shrimps injected with 1.8 µg/g shrimp of dsRNA-PmRab11 followed by YHV as compared to dsRNA-GFP and NaCl injected shrimp at various time points. The same samples that used for Western blot analysis in Fig. 6A. M represents 2 log DNA marker.

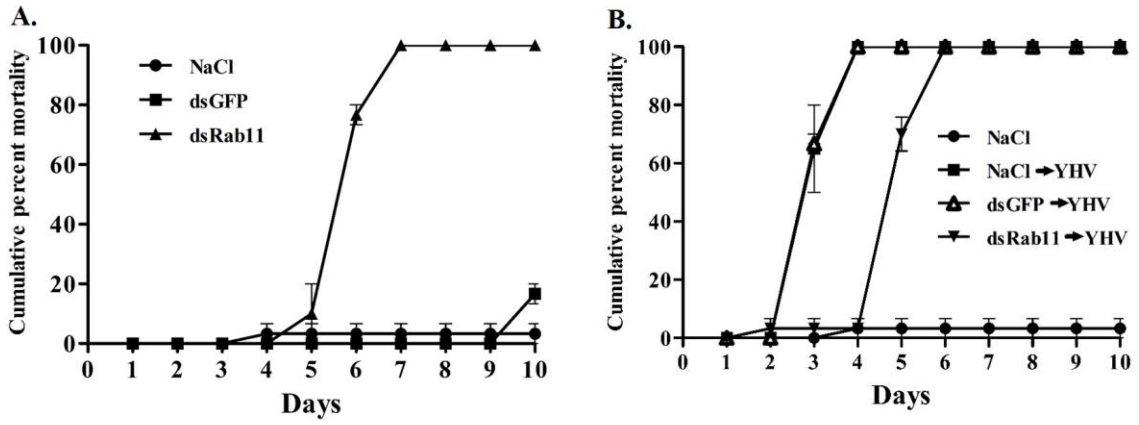

Fig. 7 Cumulative percent mortality of PmRab11-knockdown shrimp with or without YHV challenge. The cumulative percent mortality of shrimps injected with 1.25 µg/g shrimp of dsRNA-PmRab11 compared to injections of dsRNA-GFP or NaCl followed by absence (A) or presence (B) of YHV challenge were investigated. The data are presented as mean ± SEM, n=45/experiment.

3.5 Co-localization of YHV and PmRab11 in YHV infected hemocytes.

The PmRab11 protein level in individual hemocytes was observed using immunofluorescence assay. Shrimp was injected with dsRNA-PmRab11 at 1.8 µg/g shrimp, then PmRab11 protein levels were detected at various time points. The result demonstrated that the PmRab11 protein was gradually decreased from 24-96 h post-dsRNA-PmRab11 injection (Fig. 8A). Second, the localization of PmRab11 and YHV was investigated by injection with dsRNA-PmRab11 at 1.8 µg/g shrimp and followed by YHV. The low signals of PmRab11 protein and YHV glycoprotein 64 (gp64) can be observed inside the hemocytes of PmRab11 knockdown shrimp at 24 h post-infection (Fig. 8B). In contrast, high signals of PmRab11 and gp64 can be detected in shrimp that was injected with dsRNA-GFP and NaCl followed by YHV challenge at this time point. In addition, co-localization of PmRab11 and YHV can be clearly observed at 24 to 72 h post-infection in hemocytes of both control groups. In contrast, the PmRab11 knockdown group showed low level of YHV and PmRab11 at these time points (Fig. 8C, D).

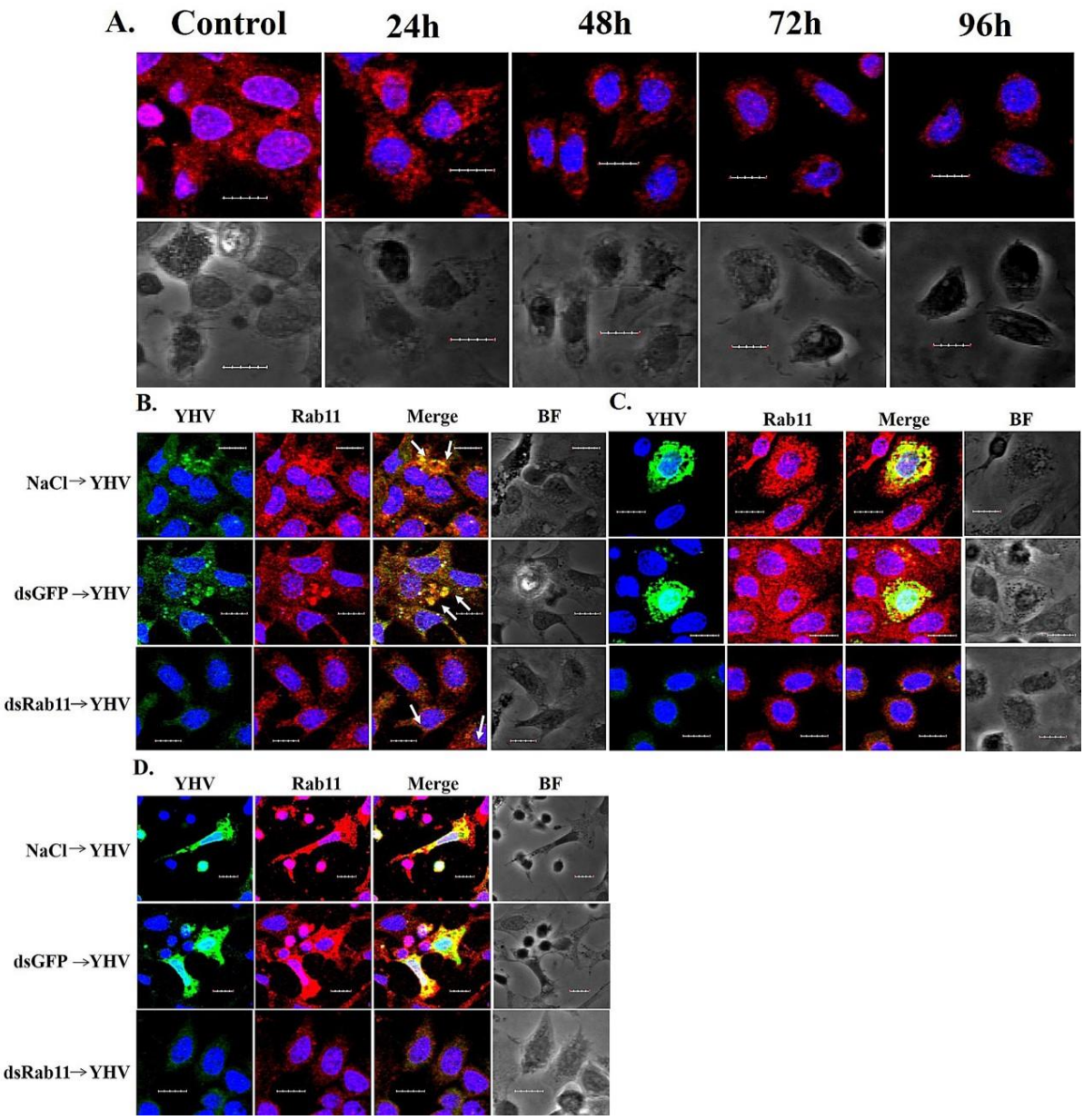

Fig. 8 Co-localization of PmRab11 and YHV in YHV-infected hemocytes. The pictures show hemocytes during PmRab1- knockdown at various times (A). Co-localization of PmRab11 and YHV was investigated at 24 h (B), 48 h (C) and 72 h (D) post-YHV challenge. Red, green and blue colours represented PmRab11, YHV-gp64 and nucleus, respectively. Arrow indicated the co-localization signal of PmRab11 and YHV. Scale is 10 μm.

4. Discussion

At present, the mechanisms of YHV internalization and transportation inside the cell have been proposed. The viral glycoprotein gp116 on YHV envelope binds to the YHV binding protein, PmYRP65 on the cell membrane [30,31] then internalizes into the cell via clathrin-dependent endocytosis [32,33]. After that, the vesicle containing YHV particle is transported to the early and late endosome by Rab5 and Rab7, respectively [11,12] before the viral genome is released to the cytoplasm for replication and translation. Electron microscopy revealed that enveloped YHV virion is formed at TGN [2,13]. However, the mechanism of the transport of YHV from TGN to PM is not well understood. The earlier studies of other (+) ssRNA viruses such as flaviviruses and coronaviruses found that viral budding from TGN to PM is dependent on Rab11-mediated pathway through cytoskeleton network [34,35]. Interestingly, Rab11 of YHV-infected shrimp was shown to be upregulated after 24 h of infection [26]. A comparative proteomic analysis showed that the protein disulfide isomerase (PDI) was increased during YHV infection [36]. PDI is normally localized in the lumen of ER catalyzing the formation and isomerization of disulfide bonds [37]. It has also been reported to be involved in the folding and assembly of viral proteins in the ER [38]. The YHV structural proteins, gp116 and gp64, contain 26 and 24 cysteine residues, respectively, suggesting a possible role for PDI to form inter- and intra-molecular disulfide bonds during the folding of these viral proteins [13]. Therefore, it is possible that PmRab11 also plays a role in the transport of YHV out of the cell.

Two forms of PmRab11 cDNAs of sizes 1200 and 1050 bp were found to be different at the 5' UTR. This may be because the gene was transcribed from different alleles. The existence of the two variants of PmRab11 was confirmed by amplification of the full-length cDNA and by 5' RACE (Supplementary Fig. 2). The nucleotide deletion at the 5' end of the two forms has not been observed for other Rab11. However, at least three isoforms of Rab11 proteins such as Rab11A, Rab11B and Rab11C (occasionally called Rab25) have been reported and shown to localize differently at specific organelles. Rab11A and B localize at the Golgi, RE and early endosomes and may be involved in membrane trafficking pathway by transportation of the target protein from TGN/RE to plasma membrane [39]. While Rab11C is expressed only in certain epithelial cells and may be involved in vesicular trafficking from recycling endosome to plasma membrane [39, 40]. The deduced PmRab11 protein shared a characteristic signature of Rab11 with other species and closely related to Rab11 in invertebrate, especially in shrimp species (100% amino acid sequence identity with Rab11 of Pacific white shrimp, *Litopenaeus vannamei*). The PmRab11 function was characterized by

using RNAi approach. Knockdown of PmRab11 by dsRNA-PmRab11 specifically inhibited PmRab11 expression within 24 h but not PmRab5 and PmRab7 expression. Suppression of PmRab11 led to 100 % shrimp death at day 7. Similar results were demonstrated in the knockdown effect of endogenous genes that are involved in the trafficking process in shrimp including PmRab5, PmRab7 and clathrin heavy chain [11,12,33]. In addition, Rab11 is an essential gene in the regulation of transportation of the endocytosed proteins [18,41,42].

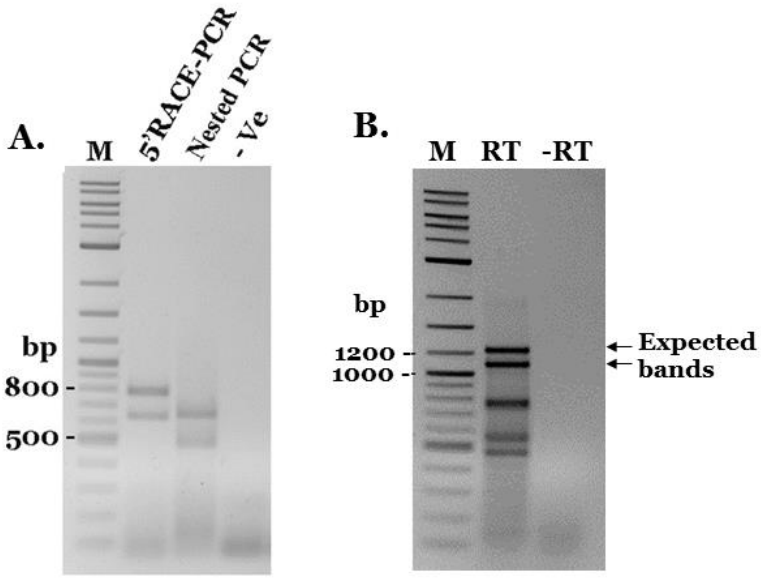

Supplementary Fig. 2 Amplification of the 5' end by 5' RACE (A) and of the full-length cDNA of PmRab11 (B) by RT-PCR. The PCR products were analysed on agarose gel electrophoresis. An expected, two bands are seen for 5' RACE and nested PCR products (A). Two bands of sizes approximately 1200 and 1050 bp were observed in the RT-PCR of the full-length cDNA of PmRab11 (B). Lane M is 2-log DNA marker.

The role of Rab11 during YHV infection was investigated by suppression of PmRab11. The PmRab11 expression was suppressed approximately 50% at 48 h post-dsRNA injection (or 24 h post-YHV infection) (Fig. 5A). This is in contrast to the result of PmRab11 knockdown alone (without YHV infection) that PmRab11 expression was inhibited more than 90% at this time point (Fig. 4A). Interestingly, subtractive hybridization found that Rab11 was upregulated at 24 h post-YHV infection [26]. Therefore, it is possible that an incomplete PmRab11 knockdown is caused by upregulation of PmRab11 expression in response to YHV infection. In addition, viral titre inside and outside the cell was determined by semi-quantitative RT-PCR. The results showed that YHV levels in hemocytes and supernatant of PmRab11 knockdown group were significantly decreased from 48 to 72 h post-YHV infection when compared to the NaCl-injected group. Notably, not only PmRab11 expression was recovered at

120 h post-dsRNA injection, but also the YHV released was increase at this time point. This relationship demonstrated that PmRab11 is required for YHV infection. Similar results were observed in the plaque assay of virus infected cells that were treated with siRNA targeting Rab11 such as hantavirus [25], Influenza A [43], and hepatitis C virus [44].

To estimate the YHV's protein level in hemocytes and supernatant, Western blot was performed using antibody against YHV-gp64 which is one of the viral glycoproteins on YHV envelope. Unfortunately, our Rab11 antibody cannot be used to detect Rab11 protein by Western blot under the denaturing condition, suggesting that it required the native structure of epitopes. The results revealed that YHV protein level cannot be observed in both fractions of all experimental groups at 24 h post-dsRNA injection (Fig. 6). Previous study in PmRab5 knockdown during YHV infection found that YHV is internalized and transported via PmRab5 from PM to early endosome around 10 min – 6 h post-infection [10]. After that, viral replication occurred and nucleocapsid was found in cytoplasm at 24 h post-YHV infection [13]. Thus, the, low level of YHV-gp64 protein at the early phase of infection and the failure to detect the protein in Western blot at this time point. At 48 h post-dsRNA injection, high YHV protein level in the NaCl-injected group can be observed. Whereas, the dsRNA-GFP injected group showed low YHV protein level at this time point. Many studies found that the innate antiviral immunity in invertebrates including shrimp was induced by any dsRNA in a sequence-independent manner [45,46]. High levels YHV protein in hemocytes and supernatant of the NaCl injected group and dsRNA-GFP injected group could be observed at 72 h. In contrast, YHV levels could not be detected in both fractions of PmRab11 knockdown group at 24-72 h post-dsRNA injection. For the (+) ssRNA virus including YHV, the replication process occurs in the cytoplasm [47] and the viral envelop glycoproteins are co-translationally inserted into ER membranes. Then, modification of the glycoproteins occurs during their passage through the secretory pathway. For example, all structural proteins of members of the Flaviviridae family such as hepatitis C and dengue virus are co-translated as a single polyprotein and are inserted into the ER membrane [48]. An individual glycoprotein is generated by proteolytic cleavage and the RNA-binding core protein that is known as the nucleocapsid is assembled within the ER, and transported to Golgi apparatus. It is possible that these events may also occur for YHV which is one of the (+) ssRNA. The single polyprotein containing gp116 and gp64 is co-translated and inserted into the ER membrane. The proteolytic cleavage resulted in individual gp116 and gp 64 that exposed the N-terminal domain to the cytosolic side [7]. Then, the viral nucleocapsid and glycoproteins are transported to the Golgi apparatus for maturation. At TGN, the budding of YHV envelope virion can be observed under electron microscope [2, 13]. Normally, Rab11 is involved in the vesicle transport from TGN to the PM [49]. After PmRab11 knockdown, YHV

cannot bud and has no target organelle to transport to. Therefore, the YHV protein in Golgi network might be transported to lysosome for degradation. However, the mechanism in this process remains to be elucidated. Similar results can be observed in the dengue virus [50]. In addition, the mortality assay revealed that injection of dsRNA-PmRab11 can delay shrimp mortality when compared to both control groups. Similar results of the delay in shrimp mortalities can be demonstrated for the knockdown effects of other Rab proteins including PmRab7 and PmRab5 during YHV infection [11,12].

Co-localization between YHV and PmRab11 was observed by immunofluorescence assay. The results showed co-localization between YHV-gp64 and PmRab11 was seen from 24-72 h post-YHV injection in both control groups (Fig. 8). Accumulation of YHV can be found at the PM of hemocytes. Similar results were also seen from other viruses that used Rab11-dependent pathway in the transportation. such as sendai virus [20], influenza A virus [21,22,43], measles virus [23], mumps virus [24], hantavirus [25], hepatitis C virus [44] and dengue virus [50]. In contrast, low level of co-localization signals between PmRab11 and YHV can be observed in the perinuclear region at 24-72 h in the PmRab11 knockdown group. This is supported by an overexpression of Rab11 dominant negative mutant in hepatitis C, hantavirus or dengue infected cell. The virus was accumulated at the perinuclear region that was identified as TGN [25,44,50]. In addition, overexpression of Rab11 constitutively active mutant in influenza A virus infection showed that Rab11 is aggregated with vRNP at the perinuclear region and cannot be transported out of the cell [21,22,23]. These evidence suggested a possible role of Rab11 in transportation of YHV.

Other Rab such as Rab6 has been shown to play important roles in virus infection of shrimp. Rab6 is involved in the regulation of phagocytosis against white spot syndrome virus (WSSV) infection through the interaction with the WSSV envelope protein VP466, β-actin, and tropomyosin which could activate the GTPase activity of Rab6 and subsequently induce the rearrangement of actin fibers in invertebrates [51,52]. An increase in Rab6 activity was demonstrated in WSSV resistant shrimp. Silencing of Rab6 by a specific siRNA significantly increased WSSV replication in shrimp [53,54]. In addition, Rab6 plays an important role in the regulation of phagocytosis against bacterial infection in *Marsupenaeus japonicus* [55].

In summary, the virus budding process and its cellular trafficking inside the cell are core study in virology, Therefore, the identification of the routes for viral infection and release including the discovery of the cellular and viral components involved in various processes are essential. These are an important knowledge that will provide insights into host-pathogen interaction in order to improve a potential approach for therapeutic intervention against viral diseases.

References

[1] Boonyaratpalin S, Supamataya K, Kasornchandra J, Direkbusarakom S, Aekpanithanpong U, Chantanachookhin C. Non-occluded baculo-like virus the causative agent of yellow-head disease in the black tiger shrimp *Penaeus monodon*. Fish Pathol 1993;28:103-109.

[2] Chantanachookin C, Boonyaratpalin S, Kasornchandra J, Direkbusarakom S, Ekpanithanpong U, Supamataya K, Siurairatana S, Flegel TW. Histology and ultrastructure reveal a new granulosis-like virus in *Penaeus monodon* affected by yellow-head disease. Dis Aquat Organ 1993;17:145-157.

[3] Walker PJ, Bonami JR, Boonsaeng V, Chang PS, Cowley JA, Enjuanes L, Flegel TW, Lightner DV, Loh PC, Snijder EJ, Tang K. Virus taxonomy: classification and nomenclature of viruses: eighth report of the international committee on the taxonomy of viruses. Elsevier. 2005:975-9.

[4] Sittidilokratna N, Hodgson RAJ, Cowley JA, Jitrapakdee S, Boonsaeng V, Panyim S, Walker PJ. Complete ORF1b gene sequence indicates yellow head virus is an invertebrate nidovirus. Dis Aquat Organ 2002;50:87–93.

[5] Sittidilokratna N, Phetchampai N, Boonsaeng V, Walker PJ. Structural and antigenic analysis of the yellow head virus nucleocapsid protein p20. Virus Res 2006;116:21-29.

[6] Jitrapakdee S, Unajak S, Sittidilokratna N, Hodgson RA, Cowley JA, Walker PJ, et al. Identification and analysis of gp116 and gp64 structural glycoproteins of yellow head nidovirus of *Penaeus monodon* shrimp. J. Gen. Virol 2003;84:863-873.

[7] Dhar AK, Cowley JA, Hasson KW, Walker PJ. Genomic organization, biology, and diagnosis of taura syndrome virus and yellow head virus of penaeid shrimp. Adv Virus Res 2004;63:353–421.

[8] Wongteerasupaya C, Vickers J, Sriurairatana S, et al. A non-occluded, systemic baculovirus that occurs in cells of ectodermal and mesodermal origin and causes high mortality in the black tiger prawn *Penaeus monodon*. Dis Aquat Organ 1995;21:66–77.

[9] Nadala ECB, Tapay LM, Loh PC. Yellow head virus: a rhabdovirus-like pathogen of penaeid shrimp. Dis Aquat Organ 1997;31:141–146.

[10] Soowannayan C, Flegel TW, Sithigorngul P, et al. Detection and differentiation of yellow head complex viruses using monoclonal antibodies. Dis Aquat Organ 2003;57:193–200.

[11] Posiri P, Panyim S, Ongvarrasopone C. Rab5, an early endosomal protein required for yellow head virus infection of *Penaeus monodon*. Aquaculture 2016;459:43-53.

[12] Ongvarrasopone C, Chanasakulniyom M, Sritunyalucksana K, Panyim S. Suppression of PmRab7 by dsRNA inhibits WSSV or YHV infection in shrimp. Mar Biotechnol 2008;10:374-381.

[13] Duangsuwan P, Tinikul Y, Withyachumnarnkul B, Chotwiwatthanakun C, Sobhon P. Cellular targets and pathways of yellow head virus infection in lymphoid organ of *Penaeus monodon* as studied by transmission electron microscopy. Songklanakarin J Sci Technol 2011;33:121-127.

[14] Dubois-Dalcq M, Holmes KV, Rentier B, Kingsbury DW. Assembly of enveloped RNA viruses. Springer-Verlag KG, Vienna, Austria 2013.

[15] Wimmer, E. Cellular receptors for animal viruses. Cold Spring Harbor Laboratory Press, Plainview, New York, USA. Volume 28, 1994.

[16] Welsch S, Müller B, Kräusslich HG. More than one door - Budding of enveloped viruses through cellular membranes. FEBS Lett 2007;581:2089-2097.

[17] Chen W, Feng Y, Chen D, Wandinger-Ness A. Rab11 is required for trans-golgi network-to-plasma membrane transport and a preferential target for GDP dissociation inhibitor. Mol Biol Cell 1998;9:3241-3257.

[18] Stenmark H. Rab GTPases as coordinators of vesicle traffic. Nat Rev Mol Cell Biol 2009;10:513-525.

[19] Das SC, Nayak D, Zhou Y, Pattnaik AK. Visualization of intracellular transport of vesicular stomatitis virus nucleocapsids in living cells. J Virol 2006;80:6368–6377.

[20] Chambers R, Takimoto T. Trafficking of Sendai virus nucleocapsids is mediated by intracellular vesicles. PLoS One 2010;5:e10994.

[21] Eisfeld AJ, Kawakami E, Watanabe T, Neumann G, Kawaoka Y. Rab11A is essential for transport of the influenza virus genome to the plasma membrane. J Virol 2011;85:6117– 6126.

[22] Amorim MJ, Bruce EA, Read EK, Foeglein A, Mahen R, Stuart AD, Digard P. A Rab11- and microtubule-dependent mechanism for cytoplasmic transport of influenza A virus viral RNA. J Virol 2011;85:4143-4156.

[23] Nakatsu Y, Ma X, Seki F, Suzuki T, Iwasaki M, Yanagi Y, Komase K, Takeda M. Intracellular transport of the measles virus ribonucleoprotein complex is mediated by Rab11A-positive recycling endosomes and drives virus release from the apical membrane of polarized epithelial cells. J Virol 2013;87:4683-4693.

[24] Katoh H, Nakatsu Y, Kubota T, Sakata M, Takeda M, Kidokoro M. Mumps virus is released from the apical surface of polarized epithelial cells, and the release is facilitated by a Rab11-mediated transport system. J Virol 2015;89:12026-12034.

[25] Rowe RK, Suszko JW, Pekosz A. Roles for the recycling endosome, Rab8, and Rab11 in hantavirus release from epithelial cells. Virology 2008;382:239-249.

[26] Prapavorarat A, Pongsomboon S, Tassanakajon A. Identification of genes expressed in response to yellow head virus infection in the black tiger shrimp, Penaeus monodon, by suppression subtractive hybridization. Dev Comp Immunol 2010;34:611-617.

[27] Dereeper A, Guignon V, Blanc G, Audic S, Buffet S, Chevenet F, et al. Phylogeny.fr: robust phylogenetic analysis for the non-specialist. Nucleic Acids Res 2008;36:W465-W469.

[28] Ongvarrasopone C, Roshorm Y, Panyim S. A simple and cost effective method to generate dsRNA for RNAi studies in invertebrates. ScienceAsia 2007;33:035-039.

[29] Posiri P, Ongvarrasopone C, Panyim S. A simple one-step method for producing dsRNA from *E. coli* to inhibit shrimp virus replication. J Virol Methods 2013;188:64-69.

[30] Assavalapsakul W, Smith DR, Panyim S. Identification and characterization of a *Penaeus monodon* lymphoid cell-expressed receptor for the yellow head virus. J Gen Virol 2006;80:262-269.

[31] Assavalapsakul W, Kiem HKT, Smith DR, Panyim S. Silencing of PmYPR65 receptor prevents yellow head virus infection in *Penaeus monodon*. Virus Res 2014;189:133-135.

[32] Jatuyosporn T, Supungul P, Tassanakajon A, Krusong K. The essential role of clathrin-mediated endocytosis in yellow head virus propagation in the black tiger shrimp *Penaeus monodon*. Dev Comp Immunol 2014;44:100-110.

[33] Posiri P, Kondo H, Hirono I, Panyim S, Ongvarrasopone C. Successful yellow head virus infection of *Penaeus monodon* requires clathrin heavy chain. Aquaculture 2015;435:480–487.

[34] Welsch S, Müller B, Kräusslich HG. More than one door - Budding of enveloped viruses through cellular membranes. FEBS Lett 2007;581:2089-2097.

[35] Weissenhorn W, Poudevigne E, Effantin G, Bassereau P. How to get out: ssRNA enveloped viruses and membrane fission. Curr Opin Virol 2013;3:159-167.

[36] Bourchookarn A, Havanapan P-O, Thongboonkerd V, Krittanai C. Proteomic analysis of altered proteins in lymphoid organ of yellow head virus infected *Penaeus monodon*. BBA-Proteins Proteom 2008;1784:504-511.

[37] Noiva R, Lennarz WJ. Protein disulfide isomerase. A multifunctional protein resident in the lumen of the endoplasmic reticulum. J Biol Chem 1992;267:3553-3566.

[38] Guichard A, Nizet V, Bier E, Doms RW, Lamb RA, Rose JK, Helenius A. Folding and assembly of viral membrane proteins. Virology 1993;193:545-562.

[39] Hutagalung AH, Novick PJ. Role of Rab GTPases in membrane traffic and cell physiology. Physiol Rev 2011;91(1):119-149.

[40] Goldenring JR, Shen KR, Vaughan HD, Modlin IM. Identification of a small GTP-binding protein, Rab25, expressed in the gastrointestinal mucosa, kidney and lung. J. Biol. Chem 1993;268(25):18419-22.

[41] Grant, B. D. and Donaldson, J. G..athways and mechanisms of endocytic recycling. Nat. Rev Mol Cell Biol 2009;10:597-608.

[42] van Ijzendoorn, S. C. D. Recycling endosomes. J Cell Sci 2006;119:1679-1681.

[43] Bruce EA, Digard P, Stuart AD. The Rab11 pathway is required for influenza A virus budding and filament formation. J Virol 2010;84:5848–5859

[44] Coller K, Heaton N, Berger K, Cooper J, Saunders J, Randall G. Molecular Determinants and Dynamics of Hepatitis C Virus Secretion. PLoS Pathog 2012;8:e1002466.

[45] Robalino J, Bartlett T, Shepard E, Prior S, Jaramillo G, Scura E, Chapman RW, Gross PS, Browdy CL, Warr GW. Double-stranded RNA induces sequence-specific antiviral silencing in addition to nonspecific immunity in a marine shrimp: convergence of RNA interference and innate immunity in the invertebrate antiviral response? J Virol 2005;79:13561-13571.

[46] Robalino J, Browdy CL, Prior S, Metz A, Parnell P, Gross P, Warr G. Induction of antiviral immunity by double-stranded RNA in a marine invertebrate. J Virol 2004;78:10442-10448.

[47] Harak C, Lohmann V. Ultrastructure of the replication sites of positive-strand RNA viruses. Virology 2015;497:418–433.

[48] Mukhopadhyay S, Kuhn R.J, Rossmann M.G. A structural perspective of the flavivirus life cycle. Nat Rev Microbiol 2005;3:13–22.

[49] Chen W, Feng Y, Chen D, Wandinger-Ness A. Rab11 is required for trans-golgi network-to-plasma membrane transport and a preferential target for GDP dissociation inhibitor. Mol Biol Cell 1998;9:3241-3257.

[50] Acosta EG, Castilla V, Damonte EB. Differential requirements in endocytic trafficking for penetration of dengue virus. PLoS One 2012;7:e44835.

[51] Ye T, TangW, Zhang X. Involvement of Rab6 in the regulation of phagocytosis against virus infection in invertebrates. J Proteome Res 2012a;11:4834–46.

[52] Ye T, Zong R, Zhang X. The role of white spot syndrome virus (WSSV) VP466 protein in shrimp antiviral phagocytosis. Fish Shellfish Immunol 2012b;33:350–8.

[53] Wu W, Zhang X. Characterization of a Rab GTPase up-regulated in the shrimp *Peneaus japonicus* by virus infection. Fish and Shellfish Immunol 2007; 23:438-445.

[54] Wu W, Zong R, Xu J, Zhang X. Antiviral phagocytosis is regulated by a novel Rab-dependent complex in shrimp *Penaeus japonicus*. J Proteome Res 2008;7: 424–31.

[55] Zong R, Wu W, Xu J, Zhang X. Regulation of phagocytosis against bacterium by Rab GTPase in shrimp *Marsupenaeus japonicus*. Fish Shellfish Immunol 2008;25:258–63.

ผลงานวิจัยที่ได้

ผลงานวิจัยที่ตีพิมพ์ในวารสารวิชาการระดับนานาชาติ

1. Posiri P, Kondo H, Hirono I, Panyim S, **Ongvarrasopone C.** (2015) Successful yellow head virus infection of *Penaeus monodon* requires clathrin heavy chain. Aquaculture. 435;480-7. Impact factor 2015: 1.893, Q1

2. Posiri P, Panyim S, **Ongvarrasopone C.** (2016) Rab5, an early endosomal protein required for yellow head virus infection of *Penaeus monodon*. Aquaculture. 459: 43-53. Impact factor 2016: 2.57, Q1

3. Kongprajug A., Panyim S., **Ongvarrasopone, C.** Suppression of PmRab11 inhibits YHV infection in *Penaeus monodon*. Fish Shellfish Immunology 2017;66:433-444. Impact factor 2017: 3.185, Q1

ผลงานวิจัยที่ส่งตีพิมพ์ในวารสารวิชาการระดับนานาชาติ

Posiri P, Thongsuksangcharoen S, Chaysri N, Panyim S, **Ongvarrasopone C.** PmEEA1, the early endosomal protein is employed by YHV for successful infection in *Penaeus monodon*. Manuscript submission.

กิจกรรมอื่น ๆที่เกี่ยวข้อง

การนำเสนอผลงานวิจัยในที่ประชุมวิชาการ

1. Thongsuksangcharoen S, Panyim S, Ongvarrasopone C. Molecular cloning and sequence analysis of *Penaeus monodon* Rab9. Proceedings for the 5th International Biochemistry and Molecular Biology Conference on Biochemistry for a Sustainable Future. May 26-27, 2016 at Prince of Songkla University, Thailand. p493-496. (Proceeding, poster presentation).

2. Kongprajug A, Panyim S, Ongvarrasopone C. Molecular cloning of the full length cDNA of Rab11 in *Penaeus monodon*. Mahidol University Research Expo 2014, Ramathibodi School of Nursing Building, Ramathibodi Hospital, Bangkok, Thailand, December 1-2, 2014. . (Proceeding, poster presentation).

ผลงานอื่น ๆ

1. ผลิตนักศึกษาปริญญาเอก หลักสูตรปรัชญาดุษฎีบัณฑิต สาขาพันธุศาสตร์ระดับโมเลกุลและพันธุวิศวกรรมศาสตร์ (5636141 MBMG/D) วิทยานิพนธ์เรื่อง กลไกระดับโมเลกุลของไวรัสหัวเหลืองในการเข้าเซลล์และการเคลื่อนที่ภายในเซลล์ของกุ้งกุลาดำ (Molecular mechanism of yellow head virus internalization and entry into *Penaeus monodon*) สำเร็จการศึกษาเมื่อ 28 ธันวาคม 2558

2. ผลิตนักศึกษาปริญญาโท หลักสูตรวิทยาศาสตรมหาบัณฑิต สาขาพันธุศาสตร์ระดับโมเลกุลและพันธุวิศวกรรมศาสตร์ นายเอกชัย คงประจักษ์ (5636141 MBMG/M) วิทยานิพนธ์เรื่องการโคลนนิ่งระดับโมเลกุลและการวิเคราะห์หน้าที่ของ Rab11 ระหว่างการติดไวรัสหัวเหลืองในกุ้งกุลาดำ (Molecular cloning and functional analysis of Rab11 during yellow head virus infection in *Penaeus monodon*) สำเร็จการศึกษาเมื่อ 28 เมษายน 2559

3. ผลิตนักศึกษาปริญญาโท หลักสูตรวิทยาศาสตรมหาบัณฑิต สาขาพันธุศาสตร์ระดับโมเลกุลและพันธุวิศวกรรมศาสตร์ นางสาว สุดารัตน์ ทองสุขแสงเจริญ (5736205 MBMG/M) วิทยานิพนธ์เรื่อง การโคลนนิ่งระดับโมเลกุลและการศึกษาหน้าที่ของ Rab9 ต่อการติดไวรัสหัวเหลืองในกุ้งกุลาดำ (Molecular cloning and characterization of Rab 9 during yellow head virus infection in *Penaeus monodon*) สำเร็จการศึกษาเมื่อ 20 มีนาคม 2560

การเชื่อมโยงกับต่างประเทศ

งานวิจัยทางด้านโคลนนิ่งและการถอดรหัสดีเอ็นเอ ได้ทำงานวิจัยร่วมกับ Prof. Ikuo Hirono และ Prof. Kondo Hidehiro ที่ Laboratory of Genome Science, Tokyo University of Marine Science and Technology, Tokyo Japan,

Aquaculture 435 (2015) 480–487

Contents lists available at ScienceDirect

Aquaculture

journal homepage: www.elsevier.com/locate/aqua-online

Successful yellow head virus infection of *Penaeus monodon* requires clathrin heavy chain

Pratsaneeyaporn Posiri [a], Hidehiro Kondo [b], Ikuo Hirono [b], Sakol Panyim [a,c], Chalermporn Ongvarrasopone [a,*]

[a] Institute of Molecular Biosciences, Mahidol University (Salaya Campus), Nakhon Pathom 73170 Thailand
[b] Laboratory of Genome Science, Tokyo University of Marine Science and Technology, Tokyo, Japan
[c] Department of Biochemistry, Faculty of Science, Mahidol University, Bangkok 10400, Thailand

ARTICLE INFO

Article history:
Received 31 August 2014
Received in revised form 10 October 2014
Accepted 12 October 2014
Available online 22 October 2014

Keywords:
Yellow head virus
Endocytosis
Double stranded RNA
RNAi
Black tiger shrimp

ABSTRACT

Viral disease caused by the Yellow head virus (YHV) had great impact on economic loss in the aquaculture industry. Prevention or curing YHV disease is still not possible due to the lack of understanding of the basic mechanisms of YHV infection. In this report, the endocytosis inhibitors (chlorpromazine (CPZ), amiloride and methyl-β-cyclodextrin (MβCD)) were used to identify the cellular entry pathway of YHV. Pretreating shrimp with CPZ but not amiloride or MβCD followed by YHV challenge resulted in a significant reduction of YHV levels, suggesting that YHV entered the shrimp cells via clathrin-mediated endocytosis. Next, the major component of the clathrin-coated vesicle, *Penaeus monodon* clathrin heavy chain (*Pm*CHC) was cloned and characterized. The complete coding sequence of PmCHC is 5055 bp encoding a putative protein of 1684 amino acids. Specific silencing of PmCHC mRNA by dsRNA-PmCHC showed an inhibition of YHV replication for 48 h post YHV injection as well as exhibiting a delay in shrimp mortality. These results indicated that PmCHC was an essential component for YHV infection of shrimp cells.

1. Introduction

Yellow head virus (YHV) is one of the most devastating shrimp pathogens as it causes mortality within 3 days. This virus was first identified in 1992 from moribund shrimp from southern Thailand (Boonyaratpalin et al., 1993). The virus was named from symptoms of the disease in which the moribund shrimp would present a yellowish cephalothorax and very sallow overall coloration. YHV can infect various penaeid shrimp such as *Penaeus aztecus*, *Penaeus duorarum*, *Penaeus merguiensis*, *Penaeus monodon*, *Penaeus setiferus*, *Penaeus stylirostris* and *Litopenaeus vannamei* (Flegel, 1997). The infected moribund shrimp shows nuclear condensation as well as pyknosis and karyorrhexis which are signs of cell apoptosis (Khanobdee et al., 2002). YHV has a positive-sense single-stranded RNA genome of approximately 27 kb with a poly (A) tail. It belongs to the genus *Okavirus*, family *Roniviridae* in the order *Nidovirales*. The morphology of YHV reveals an enveloped bacilliform which has a particle size about 50–60 × 190–200 nm, containing the internal helical nucleocapsid which is closely surrounded by an envelope studded with prominent peplomers or spikes (Nadala et al., 1997; Sittidilokratna et al., 2008). YHV contains two major structural transmembrane glycoproteins (gp116 and gp64) and a nucleoprotein (p20) (Jitrapakdee et al., 2003). Antiserum against the gp116 but not gp64 can neutralize YHV infectivity in the primary lymphoid cells of *Penaeus monodon* (Assavalapsakul et al., 2005). In addition, injection of double-stranded RNA (dsRNA) targeting to the YHV-binding protein, YRP65, inhibited YHV replication (Assavalapsakul et al., 2006). Also, suppression of PmRab7 (a late endosomal marker involved in trafficking) resulted in inhibition of YHV replication (Ongvarrasopone et al., 2008). These results imply that for successful infection, YHV requires receptor mediated endocytosis as a route of entry and takes advantage of the host cell machineries for endosomal trafficking and replication. Therefore, better understanding of the endocytosis and trafficking pathway of YHV will shed light on the mechanism of YHV infection and replication and thus will lead to the development of an antiviral agent or strategy to combat YHV infection.

Many viruses utilize well-characterized cellular endocytic mechanisms including clathrin-mediated endocytosis, lipid raft caveola-dependent endocytosis and macropinocytosis to internalize into host cells. For instance, several positive-sense ssRNA viruses such as severe acute respiratory syndrome virus (Inoue et al., 2007), hepatitis C, dengue and semliki forest virus use clathrin-mediated endocytosis (Marsh and Helenius, 2006; Meertens et al., 2006; Mercer et al., 2010) as a route of entry. In clathrin-mediated endocytosis, the cargo is trafficked through the cell via the coated vesicle which is surrounded by the polymerized clathrin in a basket-like structure. The formation of the endocytic clathrin-coated vesicles occurs through the interaction of clathrin, heterotetrameric adaptor protein-2 (AP-2), and several

* Corresponding author at: Institute of Molecular Biosciences, Mahidol University (Salaya Campus), 25/25 Phutthamonthon 4 Rd. Salaya, Phutthamonthon District, Nakhon Pathom 73170, Thailand. Tel.: +66 2 800 3624x1280; fax: +66 2 4419906.
E-mail address: chalermporn.ong@mahidol.ac.th (C. Ongvarrasopone).

http://dx.doi.org/10.1016/j.aquaculture.2014.10.018
0044-8486/

accessory proteins such as Epsin, Eps15, AP180/CALM and dynamin. Clathrin, in which the light chain and heavy chain form a unique structure called the clathrin triskelion, as well as AP-2 are recruited by epsin to the plasma membrane in response to receptor-mediated internalization signals. Epsin then mediates the assembly of a clathrin cage, which results in membrane curvature induced by the coated-pit formation. Once assembled, the clathrin-coated pits are pinched off from the plasma membrane by dynamin to form clathrin-coated vesicles which are then trafficked to endosomes (Doherty and McMahon, 2009; Mousavi et al., 2004). Whether YHV utilizes this pathway as a route of entry into shrimp cells remained to be investigated. Therefore, one purpose of this study was to characterize the YHV entry pathway by using several trafficking inhibitors. *P. monodon* clathrin heavy chain (*Pm*CHC), a major protein component in the clathrin-dependent pathway was cloned and characterized. The suppression effect of PmCHC in YHV-challenged shrimp also was investigated.

2. Materials and methods

2.1. P. monodon (black tiger shrimp) culture

Juvenile shrimp were obtained from Manoach's farm in Nakhon Pathom province, Thailand. Shrimp were sampled to determine that they were free from YHV and white spot syndrome virus (WSSV) infection using Diagnosis Strip Test YHV + WSSV (Pacific Biotech Co., Ltd, Thailand). In addition, shrimp were acclimatized for at least 5 days before use in experiments. They were maintained in large containers with oxygenated sea water at 5 ppt salinity before the experiment and fed with commercial feed every day. Half of the water was changed every 2 days.

2.2. Yellow head virus preparation

Virus stock was prepared from hemolymph of YHV infected moribund shrimp. The moribund shrimp showed signs of YHV infection for example, a yellowish cephalothorax. To confirm that the hemolymph was collected from the moribund shrimp infected with YHV not other viruses, total RNA was extracted and reverse transcription-PCR analysis was performed to detect the helicase gene of YHV and other viruses such as VP28 gene of WSSV. To prepare the viral stock, hemolymph was collected with AC-1 solution (27 mM Sodium citrate, 34.33 mM NaCl, 104.5 mM Glucose, 198.17 mM EDTA, pH 7.0), ratio 1:1, and the virus was obtained by ultracentrifugation (100,000 ×*g*) for 1 h. Viral pellet was dissolved in 150 mM NaCl and stored at −80 °C until use. The virus titer that causes 100% mortality within 3–4 days was used in this experiment.

2.3. Screening of YHV entry pathways by using drug inhibitors

The entry pathways of YHV were screened by using drug inhibitors. Various inhibitors of clathrin-dependent endocytosis, macropinocytosis and caveolar endocytosis such as chlorpromazine (CPZ), amiloride and methyl-β-cyclodextrin (MβCD), respectively, were employed at a dose of 0.25 mM g^{-1} shrimp (9 shrimp per group). The inhibitors were injected into the hemolymph using 0.5 ml U-100 insulin syringe with 29 gauge needle. Injection of PBS was used as control. At 12 h post-injection, shrimp were challenged with YHV. Then at 24 h post YHV injection, gills from individual shrimp were collected to extract the total RNA and YHV levels were determined using quantitative RT-PCR.

2.4. Cloning of the full-length of P. monodon clathrin heavy chain (PmCHC)

Specific primers, cdfullCHC-F and cdfullCHC-R (Table 1), were used to amplify PmCHC from hemocytes of *P. monodon* and were designed based on the nucleotide sequences obtained from *Marsupenaeus japonicus* clathrin heavy chain. The cDNA of PmCHC coding sequences was amplified by using Taq DNA polymerase (New England Biolabs). The PCR was performed by hot-start at 95 °C for 5 min; 30 cycles of 95 °C for 30 s, 60 °C for 30 s, and 68 °C for 6 min; followed by 68 °C for 7 min. The cDNA was cloned into pGEM-T easy vector (Promega). The recombinant plasmid containing PmCHC was sequenced using T7, SP6, walkCHC-F1, walkCHC-F2, walkCHC-R1 as primers (Table 1) by First Base Co., Ltd. (Malaysia).

Table 1
Primer sequences used in the experiments.

Primers	Sequences (5′- - → 3′)	Experiments
cdfullCHC-F	GGGGTACCATGACACAGGCGTTACCC	Full length PmCHC coding region
cdfullCHC-R	GGAATTCCATATGTTACATGCTGTAGCCTTG	Full length PmCHC coding region
walkCHC-F1	TGTATTCTTCCCACCAGAGGC	Sequencing primers
walkCHC-F2	ACGTCTGCCAGTTGTTGTGG	Sequencing primers
walkCHC-R1	CCTTGAAGTGTGACTCTCGCC	Sequencing primers
mjCHC-F	AGTGCTTTGCTGAAACTGGTC	Partial PmCHC cDNA region
mjCHC-R	CATGAATACGAGATTCCAGCC *Xba*I	Partial PmCHC cDNA region
sCHC-F1	GCTCTAGACGAAATGTAATGCGTGTC *Kpn*I	dsRNA-PmCHC construction
lpCHC-R1	GGGGTACCCTATCTGCACTACAATCTGTAG *Eco*RI	dsRNA-PmCHC construction
asCHC-F2	GGAATTCCGAAATGTAATGCGTGTC *Kpn*I	dsRNA-PmCHC construction
asCHC-R2	GGGGTACCGACCAACCATTCTGGGTT	dsRNA-PmCHC construction
PmCHC-F	CTTCTCCCAAGAACCAGAGGTGCAC	Detection of PmCHC mRNA
PmCHC-R	ATTCCTCTTCTCCACCTCTTCCACC	Detection of PmCHC mRNA
PRT-oligo dT	CCGGAATTCAAGCTTCTAGAGGATCC$(T)_{16}$	Reverse transcription
YHV(hel)-F	CAAGGACCACCTGGTACCGGTAAGAC	Detection of YHV mRNA
YHV(hel)-R	GCGGAAACGACTGACGGCTACATTCAC	Detection of YHV mRNA
PmActin-F	GACTCGTACGTGGGCGACGAGG	Detection of PmActin mRNA
PmActin-R	AGCAGCGGTGGTCATCTCCTGCTC	Detection of PmActin mRNA
qYHV-F	ATCATCAGCTCACAGGCAAGTTCC	Real time PCR
qYHV-R	GGGTCTAAATGGAGCTGGAAGACC	Real time PCR
EF-1α-F	GAACTGCTGACCAAGATCGACAGG	Real time PCR
EF-1α-R	GAGCATACTGTTGGAAGGTCTCCA	Real time PCR

2.5. Sequence analysis

The nucleotide sequence analysis was performed with BLASTN (http://blast.ncbi.nlm.nih.gov). The deduced amino acid sequence of PmCHC was used to search the NCBI database (http://www.ncbi.nlm.nih.gov/Structure/cdd/wrpsb.cgi) to predict the conserved domains. Predictions of molecular weight and isoelectric point (pI) of the protein were performed by Expert Protein Analysis System (www.expasy.org). Sequences of proteins from several organisms were obtained from GenBank database. Multiple amino acid sequence alignments were performed by VectorNTI program (Invitrogen). Phylogenetic analysis (http://www.phylogeny.fr/version2_cgi/phylogeny.cgi) was based on the neighbor-joining method (Dereeper et al., 2008, 2010).

2.6. Construction of the recombinant plasmid expressing dsRNA-PmCHC

Recombinant plasmid containing stem-loop of dsRNA was constructed in pGEM-3Zf+ (Promega) and pET-17b (Novagen) vectors. Sense-loop region of the dsRNA was amplified from the first-strand cDNA by specific primers, sCHC-F1 and lpCHC-R1 (Table 1). The antisense region was amplified by asCHC-F2 and asCHC-R2 (Table 1). Both PCR fragments were gel-purified and subjected to restriction enzyme digestion. The purified fragment of the sense-loop was cloned into the linearized fragment of pGEM-3Zf+ (digested by *Xba*I and *Kpn*I). Then, this recombinant plasmid containing the sense-loop region of PmCHC

was digested by *Kpn*I and *Eco*RI and ligated with *Kpn*I and *Eco*RI digested antisense fragment. The recombinant plasmid containing sense-loop-antisense fragments of PmCHC (pGEM-3Zf+-PmCHC) was obtained. Then, the sense-loop-antisense fragment of PmCHC was subcloned into pET-17b vector at *Xba*I and *Eco*RI sites to construct recombinant plasmid pET17b-PmCHC which was used for dsRNA production by in vivo bacterial expression.

2.7. Production of dsRNA by in vivo bacterial expression

Recombinant plasmid pET17b-PmCHC was transformed into a RNase III mutant HT115 *Escherichia coli* strain. This strain is modified to express T7 RNA polymerase from an isopropyl-β-D thiogalactopyranoside (IPTG) inducible promoter. Therefore, dsRNAs can be produced in the HT115 bacterial host after induction with IPTG. Double-stranded RNA was extracted and purified as previously described (Ongvarrasopone et al., 2007; Posiri et al., 2013). The quality of dsRNA was characterized by ribonuclease digestion assay using RNase A and RNase III. dsRNA concentration was estimated by agarose gel electrophoresis by comparing to the intensity of 100 bp DNA marker.

2.8. Suppression of PmCHC by dsRNA-PmCHC

The knockdown effect of dsRNA-PmCHC was tested by injection of dsRNA into hemolymph. Shrimp were injected with 2.5 μg g^{-1} shrimp of dsRNA-PmCHC or an unrelated gene of dsRNA-GFP dissolved in 150 mM NaCl. Injection of 150 mM NaCl was used as control. After 24 h post dsRNA injection, gills of individual shrimp were collected to extract total RNA. Suppression effect of dsRNA was analyzed by reverse-transcription PCR (RT-PCR) to determine PmCHC mRNA level. To study the knockdown effect of PmCHC in YHV-challenged shrimp, shrimp were injected with dsRNA-PmCHC for 24 h before YHV challenge. Forty-eight hours later, gills of individual shrimp were collected to extract total RNA to detect YHV (helicase gene) and PmCHC mRNA expression levels. PmActin mRNA was used as an internal control.

2.9. Shrimp mortality assay

The mortality of shrimp injected with dsRNA followed by YHV challenge were observed every 6 h. Shrimp were about 1 g with 15 shrimp per group. Three independent experiments were performed. Shrimp were injected with 150 mM NaCl, 2.5 μg g^{-1} shrimp of dsRNA-PmCHC or dsRNA-GFP. After 24 h post injection, shrimp were challenged with YHV. Mortality was plotted every 12 h.

2.10. RNA isolation and RT-PCR analysis

Total RNA from gill tissues was isolated by Trizol® reagent (Molecular Research Center) following the manufacturer's procedure. The RNA concentration was measured by Nanodrop ND-1000 spectrophotometer (Nanodrop Technologies). Total RNA (2 μg) was used to generate first-strand cDNA by Improm-II™ reverse transcriptase (Promega) and PRT primer (Table 1). PmCHC mRNA level was amplified by primers; PmCHC-F1 and PmCHC-R1 (Table 1). PmActin mRNA expression, used as internal control, was amplified by specific primers, PmActin-F and PmActin-R1 (Table 1). Multiplex PCR for PmCHC and PmActin was performed according to this condition: 95 °C for 5 min; 25 cycles of 95 °C for 30 s, 60 °C for 30 s, and 72 °C for 45 s; followed by 72 °C for 7 min. YHV mRNA level was amplified using primers, YHV(hel)-F and YHV(hel)-R (Table 1). The multiplex PCR condition for YHV and PmActin was as above except that the annealing temperature was changed to 55 °C for 30 s. The PCR products were analyzed on 1.5% agarose gel. The intensity of each band after subtracting the background was quantified by using ImageJ analysis program (version 1.46r). The relative expression level of PmCHC and YHV was normalized with PmActin levels and expressed as an arbitrary unit.

2.11. Quantitative real time PCR (qPCR)

Total RNA 2 μg was used for the first-strand cDNA synthesis by Improm-II™reverse transcriptase (Promega) using PRT primer. Dilution of cDNA at 1:32 was mixed with qPCR reaction using KAPA™ SYBR®Fast master mix (2×) ABI Prism™ (KAPA Biosystems) following the manufacturer's protocol. qYHV-F and qYHV-R specific primers (Table 1) were used to amplify YHV mRNA; EF1-α (EF1α-F and EF1α-R) is used as internal control: 95 °C for 3 min; 40 cycles of 95 °C for 5 s, 60 °C for 30 s. The qPCR was analyzed in an ABI 7500 real-time detection system (Applied Biosystems). The cycle threshold (Ct) value of YHV and EF1-α was compared and calculated by $2^{-\Delta\Delta C}{}_T$ method (Livak and Schmittgen, 2001).

2.12. Statistical analysis

The relative mRNA levels of PmCHC or YHV normalized with PmActin and fold change in PmCHC expression were presented as mean ± SEM. Cumulative percent mortality was plotted as mean ± SEM. In addition, significant differences of each experimental group were tested by using analysis of variance (ANOVA). A probability (P) value of 0.05 was used to define significant difference.

3. Results

3.1. Analysis of YHV entry pathway

To identify the pathway for YHV internalization into shrimp cell, shrimp of about 2 g were pretreated with inhibitors of clathrin-mediated endocytosis (chlorpromazine, CPZ), macropinocytosis (amiloride) or the caveolar dependent pathway (methyl-β-cyclodextrin, MβCD), and this was followed by YHV challenge. All shrimp receiving inhibitors survived throughout the experiment. Quantitative RT-PCR of the shrimp pretreated with chlorpromazine showed a significant reduction of YHV mRNA levels, approximately 77%, when compared to the PBS-YHV injected group, whereas shrimp pretreated with amiloride and MβCD demonstrated no significant difference to the YHV control group (Fig. 1).

3.2. Cloning of PmCHC coding region and sequence analysis

The sequence of *M. japonicus* clathrin heavy chain was used to design specific-primers to amplify the full-length coding region of *P. monodon*

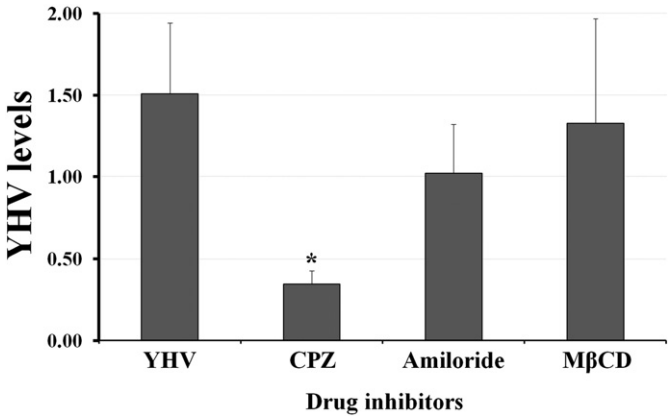

Fig. 1. Effect of inhibitors on YHV internalization into shrimp cell. Graphs represent the quantitative RT-PCR of YHV mRNA levels (fold change) of YHV-challenged shrimp pretreated with inhibitors which are chlorpromazine (CPZ), amiloride and methyl-β-cyclodextrin (MβCD). Nine shrimp per group were analyzed. (*) represents significant difference ($P < 0.05$) of YHV mRNA levels compared between the YHV- challenged groups pretreated with or without inhibitors.

Table 2
Accession number of organisms used for phylogenetic analysis.

Organisms	Accession number
Acromyrmex echinator	EGI60613
Aedes aegypti	XP_001656878
Bombyx mori	NP_001136443
Bos taurus	AAC48524
Ciona intestinalis	XP_002130279
Culex quinquefasciatus	EDS40945
Danaus plexippus	EHJ79063
Danio rerio	NP_001005391
Drosophila melanogaster	NP_001096993
Gallus gallus	NP_001073586
Glycine max	AAC49294
Homo sapiens	NP_004850
Medicago truncatula	AES71175
Penaeus monodon	KJ700941
Populus trichocarpa	EEF02372
Rattus norvegicus	AAA40874
Riptortus pedestris	BAN20627
Sus scrofa	NP_001139599
Theobroma cacao	EOY34523
Tribolium castaneum	XP_967829
Zea mays	AGC82051

clathrin heavy chain from hemocytes. The open reading frame of PmCHC is 5055 bp, encoding a protein of 1684 amino acids, with an estimated molecular weight of 192.5 kDa and a pI of 5.53. The nucleotide sequence is deposited in the GenBank database under the accession number KJ700941. The protein contains several conserved domains: clathrin propeller repeat (amino acid: 205–241, 259–295, 303–337), clathrin heavy chain linker (amino acid 338–361), clathrin-H-link (amino acid 363–428), and clathrin heavy chain repeat homology (amino acid: 544–682, 693–831, 844–978, 986–1127, 1139–1275, 1281–1423, 1434–1572) (Supplementary Fig. 1). For most organisms (Table 2, Fig. 2), conserved domains of CHC consist of a seven CHC repeat homology, one CHC H-linker and one CHC linker. One clathrin propeller repeat is observed in plants including *Zea mays* and *Theobroma cacao*. However, three to four clathrin propeller repeats are found in both invertebrate and vertebrate species including *P. monodon*, *Aedes aegypti*, *Drosophila melanogaster*, *Homo sapiens* and *Danio rerio* (Table 2). Phylogenetic tree analysis clustered organisms in three groups which are plants, invertebrates and vertebrates. PmCHC was clustered into an invertebrate group (Fig. 3).

3.3. Production of dsRNA-PmCHC and its suppression effect

Recombinant plasmid pET17b containing a stem loop of PmCHC was constructed and transformed into HT115 *E. coli* strain to be used as template for *Pm*CHC dsRNA production (dsRNA-PmCHC) by in vivo bacterial expression. Then, hairpin dsRNA-PmCHC was extracted using an ethanol method (Posiri et al., 2013). The quality of dsRNA-PmCHC was characterized by ribonuclease III (RNase III) and by ribonuclease A (RNase A) digestion assay. DsRNA-GFP was also produced for nonspecific dsRNA injection. The hairpin dsRNA-PmCHC and dsRNA-GFP could be cleaved by RNase III but not by RNase A, suggesting that good quality dsRNA were obtained (Fig. 4A). Injection of dsRNA-PmCHC resulted in a significant reduction of PmCHC mRNA levels, approximately 90% when compared to the NaCl injected group ($P < 0.01$; $n = 5$). In contrast, no significant difference in PmCHC expression levels was observed between dsRNA-GFP- and NaCl-injected groups (Fig. 4B and 4C).

3.4. Suppression effect of PmCHC in YHV-challenged shrimp inhibited YHV mRNA levels

To determine whether PmCHC is required for YHV internalization into shrimp cells, the PmCHC-knockdown shrimp were challenged with YHV. After 48 h, gills were collected for total RNA extraction and RT-PCR analysis to determine mRNA expression of YHV and PmCHC. The results demonstrated the suppression effect of PmCHC, by dsRNA-PmCHC, and resulted in almost complete inhibition of YHV mRNA expression. However, high levels of YHV mRNA were still observed in both NaCl-injected and dsRNA-GFP injected groups (Fig. 5A and B).

3.5. Suppression of PmCHC in YHV-challenged shrimp delayed mortality

Shrimp receiving dsRNA-*Pm*CHC, followed by YHV challenge, reached 100% cumulative mortality at 120 h post YHV injection (hpi) whereas NaCl- and dsRNA-GFP-injected groups gave 100% mortality at 108 hpi. Furthermore, shrimp injected with dsRNA-PmCHC followed by YHV challenge showed significant reduction in cumulative percent mortality at 84–108 hpi when compared with the NaCl injection group (Fig. 6A). This result suggested that clathrin heavy chain is required for YHV infection. However, shrimp injected with dsRNA-PmCHC at 2.5 μg g^{-1} shrimp without YHV challenge reached 100% mortality at 156 h post dsRNA injection whereas shrimp injected with NaCl or dsRNA-GFP showed no mortality (Fig. 6B). In addition, shrimp injected with dsRNA-PmCHC at lower dosage, 1.25 μg g^{-1} shrimp,

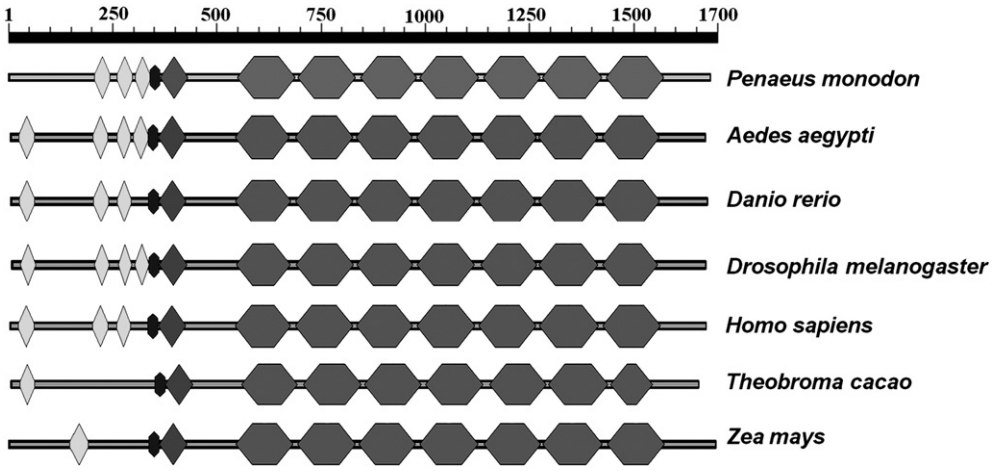

Fig. 2. Comparison of the clathrin heavy chain protein domains among several organisms. The protein domains comprising of clathrin propeller repeat (), clathrin heavy chain linker (), clathrin-H-link (), clathrin heavy chain repeat homology (). *Aedes aegypti*, *Drosophila melanogaster*, *Homo sapiens*, *Danio rerio*, *Zea mays* and *Theobroma cacao* were compared to *Penaeus monodon*.

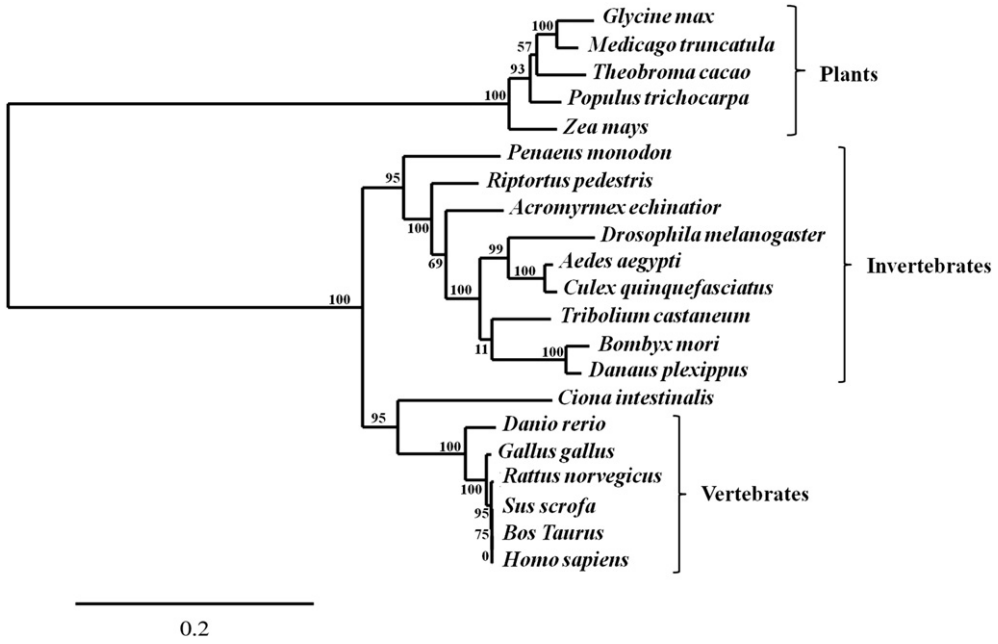

Fig. 3. Phylogenetic analysis of the clathrin heavy chain based on amino acid sequence of various species (*Glycine max*, *Medicago truncatula*, *Theobroma cacao*, *Populus trichocarpa*, *Zea mays*, *Penaeus monodon*, *Riptortus pedestris*, *Acromyrmex echinatior*, *Drosophila melanogaster*, *Aedes aegypti*, *Culex quinquefasciatus*, *Tribolium castaneum*, *Bombyx mori*, *Danaus plexippus*, *Ciona intestinalis*, *Danio rerio*, *Gallus gallus*, *Rattus norvegicus*, *Sus scrofa*, *Bos taurus*, and *Homo sapiens*) using neighbor-joining distance analysis. The GenBank accession numbers of CHC from each organism are in Table 2. Bootstrap values from 1000 replicates are indicated at the node.

without YHV challenge reached 100% mortality at a later time, 180 h post dsRNA injection. A 75% mortality was observed in shrimp injected with dsRNA-PmCHC at 0.63 μg g^{-1} without YHV challenge during 144–240 h post dsRNA injection (Supplementary Fig. 2). Dead shrimp were sampled for viral load detection. The results showed that dsRNA-PmCHC → YHV group (Fig. 6C (b)) demonstrated lower YHV mRNA levels when compared to NaCl → YHV group (Fig. 6C (a)) and dsRNA-GFP → YHV group (Fig. 6C (c)). All dead shrimp except samples from lanes 2, 3, 8, 11, and 12 in the dsRNA-PmCHC → YHV group showed the presence of YHV. This suggested that the shrimps in lanes 2, 3, 8,

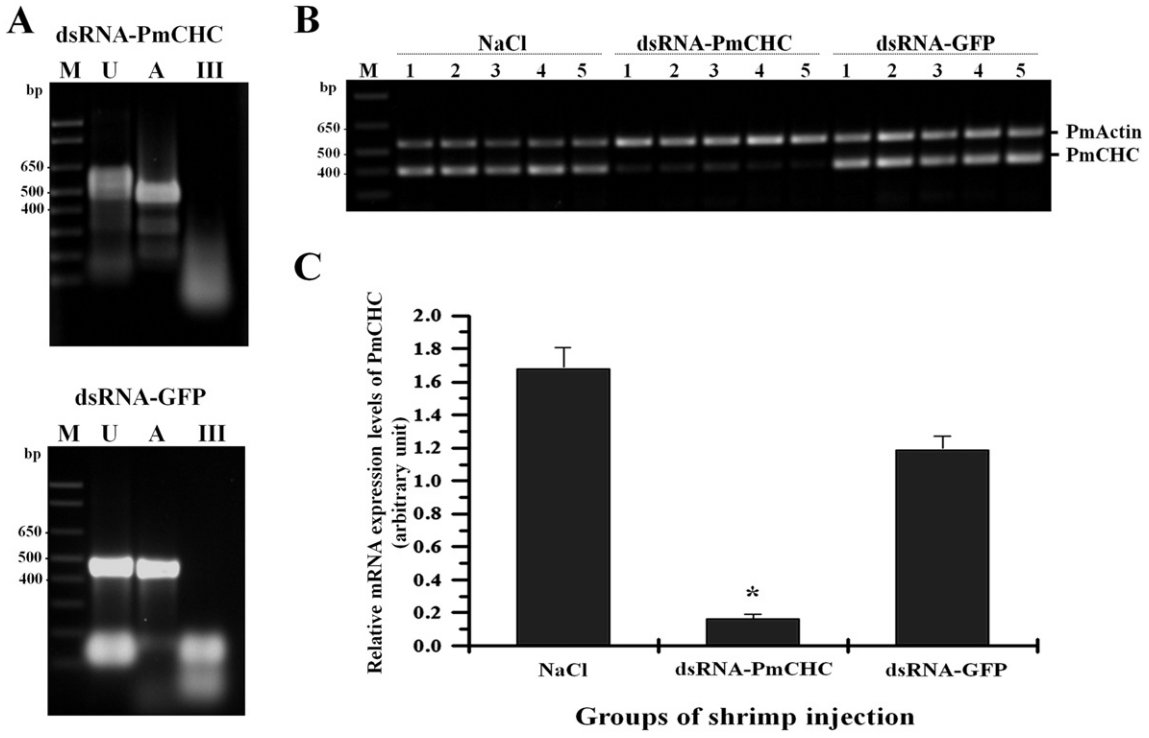

Fig. 4. Effectiveness of dsRNA-PmCHC on silencing of PmCHC mRNA. (A) Quality of dsRNA-PmCHC and dsRNA-GFP produced by in vivo bacterial expression. M is 1 kb plus DNA ladder. U, A and III are undigested dsRNA, dsRNA treated with RNase A and dsRNA treated with RNase III, respectively. (B) Representative agarose gel of RT-PCR products of PmCHC and PmActin expression of NaCl control, injected with dsRNA-PmCHC or dsRNA-GFP groups. M is 1 kb plus DNA marker. (C) The relative mRNA expression levels of PmCHC when normalized with PmActin are presented as mean ± SEM (n = 5). (*) Statistically significant difference between dsRNA-CHC compared to NaCl injected group ($P < 0.01$).

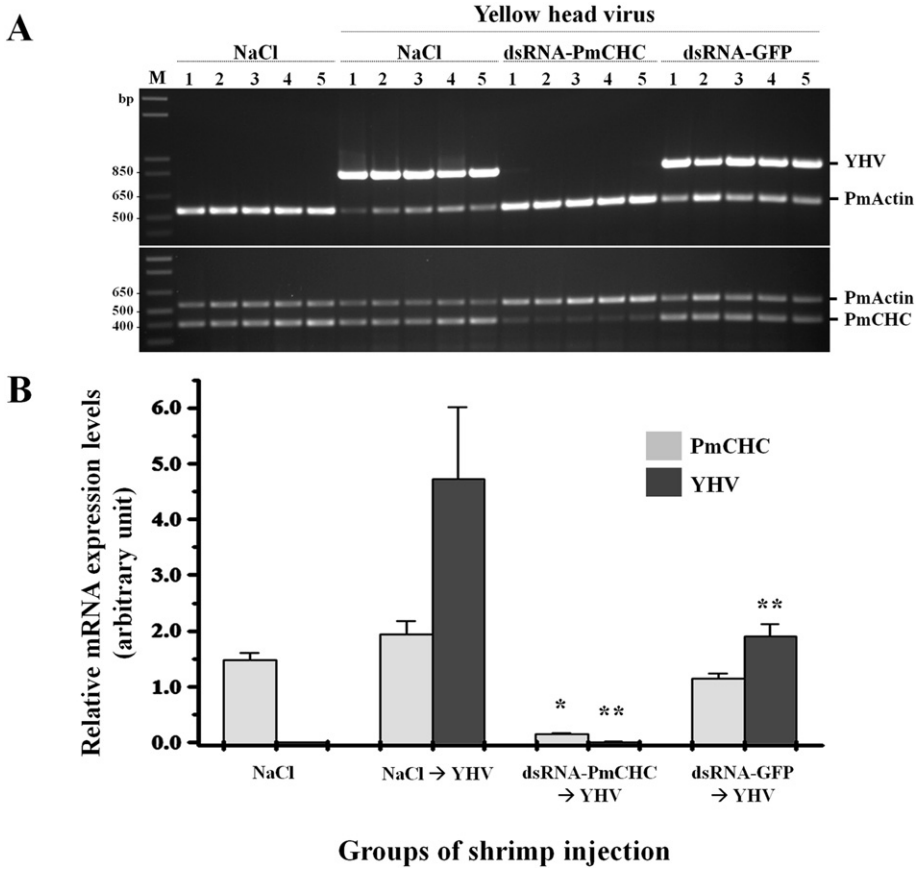

Fig. 5. Suppression effect of PmCHC upon YHV infection. (A) A representative gel of RT-PCR products of YHV (top panel) and PmCHC (bottom panel) mRNA levels. PmActin was used as an internal control. Shrimp were divided into 4 groups: NaCl alone and NaCl + YHV challenge, dsRNA-PmCHC + YHV challenge or dsRNA-GFP + YHV challenge (n = 5 per group). M is 1 kb plus DNA marker. (B) The relative mRNA expression levels of PmCHC (gray bar) and YHV normalized with PmActin (light black bar). Data is expressed as mean ± SEM in an arbitrary unit. (*) represents significant difference ($P < 0.05$) of PmCHC mRNA levels between dsRNA-PmCHC → YHV and NaCl injected group. (**) represents statistically significant difference ($P < 0.05$) of YHV mRNA levels between dsRNA-injected group and NaCl → YHV group.

11, and 12 were protected from YHV infection but were dead from the PmCHC knockdown. Taken together, the results strongly suggested that clathrin heavy chain is essential for YHV infection.

4. Discussion

Clathrin heavy chain (CHC) is a major protein in clathrin-coated pit and clathrin-coated vesicle. Clathrin heavy and light chains are assembled to form a three-legged structure, called a triskelion. Clathrin heavy chain together with adaptor and accessory proteins, including AP2, EPS15, AP-180, epsin or dynamin (McMahon and Boucrot, 2011; Mousavi et al., 2004; Young, 2007) are involved in endocytosis. The functions of clathrin heavy chain are believed to be involved in sorting cargo protein in the membrane and membrane curvature.

In black tiger shrimp, the role of clathrin heavy chain in virus infection has not been previously investigated. In this study, we have cloned *P. monodon* clathrin heavy chain (*Pm*CHC). The function of PmCHC especially for yellow head virus (YHV) infection was tested to study the major route for YHV internalization. RNA interference (RNAi) was used as a tool to study the function of PmCHC. Shrimp injected with dsRNA-PmCHC showed reduction of PmCHC mRNA levels up to 90% when compared to the NaCl-injected control group. In addition, knockdown of PmCHC mRNA in YHV-challenged shrimp exhibited low levels of YHV expression (Figs. 5 and 6C) and a delay in shrimp mortality up to 24 h post YHV injection (84–108 hpi) (Fig. 6A). These effects may be due to suppression of PmCHC gene (Fig. 6B and Supplementary Fig. 2). After knocking down of PmCHC mRNA, low levels of PmCHC present may slow down the entry of YHV into the cell, thus resulting in a delay of shrimp mortality. Moreover, the shrimp death may also be due to the depletion of clathrin heavy chain (Fig. 6B and Supplementary Fig. 2). This is because clathrin heavy chain has diverse cellular functions such as transportation of cargo inside the cell, cytokinesis and glucose metabolism (Brodsky, 2012). Depletion of PmCHC may inhibit some cellular functions which are essential for cell survival. Several studies have shown that some viruses require clathrin heavy chain for infection (Bhattacharyya et al., 2010; Hongliang and Chengyu, 2009; Hussain et al., 2011). For instance, confocal microscopy demonstrated the colocalization between rhesus rhadinovirus and clathrin heavy chain (Zhang et al., 2010). Similar to this study, suppression of the clathrin heavy chain by small interfering RNA exhibited a reduction of viral load in the host cells, including influenza A virus, severe acute respiratory syndrome coronavirus or human enterovirus 71 (Hongliang and Chengyu, 2009; Hussain et al., 2011; Inoue et al., 2007). It has been shown that the cargo molecules that can be transported via clathrin-meditated endocytosis are size dependent, approximately 200 nm (Rejman et al., 2004) which nicely fit with the YHV virion, whose size is ~50–60 × 190–200 nm (Nadala et al., 1997). In addition, a recent report showed the reduction of YHV level in clathrin coat AP17 knockdown shrimp (Jatuyosporn et al., 2014). Moreover, by using various inhibitors (CPZ, MβCD and amiloride), only the YHV-challenged shrimp pretreated with CPZ showed a significant reduction of YHV levels. These results suggested that the major route of YHV into the shrimp cells was via clathrin-mediated endocytosis pathway.

In shrimp, a previous study has identified a protein in the endocytosis pathway, *P. monodon* Rab7 (PmRab7) (Sritunyalucksana et al, 2006). Rab7 is a small GTPase protein and plays a crucial role to regulate the

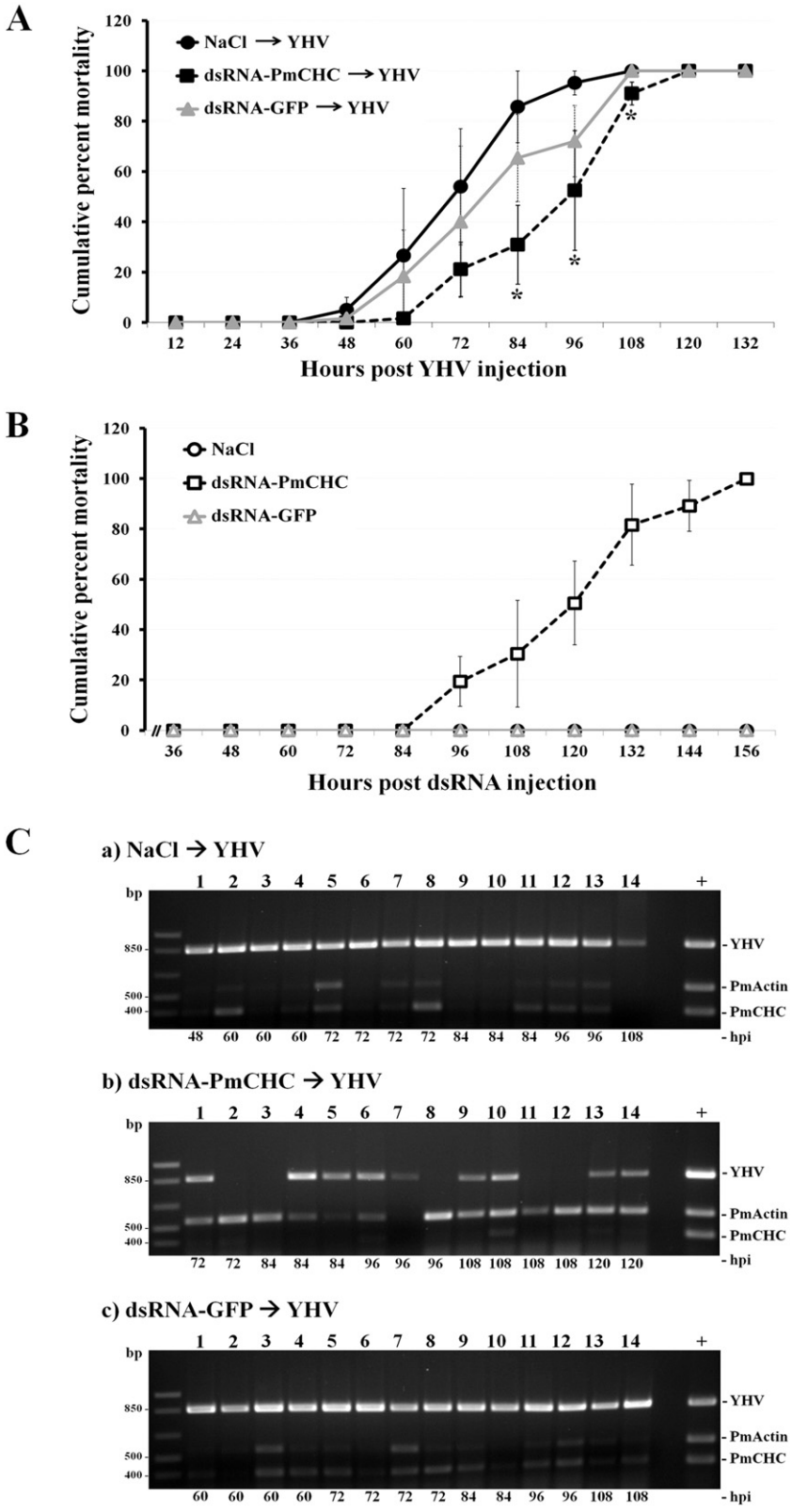

Fig. 6. The cumulative percent mortality of shrimp injected with NaCl, dsRNA-PmCHC, or dsRNA-GFP followed by YHV challenge (A) or without YHV challenge (B). (*) represents significant difference between dsRNA-PmCHC → YHV and NaCl → YHV group. (C) A representative gel of RT-PCR products of YHV and PmCHC mRNA levels of dead shrimp. a) NaCl → YHV group, b) dsRNA-PmCHC → YHV group and c) dsRNA-GFP → YHV group. PmActin was used as internal control. The number on the bottom of the each lane represents the time (hours of post YHV challenge, hpi) that the shrimp die. The expression of PmActin in dead shrimp samples that showed high expression levels of YHV were very faint. This result was also demonstrated in a previous study (Posiri et al., 2011).

transportation from late endosome to lysosome during endosome maturation (Huotari and Helenius, 2011). In addition, PmRab7 is required for several shrimp viruses such as white spot syndrome virus (WSSV), taura syndrome virus (TSV) Laem-Singh virus (LSNV) or YHV for intracellular trafficking inside the cell (Ongvarrasopone et al., 2008, 2010, 2011). Therefore based on the previous evidence and this study, the

mechanism of YHV entry and intracellular trafficking can be proposed. YHV enters the shrimp cells by using the envelop protein gp116 to bind to YHV binding protein, PmYRP65 (Assavalapsakul et al., 2006). Then, many adaptor proteins which are involved in clathrin-coated pit formation including AP2, AP17 and PmCHC are recruited to induce membrane invagination to form clathrin-coated vesicles which then transport YHV to the early endosome which also may require Rab5 protein (Hutagalung and Novick, 2011; Stenmark, 2009). After that, YHV may be transported toward the late endosome and lysosome via the regulation by PmRab7 for viral uncoating. The intracellular trafficking process of YHV may be similar to that of semliki forest virus (SFV) which is internalized via clathrin mediated endocytosis and requires Rab7 for transportation inside the cell (Vonderheit and Helenius, 2005).

Taken together, this study demonstrated that PmCHC is an essential protein required for YHV internalization into the shrimp cell. Knockdown of PmCHC by dsRNA-PmCHC resulted in inhibition of YHV levels suggesting that clathrin-mediated endocytosis is a major route for YHV infection.

Supplementary data to this article can be found online at http://dx.doi.org/10.1016/j.aquaculture.2014.10.018.

Acknowledgments

We would like to thank Assoc. Prof. Albert Ketterman and Asst. Prof. Dr. Kusol Pootanakit for critically reading the manuscript, and Ms. Chaweewan Chimawei, Mrs. Suparb Hongthong and Ms. Punnee Tongboonsong for technical assistance in culturing shrimp. This work was supported by grants from Mahidol University and Thailand Research Fund (BRG5780006 to C.O. and DPG5680001 to S.P.). PP is supported by the grant DPG5680001.

References

Assavalapsakul, W., Tirasophon, W., Panyim, S., 2005. Antiserum to the gp116 glycoprotein of yellow head virus neutralizes infectivity in primary lymphoid organ cells of *Penaeus monodon*. Dis. Aquat. Org. 63, 85–88.

Assavalapsakul, W., Smith, D.R., Panyim, S., 2006. Identification and characterization of a *Penaeus monodon* lymphoid cell-expressed receptor for the yellow head virus. J. Virol. 80 (1), 262–269.

Bhattacharyya, S., Warfield, K.L., Ruthel, G., Bavari, S., Aman, M.J., Hope, T.J., 2010. Ebola virus uses clathrin-meditated endocytosis as and entry pathway. Virology 401, 18–28.

Boonyaratpalin, S., Supamattaya, K., Kasornchandra, J., Direkbusaracom, S., Aekpanithanpong, U., Chantanachooklin, C., 1993. Non-occluded baculo-like virus, the causative agent of yellow head disease in the black tiger shrimp (*Penaeus monodon*). Fish Pathol. 28 (3), 103–109.

Brodsky, F.M., 2012. Diversity of clathrin function: new tricks for an old protein. Annu. Rev. Cell Dev. Biol. 28, 309–336.

Dereeper, A., Guignon, V., Blanc, G., Audic, S., Buffet, S., Chevenet, F., Dufayard, J.-F., Guindon, S., Lefort, V., Lescot, M., Claverie, J.-M., Gascuel, O., 2008. Phylogeny.fr: robust phylogenetic analysis for the non-specialist. Nucleic Acids Res. 36, W465–W469.

Dereeper, A., Audic, S., Claverie, J.-M., Blanc, G., 2010. BLAST-EXPLORER helps you building datasets for phylogenetic analysis. BMC Evol. Biol. 12, 10:8.

Doherty, G.J., McMahon, H.T., 2009. Mechanisms of endocytosis. Annu. Rev. Biochem. 78, 31.1–31.46.

Flegel, T.W., 1997. Major viral diseases of the black tiger prawn (*Penaeus monodon*) in Thailand. World J. Microbiol. Biotechnol. 13, 433–442.

Hongliang, W., Chengyu, J., 2009. Influenza A virus H5N1 entry into host cells is through clathrin-dependent endocytosis. Sci. China C Life Sci. 52 (5), 464–469.

Huotari, J., Helenius, A., 2011. Endosome maturation. EMBO J. 30 (17), 3481–3500.

Hussain, K.M., Leong, K.L., Ng, M.M., Chu, J.J., 2011. The essential role of clathrin-mediated endocytosis in the infectious entry of human enterovirus 71. J. Biol. Chem. 286 (1), 309–321.

Hutagalung, A.H., Novick, P.J., 2011. Role of Rab GTPases in membrane traffic and cell physiology. Physiol. Rev. 91, 119–149.

Inoue, Y., Tanaka, N., Tanaka, Y., Inoue, S., Morita, K., Zhuang, M., Hattori, T., Sugamura, K., 2007. Clathrin-dependent entry of severe acute respiratory syndrome coronavirus into target cells expressing ACE2 with the cytoplasmic tail deleted. J. Virol. 81 (16), 8722–8729.

Jatuyosporn, T., Supungul, P., Tassanakajon, A., Krusong, K., 2014. The essential role of clathrin-mediated endocytosis in yellow head virus propagation in the black tiger shrimp *Penaeus monodon*. Dev. Comp. Immunol. 44, 100–110.

Jitrapakdee, S., Unajak, S., Sittidilokratna, N., Hodgson, R.A., Cowley, J.A., Walker, P.J., Panyim, S., Boonsaeng, V., 2003. Identification and analysis of gp116 and gp64 structural glycoproteins of yellow head nidovirus of *Penaeus monodon* shrimp. J. Gen. Virol. 84, 863–873.

Khanobdee, K., Soowannayan, C., Flegel, T.W., Ubol, S., Withyachumnarnkul, B., 2002. Evidence for apoptosis correlated with mortality in the giant black tiger shrimp *Penaeus monodon* infected with yellow head virus. Dis. Aquat. Org. 48, 79–90.

Livak, K.J., Schmittgen, T.D., 2001. Analysis of relative gene expression data using real-time quantitative PCR and the $2^{-\Delta\Delta CT}$ method. Methods 25, 402–408.

Marsh, M., Helenius, A., 2006. Virus entry: open sesame. Cell 124, 729–740.

McMahon, H.T., Boucrot, E., 2011. Molecular mechanism and physiological functions of clathrin-mediated endocytosis. Nat. Rev. Mol. Cell Biol. 12, 517–533.

Meertens, L., Bertaux, C., Dragic, T., 2006. Hepatitis C Virus entry requires a critical postinternalization step and delivery to early endosomes via clathrin-coated vesicles. J. Virol. 80 (23), 11571–11578.

Mercer, J., Schelhaas, M., Helenius, A., 2010. Virus entry by endocytosis. Annu. Rev. Biochem. 79, 803–833.

Mousavi, S.A., Malerod, L., Berg, T., Kjeken, R., 2004. Clathrin-dependent endocytosis. Biochem. J. 377, 1–16.

Nadala Jr., C.B., Tapay, L.M., Loh, P.C., 1997. Yellow-head virus: a rhabdovirus-like pathogen of penaeid shrimp. Dis. Aquat. Org. 31, 141–146.

Ongvarrasopone, C., Roshorm, Y., Panyim, S., 2007. A simple and cost effective method to generate dsRNA for RNAi studies in invertebrates. ScienceAsia 33, 35–39.

Ongvarrasopone, C., Chanasakulniyom, M., Sritunyalucksana, K., Panyim, S., 2008. Suppression of PmRab7 by dsRNA inhibits WSSV or YHV infection in shrimp. Mar. Biotechnol. 10 (4), 374–381.

Ongvarrasopone, C., Chomchay, E., Panyim, S., 2010. Antiviral effect of PmRab7 knockdown on inhibition of Laem-Singh virus replication in black tiger shrimp. Antiviral Res. 88, 116–118.

Ongvarrasopone, C., Saejia, P., Chanasakulniyom, M., Panyim, S., 2011. Inhibition of Taura syndrome virus replication in *Litopenaeus vannamei* through silencing LvRab7 gene by double-stranded RNA. Arch. Virol. 156, 1117–1123.

Posiri, P., Ongvarrasopone, C., Panyim, S., 2011. Improved preventive and curative effects of YHV infection in *Penaeus monodon* by a combination of two double stranded RNAs. Aquaculture 314, 34–38.

Posiri, P., Ongvarrasopone, C., Panyim, S., 2013. A simple one-step method for producing dsRNA from *E. coli* to inhibit shrimp virus replication. J. Virol. Methods 188, 64–69.

Rejman, J., Oberle, V., Zuhorn, I.S., Hoekstra, D., 2004. Size-dependent internalization of particles via the pathways of clathrin and caveolae-mediated endocytosis. Biochem. J. 377, 159–169.

Sittidilokratna, N., Dangtip, S., Cowley, J.A., Walker, P.J., 2008. RNA transcription analysis and completion of the genome sequence of yellow head nidovirus. Virus Res. 136, 157–165.

Sritunyalucksana, K., Wannapapho, W., Lo, C.F., Flegel, T.W., 2006. PmRab7 is a VP28-binding protein involved in white spot syndrome virus infection in shrimp. J. Virol. 80 (21), 10734–10742.

Stenmark, H., 2009. Rab GTPases as coordinators of vesicle traffic. Nat. Rev. Mol. Cell Biol. 10, 513–525.

Vonderheit, A., Helenius, A., 2005. Rab7 associates with early endosomes to mediate sorting and transport of semliki forest virus to late endosomes. PLoS Biol. 3 (7), 1225–1238.

Young, A., 2007. Structural insights into the clathrin coat. Semin. Cell Dev. Biol. 18, 448–458.

Zhang, W., Zhou, F., Greene, W., Gao, S.-J., 2010. Rhesus rhadinovirus infection of rhesus fibroblasts occurs through clathrin-mediated endocytosis. J. Virol. 84 (22), 11709–11717.

Aquaculture 459 (2016) 43–53

Contents lists available at ScienceDirect

Aquaculture

journal homepage: www.elsevier.com/locate/aquaculture

Rab5, an early endosomal protein required for yellow head virus infection of *Penaeus monodon*

Pratsaneeyaporn Posiri [a], Sakol Panyim [a,b], Chalermporn Ongvarrasopone [a,*]

[a] Institute of Molecular Biosciences, Mahidol University (Salaya Campus), Nakhon Pathom 73170, Thailand
[b] Department of Biochemistry, Faculty of Science, Mahidol University, Bangkok 10400, Thailand

ARTICLE INFO

Article history:
Received 30 January 2016
Received in revised form 11 March 2016
Accepted 13 March 2016
Available online 15 March 2016

Keywords:
Double stranded RNA
RNAi
Black tiger shrimp
Endocytosis
Yellow head disease

ABSTRACT

Yellow head virus (YHV) is a virulent pathogen in black tiger shrimp. It causes high mortality within a few days after infection. In this study, colocalization between YHV and *P. monodon* Rab5 (PmRab5) which is a small GTPase protein was visualized at 10 min to 3 h post-YHV challenge under a confocal microscope. The result indicated that PmRab5 plays a key role in the early stage of endocytosis, and is involved in YHV trafficking process. Molecular cloning showed that the open reading frame of PmRab5 is 633 bp encoding a putative protein of 210 amino acids with an estimated molecular weight of 23 kDa. PmRab5 contained all Rab-specific signature motifs: Rab family motif (RabF), Rab subfamily motif (RabSF), G-boxes and cysteine prenylation signal. Silencing of PmRab5 by specific dsRNA reduced YHV replication inside the cells. Furthermore, lack of PmRab5 expression exhibited a delay of shrimp mortality after YHV infection. The results demonstrated that PmRab5 is involved in YHV early endosomal trafficking, suggesting its role in the early step of infection.
Statement of relevance: Silencing of PmRab5 may be applicable for inhibition of YHV.

1. Introduction

Enveloped yellow head virus (YHV) belongs to the genus *Okavirus*, family *Roniviridae* in the order *Nidovirales* which is a highly virulent pathogen against *Penaeus monodon* or black tiger shrimp. *P. monodon* is an economically important aquaculture shrimp in Thailand. YHV is a positive-sense ssRNA virus of approximately 27 kb, with poly-(A) tail. Morphology of YHV revealed an envelope bacilliform which has a particle size of about 50–60 × 190–200 nm. Within the YHV particle, it contains the internal helical nucleocapsid which is closely surrounded by an envelope studded with prominent peplomers or spikes (Nadala et al., 1997; Sittidilokratna et al., 2008). YHV contains three structural proteins: two major structural transmembrane glycoproteins (gp116 and gp64) and a nucleoprotein (p20) (Jitrapakdee et al., 2003).

Infection of several enveloped viruses is initiated by the viral glycoprotein binding to its cellular receptor. The conformational change in the virus particle promotes endocytic internalization into the host cell. The virus is delivered from the surface membrane toward early endosomes, maturing endosomes, late endosomes and lysosomes. The acidic condition of the endosomal compartment can trigger the penetration of the viral genome into cytosol. The low pH induces conformational changes of the fusion protein which exists in the viral membrane resulting in host-virus membrane fusion. The virus then uncoats and releases the genome into the cytoplasm (Greber et al., 1994; Marsh and Helenius, 2006; Mercer et al., 2010). Intracellular membrane traffic between these membranous organelles by vesicular transport requires tight regulation to ensure both fidelity and efficiency. The Rab GTPase family which belongs to the Ras superfamily plays a central role in regulating vesicle transports, including vesicle budding, delivery, tethering and fusion with the target membrane (Hutagalung and Novick, 2011; Stenmark, 2009). The intracellular localization and associated vesicle transport of plasma membrane to early endosome and mature endosome requires Rab5 protein. Rab5 associates with plasma membrane-derived clathrin-coated vesicles (Bucci et al., 1992) and mediates tethering with Early Endosome Antigen1 (EEA1), a Rab5 effector protein (Merithew et al., 2003). Then, the trafficking of vesicles from mature endosome to late endosome and lysosome is regulated by Rab7 (Hutagalung and Novick, 2011; Mercer et al., 2010; Stenmark, 2009).

However, molecular mechanisms of the early steps in intracellular trafficking of YHV entry into the shrimp cell are poorly defined. Recently, it has been demonstrated that YHV utilizes clathrin-mediated endocytosis to invade shrimp cells (Jatuyosporn et al., 2014, Posiri et al., 2015). In addition, silencing of *P. monodon* Rab7 (PmRab7), a late endosomal marker resulted in inhibition of YHV replication, suggesting that YHV could not move from the late endosome to the lysosome where its genome was uncoated and released into the cytoplasm for replication (Ongvarrasopone et al., 2008). How YHV is trafficked from the plasma membrane toward late endosomal

* Corresponding author at: Institute of Molecular Biosciences, Mahidol University (Salaya Campus), 25/25 Phutthamonthon 4 Rd. Salaya, Phutthamonthon district, Nakhon Pathom 73170, Thailand.
E-mail address: chalermporn.ong@mahidol.ac.th (C. Ongvarrasopone).

http://dx.doi.org/10.1016/j.aquaculture.2016.03.026
0044-8486/

Table 1
Primer sequences of the experiments.

Primers	Sequences (5′–3′)	Experiments
dRab5-F	AAGGGCCAGTTCCACGAGTACCA(G/A)GA	Amplify PmRab5 partial sequences
dRab5-R	AAGATGTCGTTCACGTTCATGGCGGT	
PmRab5-R1	GGTCTGGGCCTCTTCATATTCAACC	5′ RACE of PmRab5
PRT	CCGGAATTCAAGCTTCTAGAGGATCCTTTTTTTTTTTTTTT	Reverse transcription and RACE assay
PmRab5-R2	CCTTTACCCAGGTCTTAGCACGACC	5′ RACE of PmRab5
PM1	CCGGAATTCAAGCTTCTAGAGGATCC	5′ RACE of PmRab5
FullR5-F2	GGTTGTGTGGTTGATCCTG	Full-length of PmRab5 cDNA
FullR5-R	TTTTTTCTTAAAAATGTCTAACAC	
stPmRab5-F1-*Xba*I	*Xba*I GCTCTAGAGTCAACTATTGGAGCTGCA	Amplification of sense-loop region of dsRNA-PmRab5
lpPmRab5-R1-*Kpn*I	*Xba*I GGGGTACCTATTGGACAGGCTGACATC	
stPmRab5-F2-*Eco*RI/*Xho*I	*Eco*RI *Xbo*I GGAATTCCTCGAGGTCAACTATTGGAGCTGCA	Amplification of antisense region of dsRNA-PmRab5
stPmRab5-R2-*Kpn*I	*Kpn*I GGGGTACCCTTAGCAGAGGTCTCCATAA	
PmRab5-F1	GGAGCTGCATTTCTGACACAGACAG	3′ RACE of PmRab5 and detection of PmRab5 mRNA
PmRab5-R1	GGTCTGGGCCTCTTCATATTCAACC	Detection of PmRab5 mRNA
PmActin-F	GACTCGTACGTGGGCGACGAGG	Detection of PmActin mRNA
PmActin-R	AGCAGCGGTGGTCATCTCCTGCTC	
YHV(hel)-F	CAAGGACCACCTGGTACCGGTAAGAC	Detection of YHV mRNA
YHV(hel)-R	GCGGAAACGACTGACGGCTACATTCAC	

compartment has not been investigated. An increasing evidence for the requirement of Rab5 in the early entry step of several viruses including dengue virus, West Nile virus and foot-and-mouth disease virus (Johns et al., 2009; Krishnan et al., 2007) could suggest a possible role of Rab5 for YHV entry into shrimp cells. Therefore, in this study, the molecular mechanism of Rab5 in YHV entry into the shrimp cells was investigated.

2. Materials and methods

2.1. Primary hemocyte culture

Hemolymph was collected from *P. monodon* using sterile syringe and 18 gauge needle with anticoagulant AC-1 (27 mM Sodium citrate, 34.33 mM NaCl, 104.5 mM Glucose, 198.17 mM EDTA, pH 7.0) in a ratio 1:1. The mixture of hemolymph and anticoagulant was centrifuged at 550 ×*g* for 10 min to separate the hemocyte pellet from the hemolymph. The hemocyte pellet was washed in 1 ml of L-15 culture medium washing solution (2× Leibovitz L-15 medium, 15% (*v*/*v*) fetal bovine serum, 200 IU/ml penicillin and 200 μg/ml streptomycin). Then the washing step was repeated three times. After that, the hemocytes were resuspended in 1 ml of L-15 culture medium working solution (2× Leibovitz L-15 medium, 15% (*v*/*v*) fetal bovine serum, 200 IU/ml penicillin, 200 μg/ml streptomycin, and 15% (*v*/*v*) shrimp meat extract). The hemocyte number was counted under a light microscope by using hemocytometer. The cells (10^5 cells per well) were seeded into a 24-well plate.

2.2. Yellow head virus (YHV) stock

Viral free shrimp was injected with YHV to propagate the virus. All use of 'shrimp' refers to *P. monodon*. Hemolymph was collected with AC-1 solution from YHV infected moribund shrimp. The hemolymph was centrifuged at 20,000 ×*g* for 20 min at 4 °C to remove hemocyte debris. Then, free YHV particles were collected by ultracentrifugation (100,000 ×*g*) for 1 h. Virus pellets were dissolved with 150 mM NaCl and stored at −80 °C until used. YHV titer was determined by using RT-PCR with YHV helicase gene.

Table 2
Percent amino acid sequence identity of PmRab5 compared with each organism. Accession number of organisms used for Rab5 protein domain and phylogenetic analysis are listed.

Organisms	Accession number	Rab5 isoforms	Percent identity of PmRab5 compared with each organism
Aedes aegypti	XP_001658691	AaRab5	77
Aiptasia pulchella	AAV34202	ApRab5	85
Apis mellifera	XP_003251474	AmRab5B	76
Ascaris suum	ADY48161	AsRab5B	79
Bombyx mori	NP_001037614	BmRab5	78
Canis lupus	NP_001003317	ClRab5A	75
	XP_531627	ClRab5B	81
	CAA81626	ClRab5C	81
Danaus plexippus	EHJ77299	DpRab5	81
Danio rerio	NP_957264	DrRab5A	75
	AAI65047	DrRab5C	77
Homo sapiens	CAG38731	HsRab5A	75
	CAG46491	HsRab5B	81
	CAG46699	HsRab5C	81
Litopenaeus vannamei	AFK08607	LvRab5	100
Loa loa	XP_003136717	LlRab5	77
Medicago truncatula	AES68021	MtRab5C	48
Mus musculus	BAF02855	MmRab5A	75
	CAA59016	MmRab5B	81
	BAF02857	MmRab5C	80
Oryza sativa	AAK38149	OsRab5	60
Penaeus monodon	KT896540	PmRab5	–
Physcomitrella patens	BAG09234	PpRab5	48
Suberites domuncula	ABD65432	SdRab5	76
Tribolium castaneum	EFA04701	TcRab5	84
Xenopus tropicalis	NP_001008068	XtRab5A	76
	AAH75323	XtRab5B	80
	CAJ81259	XtRab5C	76

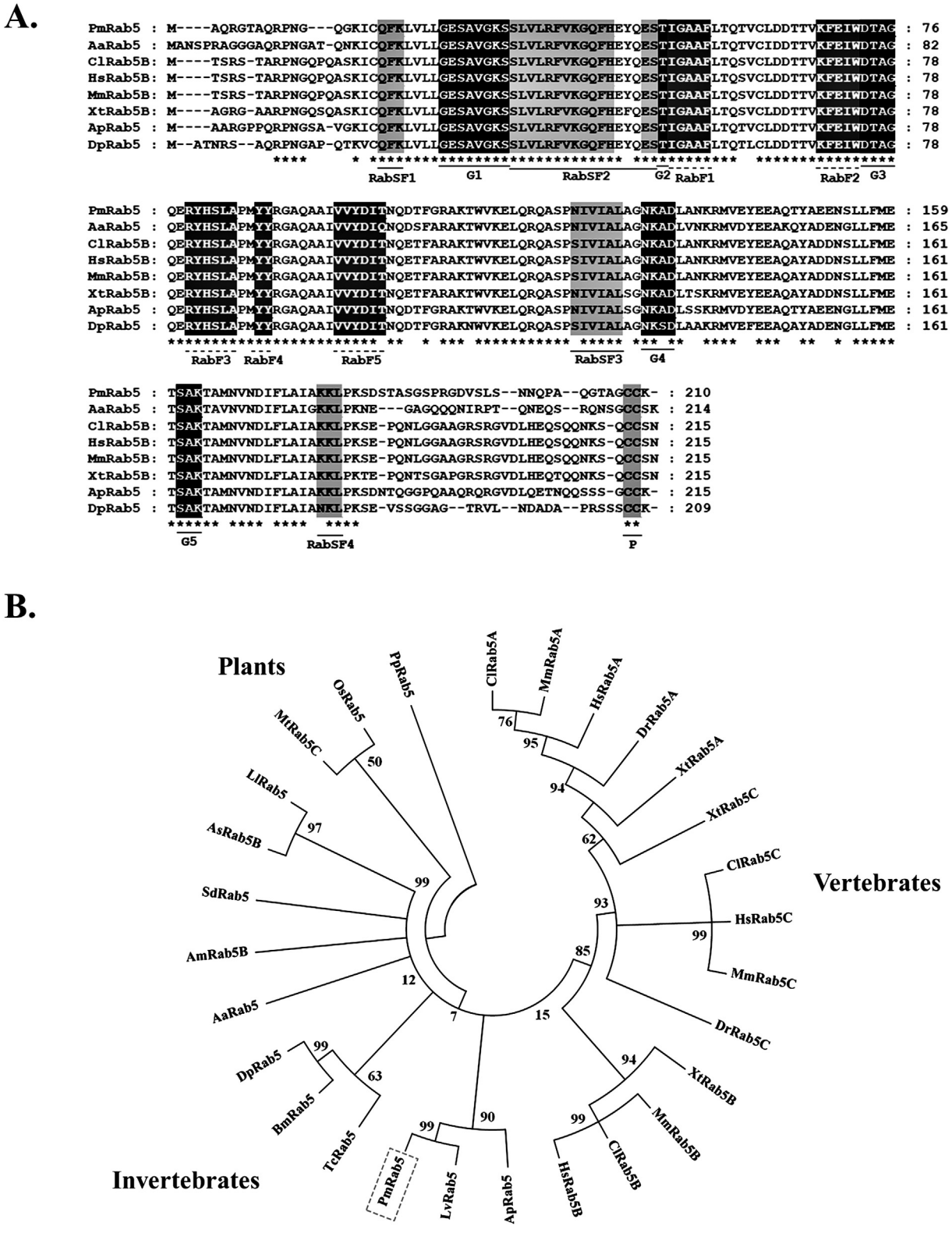

Fig. 1. PmRab5 domains and phylogenetic tree analysis. (A) Amino acid sequence alignment of Rab5 proteins from selected organisms demonstrated a signature of five Rab family motifs (RabF1–RabF5) (light gray shade), four Rab subfamily domains (RabSF1–RabSF4) (heavy gray), five G-boxes (G1–G5) (black) and a prenylation site (P). Star (*) represents the consensus amino acid sequence. (B) Phylogenetics tree analysis of Rab5 based on amino acid sequences. Molecular Evolutionary Genetics Analysis (MEGA) 4.1 program was used for phylogenetic tree construction from several species: *Aedes aegypti* (Aa), *Aiptasia pulchella* (Ap), *Apis mellifera* (Am), *Ascaris suum* (As), *Bombyx mori* (Bm), *Canis lupus* (Cl), *Danaus plexippus* (Dp), *Danio rerio* (Dr), *Homo sapiens* (Hs), *Litopenaeus vannamei* (Lv), *Loa loa* (Ll), *Medicago truncatula* (Mt), *Mus musculus* (Mm), *Oryza sativa* (Os), *Penaeus monodon* (Pm), *Physcomitrella patens* (Pp), *Suberites domuncula* (Sd), *Tribolium castaneum* (Tc), and *Xenopus tropicalis* (Xt).

2.3. Immunofluorescence staining of YHV and P. monodon Rab5 (PmRab5)

The primary hemocytes (10^5 cells) in 24-well plates with cover-slip were incubated at 4 °C. After 30 min, the cells were washed with ice-cold phosphate buffer saline (1× PBS, pH 7.4) and then infected with YHV at a multiplicity of infection (MOI) of 10 for 30 min at 4 °C. The cells were then transferred to 28 °C for 10 min to allow the cells to recover (specified as time 0). Next, the cells were fixed in ice-cold 4% paraformaldehyde at different time points, 0 min, 10 min, 30 min, 1 h, 3 h, 6 h, and 12 h, followed by three washing steps with ice-cold 1× PBS pH 7.4 for 5 min each. The fixed hemocytes were permeabilized with 0.1% Triton X-100 in 1× PBS, pH 7.4, and then blocked with 10% fetal bovine serum. Then, the cells were incubated with rabbit anti-Rab5 primary antibody (ab94690, abcam, USA) at 1:400 dilution at room temperature, overnight. Then the cells were incubated with mouse anti-gp64, a YHV detecting antibody (kindly provided by Professor Paisarn Sithigorngul, Department of Biology, Faculty of Science, Srinakharinwirot University) at 1:200 dilution. After 2 h, the cells were washed 3 times with 0.05% Tween-20 in 1× PBS, pH 7.4, and then incubated with secondary antibody, goat anti-mouse Alexa Fluor® 488 and goat anti-rabbit Alexa Fluor® 594 (Invitrogen), (1:500 dilution) for 1 h in the dark, and washed three times with 0.05% Tween-20 in 1× PBS, pH 7.4. Subsequently, the nuclei of the hemocytes were stained with TO-PRO®-3 iodide at 1:500 dilution (Invitrogen) in 1× PBS, pH 7.4, at room temperature for 1 h in the dark, and washed three times with 0.05% Tween-20 in 1× PBS, pH 7.4. The cover slips were mounted with anti-fade permount (Invitrogen). Fluorescence signals were detected by using a confocal microscope (FluoView FV10i — Olympus).

2.4. Cloning of the full-length PmRab5 cDNA from P. monodon

Multiple sequence alignment of Rab5 proteins from several species (Table 2) was aligned and used to design degenerate primers, dRab5-F

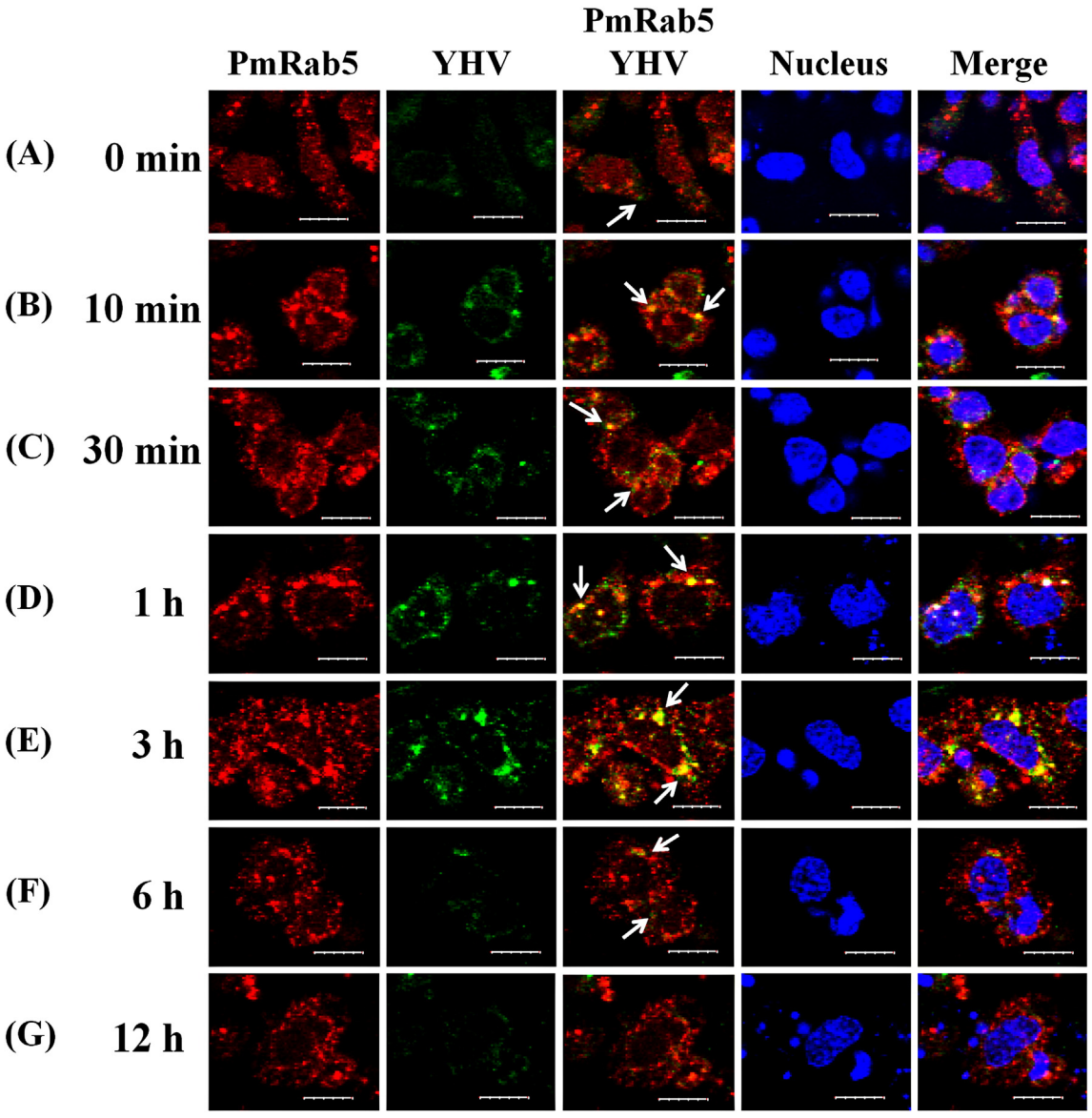

Fig. 2. Visualization of the interaction between PmRab5 protein and YHV particles. The primary hemocytes were first incubated with YHV and then the infected cells were fixed at various time points. (A) At time point 0 min post-infection, no colocalization between YHV and PmRab5 was observed. YHV particles could be detected around the cell (arrow). (B and C) YHV particles demonstrated colocalizing with PmRab5 (arrow) at 10 and 30 min post-infection. (D and E) Increased intensity of the colocalization signal (arrow) was observed at 1 to 3 h post-infection. (F) The signal of YHV particles at time 6 hpi showed inside the cells without colocalization with PmRab5 (arrow). (G) At 12 hpi, YHV signal was hardly detected. PmRab5 signal was detected by anti-Rab5 antibody and showed in red. YHV particle was detected by anti-gp64 antibody and showed in green. Colocalization of PmRab5 and YHV was shown as yellow. Cell nuclei were stained blue with TOPRO®-3 iodide. Scale bar is 10 μm.

and dRab5-R (Table 1), to PCR amplify the partial sequence of PmRab5. The PCR condition was: a hot-start at 95 °C for 5 min, then 30 cycles of 95 °C for 30 s, 46 °C for 30 s, and 72 °C for 45 s, followed by 72 °C for 7 min. Next, the expected PmRab5 band was cut and gel purified using Gel/PCR DNA fragments extraction kit (Geneaid). The fragment (346 bp) was cloned into pGEM-T easy vector (Promega) and sequenced (First Base Co, Ltd., Malaysia).

The 5′ and 3′ ends of PmRab5 were amplified by using rapid amplification of cDNA ends (RACE) approach. For 5′-RACE, the cDNA was first generated by using Superscript III® reverse transcriptase (Invitrogen) with a PmRab5-specific primer, PmRab5-R1 (Table 1). Then, the RNA template was removed by RNaseH (Promega) and the first-stranded cDNA was purified by ethanol precipitation, followed by Geneaid spin column (Geneaid). The purified cDNA was performed an polyA-tailing by terminal deoxynucleotidyl transferase (TdT) (Promega). Then, polyA-tailed cDNA was used as template to perform the first PCR with PmRab5-R1 and PRT primers. Next, the obtained PCR product was diluted at 1:100 and used as template for nested PCR with PmRab5-R2 and PM1 nested primer (Table 1). For 3′ RACE, first-strand cDNA was generated by Impromp II™ reverse transcriptase (Promega) with PRT primer (Table 1). Then, cDNA was used as template for the first PCR with PmRab5-F1 (Table 1) and PRT primer. All of RACE products were purified, cloned and sequenced as described above.

The 3 partial sequences obtained from PCR using degenerate primers, 5′ and 3′ RACE products were *in silico* assembled to obtain the full-length PmRab5 cDNA. In order to verify that the assembled sequence is indeed corresponded to the full-length PmRab5 sequence, PCR was performed using primers targeting to the 5′ and 3′ ends, fullR5-F2 and fullR5-R (Table 1), and Vent® DNA polymerase (New England Biolabs). The PCR condition was as follow: denaturation at 95 °C for 5 min, 30 cycles of 95 °C for 30 s, 51 °C for 30 s, and 72 °C for 2 min 30 s, followed by 72 °C for 7 min. PCR products were purified, cloned and sequenced as previously described.

2.5. Sequence analysis of PmRab5 cDNA

Sequence analysis was performed with BLASTN (http://blast.ncbi.nlm.nih.gov). The conserved domain of the deduced amino acid sequences were predicted using NCBI database (Zhu et al., 2004). Molecular weight and isoelectric point (pI) of the protein were performed with Expert Protein Analysis System (www.expasy.org). Rab5 protein sequences from several organisms were obtained from GenBank database. Multiple alignments were performed using VectorNTI program

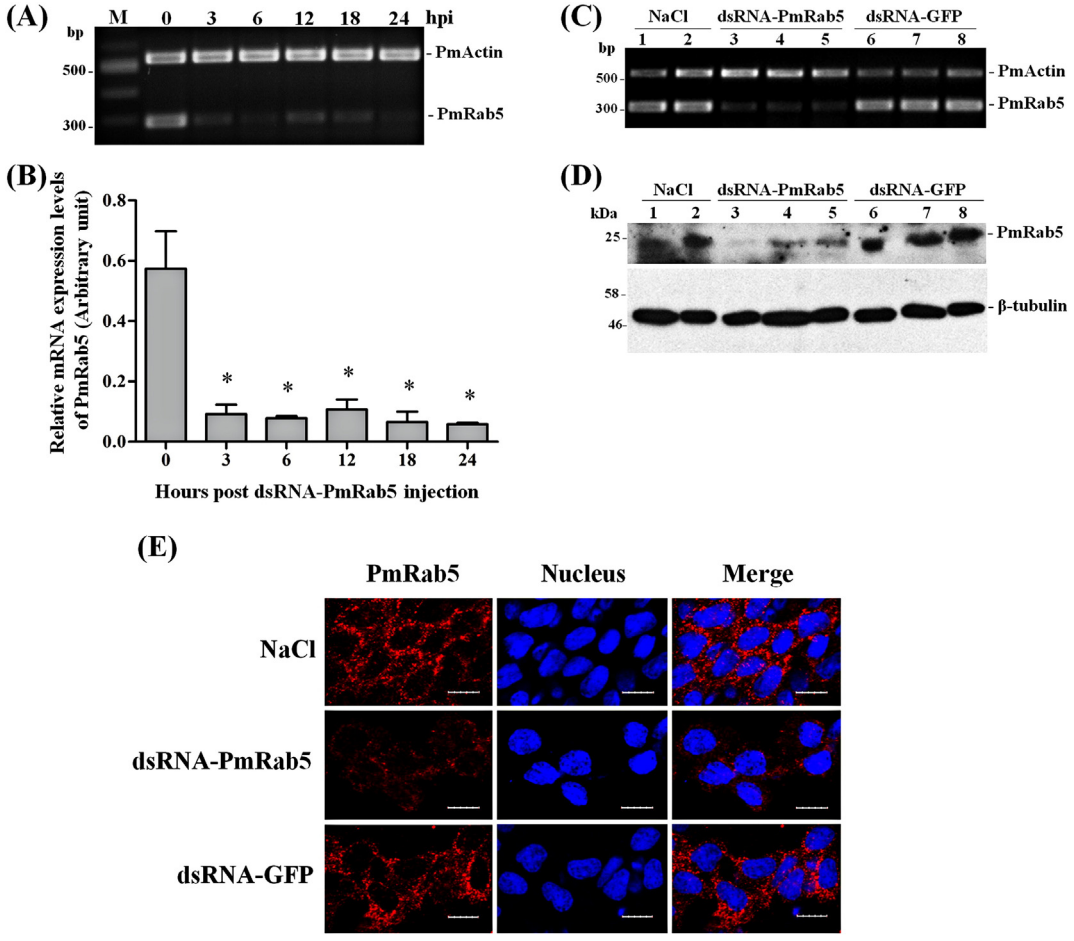

Fig. 3. Knockdown effect of PmRab5 by dsRNA-PmRab5. (A) A representative gel of RT-PCR products of PmRab5 and PmActin expression of shrimp injected with dsRNA-PmRab5. The hemolymph was collected at 0, 3, 6, 12, 18 and 24 h post-dsRNA injection. M is 1 kb+ DNA marker. (B) The relative mRNA expression levels (mean ± SEM) of PmRab5 normalized with PmActin and expressed as arbitrary unit (n = 3 for each time course of post-dsRNA injection). (*) represents statistically significant difference between before (time 0) and after dsRNA-PmRab5 injection at various time courses ($p < 0.05$). The mRNA level of PmRab5 and PmActin (C); and, protein level of PmRab5 and β-tubulin (D) of shrimp injected with NaCl (lanes 1–2), dsRNA-PmRab5 (lanes 3–5) and dsRNA-GFP (lanes 6–8) at 24-h post-dsRNAs injection. (E) Confocal immunofluorescence study of the hemocytes collected at 24-h post-dsRNAs injection compared to the NaCl and unrelated dsRNA-GFP control groups. The localization of PmRab5 was represented in red. Cell nuclei were stained blue with TOPRO®-3 iodide. Scale bar is 10 μm.

(Invitrogen). Molecular Evolutionary Genetics Analysis (MEGA) 4.1 program was used for phylogenetic analysis based on the neighbor-joining method (Kumar et al., 2008).

2.6. Construction of the recombinant plasmid for production of dsRNA-PmRab5

Recombinant plasmid containing stem-loop of dsRNA-PmRab5 was constructed in pGEM-3Zf+ (Promega) and pET-17b (Novagen) vectors. Sense-loop region of the dsRNA, size 494 bp, was amplified from the first-strand cDNA by stPmRab5-F1-*Xba*I and lpPmRab5-R1-*Kpn*I specific primers (Table 1). Antisense region, size 394 bp, was amplified by stPmRab5-F2-*EcoR*I/*Xho*I and stPmRab5-R2-*Kpn*I primers (Table 1). The PCR fragment of sense-loop was cloned into pGEM-3Zf+ followed by the antisense fragment in the sense and antisense orientation, respectively. Then, this stem-loop fragment of size about 888 bp was subcloned into *Xba*I and *Xho*I sites of pET-17b vector for construction of recombinant plasmid, named pET17b-PmRab5, which was used for *in vivo* bacterial expression of dsRNA-PmRab5. In addition, recombinant plasmid containing stem-loop of dsRNA-GFP (kindly provided by Asst. Prof. Witoon Tirasophon) was used to express dsRNA-GFP which was used as an unrelated dsRNA (Ongvarrasopone et al., 2007).

2.7. Production of dsRNA-PmRab5 by in vivo bacterial expression

Recombinant plasmid pET17b-PmRab5 was transformed into a ribonuclease (RNase) III mutant HT115 *Escherichia coli* strain. This strain is modified to express T7 RNA polymerase from an isopropyl-β-D thiogalactopyranoside (IPTG) inducible promoter. Therefore, dsRNAs can be produced in the HT115 bacterial host after induction with 0.1 mM IPTG. Double stranded RNA was extracted and purified as previously described (Ongvarrasopone et al., 2007; Posiri et al., 2013). The quality of dsRNA was characterized by ribonuclease digestion assay using RNase A and RNase III. dsRNA concentration was estimated by agarose gel electrophoresis and compared to the intensity of 100 bp DNA marker.

2.8. Black tiger shrimp culture

Juvenile shrimp, sizes about 10 g, were obtained from commercial shrimp farms in Thailand. The shrimp were maintained in large boxes with oxygenated sea water at 20 ppt salinity for 1 day before experiment and fed with commercial diet every day. Half of the water was exchanged every 2 days.

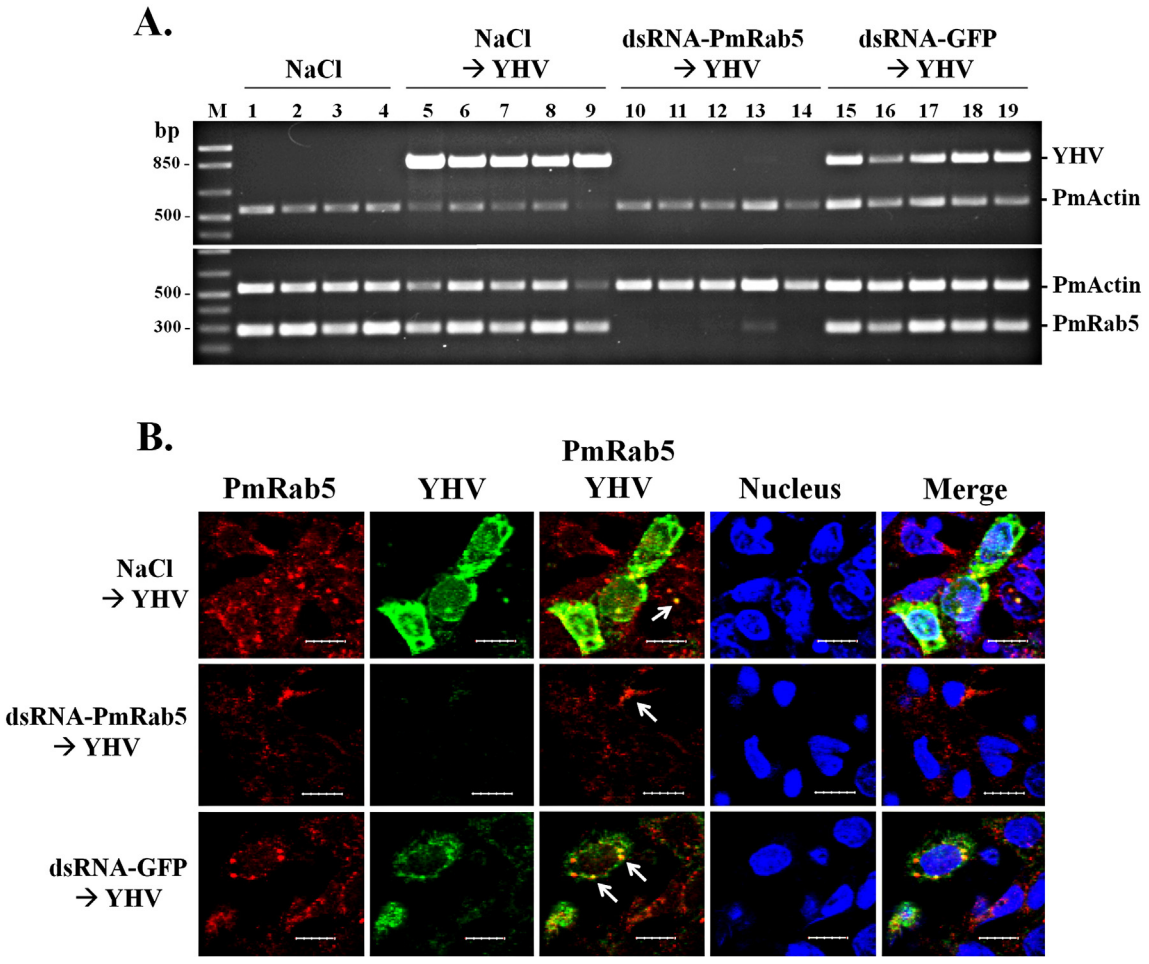

Fig. 4. Depletion of PmRab5 during YHV infection. (A) A representative gel of RT-PCR products of YHV (top panel), PmRab5 (bottom panel) and PmActin from gill tissues of shrimp injected with NaCl only (lanes 1–4) and challenged with YHV (lanes 5–9) and shrimp injected with dsRNA-PmRab5 (lanes 10–14) or dsRNA-GFP (lanes 15–19) prior to YHV challenge. M is 1 kb+ DNA marker. (B) Confocal immunofluorescence study demonstrated that knockdown of PmRab5 by dsRNA-PmRab5 disrupted YHV trafficking during the early-stage of YHV infection. The hemocytes were collected at 48 h post-YHV injection from shrimp injected with NaCl, 2.5 $\mu g \cdot g^{-1}$ shrimp of dsRNA-PmRab5 or 2.5 $\mu g \cdot g^{-1}$ shrimp of dsRNA-GFP prior to YHV challenge. The PmRab5 signal is represented in red. YHV is represented in green. The colocalization between YHV particles and PmRab5 are shown by arrows. Cell nuclei were stained blue with TOPRO®-3 iodide. Scale bar is 10 μm.

2.9. Suppression of PmRab5 mRNA by dsRNA-PmRab5 in P. monodon

The knockdown effect of PmRab5 mRNA using dsRNA-PmRab5 was tested by injection of dsRNA into hemolymph. Shrimp were injected with 2.5 $\mu g \cdot g^{-1}$ shrimp of dsRNA-PmRab5 dissolved in 150 mM NaCl. Then, hemolymph was collected at time 0, 3, 6, 12, 18 and 24 h post-dsRNA injection to extract total RNA. Suppression effect of the PmRab5 was analyzed by RT-PCR to determine mRNA level.

In addition, hemocytes of shrimp injected with 2.5 $\mu g \cdot g^{-1}$ shrimp of dsRNA-PmRab5, unrelated dsRNA-GFP and NaCl were collected to observe PmRab5 mRNA by using RT-PCR and protein level by western blot analysis and an immunofluorescence assay.

2.10. Effect of dsRNA-PmRab5 during YHV infection

To study the function of PmRab5 on YHV infection, shrimp was injected into hemocoel with dsRNA-PmRab5 or dsRNA-GFP at 2.5 $\mu g \cdot g^{-1}$ shrimp. After 24-h post-injection (hpi), YHV was injected. Then, gill was collected at 48 h post-YHV challenge to detect PmRab5 and YHV mRNA expressions. Hemocytes of each group were collected to investigate PmRab5 and YHV protein levels by an immunofluorescence assay. Injection of 150 mM NaCl alone or prior to YHV challenge was used as experimental controls.

2.11. Shrimp mortality assay

The mortality of shrimp injected with dsRNA-Rab5 with YHV challenge was observed every 12 h. Shrimp size about 1 g and 15 shrimps per group were tested. Four independent experiments were performed. Shrimps were injected with 150 mM NaCl, 2.5 $\mu g \cdot g^{-1}$ shrimp of dsRNA-PmRab5 or unrelated dsRNA-GFP. After 24-h post-injection, YHV was injected. Dead shrimps were recorded every 12 h.

2.12. RNA isolation and RT-PCR

Total RNA from gill tissues or hemolymph was isolated by Trizol® reagent (Molecular Research Center) following the manufacturer's procedure. The RNA concentration was measured by Nanodrop ND-1000

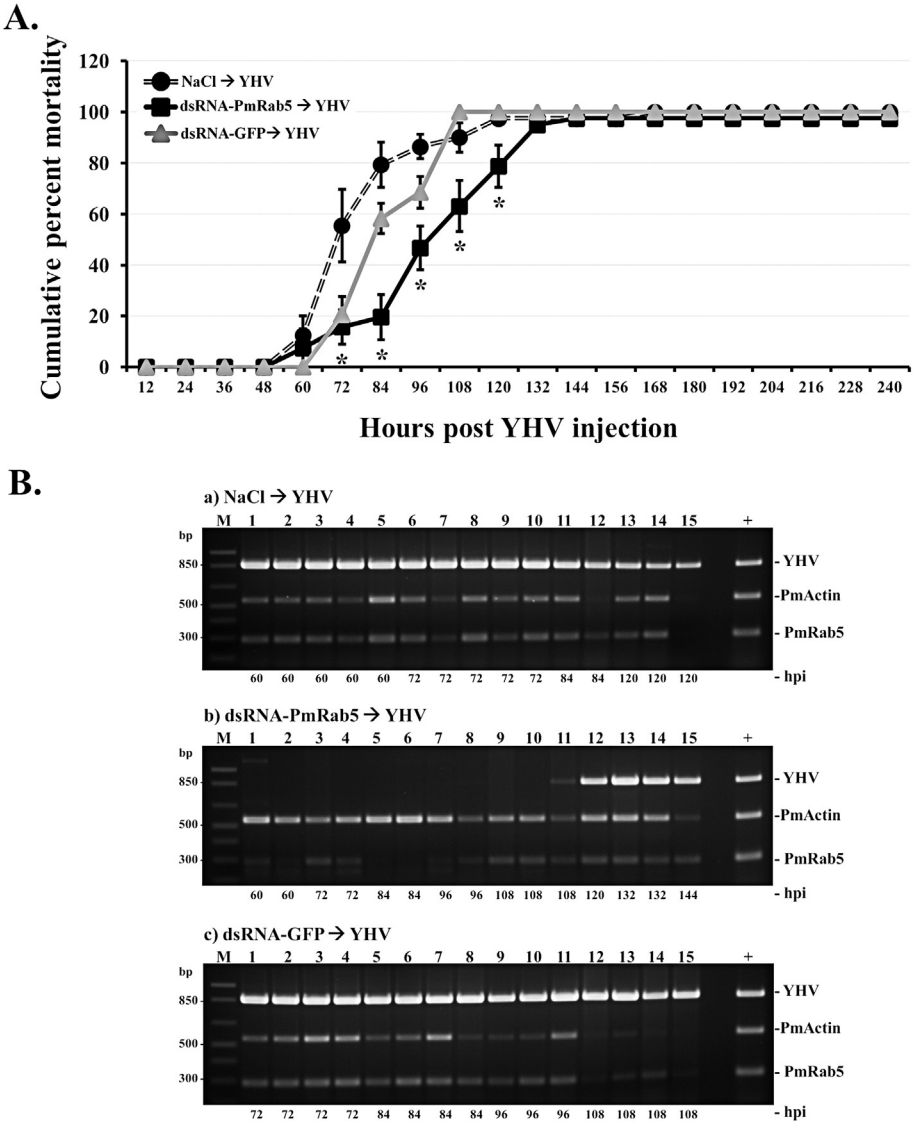

Fig. 5. Cumulative mortality assay in the PmRab5 knockdown shrimp upon YHV infection. (A) The cumulative percent mortality of shrimp injected with NaCl, 2.5 $\mu g \cdot g^{-1}$ shrimp of dsRNA-PmRab5, or 2.5 $\mu g \cdot g^{-1}$ shrimp of dsRNA-GFP 24 h before YHV challenge. Dead shrimps were recorded every 12 h post-YHV injection. (*) represents statistically significant difference between NaCl → YHV and dsRNA-PmRab5 → YHV injection ($p < 0.05$). (B) A representative gel of RT-PCR products for YHV and PmRab5 mRNA levels of dead shrimp. PmActin was used as internal control. (a) NaCl → YHV group, (b) dsRNA-PmRab5 → YHV group and (c) dsRNA-GFP → YHV group. The number on the bottom of each lane demonstrated the time (hours of post-YHV challenge, hpi) of dead shrimp. M is 1 kb+ DNA marker.

spectrophotometer (Nanodrop Technologies). RNA (2 μg) was used as template to generate the first-strand cDNA by Improm-II™ reverse transcriptase (Promega) using PRT primer (Table 1). PmRab5 was amplified by PCR using primers PmRab5-F1 and PmRab5-R1. PmActin mRNA expression, used for internal control, was amplified by PmActin-F and PmActin-R1 specific primers (Table 1). Multiplex PCR for PmRab5 and PmActin was amplified according to this condition: 95 °C for 5 min, 25 cycles of 95 °C for 30 s, 60 °C for 30 s, and 72 °C for 45 s, followed by 72 °C for 7 min. YHV expression was amplified by using YHV(hel)-F and YHV(hel)-R primers (Table 1). PCR products were electrophoresed on 1.5% agarose gel. The intensity of each band after subtracting the background was quantified by using ImageJ (version 1.46r) program. The relative expression level of PmRab5 was normalized with PmActin level and expressed as an arbitrary unit.

2.13. Western blot analysis

Hemocyte proteins were extracted by using Buffer T (8 M Urea, 2 M Thiourea, 0.4% Triton X-100, 60 mM DTT, 1 mM PMSF, 1× Protease inhibitor cocktail (Sigma)). The protein lysate of each shrimp was electrophoresed in 10% SDS-polyacrylamide gel (SDS-PAGE). The proteins in SDS-PAGE were transferred from gel onto a PVDF membrane (Bio-Rad) by electrophoresis with 1× transfer buffer [0.025 M Tris–HCl pH 8.3, 0.192 M glycine, and 20% (*v*/*v*) methanol]. The membrane was blocked in 5% skimmed milk in 1× PBS containing 0.05% Tween-20 (PBST). PmRab5 and β-tubulin were detected by incubating the membrane with rabbit anti-Rab5 (ab94690, abcam, USA) and anti-β-tubulin (kindly provided by Dr. Phattara-Orn Havanapan) antibody, respectively. Then, the membrane was washed with PBST for 10 min at least 3 times. After that, it was incubated with horseradish peroxidase conjugated to goat anti-rabbit polyclonal antibodies (Sigma), followed by washing as described above. The signal was detected by Luminata™ Forte Western HRP Substrate (Millipore Corporation). PmRab5 and β-tubulin have sizes about 23 and 50 kDa, respectively.

2.14. Statistical analysis

The relative mRNA levels of PmRab5 normalized with PmActin were presented as mean ± SEM. Cumulative percent mortality was plotted as mean ± SEM. Moreover, significant differences of each experimental group were tested by analysis of variance (ANOVA). A probability (p) value less than 0.05 was used to define significant difference.

3. Results

3.1. Full-length cDNA and amino acid sequences of PmRab5

The conserved domains from the alignment of Rab5 proteins from several organisms were used to design primers to amplify the partial sequence of Rab5 from gill tissue of *P. monodon* by PCR. A partial sequence of 346 nucleotides of the putative PmRab5 showed more than 90% sequence identity to Rab5 protein of other species (data not shown). The 5′ and 3′ ends of PmRab5 were obtained by using RACE approach. The full-length cDNA of PmRab5 was confirmed by using specific primers targeting the 5′ and 3′ ends. It comprised of 1293 bp with a 113 bp 5′ untranslated region (UTR), a 633 bp of open reading frame (ORF) (nucleotide 114–746), a 547 bp 3′ UTR with polyadenylation (poly-A) signal. The Kozak's consensus sequence (*AXXATGG*) was present at nucleotide 111–117 (*ATTATGG*). Moreover, a typical poly-A signal (*AATATTA*) was found at nucleotide 1252–1258 (Supplementary Fig. 1). The sequence of PmRab5 cDNA was submitted into the GenBank database under the accession number KT896540.

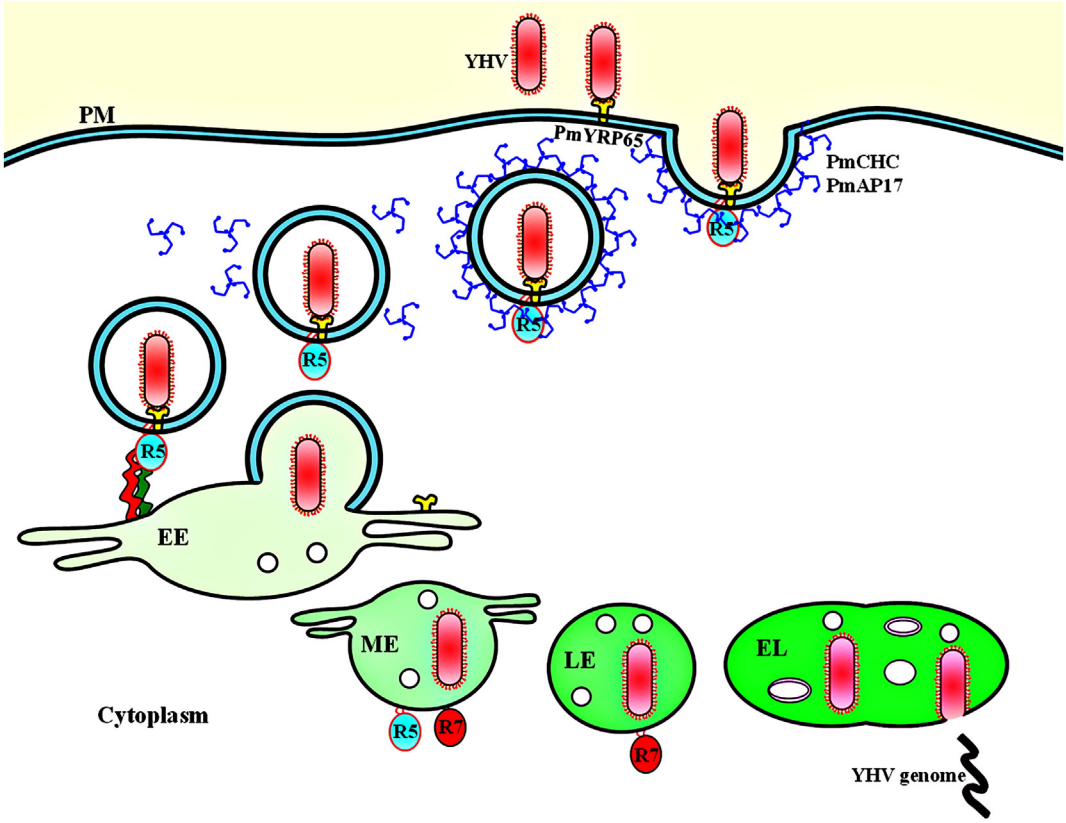

Fig. 6. Schematic model of YHV trafficking into shrimp cell. YHV binds with its receptor (PmYRP65) and internalizes into the cells *via* clathrin-mediated endocytosis which required PmCHC and PmAP17 proteins. Vesicle containing the virus is transported from plasma membrane (PM) to early endosome (EE) and then moved toward maturing endosome (ME), late endosome (LE) and endolysosome (EL). These processes, PM to EE and to ME are regulated by PmRab5 (R5) whereas ME to LE and to EL are regulated by PmRab7 (R7) protein. YHV genome may be released by acidic condition in endolysosome into the cytoplasm where the replication process begins.

The deduced amino acid sequence of PmRab5 is 210 amino acids with an estimated molecular weight of 22.97 kDa and a pI of 8.29. Blastp search of NCBI database showed high sequence homology of PmRab5 protein with other known Rab5 proteins in the database (Table 2). Moreover, the alignment of PmRab5 to Rab5 proteins from several organisms such as mosquito (*Aedes aegypti*), dog (*Canis lupus*), human (*Homo sapiens*), mouse (*Mus musculus*), frog (*Xenopus tropicalis*), sea anemone (*Aiptasia pulchella*) and butterfly (*Danaus plexippus*) demonstrated the conserved motifs of Rab protein family, including five Rab family motifs (RabF1–5), four Rab subfamily motifs (RabSF1–4) which defined Rab5 protein, five signature domains for GTP-binding sites (G1–G5) and a putative prenylation signal (*XCCX*) at the C-terminal of the invertebrates sequence (Stenmark and Olkkonen, 2001; Zhu et al., 2004) (Fig. 1A). Phylogenetic tree analysis separated Rab5 protein into 3 clusters, including vertebrate, invertebrate and plant. The tree revealed that PmRab5 is in the invertebrates group (Fig. 1B). The expression of PmRab5 in *P. monodon* was examined by multiplex RT-PCR. The results demonstrated that PmRab5 was expressed at similar levels in several tissues including brain, thoracic ganglia, nerve cord, gill, lymphoid organ, hepatopancreas, ovary and hemocytes (Supplementary Fig. 2).

3.2. YHV and PmRab5 are colocalized in the hemocytes during YHV infection

Rab5 protein regulates endocytic vesicle membrane that transports the cargo from plasma membrane to the early endosome (Bucci et al., 1992). This process is an early step for many viruses to enter into the cells (Cheng et al., 2012; Clemente and de la Torre, 2009; Johns et al., 2009; Macovei et al., 2013). To elucidate the function of PmRab5 that is possibly involved in the molecular trafficking process of YHV entry into hemocytes, colocalization of YHV and PmRab5 was investigated. Primary hemocyte culture was infected with YHV. Localization of YHV and PmRab5 were investigated at 0 min, 10 min, 30 min, 1 h, 3 h, 6 h and 12 h post-infection (pi.). The signal of YHV was detected around the cell surface and no colocalization of YHV particles and PmRab5 was observed at 0 min. From 10 to 30 min, strong colocalized signals of YHV and PmRab5 were detected. The signals were strongest at time 1 to 3 hpi. Interestingly, the colocalization signal was faint at 6 hpi and completely absent at 12 hpi (Fig. 2).

3.3. PmRab5 was suppressed by specific dsRNA in shrimp

In order to study the function of PmRab5 in shrimp, RNA interference (RNAi) was used as a tool to investigate its role. First, dsRNA targeting PmRab5 (dsRNA-PmRab5) was constructed and tested for its suppression of endogenous PmRab5 transcript. Shrimps received dsRNA-PmRab5 injection showed significant reduction of PmRab5 transcript at more than 85% from 3 hpi to 24 hpi (Fig. 3A and 3B). Moreover, specificity of the knockdown effect by dsRNA-PmRab5 was also tested. Shrimps received dsRNA-PmRab5 demonstrated reduction of PmRab5 at both the mRNA and protein levels. In contrast, the knockdown effect of PmRab5 was not seen in shrimp injected with unrelated dsRNA-GFP or NaCl-injected groups (Fig. 3C and 3D). In addition, immunofluorescence staining of the hemocytes obtained from shrimps injected with dsRNA-PmRab5 demonstrated faint PmRab5 signal when compared to that of the NaCl and dsRNA-GFP groups (Fig. 3E).

3.4. YHV requires PmRab5 for entry into shrimp cells

To study the suppression effect of PmRab5 during YHV challenge, shrimps were injected with dsRNA-PmRab5 at 2.5 $\mu g \cdot g^{-1}$ shrimp 24 h prior to YHV challenge. Injection of dsRNA-GFP was used as an unrelated control group. Then, gills were collected for total RNA extraction after 48 h post-YHV challenge. Injection of dsRNA-PmRab5 demonstrated approximately 97% reduction of PmRab5 transcript when compared to the NaCl and dsRNA-GFP groups, resulting in hardly observable YHV mRNA level. On the other hand, injection of NaCl or dsRNA-GFP prior to YHV challenge showed high levels of YHV (Fig. 4A). Moreover, immunofluorescence staining of hemocytes collected 48 h post-YHV challenge in dsRNA-PmRab5 injected group showed faint signal of PmRab5 protein when compared to the hemocytes from NaCl or dsRNA-GFP group. Interestingly, the depleted PmRab5 cells hardly showed any YHV particles inside the cells. Colocalization between YHV particles with PmRab5 could be barely detected in the PmRab5-knockdown cells. However, a clear colocalization signal of PmRab5 and YHV could be clearly observed in the hemocytes from NaCl and dsRNA-GFP injected group (Fig. 4B).

3.5. Silencing of PmRab5 levels delayed YHV replication and shrimp mortality in infected shrimp

To further investigate the suppression effect of PmRab5 in YHV infected shrimp, shrimp mortality assay was performed. Shrimp injected with dsRNA-PmRab5 followed by YHV challenge exhibited 97.5% cumulative mortality at 132 hpi. Rate of shrimp death in this group still unchanged after 240 hpi. On the other hand, shrimp challenged with YHV alone or injected with unrelated dsRNA-GFP followed by YHV challenge that used as the control groups demonstrated 100% mortality at 168 and 108 hpi, respectively. A significant decrease of cumulative percent mortality in YHV infected shrimp could be observed at 72–120 hpi in the PmRab5 knockdown group when compared to the control groups (Fig. 5). To check YHV levels, shrimps died at various time points were sampled. YHV mRNA levels could not be detected during 60–108 hpi in dead shrimp that the PmRab5 expression was suppressed. However, YHV mRNA levels could be observed after 120 hpi (Fig. 5B (b)). In contrast, high levels of YHV expression can be detected in all dead shrimps from the control groups (Fig. 5B (a and c)).

4. Discussion

Yellow head virus is a serious causative agent that led to high mortality rate in *P. monodon*. Understanding of the virus trafficking pathway especially the mechanism of YHV infection is still poorly understood. Knowledge of the virus life cycles needs to be examined to shed light on providing useful information and to develop approaches for prevention and cure of shrimp from YHV infection. The endocytosis pathway of YHV has been characterized. Specifically, YHV utilized clathrin-mediated endocytosis which required clathrin coated vesicle protein including *P. monodon* clathrin heavy chain (PmCHC) and clathrin coat assembly protein 17 (AP17) to invade shrimp cells (Jatuyosporn et al., 2014; Posiri et al., 2015). Moreover, Rab5, a small GTPase protein formed complex with guanine-nucleotide dissociation inhibitor (GDI) and then associated into clathrin-coated vesicle membrane. After the association, GDI is released and Rab5 is converted into GTP-bound form to regulate downstream processing (Horiuchi et al., 1995; McLauchlan et al., 1997). Rab5 protein regulates the transportation of the vesicle from plasma membrane to early endosome of the endocytic pathway (Bucci et al., 1992). Therefore, YHV possibly utilizes the Rab5 protein to invade the host cells. In addition, previous study in *P. monodon* has identified a small GTPase Rab7 protein as a WSSV-VP28 binding protein in shrimp (Sritunyalucksana et al., 2006). The protein plays a crucial role in regulation of vesicle formation and membrane trafficking from late endosome to lysosome which is a sequential process from early endosome (Hutagalung and Novick, 2011; Stenmark, 2009). Interestingly, the *P. monodon* Rab7 (PmRab7) was involved in YHV replication in shrimp (Ongvarrasopone et al., 2008). However, this is the first report demonstrating that Rab5 protein is involved in YHV infection in *P. monodon*.

In this study, PmRab5 demonstrated conserved regions of Rab family and Rab5 subfamily which were similar to other organisms including *Aiptasia pulchella* (Chen et al., 2004) and many other vertebrates

(Fig. 2). In shrimp, its amino acid sequence identity is highly conserved to human Rab5B (81.1%). Differences in the three isoforms of Rab5 proteins (Rab5A, 5B, and 5C) have no effect in the regulation of trafficking pathway from plasma membrane to early endosome but they are differentially recognized by different specific kinases (Bucci et al., 1995; Chiariello et al., 1999). In addition, colocalization between YHV and PmRab5 was observed in the hemocytes from 10 min to 3 h and rarely observed from 6 to 12 hpi. These results suggested that YHV and PmRab5 were transported together until 3 hpi. Then, YHV may be uncoated and released into the cytoplasm for replication process. Previously, Semliki Forest virus (SFV) and dengue virus (DENV) demonstrated colocalization with early endosome antigen 1 (EEA1), an effector protein of Rab5, at early time of infection and then later associated with Rab7. After that the viruses which were in hybrid organelles would separate from Rab5 and colocalize with only Rab7 (van der Schaar et al., 2008; Vonderheit and Helenius, 2005). The colocalization of YHV and Rab7 has not been reported but this event may be similar to SFV and DENV.

The function of PmRab5 on YHV replication was also investigated by using RNA interference technique. Levels of PmRab5 mRNA were suppressed at more than 85% by specific dsRNA after 3 hpi and showed partial recovery after 3 dpi (data not shown). Depletion of Rab5 protein causes accumulation of small vesicles around the cytoplasm due to the vesicles could not be fused with early endosome (Bucci et al., 1992). The fusion of the vesicles from plasma membrane with early endosome occurred from specific interaction of Rab5 and EEA1 protein. Rab5 protein could bind to both $C_2H_2Zn^{2+}$ finger and FYVE domain of EEA1 protein (Lawe et al., 2000; Merithew et al., 2003). Inhibition of the membrane fusion might block the transportation of many essential cargo proteins and might lead to cell death. Moreover, Rab5 protein is involved in the internalization of integrin which is critical for caspase-8 functions to regulate cell motility, metastasis and survival (Torres et al., 2010). Therefore, silencing of PmRab5 may cause a loss of cell equilibrium and induces death in shrimps. Furthermore, depletion of PmRab5 by using dsRNA could silence YHV mRNA levels and suppressed YHV infection in shrimp cells. These results suggested that YHV required PmRab5 for transportation into the cell similar to other envelope positive-sense single-stranded RNA viruses such as dengue virus (DENV), West Nile virus (WNV) or hepatitis C virus (HCV). Knockdown of Rab5 by siRNA showed the reduction of both DENV and WNV (Krishnan et al., 2007) while a dominant negative mutant of Rab5 could be used to decrease RNA progeny of HCV (Stone et al., 2007). Moreover, Rab5 protein is required for many viruses such as Borna disease virus (BDV), bovine ephemeral fever virus (BEFV), hepatitis B virus, and foot and mouth disease virus (FMDV) to transport within the host cell (Cheng et al., 2012; Clemente and de la Torre, 2009; Johns et al., 2009; Macovei et al., 2013). Taken together, the model of YHV entry into shrimp cell is proposed (Fig. 6). First, YHV glycoprotein 116 binds with PmYRP65, a shrimp cell receptor. Then, it utilizes clathrin dependent endocytosis to enter into the cells. The virus requires PmRab5 and PmRab7 to regulate the transportation from plasma membrane to early endosome and from early endosome to late endosome, respectively (Assavalapsakul et al., 2006; Jatuyosporn et al., 2014; Ongvarrasopone et al., 2008; Posiri et al., 2015). When the pH was lowered, YHV genome may be released into the cytoplasm for replication process which is similar to other enveloped RNA viruses, such as SFV and Sindbis virus (Glomb-Reinmund and Kielian, 1998; Helenius et al., 1980). In conclusion, YHV requires PmRab5 transport within the shrimp cell.

Supplementary data to this article can be found online at http://dx.doi.org/10.1016/j.aquaculture.2016.03.026.

Acknowledgments

We would like to thank Asst. Prof. Dr. Kusol Pootanakit for critically reading the manuscript, Prof. Dr. Paisarn Sithigorngul and Dr. Phattara-Orn Havanapan for providing anti-YHV gp64 antibody and anti-β-tubulin antibody, respectively and Ms. Chaweewan Chimawei, Mrs. Suparb Hongthong and Ms. Punnee Tongboonsong for technical assistance on culturing shrimp. We also would like to thank Mr. Wichai Boonsai from Choochai farm in Chonburi province and shrimp genetic improvement center in Surat Thani province, Thailand for providing shrimp samples. This work was supported by grants from Mahidol University under the National Research University Initiative (NRU) and Thailand Research Fund (BRG5780006 to C.O., DPG5680001 to S.P. and IRG 5780009). PP is supported by the grant DPG5680001.

References

Assavalapsakul, W., Smith, D.R., Panyim, S., 2006. Identification and characterization of a *Penaeus monodon* lymphoid cell-expressed receptor for the yellow head virus. J. Virol. 80 (1), 262–269.

Bucci, C., Lütcke, A., Steele-Mortimer, O., Olkkonen, V.M., Dupree, P., Chiariello, M., Bruni, C.B., Simons, K., Zerial, M., 1995. Co-operative regulation of endocytosis by three Rab5 isoforms. FEBS Lett. 366, 65–71.

Bucci, C., Parton, R.G., Mather, I.H., Stunnenberg, H., Simons, K., Hoflack, B., Zerial, M., 1992. The small GTPase Rab5 functions as a regulatory factor in the early endocytic pathway. Cell 70, 715–728.

Chen, M.C., Cheng, Y.M., Hong, M.C., Fang, L.S., 2004. Molecular cloning of Rab5 (ApRab5) in *Aiptasia pulchella* and its retention in phagosomes harboring live zooxanthellae. Biochem. Biophys. Res. Commun. 324, 1024–1033.

Cheng, C.Y., Shih, W.L., Huang, W.R., Chi, P.I., Wu, M.H., Liu, H.J., 2012. Bovine ephemeral fever virus uses a clathrin-mediated and dynamin 2-dependent endocytosis pathway that requires Rab5 and Rab7 as well as microtubules. J. Virol. 86, 13653–13661.

Chiariello, M., Bruni, C.B., Bucci, C., 1999. The small GTPases Rab5a, Rab5b and Rab5c are differentially phosphorylated *in vitro*. FEBS Lett. 453, 20–24.

Clemente, R., de la Torre, J.C., 2009. Cell entry of Borna disease virus follows a clathrin-mediated endocytosis pathway that requires Rab5 and microtubules. J. Virol. 83, 10406–10416.

Glomb-Reinmund, S., Kielian, M., 1998. The role of low pH and disulfide shuffling in the entry and fusion of semliki forest virus and sindbis virus. Virology 248, 372–381.

Greber, U.F., Singh, I., Helenius, A., 1994. Mechanisms of virus uncoating. Trends Microbiol. 2, 52–56.

Helenius, A., Kartenbeck, J., Simons, K., Fries, E., 1980. On the entry of Semliki Forest virus into BHK-21 cells. J. Cell Biol. 84, 404–420.

Horiuchi, H., Giner, A., Hoflack, B., Zerial, M., 1995. A GDP/GTP exchange-stimulatory activity for the Rab5-RabGDI complex on clathrin-coated vesicles from bovine brain. J. Biol. Chem. 270, 11257–11262.

Hutagalung, A.H., Novick, P.J., 2011. Role of Rab GTPases in membrane traffic and cell physiology. Physiol. Rev. 91, 119–149.

Jatuyosporn, T., Supungul, P., Tassanakajon, A., Krusong, K., 2014. The essential role of clathrin-mediated endocytosis in yellow head virus propagation in the black tiger shrimp *Penaeus monodon*. Dev. Comp. Immunol. 44, 100–110.

Jitrapakdee, S., Unajak, S., Sittidilokratna, N., Hodgson, R.A., Cowley, J.A., Walker, P.J., Panyim, S., Boonsaeng, V., 2003. Identification and analysis of gp116 and gp64 structural glycoproteins of yellow head nidovirus of *Penaeus monodon* shrimp. J. Gen. Virol. 84, 863–873.

Johns, H.L., Berryman, S., Monaghan, P., Belsham, G.J., Jackson, T., 2009. A dominant-negative mutant of Rab5 inhibits infection of cells by foot-and-mouth disease virus: implications for virus entry. J. Virol. 83, 6247–6256.

Krishnan, M.N., Sukumaran, B., Pal, U., Agaisse, H., Murray, J.L., Hodge, T.W., Fikrig, E., 2007. Rab 5 is required for the cellular entry of dengue and West Nile viruses. J. Virol. 81, 4881–4885.

Kumar, S., Nei, M., Dudley, J., Tamura, K., 2008. MEGA: a biologist-centric software for evolutionary analysis of DNA and protein sequences. Brief. Bioinform. 9, 299–306.

Lawe, D.C., Patki, V., Heller-Harrison, R., Lambright, D., Corvera, S., 2000. The FYVE domain of early endosome antigen 1 is required for both phosphatidylinositol 3-phosphate and Rab5 binding. J. Biol. Chem. 275, 3699–3705.

Macovei, A., Petrareanu, C., Lazar, C., Florian, P., Branza-Nichita, N., 2013. Regulation of hepatitis B virus infection by Rab5, Rab7, and the endolysosomal compartment. J. Virol. 87, 6415–6427.

Marsh, M., Helenius, A., 2006. Virus entry: open sesame. Cell 124, 729–740.

McLauchlan, H., Newell, J., Morrice, N., Osborne, A., West, M., Smythe, E., 1997. A novel role for Rab5-GDI in ligand sequestration into clathrin-coated pits. Curr. Biol. 8, 34–45.

Mercer, J., Schelhaas, M., Helenius, A., 2010. Virus entry by endocytosis. Annu. Rev. Biochem. 79, 803–833.

Merithew, E., Stone, C., Eathiraj, S., Lambright, D.G., 2003. Determinants of Rab5 interaction with the N terminus of early endosome antigen 1. J. Biol. Chem. 278, 8494–8500.

Nadala, E.C.B., Tapay, L.M., Loh, P.C., 1997. Yellow-head virus: a rhabdovirus-like pathogen of penaeid shrimp. Dis. Aquat. Org. 31, 141–146.

Ongvarrasopone, C., Chanasakulniyom, M., Sritunyalucksana, K., Panyim, S., 2008. Suppression of PmRab7 by dsRNA inhibits WSSV or YHV infection in shrimp. Mar. Biotechnol. 10, 374–381.

Ongvarrasopone, C., Roshorm, Y., Panyim, S., 2007. A simple and cost effective method to generate dsRNA for RNAi studies in invertebrates. Sci. Asia 33, 35–39.

Posiri, P., Kondo, H., Hirono, I., Panyim, S., Ongvarrasopone, C., 2015. Successful yellow head virus infection of *Penaeus monodon* requires clathrin heavy chain. Aquaculture 435, 480–487.

Posiri, P., Ongvarrasopone, C., Panyim, S., 2013. A simple one-step method for producing dsRNA from *E. coli* to inhibit shrimp virus replication. J. Virol. Methods 188, 64–69.
Sittidilokratna, N., Dangtip, S., Cowley, J.A., Walker, P.J., 2008. RNA transcription analysis and completion of the genome sequence of yellow head nidovirus. Virus Res. 136, 157–165.
Sritunyalucksana, K., Wannapapho, W., Lo, C.F., Flegel, T.W., 2006. PmRab7 is a VP28-binding protein involved in white spot syndrome virus infection in shrimp. J. Virol. 80, 10734–10742.
Stenmark, H., 2009. Rab GTPases as coordinators of vesicle traffic. Nat. Rev. Mol. Cell Biol. 10, 513–525.
Stenmark, H., Olkkonen, V.M., 2001. The Rab GTPase family. Genome Biol. 2, 3007.1–3007.7.
Stone, M., Jia, S., Heo, W.D., Meyer, T., Konan, K.V., 2007. Participation of Rab5, an early endosome protein, in hepatitis C virus RNA replication machinery. J. Virol. 81, 4551–4563.
Torres, V.A., Mielgo, A., Barbero, S., Hsiao, R., Wilkins, J.A., Stupack, D.G., 2010. Rab5 mediates caspase-8-promoted cell motility and metastasis. Mol. Biol. Cell 21, 369–376.
van der Schaar, H.M., Rust, M.J., Chen, C., van der Ende-Metselaar, H., Wilschut, J., Zhuang, X., Smit, J.M., 2008. Dissecting the cell entry pathway of dengue virus by single-particle tracking in living cells. PLoS Pathog. 4, e1000244.
Vonderheit, A., Helenius, A., 2005. Rab7 associates with early endosomes to mediate sorting and transport of semliki forest virus to late endosomes. PLoS Biol. 3, 1225–1238.
Zhu, G., Zhai, P., Liu, J., Terzyan, S., Li, G., Zhang, X.C., 2004. Structural basis of Rab5-Rabaptin5 interaction in endocytosis. Nat. Struct. Mol. Biol. 11, 975–983.

Fish & Shellfish Immunology 66 (2017) 433–444

Contents lists available at ScienceDirect

Fish & Shellfish Immunology

journal homepage: www.elsevier.com/locate/fsi

Full length article

Suppression of PmRab11 inhibits YHV infection in *Penaeus monodon*

Akechai Kongprajug [a], Sakol Panyim [a, b], Chalermporn Ongvarrasopone [a, *]

[a] Institute of Molecular Biosciences, Mahidol University (Salaya Campus), Nakhon Pathom, 73170 Thailand
[b] Department of Biochemistry, Faculty of Science, Mahidol University, Bangkok, 10400 Thailand

ARTICLE INFO

Article history:
Received 16 December 2016
Received in revised form
16 April 2017
Accepted 15 May 2017
Available online 17 May 2017

Keywords:
Exocytosis
Recycling endosome
Viral budding
Black tiger shrimp
Viral transportation

ABSTRACT

Yellow head virus (YHV) is one of the most serious pathogens that causes worldwide shrimp production loss. It enters the cells via clathrin-mediated endocytosis and utilizes small GTPase Rab proteins such as PmRab5 and PmRab7 for intracellular trafficking. In this study, molecular cloning and functional analysis of Rab11 during YHV infection were investigated. PmRab11 cDNA was cloned by Rapid amplification of cDNA ends (RACEs). It contained two forms of sizes 1200 and 1050 bp distinct at the 5′ UTR. The coding region of PmRab11 was 645 bp, encoding 214 amino acids. It also demonstrated the characteristics of Rab11 proteins containing five GTP-binding domains, five Rab family domains, four Rab subfamily domains and a prenylation site at the C-terminus. Suppression of PmRab11 using dsRNA-PmRab11 either before or after YHV-challenge resulted in significant inhibition of YHV levels in the hemocytes and viral release in the supernatant in both mRNA and protein levels. In addition, the silencing effect of PmRab11 in YHV-infected shrimps resulted in a delay in shrimp mortality for at least 2 days. Immunofluorescence study showed co-localization between PmRab11 and YHV at 24–72 h post YHV-challenge. In contrast, the co-localization signals were absence in the PmRab11 knockdown hemocytes and the YHV signals accumulated at the perinuclear region at 24 h post YHV-challenge. Then, accumulation of YHV was hardly observed after 48–72 h. These results suggested that PmRab11 is required for YHV infection in shrimp.

1. Introduction

Thailand is the world's important exporter of shrimp products, especially the black tiger shrimp, *Penaeus monodon*. At present, losses of shrimp production are caused by various viral diseases. One of the major causative agents is the yellow head virus (YHV) which causes extensive and rapid mortality in black tiger shrimp [1,2]. YHV is a positive sense, single-stranded RNA virus that is classified as a member of Gill-associated virus, belonging to the genus Okavirus, family Roniviridae in the order Nidovirales [3]. YHV genome is approximately 26 kb, containing four long open reading frames (ORF1a, ORF1b, ORF2, and ORF3) [4–6]. The enveloped rod-shaped YHV particles are 150–200 nm in length and 40–50 nm in diameter [1,7]. The virion has prominent surface spikes and contains internal helical nucleocapsid [8,9]. It contains three structural proteins, the transmembrane glycoproteins gp116 and gp64 are found in the viral envelope, and the nucleoprotein p20 [6,10].

Recently, the mechanism of YHV transportation has been proposed. After YHV enters into the cell, it is transported via endosomal compartments [11,12] and released its genome into the cytoplasm for replication. Then, the nucleocapsid is synthesized and transported to the ER-Golgi compartment where the envelope is formed [2,13]. Finally, the enveloped viral particle is exocytosed at the plasma membrane. However, this exocytosis process of YHV out of the cells is not well understood. Normally, enveloped viruses are budded at the membrane in order to generate the envelope that surrounded the nucleocapsid [14]. In this process, the nucleocapsid is wrapped in a cellular membrane containing virus-specific envelope proteins. The viral envelope protein serves to target the host cell receptor [15]. Some viruses bud at the plasma membrane (PM), whereas others are assembled and budded at intracellular membranes along the secretory pathway such as the nuclear envelope, rough and smooth endoplasmic reticulum (ER), endosomes, intermediate or pre-Golgi compartment, Golgi cisternae and the *trans*-Golgi-network (TGN) [16]. However, the cytoplasmic transportation of viral genome or viral particle to plasma membrane

* Corresponding author. Institute of Molecular Biosciences, Mahidol University (Salaya Campus), 25/25 Phutthamonthon 4 Rd. Salaya, Phutthamonthon district, Nakhon Pathom, 73170 Thailand.
E-mail address: chalermporn.ong@mahidol.ac.th (C. Ongvarrasopone).

http://dx.doi.org/10.1016/j.fsi.2017.05.039
1050-4648/

requires the host proteins.

One of the cellular proteins that is involved in intracellular trafficking process is Rab11. Rab11 is a small GTPase protein belongs to the Ras superfamily, whose function is in transportation of the vesicles through the TGN [17], apical recycling of endosomes [18] and the perinuclear recycling of endosomal compartments before redirecting the vesicular cargo back to the apical plasma membrane. The Rab GTPase protein acts as molecular switches that shuffle between two conformational states, the GTP bound 'active' form and the GDP-bound 'inactive' form. In the active form, Rab protein is associated with membranes by hydrophobic geranylgeranyl groups at the C-terminal and recruited the specific effector molecules such as sorting adaptors, tethering factors, kinases, phosphatases and motor proteins in vesicle transport process [18]. Our previous studies found that several Rab proteins are hijacked by YHV [11,12]. Specifically, the transportation of YHV particles required PmRab5 which is a key protein in vesicles transport to early endosome; whereas, PmRab7 is involved in YHV transportation from early endosome to late endosome and lysosome. The silencing effects of PmRab5 or PmRab7 in YHV-infected *P. monodon* inhibited YHV expression, suggesting that PmRab5 and PmRab7 are involved in intracellular trafficking of YHV [11,12].

Recently, several evidence revealed that some RNA viruses such as vesicular stomatitis virus, sendai virus, influenza A, measles virus, mumps virus, and hantavirus use Rab11-dependent pathway to assemble and release out of the cells [19–25]. Whether YHV which is also a e RNA viruse requires Rab11 for its transport out of the cell remains to be elucidated. Furthermore, subtractive hybridization study found that *RAB11* is one of the responsive genes that is upregulated after YHV infection [26]. Therefore, here, molecular cloning of the full-length cDNA in *P. monodon* Rab11 (PmRab11) and its probable function during YHV infection were performed.

2. Materials and methods

2.1. Black tiger shrimp culture

Juvenile viral-free pathogen black tiger shrimps (*P. monodon*) of about 10–30 g were obtained from commercial shrimp farms in Thailand. Before use, shrimps were tested for YHV and white spot syndrome virus infection by using diagnostic strip test (Pacific Biotech Co. Ltd., Thailand). Shrimps were grown in a plastic box containing oxygenated seawater at 10 ppt salinity and were acclimatized for 2 days before the experiment was carried out. They were fed with commercial shrimp feed every day. The salt water was changed every 2 days.

2.2. Yellow head virus (YHV) stock

The infectious YHV was propagated by injection of YHV to viral-free shrimp. Then, hemolymph was collected from YHV-infected moribund shrimp and mixed with AC-1 solution (27 mM Sodium citrate, 34.33 mM NaCl, 104.5 mM Glucose, 198.17 mM EDTA, pH 7.0). Next, the hemolymph was centrifuged at 20,000×*g* for 20 min at 4 °C to remove hemocyte debris. Free YHV particles were collected by ultracentrifugation (100,000×*g*) for 1 h. Virus pellets were suspended with 150 mM NaCl and stored at −80 °C until used. The viral nucleic acid was purified from the YHV stock using high pure viral nucleic acid kit (Roache Diagnostics, Germany) and subjected to RT-PCR to determine viral titer using primers YHV_F: 5′-CAAGGACCACCTGGTACCGGTTAAGAC-3′ and YHV_R: 5′-GCGGAAACGACTGACGGCTACATTCAC-3′ [11].

2.3. Molecular cloning of the full length PmRab11cDNA

The partial sequence of PmRab11 served as template to design primers for 5′ and 3′ RACE. 5′ and 3′ RACE were performed as previously described [11]. Briefly, 5′ RACE method was performed by using 5Rab11_R1 specific primer (Table 1) to generate the first-strand cDNAs by Superscript III® reverse transcriptase (Invitrogen). Then, 5Rab11_R1 and PRT primers (Table 1) were used to synthesize the first PCR product which was diluted to 1:100 for used as template in the nested PCR with 5Rab11_R2 and PM1 primers (Table 1). To obtain the 3′ end of PmRab11 cDNA, 3′ RACE PCR was performed by PRT primer to generate the first-strand cDNAs. Then, the PCR reaction containing 3Rab11_F1 and PM-1 primers was performed. Next, two nested PCRs were performed using 3Rab11_F2 and PM-1 primers and 3Rab11_F3 and PM-1 primers (Table 1). Then, all expected bands of the 5′ and 3′ RACE PCR products were purified by Gel/PCR fragments extraction kit (Geneaid), cloned into pGEM-T-easy vector (Promega) and sequenced (First Base Co. Ltd, Malaysia).

The sequences of the 5′ and 3′ ends obtained from RACE-RCR were assembled together with the partial sequence of PmRab11 in order to obtain the full-length cDNA by using ContigExpress tool from Vector NTI Advance 11.5.1 program. Finally, a PCR was performed to amplify the full-length PmRab11 cDNA using Taq DNA polymerase (New England Biolabs) with primers that were designed based on the 5′ and 3′ end sequences, fullRab11_F and fullRab11_R primers (Table 1). PCR condition was: 95 °C for 5 min, followed by 30 cycles of 95 °C for 30 s, 51 °C for 30 s, 72 °C for 1.30 min and 72 °C for 7 min in the final step. Finally, the PCR product was purified, cloned and subjected to sequence following the protocol that was described earlier.

2.4. Sequence analysis of PmRab11

The full-length cDNA sequence of PmRab11 was analyzed against the NCBI's blastn database (http://blast.ncbi.nlm.nih.gov/Blast.cgi). The coding sequences were translated to amino acid sequence by using Expasy's tool (http://web.expasy.org/translate/). Amino acid sequence identity between PmRab11 and Rab11 proteins of other species was performed by using alignX of Vector NTI. In addition, the initiation codon and poly-A signal were identified by using ATGpr (http://atgpr.dbcls.jp/) and Poly (A) signal miner (http://dnafsminer.bic.nus.edu.sg/PolyA.html). Multiple sequence alignment of PmRab11 was performed to identify the conserved domains of Rab11 protein by using the conserved domain database of NCBI (http://www.ncbi.nlm.nih.gov/Structurecdd/wrpsb.cgi). Prenylation site was identified by using Prenylation Prediction Suite (http://mendel.imp.ac.at/PrePS/)., Phylogenetic tree analysis of PmRab11 was performed based on the neighbor-joining methods (http://www.phylogeny.fr/) [27]. The phylogeny was constructed by phylogeny.fr under "One Click" mode. The pipeline is already set up to run and connect well recognized programs: MUSCLE for multiple alignment, Gblocks for automatic alignment curation, PhyML for tree building and TreeDyn for tree drawing.

2.5. Construction of recombinant plasmid expressing dsRNA-PmRab11

A recombinant plasmid containing sense-loop and antisense fragment of PmRab11 was constructed using pGEM®-3zf(+) vector (Promega) as a plasmid backbone. A sense-loop fragment of size 494 bp was amplified from PmRab11 cDNA using slRab11_F and slRab11_R primers containing *Xba*I and *Kpn*I sites, respectively (Table 1). The amplification of the antisense fragment of size 404 bp was performed using asRab11_F and asRab11_R primers containing

Table 1
List of synthetic oligonucleotide primers.

Name	Sequences (5′……3′)	Experiments
PRT	CCGGAATTCAAGCTTCTAGAGGATCCTTTTTTTTTTTTTTT	Reverse transcription
5Rab11_R1	GGCCGTCTCTACATTAGTGGAGCC	5′RACE
5Rab11_R2	ATTCTGATCTGCATGATCTCTGAGC	
3Rab11_F1	CACTTACACTAATGTAGAACGTTGGC	3′RACE
3Rab11_F2	GCTGATGTTAAGGCTATTCACGTGG	
3Rab11_F3	AAGGCATTTGCAGAAAAGGAGGGAC	
PM1	CCGGAATTCAAGCTTCTAGAGGATCC	
FullRab11_F	GGA GAG GCG TAA CGG TTC GC	Full-length
FullRab11_R	TTTTTTTTTTAGAGAACAGGACAAACAGAG	
slRab11_F	GCTCTAGATCCACCATTGGTGTTGAG	Sense-loop of dsRNA
slRab11_R	GGGGTACCGCATTTACAGTTGGTTCCAC	
asRab11_F	GGAATTCCCCTCGAGTCCACCATTGGTGTTGAG	Antisense of dsRNA
asRab11_R	GGGGTACCACAATGCGGTAGATTTCTG	
PmRab11_F	ATGGGGAACAGGGACGACGAGTATG	Detection of PmRab11
PmRab11_R	GGCCTCTTCTGTGGGAACTGACCGC	
PmRab5_F	GGAGCTGCATTTCTGACACAGACAG	Detection of PmRab5
PmRab5_R	GGTCTGGGCCTCTTCATATTCAACC	
PmRab7_F	ATGGCATCTCGCAAGAAGATT	Detection of PmRab7
PmRab7_R	TTAGCAAGAGCATGCATCCTG	
PmActin_F	GACTCGTACGTCGGGCGACGA	Detection of PmActin
PmActin_R1	AGCAGCGGTGGTCATCACCTG	
PmActin_R2	CGTAGATGGGCACGGTGTGGG	
YHV_F	CAAGGACCACCTGGTACCGGTTAAGAC	Detection of YHV
YHV_R	GCGGAAACGACTGACGGCTACATTCAC	

*Eco*RI/*Xho*I and *Kpn*I, respectively (Table 1). Then, the sense and antisense fragments were cloned into pGEM®-3zf(+) vector to obtain a recombinant clone containing the stem-loop fragment of PmRab11. Then, the stem-loop fragment, size 898 bp, was digested by *Hin*dIII and *Xho*I and subcloned to an expression vector, pET-17b to produce dsRNA-PmRab11 by *in vivo* bacterial expression. The region of dsRNA-PmRab11 is located at the nucleotides 124–510 from the start codon. In addition, a recombinant plasmid containing a stem-loop fragment of GFP (kindly provided by Asst. Prof. Witoon Tirasophon) was used to express dsRNA-GFP which served as an unrelated dsRNA [28].

2.6. Expression and extraction of dsRNA-PmRab11

A recombinant plasmid pET-17b containing a stem-loop of PmRab11 was transformed into *E. coli* HT115 which is a ribonuclease III mutant strain to produce dsRNA-PmRab11 [28]. dsRNA-PmRab11 expression was induced by 0.1 mM IPTG. dsRNA-PmRab11 was extracted and purified by ethanol method [29]. The quality of dsRNA was characterized by ribonuclease digestion assay using RNase A and RNase III (New England Biolab, USA). Yield of dsRNA-PmRab11 was determined by agarose gel electrophoresis and compared to the intensity of 2-log DNA marker. The intensity was measured by an ImageJ program.

2.7. Suppression of PmRab11 expression by dsRNA-PmRab11

In order to determine specific inhibition of PmRab11 expression, injection of dsRNA-PmRab11 was performed. Shrimps were injected in the muscle with 1.25 or 2.5 μg/g shrimp of dsRNA-PmRab11. Injection of unrelated dsRNA-GFP and 150 mM NaCl were used as controls. Then, hemolymph from individual shrimp was collected at 24, 48 and 72 h post-dsRNA or NaCl injection and mixed with anticoagulants I (27 mM sodium citrate, 34.33 mM NaCl, 104.5 mM glucose, 198.17 mM EDTA, pH 7.0) in a ratio 1:1. Total RNAs was extracted from hemolymph by TRI REAGENT® LS (Molecular Research Center). Semi-quantitative RT-PCR was performed to monitor the levels of PmRab11 expression using PmRab11 specific primers. In addition, to examine the specificity of the knockdown effect of PmRab11, these cDNAs were used as templates for detection of other Rab genes expression using PmRab5 and PmRab7 specific primers (Table 1) [11,12].

2.8. Suppression effect of PmRab11 during YHV infection

To investigate the function of PmRab11 on YHV infection, shrimps were intramuscularly injected with dsRNA-PmRab11 at 1.25 μg/g shrimp. Injection of 150 mM NaCl and unrelated dsRNA-GFP were used as control groups. After 24 h, shrimps were challenged with 10^{-2} dilution of YHV (dose of YHV that leads to 100% mortality within 3 days). The hemolymph was collected at 24, 48, 72 and 96 h post-YHV challenge. Then, the hemocytes and supernatant were fractionated by centrifugation at 650×*g* for 15 min. Total RNAs in hemocytes and supernatant were extracted by TRI REAGENT® and TRI REAGENT® LS (Molecular Research Center), respectively. The levels of PmRab11 and YHV expression were monitored by semi-quantitative RT-PCR using PmRab11 and YHV specific primers (Table 1), respectively. PmActin was used as an internal control. Finally, the relative expressions of PmRab11 and YHV in hemocytes were normalized by PmActin. However, PmActin cannot be amplified from the supernatant fraction, thus the YHV levels was analyzed from equal amount of the total RNAs.

2.9. RNA isolation and RT-PCR

Total RNA from hemocytes or supernatant was isolated by Trizol® reagent (Molecular Research Center) following the manufacturer's procedure. The RNA concentration was measured by Nanodrop ND-1000 spectrophotometer (Nanodrop Technologies). Total RNAs (2 μg) was used as template to generate the first-strand cDNA by Improm-II™reverse transcriptase (Promega) using PRT primer (Table 1). PmRab11 expression was monitored by multiplex PCR using PmRab11-F and PmRab11-R primers and PmActin-F and PmActin-R1 primers for PmActin detection which served as an internal control. The PCR was carried out according to this condition: 95 °C for 5 min, followed by 30 cycles of 95 °C for 30 s, 61 °C for 30 s, 72 °C for 45 s and 72 °C for 7 min in the final step. Expressions of PmRab5, PmRab7 and YHV were determined according to the

previous methods [11,12]. PCR products were analyzed on 1.5% agarose gel electrophoresis. The intensity of each band after subtracting the background was quantified by using ImageJ program (Version 1.50b). The relative expression level of the gene of interest was normalized against PmActin level and expressed as an arbitrary unit.

2.10. Investigation of protein levels of YHV in hemocytes and supernatant

In order to investigate YHV protein levels in hemocytes and supernatant of the complete PmRab11 knockdown shrimp, shrimps were injected with dsRNA-PmRab11 at 1.8 μg/g shrimp by intramuscular injection. Injection of NaCl and unrelated dsRNA-GFP were used as control groups. After 24 h, shrimps were challenged with 10^{-2} dilution of YHV by intramuscular injection. The hemolymph was collected at 24, 48, 72 and 96 h post-YHV injection. The hemolymph from 3 shrimps in the same group at the same time was pooled. Then, total RNA from 200 μl of the pooled hemolymph was extracted by TRI REAGENT® LS method and RT-PCR was performed in order to detect PmRab11 and YHV expression at mRNA level. To extract total protein for Western blot analysis, 2 ml of the pooled hemolymph was fractionated to separate hemocytes and supernatant by centrifugation at 650×*g*. Total proteins from hemocytes were extracted by using 100 μl buffer T (8M urea, 2 M thiourea, 0.4% Triton X-100, 60 mM DTT, 1 mM PMSF, 1 × Protease inhibitor cocktail (Sigma)). Whereas, total proteins from 100 μl of supernatant were precipitated by 10% TCA at final concentration and dissolved in 100 μl of buffer T. Then, Western blot was performed to detect YHV level in both fractions.

2.11. Western blot analysis

Hemocyte and supernatant proteins were extracted by using buffer T. The protein lysate (50 μg) was electrophoresed in 12% SDS-polyacrylamide gel (SDS-PAGE). Then, proteins were transferred from gel onto a nitrocellulose membrane (Bio-Rad) by electrophoresis with 1X transfer buffer [0.025 M Tris–HCl pH 8.3, 0.192 M glycine, and 20% (v/v) methanol]. Then the membrane was blocked with blocking solution [5% skimmed milk in 0.2% PBST (0.2% (v/v) Tween-20 in 1X PBS)] for 2 h. Next, the membrane was soaked with 0.05% PBST (0.2% (v/v) Tween-20 in 1X PBS) containing primary antibody for 2 h. To detect YHV levels, the mouse anti-gp64 antibody was used as primary antibody at the dilution 1: 1000 in 0.2% PBST. In addition, dilution 1: 1000 in 0.2% PBST of the rabbit anti- β-tubulin primary antibody was used to detect β-tubulin which is an internal control. Then, the primary antibody was removed. The membrane was washed with 0.2% PBST for 10 min, 3 times and incubated with blocking solution containing horseradish peroxidase-conjugated secondary antibody (Sigma) in dilution 1:5000. Then, the membrane was washed 1 time with 0.2% PBST and 3 times with 1X PBST. Finally, the signal was detected by adding the Luminata™ Forte Western HRP Substrate (Millipore Corporation) for 5 min and exposed to X-ray film. PmRab11 and β-tubulin have sizes of about 23 and 60 kDa, respectively.

2.12. Shrimp mortality assay

Suppression effects of PmRab11 with or without YHV challenge on shrimp mortality were investigated. Shrimps size about 1 g (n = 15 shrimps per group) were injected with 1.25 or 2.5 μg/g shrimp of dsRNA-PmRab11 24 h with or without YHV challenge. Injection of 150 mM NaCl and unrelated dsRNA-GFP were used as controls. The experiment was performed in triplicates and the number of dead shrimps were recorded every day for 10 days.

2.13. Immunofluorescence assay of YHV and PmRab11 in YHV-infected hemocytes

Shrimp was injected with 1.8 μg/g shrimp of dsRNA-PmRab11 24 h prior to YHV challenge. The injection of 150 mM NaCl and unrelated dsRNA-GFP were used as control groups. Then, 250 μl of hemolymph was collected at 24, 48 and 72 h after YHV challenge. The hemocytes were separated by centrifugation at 550×*g* for 10 min at 4 °C. Cell pellet was resuspended in 500 μl of L-15 medium. Then, hemocytes mixture was seeded in 24 wells plate containing a coverslip and incubated at room temperature. After for 2 h, culture media was discarded and 500 μl of ice cold 4% (w/v) paraformaldehyde was added into each wells. After incubation at room temperature for 20 min, the supernatant was removed and fixed hemocytes were washed with 1X PBS for 5 min, 3 times. Then, they were permeabilized by adding 350 μl of 0.1% (v/v) Triton X-100 in 1X PBS for 5 min. After the supernatant was discarded and the permeabilized hemocytes were proceeded to immunofluorescence staining according to the previous method [10]. Except that the rabbit polyclonal anti-Rab11 antibody (ab3612, Abcam, USA) and mouse monoclonal anti-gp64 of YHV antibody (kindly provided by Professor Paisarn Sithigorngul, Department of Biology, Faculty of Science, Srinakharinwirot University) were used. After washing, the secondary antibodies which are goat anti-rabbit IgG, Alexa Fluor® 596 and goat anti-mouse IgG, Alexa Fluor® 488 (Invitrogen) were used for detection of PmRab11 and YHV. The nuclei were stained by TO-PRO®-3 iodide (Invitrogen). Finally, a cover slip was mounted with 8 μl of ProLong antifade (Invitrogen). The slide was kept at 4 °C until visualized under confocal microscope (Fluoview FV10i – DOC, Olympus).

2.14. Statistical analysis

The relative mRNA levels of PmRab11 normalized with PmActin were presented as mean ± standard error of mean (SEM). The statistical analysis of the relative mRNA expression levels was tested by using analysis of variance (ANOVA). A probability (P) value at less than 0.05 was used to define significant difference. Cumulative percent mortality was plotted as mean ± SEM.

3. Results

3.1. Full-length cDNA cloning and sequences analysis of PmRab11

The full-length cDNA was obtained from 5′ and 3′ RACE protocol. It has 2 forms of sizes 1217 and 1065 bp with the same coding sequences of 645 bp. The 5′ and 3′ untranslated region (UTR) have sizes 247 bp and 324 bp, respectively (Fig. 1). The sequence of PmRab11 cDNA of 2 variants were submitted into the GenBank database under the accession number KY241479 and KY241480, respectively. PmRab11 protein has size of 214 aa. The theoretical pI and molecular weight are 5.22 and 23.85 kDa, respectively. In addition, this protein shared the characteristics of Rab11 protein family when compared to others species such as five GTP biding domains (G1-G5), five Rab family domains (RabF1-5), four Rab subfamily domains (RabSF1-4) and a prenylation site that usually terminated in CC or CXC motif at the C-terminus (Fig. 2). The amino acid sequence identity showed that PmRab11 protein shared 100% amino sequence identity with Rab11 of Pacific white shrimp (*Litopenaeus vannamei*) and shared approximately 80% with Rab11 of vertebrates such as zebrafish (*Danio rerio*). In addition, the phylogenetic tree revealed that PmRab11 protein was closely related to Rab11 of vertebrate and arthropods (Fig. 3). It was not clustered with other Rab proteins including Rab5, Rab6 and Rab7. These results indicate that PmRab11 is a highly conserved protein.

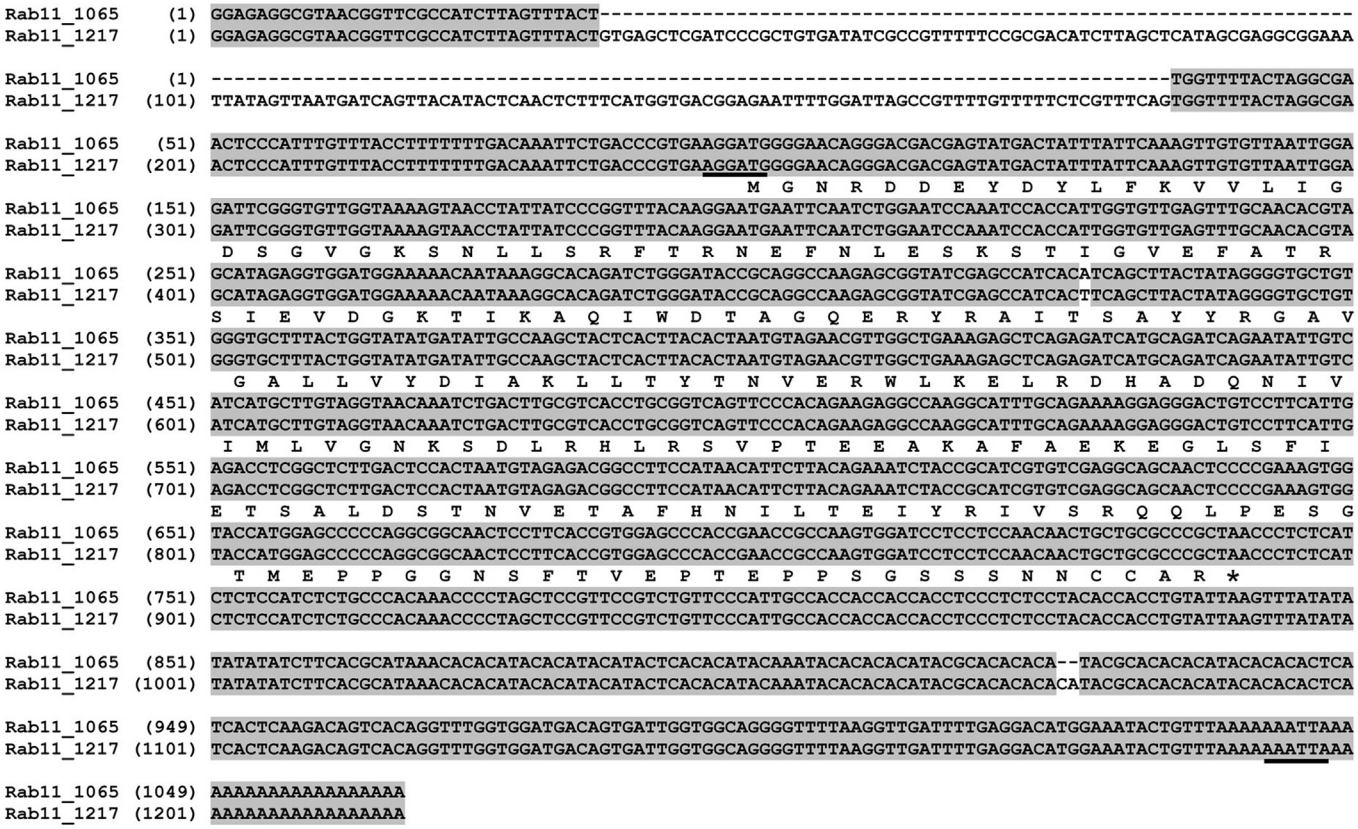

Fig. 1. Two forms of the full-length cDNAs and their deduced amino acid sequences of PmRab11. The full-length cDNA of PmRab11 has 2 forms of sizes 1217 and 1065 bp containing the open reading frame of size 645 bp. The deduced amino acid sequences of PmRab11 is represented in the capital letter under the respective codon. Kozak consensus sequences (AGGATG) and poly A signal (AAATTA) are indicated in underline.

3.2. Suppression of PmRab11 expression by dsRNA-PmRab11

To investigate whether the PmRab11 expression can be suppressed by using RNAi approach. Double-strands RNA targeting PmRab11 was produced and injected into shrimp muscle. The expression levels of PmRab11 in dsRNA-PmRab11 injected shrimp were significantly reduced at more than 90%, 24 h post-dsRNA-PmRab11 injection at both dosages (1.25 and 2.5 μg/g shrimp) when compared to 0 h. The suppression effect of PmRab11 was maintained for at least 72 h post-dsRNA injection ($P < 0.001$, $n = 4$/time point) (Fig. 4A). As the nucleotide sequences of dsRNA-PmRab11 contained many conserved domains such as Rab family domains, Rab subfamily domains and GTP binding domains, it is possible that some of the regions of dsRNA-PmRab11 are similar to other Rab genes. Therefore, a specific inhibition to PmRab11 expression was investigated. The results showed that suppression of PmRab11 by injection of dsRNA-PmRab11 has no effect on the levels of PmRab5 and PmRab7 expression from 24 to 72 h post-dsRNA injection (Fig. 4B). Large standard deviation of PmRab7 after 24 h dsRNA injection may be due to varying expression of PmRab7 among shrimp samples.

3.3. Suppression effect of PmRab11 during YHV infection

To investigate whether PmRab11 protein is essential for YHV transport out of the cell, suppression of PmRab11 was performed 24 h prior to YHV challenge. PmRab11 expression level in hemocytes was significantly decreased approximately 50% in shrimp injected with dsRNA-PmRab11 within 48 h post-dsRNA-PmRab11 injection. The knockdown effect of PmRab11 was increased to 75% at 72 and 96 h post-dsRNA injection ($P < 0.001$, $n = 4$/time point) (Fig. 5A). In addition, YHV levels in hemocytes and supernatant of PmRab11 knockdown group were significantly decreased from 48 to 72 h post-YHV infection when compared to NaCl injected group ($P < 0.01$ for hemocytes and $P < 0.001$ for supernatant, $n = 4$/time point) (Fig. 5B and C). Notably, shrimps in 2 control groups died at 96 h while shrimp in PmRab11 knockdown group still alive at this time point.

Protein analysis revealed that an envelope glycoprotein gp64 of YHV cannot be detected in the hemocytes and supernatant of the PmRab11 knockdown group from 24 to 72 h post-YHV challenge. At 96 h post-YHV challenge, low levels of YHV can be detected in both hemocytes and supernatant while shrimp in both control groups died at this time point. On the other hand, high YHV level can be detected in hemocytes and supernatant of NaCl-injected groups at 48 and 72 h. However, low level of YHV expression can still be observed in dsRNA-GFP injected group at 48 h and even increased at 72 h post-YHV infection (Fig. 6A and B, Supplementary Fig. 1).

3.4. Shrimp mortality assay

To investigate the suppression effect of PmRab11 on shrimp mortality, shrimp was injected with 1.25 μg/g shrimp of dsRNA-PmRab11. Then, shrimp mortality was recorded for 10 days. The results showed that injection of dsRNA-PmRab11 caused 100% shrimp death at day 7. In contrast, injection of 1.25 μg/g shrimp dsRNA-GFP and NaCl resulted in less than 10% shrimp mortality within 10 days (Fig. 7A). In addition, the cumulative mortalities of

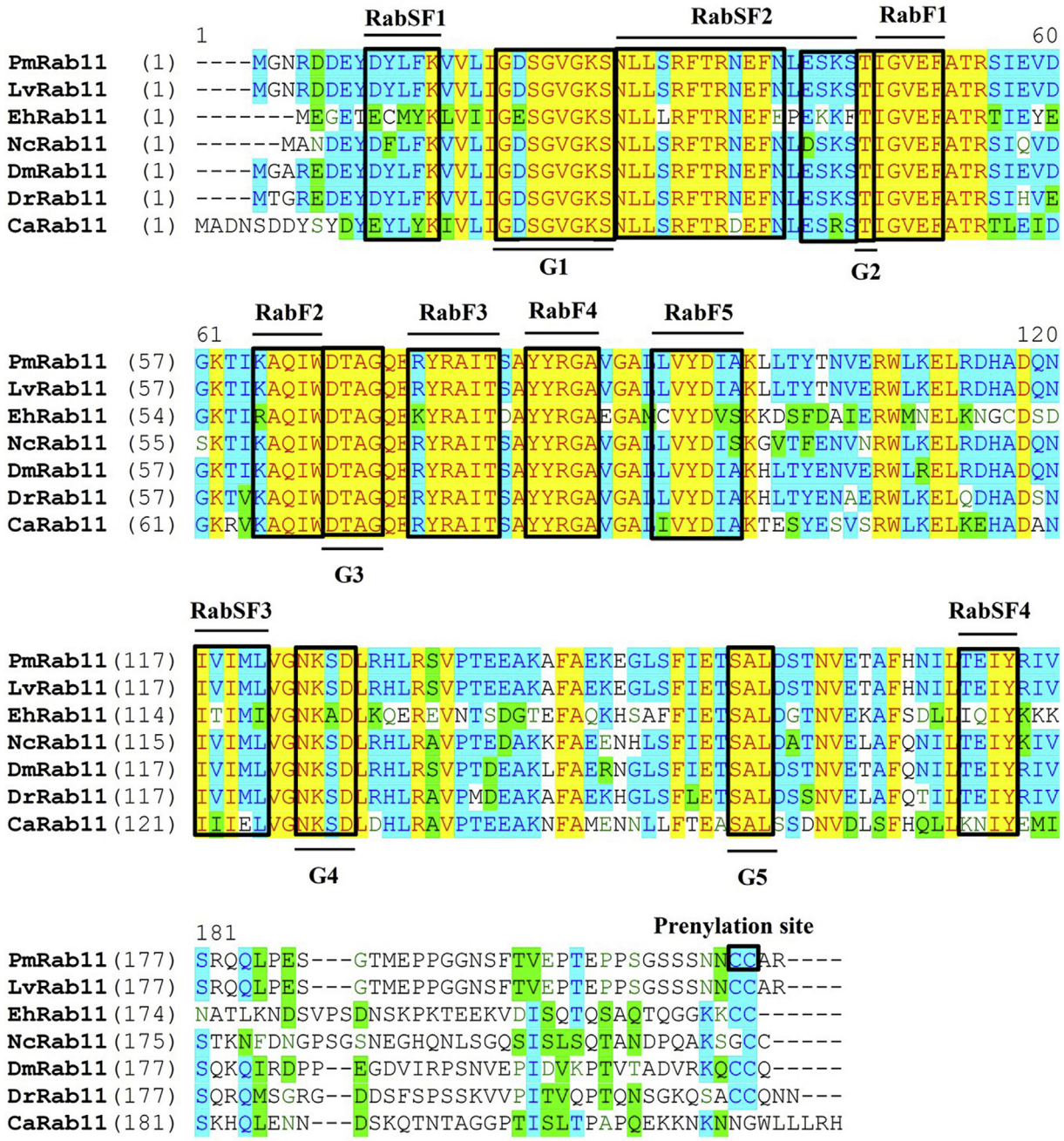

Fig. 2. Multiple sequence alignment showing conserved domains of PmRab11 compared to Rab11 proteins from other species. The conserved domains of PmRab11 shared characteristics of Rab11 among other species such as five GTP binding domains (G1-G5), five Rab family (RabF1-5) domains, four Rab subfamily (RabSF1-4) domains and a prenylation site (CCXX motif) at the C-terminus.

shrimp that injected with dsRNA-PmRab11 at 1.25 μg/g shrimp followed by YHV challenge was delayed at least 2 days when compared to the control groups (Fig. 7B).

3.5. Co-localization of YHV and PmRab11 in YHV infected hemocytes

The PmRab11 protein level in individual hemocytes was observed using immunofluorescence assay. Shrimp was injected with dsRNA-PmRab11 at 1.8 μg/g shrimp, then PmRab11 protein levels was detected at various time points. The result demonstrated that the PmRab11 protein was gradually decreased from 24 to 96 h post-dsRNA-PmRab11 injection (Fig. 8A). Second, the localization of PmRab11 and YHV was investigated by injection with dsRNA-PmRab11 at 1.8 μg/g shrimp and followed by YHV. The low signals of PmRab11 protein and YHV glycoprotein 64 (gp64) can be observed inside the hemocytes of PmRab11 knockdown shrimp at 24 h post-infection (Fig. 8B). In contrast, high signals of PmRab11 and gp64 can be detected in shrimp that was injected with dsRNA-GFP and NaCl followed by YHV challenge at this time point. In addition, co-localization of PmRab11 and YHV can be clearly observed at 24–72 h post-infection in hemocytes of both control groups. In contrast, the PmRab11 knockdown group showed low level of YHV and PmRab11 at these time points (Fig. 8C and D).

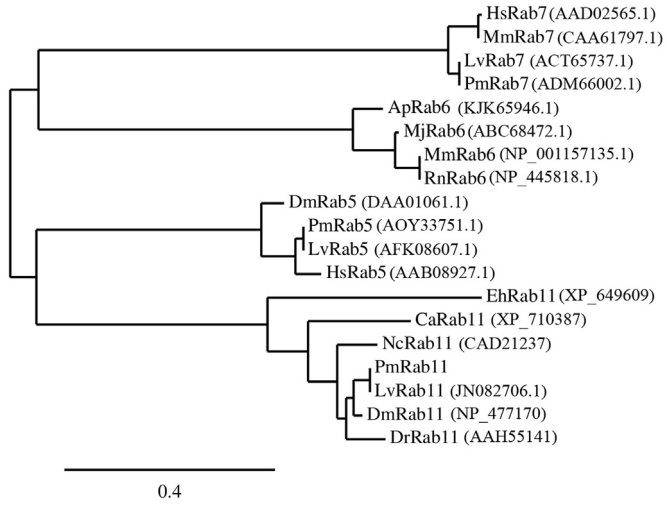

Fig. 3. Phylogenetic analysis of Rab11 of *P. monodon* compared with Rab11, Rab5, Rab6 and Rab7 of other species. The amino acid sequences of the coding region of Rab proteins of *P. monodon* and of other species were used to perform phylogenetic tree analysis based on the neighbor-joining methods by using the program from (http://www.phylogeny.fr/). The abbreviation of species is as follows: *Homo sapiens (Hs)*, *Mus musculus (Mm)*, *Litopenaeus vannamei (Lv)*, *Penaeus monodon (Pm)*, *Aspergillus parasiticus (Ap)*, *Marsupeneus japonicus (Mj)*, *Rattus norvegicus (Rn)*, *Drosophila melanogaster (Dm)*, *Entamoeba histolytica (Eh)*, *Candida albicans (Ca)*, *Neurospora crassa (Nc)*, and *Danio rerio (Dr)*. The accession number is in the parenthesis. PmRab11 cDNA of 2 variants were submitted into the GenBank database under the accession number KY241479 and KY241480, respectively.

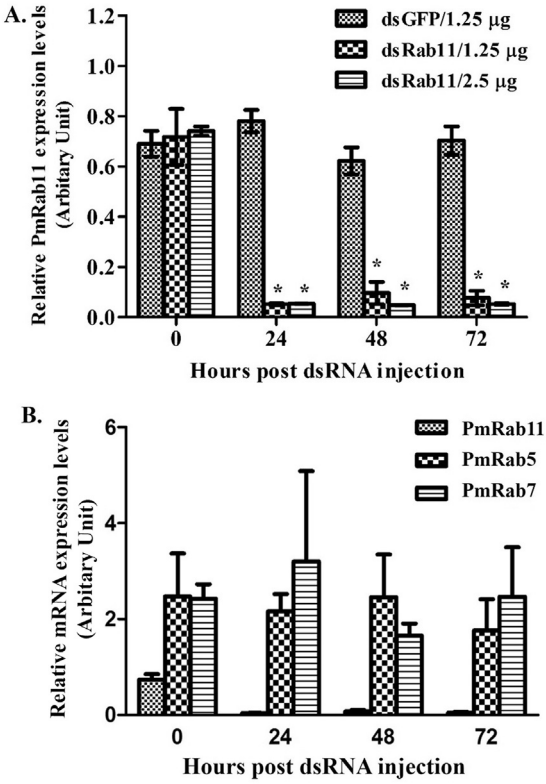

Fig. 4. Suppression of PmRab11 gene by dsRNA-PmRab11. (A) Relative mRNA expression levels of PmRab11 in shrimps injected with dsRNA-PmRab11 at 1.25 and 2.5 µg/g shrimp compared with 1.25 µg/g shrimp of dsRNA-GFP injection are presented as mean ± SEM, n = 4/time point. (B) Relative mRNA expression levels of PmRab11, PmRab5 and PmRab7 are presented as mean ± SEM, n = 3–4/time point. The relative mRNA expression levels of these genes were normalized with PmActin. (*) statistically significant difference between dsRNA-PmRab11 and dsRNA-GFP injected groups at each time point.

4. Discussion

At present, the mechanisms of YHV internalization and transportation inside the cell have been proposed. The viral glycoprotein gp116 on YHV envelope binds to the YHV binding protein, PmYRP65 on the cell membrane [30,31] then internalizes into the cell via clathrin-dependent endocytosis [32,33]. After that, the vesicle containing YHV particle is transported to the early and late endosome by Rab5 and Rab7, respectively [11,12] before the viral genome is released to the cytoplasm for replication and translation. Electron microscopy revealed that enveloped YHV virion is formed at TGN [2,13]. However, the mechanism of the transport of YHV from TGN to PM is not well understood. The earlier studies of other (+) ssRNA viruses such as flaviviruses and coronaviruses found that viral budding from TGN to PM is dependent on Rab11-mediated pathway through cytoskeleton network [34,35]. Interestingly, Rab11 of YHV-infected shrimp was shown to be upregulated after 24 h of infection [26]. A comparative proteomic analysis showed that the protein disulfide isomerase (PDI) was increased during YHV infection [36]. PDI is normally localized in the lumen of ER catalyzing the formation and isomerization of disulfide bonds [37]. It has also been reported to be involved in the folding and assembly of viral proteins in the ER [38]. The YHV structural proteins, gp116 and gp64, contain 26 and 24 cysteine residues, respectively, suggesting a possible role for PDI to form inter- and intra-molecular disulfide bonds during the folding of these viral proteins [13]. Therefore, it is possible that PmRab11 also play a role in the transport of YHV out of the cell.

Two forms of PmRab11 cDNAs of sizes 1200 and 1050 bp were found to be different at the 5′ UTR. This may be because the gene was transcribed from different alleles. The existence of the two variants of PmRab11 was confirmed by amplification of the full-length cDNA and by 5′ RACE (Supplementary Fig. 2). The nucleotide deletion at the 5′ end of the two forms has not been observed for other Rab11. However, at least three isoforms of Rab11 proteins such as Rab11A, Rab11B and Rab11C (occasionally called Rab25) have been reported and shown to localize differently at specific organelles. Rab11A and B localize at the Golgi, RE and early endosomes and may be involved in membrane trafficking pathway by transportation of the target protein from TGN/RE to plasma membrane [39]. While Rab11C is expressed only in certain epithelial cells and may be involved in vesicular trafficking from recycling endosome to plasma membrane [39,40]. The deduced PmRab11 protein shared a characteristic signature of Rab11 with other species and closely related to Rab11 in invertebrate, especially in shrimp species (100% amino acid sequence identity with Rab11 of Pacific white shrimp, *Litopenaeus vannamei*). The PmRab11 function was characterized by using RNAi approach. Knockdown of PmRab11 by dsRNA-PmRab11 specifically inhibited PmRab11 expression within 24 h but not PmRab5 and PmRab7 expression. Suppression of PmRab11 led to 100% shrimp death at day 7. Similar results were demonstrated in the knockdown effect of endogenous genes that are involved in the trafficking process in shrimp including PmRab5, PmRab7 and clathrin heavy chain [11,12,33]. In addition, Rab11 is an essential gene in the regulation of transportation of the endocytosed proteins [18,41,42].

The role of Rab11 during YHV infection was investigated by suppression of PmRab11. The PmRab11 expression was suppressed approximately 50% at 48 h post-dsRNA injection (or 24 h post-YHV infection) (Fig. 5A). This is in contrast to the result of PmRab11 knockdown alone (without YHV infection) that PmRab11 expression was inhibited more than 90% at this time point (Fig. 4A).

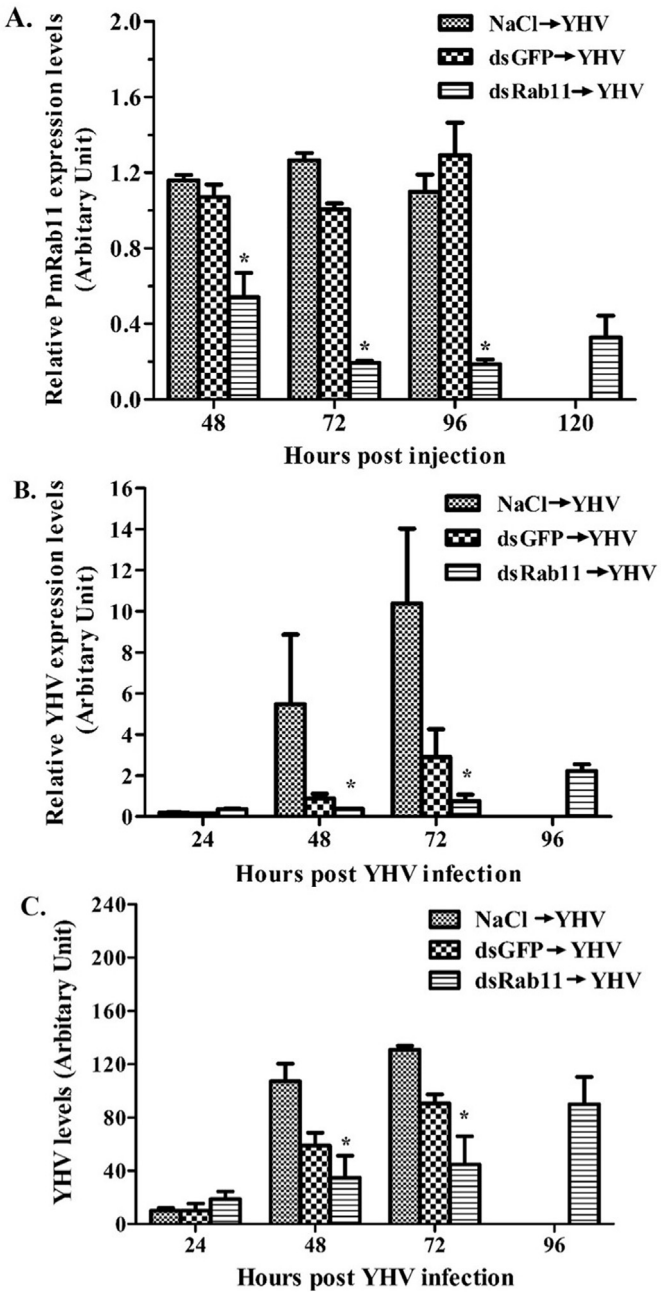

Fig. 5. Suppression of PmRab11 during YHV infection. (A) Relative expression of PmRab11 was detected from hemocytes of shrimps injected with 1.25 μg/g shrimp of dsRNA-PmRab11 followed by YHV, compared with dsRNA-GFP and NaCl injected shrimps at various time courses. Relative mRNA expression levels of YHV in hemocytes (B) and YHV levels in supernatant (C) was monitored. The data are presented as mean ± SEM, n = 4/time point. (*) statistically significant difference between dsRNA-PmRab11 and NaCl injected groups at each time point.

Interestingly, subtractive hybridization found that Rab11 was upregulated at 24 h post-YHV infection [26]. Therefore, it is possible that an incomplete PmRab11 knockdown is caused by upregulation of PmRab11 expression in response to YHV infection. In addition, viral titre inside and outside the cell was determined by semi-quantitative RT-PCR. The results showed that YHV levels in hemocytes and supernatant of PmRab11 knockdown group were significantly decreased from 48 to 72 h post-YHV infection when compared to the NaCl-injected group. Notably, not only PmRab11 expression was recovered at 120 h post-dsRNA injection, but also the YHV released was increase at this time point. This relationship demonstrated that PmRab11 is required for YHV infection. Similar results were observed in the plaque assay of virus infected cells that were treated with siRNA targeting Rab11 such as hantavirus [25], Influenza A [43], and hepatitis C virus [44].

To estimate the YHV's protein level in hemocytes and supernatant, Western blot was performed using antibody against YHV-gp64 which is one of the viral glycoproteins on YHV envelope. Unfortunately, our Rab11 antibody cannot be used to detect Rab11 protein by Western blot under the denaturing condition, suggesting that it required the native structure of epitopes. The results revealed that YHV protein level cannot be observed in both fractions of all experimental groups at 24 h post-dsRNA injection (Fig. 6). Previous study in PmRab5 knockdown during YHV infection found that YHV is internalized and transported via PmRab5 from PM to early endosome around 10 min–6 h post-infection [10]. After that, viral replication occurred and nucleocapsid was found in cytoplasm at 24 h post-YHV infection [13]. Thus, the, low level of YHV-gp64 protein at the early phase of infection and the failure to detect the protein in Western blot at this time point. At 48 h post-dsRNA injection, high YHV protein level in the NaCl-injected group can be observed. Whereas, the dsRNA-GFP injected group showed low YHV protein level at this time point. Many studies found that the innate antiviral immunity in invertebrates including shrimp was induced by any dsRNA in a sequence-independent manner [45,46]. High levels YHV protein in hemocytes and supernatant of the NaCl injected group and dsRNA-GFP injected group could be observed at 72 h. In contrast, YHV levels could not be detected in both fractions of PmRab11 knockdown group at 24–72 h post-dsRNA injection. For the (+) ssRNA virus including YHV, the replication process occurs in the cytoplasm [47] and the viral envelop glycoproteins are co-translationally inserted into ER membranes. Then, modification of the glycoproteins occurs during their passage through the secretory pathway. For example, all structural proteins of members of the Flaviviridae family such as hepatitis C and dengue virus are co-translated as a single polyprotein and are inserted into the ER membrane [48]. An individual glycoprotein is generated by proteolytic cleavage and the RNA-binding core protein that is known as the nucleocapsid is assembled within the ER, and transported to Golgi apparatus. It is possible that these events may also occur for YHV which is one of the (+) ssRNA. The single polyprotein containing gp116 and gp64 is co-translated and inserted into the ER membrane. The proteolytic cleavage resulted in individual gp116 and gp 64 that exposed the N-terminal domain to the cytosolic side [7]. Then, the viral nucleocapsid and glycoproteins are transported to the Golgi apparatus for maturation. At TGN, the budding of YHV envelope virion can be observed under electron microscope [2,13]. Normally, Rab11 is involved in the vesicle transport from TGN to the PM [49]. After PmRab11 knockdown, YHV cannot bud and has no target organelle to transport to. Therefore, the YHV protein in Golgi network might be transported to lysosome for degradation. However, the mechanism in this process remains to be elucidated. Similar results can be observed in the dengue virus [50]. In addition, the mortality assay revealed that injection of dsRNA-PmRab11 can delay shrimp mortality when compared to both control groups. Similar results of the delay in shrimp mortalities can be demonstrated for the knockdown effects of other Rab proteins including PmRab7 and PmRab5 during YHV infection [11,12].

Co-localization between YHV and PmRab11 was observed by immunofluorescence assay. The results showed co-localization between YHV-gp64 and PmRab11 was seen from 24 to 72 h post-YHV injection in both control groups (Fig. 8). Accumulation of YHV can be found at the PM of hemocytes. Similar results were also seen from other viruses that used Rab11-dependent pathway in the

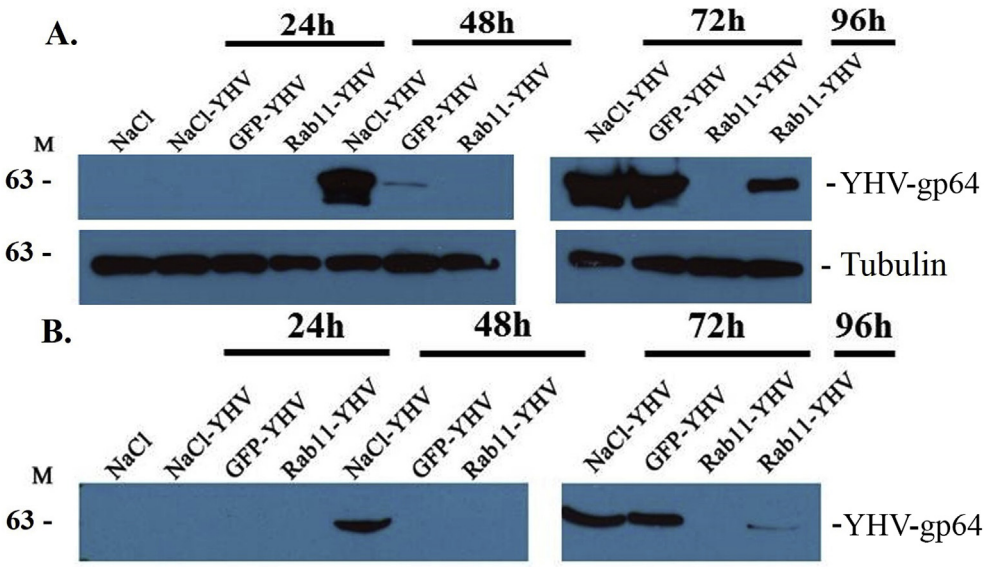

Fig. 6. Suppression effect of PmRab11 on YHV protein levels. Western blot analysis showed protein levels of YHV in hemocytes (A) and supernatant (B) of shrimps injected with 1.8 μg/g shrimp of dsRNA-PmRab11 followed by YHV, compared with dsRNA-GFP and NaCl injected shrimps at various times. Monoclonal antibody to YHV-gp64 was used to detect YHV while tubulin was used as a control.

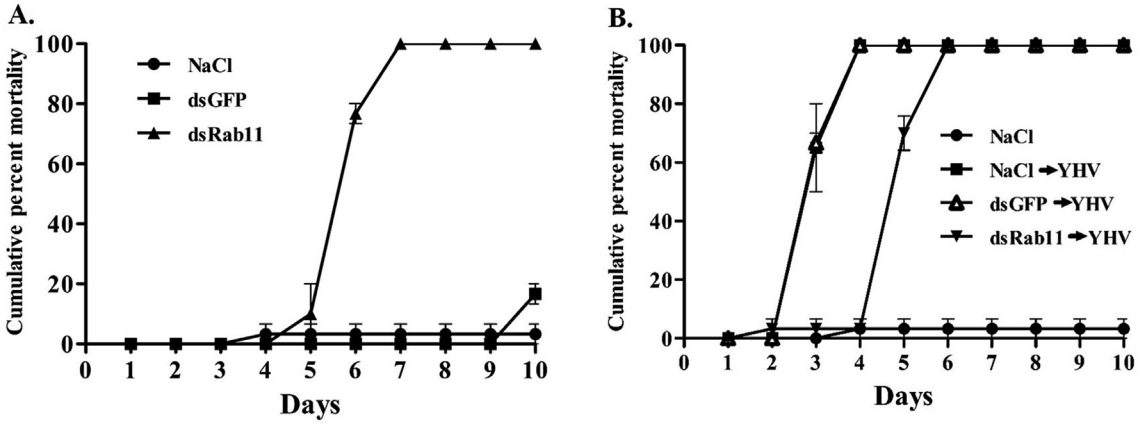

Fig. 7. Cumulative percent mortality of PmRab11-knockdown shrimp with or without YHV challenge. The cumulative percent mortality of shrimps injected with 1.25 μg/g shrimp of dsRNA-PmRab11 compared to injections of dsRNA-GFP or NaCl followed by absence (A) or presence (B) of YHV challenge were investigated. The data are presented as mean ± SEM, n = 45/experiment.

transportation. Such as sendai virus [20], influenza A virus [21,22,43], measles virus [23], mumps virus [24], hantavirus [25], hepatitis C virus [44] and dengue virus [50]. In contrast, low level of co-localization signals between PmRab11 and YHV can be observed in the perinuclear region at 24–72 h in the PmRab11 knockdown group. This is supported by an overexpression of Rab11 dominant negative mutant in hepatitis C, hantavirus or dengue infected cell. The virus was accumulated at the perinuclear region that was identified as TGN [25,44,50]. In addition, overexpression of Rab11 constitutively active mutant in influenza A virus infection showed that Rab11 is aggregated with vRNP at the perinuclear region and cannot be transported out of the cell [21–23]. These evidence suggested a possible role of Rab11 in transportation of YHV.

Other Rab such as Rab6 has been shown to play important roles in virus infection of shrimp. Rab6 is involved in the regulation of phagocytosis against white spot syndrome virus (WSSV) infection through the interaction with the WSSV envelope protein VP466, β-actin, and tropomyosin which could activate the GTPase activity of Rab6 and subsequently induce the rearrangement of actin fibers in invertebrates [51,52]. An increase in Rab6 activity was demonstrated in WSSV resistant shrimp. Silencing of Rab6 by a specific siRNA significantly increased WSSV replication in shrimp [53,54]. In addition, Rab6 plays an important role in the regulation of phagocytosis against bacterial infection in *Marsupenaeus japonicus* [55].

In summary, the virus budding process and its cellular trafficking inside the cell are core study in virology, Therefore, the identification of the routes for viral infection and release including the discovery of the cellular and viral components involved in various processes are essential. These are an important knowledge that will provide insights into host-pathogen interaction in order to improve a potential approach for therapeutic intervention against viral diseases.

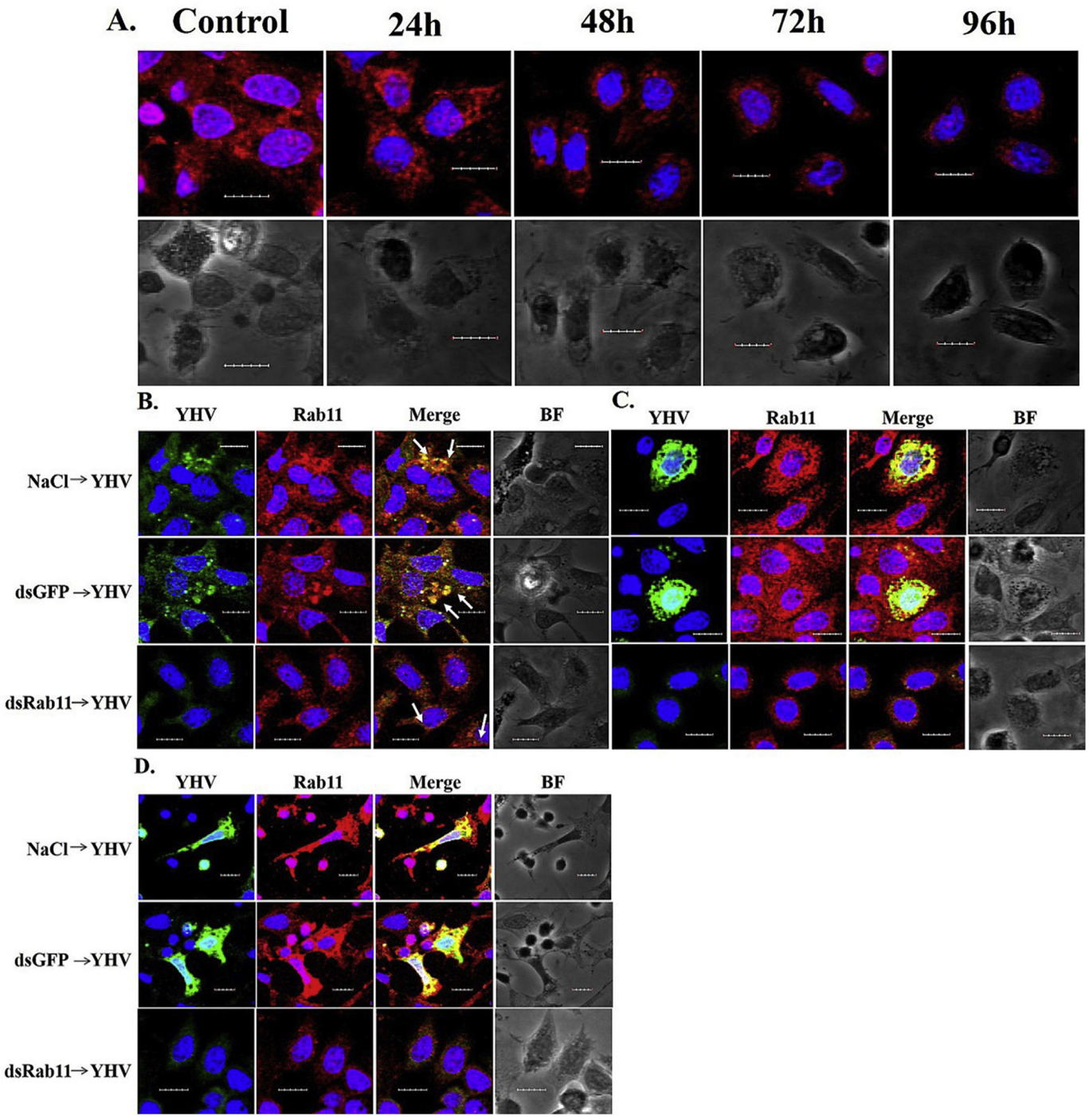

Fig. 8. Co-localization of PmRab11 and YHV in YHV-infected hemocytes. The pictures show hemocytes during PmRab1-knockdown at various times (A). Co-localization of PmRab11 and YHV was investigated at 24 h (B), 48 h (C) and 72 h (D) post-YHV challenge. Red, green and blue colours represented PmRab11, YHV-gp64 and nucleus, respectively. Arrow indicated the co-localization signal of PmRab11 and YHV. Scale is 10 μm. (For interpretation of the references to colour in this figure legend, the reader is referred to the web version of this article.)

Acknowledgement

We would like to thank Asst. Prof. Dr. Kusol Pootanakit for critically reading the manuscript, Prof. Dr. Paisarn Sithigorngul and Dr. Phattara-Orn Havanapan for providing anti-YHV-gp64 monoclonal antibody and anti-β-tubulin antibody, respectively and Ms. Chaweewan Chimawei, Mrs. Suparb Hongthong and Ms. Punnee Tongboonsong for technical assistance on culturing shrimp. We also would like to thank Shrimp Genetic Improvement Center in Surat Thani province, Thailand for providing shrimp samples. This work was supported by grants from Mahidol University under the National Research University initiative (NRU) and Thailand Research Fund (BRG5780006 to C.O, DBG5980011 to S.P. and IRG 5780009). A.K. is supported by the 60th Year Supreme Reign of His Majesty King Bhumibol Adulyadej.

Appendix A. Supplementary data

Supplementary data related to this article can be found at http://dx.doi.org/10.1016/j.fsi.2017.05.039.

References

[1] S. Boonyaratpalin, K. Supamataya, J. Kasornchandra, S. Direkbusarakom, U. Aekpanithanpong, C. Chantanachookhin, Non-occluded baculo-like virus the causative agent of yellow-head disease in the black tiger shrimp *Penaeus monodon*, Fish. Pathol. 28 (1993) 103–109.

[2] C. Chantanachookin, S. Boonyaratpalin, J. Kasornchandra, S. Direkbusarakom, U. Ekpanithanpong, K. Supamataya, S. Siurairatana, T.W. Flegel, Histology and ultrastructure reveal a new granulosis-like virus in *Penaeus monodon* affected by yellow-head disease, Dis. Aquat. Organ 17 (1993) 145–157.

[3] P.J. Walker, J.R. Bonami, V. Boonsaeng, P.S. Chang, J.A. Cowley, L. Enjuanes, T.W. Flegel, D.V. Lightner, P.C. Loh, E.J. Snijder, K. Tang, Virus Taxonomy: Classification and Nomenclature of Viruses: Eighth Report of the International Committee on the Taxonomy of Viruses, Elsevier, 2005, pp. 975–979.

[4] N. Sittidilokratna, R.A.J. Hodgson, J.A. Cowley, S. Jitrapakdee, V. Boonsaeng, S. Panyim, P.J. Walker, Complete ORF1b gene sequence indicates yellow head virus is an invertebrate nidovirus, Dis. Aquat. Organ 50 (2002) 87–93.

[5] N. Sittidilokratna, N. Phetchampai, V. Boonsaeng, P.J. Walker, Structural and antigenic analysis of the yellow head virus nucleocapsid protein p20, Virus Res. 116 (2006) 21–29.

[6] S. Jitrapakdee, S. Unajak, N. Sittidilokratna, R.A. Hodgson, J.A. Cowley, P.J. Walker, et al., Identification and analysis of gp116 and gp64 structural glycoproteins of yellow head nidovirus of *Penaeus monodon* shrimp, J. Gen. Virol. 84 (2003) 863–873.

[7] A.K. Dhar, J.A. Cowley, K.W. Hasson, P.J. Walker, Genomic organization, biology, and diagnosis of taura syndrome virus and yellow head virus of penaeid shrimp, Adv. Virus Res. 63 (2004) 353–421.

[8] C. Wongteerasupaya, J. Vickers, S. Sriurairatana, et al., A non-occluded, systemic baculovirus that occurs in cells of ectodermal and mesodermal origin and causes high mortality in the black tiger prawn *Penaeus monodon*, Dis. Aquat. Organ 21 (1995) 66–77.

[9] E.C.B. Nadala, L.M. Tapay, P.C. Loh, Yellow head virus: a rhabdovirus-like pathogen of penaeid shrimp, Dis. Aquat. Organ 31 (1997) 141–146.

[10] C. Soowannayan, T.W. Flegel, P. Sithigorngul, et al., Detection and differentiation of yellow head complex viruses using monoclonal antibodies, Dis. Aquat. Organ 57 (2003) 193–200.

[11] P. Posiri, S. Panyim, C. Ongvarrasopone, Rab5, an early endosomal protein required for yellow head virus infection of *Penaeus monodon*, Aquaculture 459 (2016) 43–53.

[12] C. Ongvarrasopone, M. Chanasakulniyom, K. Sritunyalucksana, S. Panyim, Suppression of PmRab7 by dsRNA inhibits WSSV or YHV infection in shrimp, Mar. Biotechnol. 10 (2008) 374–381.

[13] P. Duangsuwan, Y. Tinikul, B. Withyachumnarnkul, C. Chotwiwatthanakun, P. Sobhon, Cellular targets and pathways of yellow head virus infection in lymphoid organ of *Penaeus monodon* as studied by transmission electron microscopy, Songklanakarin J. Sci. Technol. 33 (2011) 121–127.

[14] M. Dubois-Dalcq, K.V. Holmes, B. Rentier, D.W. Kingsbury, Assembly of Enveloped RNA Viruses, Springer-Verlag KG, Vienna, Austria, 2013.

[15] E. Wimmer, Cellular Receptors for Animal Viruses, vol. 28, Cold Spring Harbor Laboratory Press, Plainview, New York, USA, 1994.

[16] S. Welsch, B. Müller, H.G. Kräusslich, More than one door - budding of enveloped viruses through cellular membranes, FEBS Lett. 581 (2007) 2089–2097.

[17] W. Chen, Y. Feng, D. Chen, A. Wandinger-Ness, Rab11 is required for trans-golgi network-to-plasma membrane transport and a preferential target for GDP dissociation inhibitor, Mol. Biol. Cell 9 (1998) 3241–3257.

[18] H. Stenmark, Rab GTPases as coordinators of vesicle traffic, Nat. Rev. Mol. Cell Biol. 10 (2009) 513–525.

[19] S.C. Das, D. Nayak, Y. Zhou, A.K. Pattnaik, Visualization of intracellular transport of vesicular stomatitis virus nucleocapsids in living cells, J. Virol. 80 (2006) 6368–6377.

[20] R. Chambers, T. Takimoto, Trafficking of Sendai virus nucleocapsids is mediated by intracellular vesicles, PLoS One 5 (2010) e10994.

[21] A.J. Eisfeld, E. Kawakami, T. Watanabe, G. Neumann, Y. Kawaoka, Rab11A is essential for transport of the influenza virus genome to the plasma membrane, J. Virol. 85 (2011) 6117–6126.

[22] M.J. Amorim, E.A. Bruce, E.K. Read, A. Foeglein, R. Mahen, A.D. Stuart, P. Digard, A Rab11- and microtubule-dependent mechanism for cytoplasmic transport of influenza A virus viral RNA, J. Virol. 85 (2011) 4143–4156.

[23] Y. Nakatsu, X. Ma, F. Seki, T. Suzuki, M. Iwasaki, Y. Yanagi, K. Komase, M. Takeda, Intracellular transport of the measles virus ribonucleoprotein complex is mediated by Rab11A-positive recycling endosomes and drives virus release from the apical membrane of polarized epithelial cells, J. Virol. 87 (2013) 4683–4693.

[24] H. Katoh, Y. Nakatsu, T. Kubota, M. Sakata, M. Takeda, M. Kidokoro, Mumps virus is released from the apical surface of polarized epithelial cells, and the release is facilitated by a Rab11-mediated transport system, J. Virol. 89 (2015) 12026–12034.

[25] R.K. Rowe, J.W. Suszko, A. Pekosz, Roles for the recycling endosome, Rab8, and Rab11 in hantavirus release from epithelial cells, Virology 382 (2008) 239–249.

[26] A. Prapavorarat, S. Pongsomboon, A. Tassanakajon, Identification of genes expressed in response to yellow head virus infection in the black tiger shrimp, Penaeus monodon, by suppression subtractive hybridization, Dev. Comp. Immunol. 34 (2010) 611–617.

[27] A. Dereeper, V. Guignon, G. Blanc, S. Audic, S. Buffet, F. Chevenet, et al., Phylogeny.fr: robust phylogenetic analysis for the non-specialist, Nucleic Acids Res. 36 (2008) W465–W469.

[28] C. Ongvarrasopone, Y. Roshorm, S. Panyim, A simple and cost effective method to generate dsRNA for RNAi studies in invertebrates, ScienceAsia 33 (2007) 035–039.

[29] P. Posiri, C. Ongvarrasopone, S. Panyim, A simple one-step method for producing dsRNA from *E. coli* to inhibit shrimp virus replication, J. Virol. Methods 188 (2013) 64–69.

[30] W. Assavalapsakul, D.R. Smith, S. Panyim, Identification and characterization of a *Penaeus monodon* lymphoid cell-expressed receptor for the yellow head virus, J Gen. Virol. 80 (2006) 262–269.

[31] W. Assavalapsakul, H.K.T. Kiem, D.R. Smith, S. Panyim, Silencing of PmYPR65 receptor prevents yellow head virus infection in *Penaeus monodon*, Virus Res. 189 (2014) 133–135.

[32] T. Jatuyosporn, P. Supungul, A. Tassanakajon, K. Krusong, The essential role of clathrin-mediated endocytosis in yellow head virus propagation in the black tiger shrimp *Penaeus monodon*, Dev. Comp. Immunol. 44 (2014) 100–110.

[33] P. Posiri, H. Kondo, I. Hirono, S. Panyim, C. Ongvarrasopone, Successful yellow head virus infection of *Penaeus monodon* requires clathrin heavy chain, Aquaculture 435 (2015) 480–487.

[34] S. Welsch, B. Müller, H.G. Kräusslich, More than one door - budding of enveloped viruses through cellular membranes, FEBS Lett. 581 (2007) 2089–2097.

[35] W. Weissenhorn, E. Poudevigne, G. Effantin, P. Bassereau, How to get out: ssRNA enveloped viruses and membrane fission, Curr. Opin. Virol. 3 (2013) 159–167.

[36] A. Bourchookarn, P.-O. Havanapan, V. Thongboonkerd, C. Krittanai, Proteomic analysis of altered proteins in lymphoid organ of yellow head virus infected *Penaeus monodon*, BBA-Proteins Proteom 1784 (2008) 504–511.

[37] R. Noiva, W.J. Lennarz, Protein disulfide isomerase. A multifunctional protein resident in the lumen of the endoplasmic reticulum, J. Biol. Chem. 267 (1992) 3553–3566.

[38] A. Guichard, V. Nizet, E. Bier, R.W. Doms, R.A. Lamb, J.K. Rose, A. Helenius, Folding and assembly of viral membrane proteins, Virology 193 (1993) 545–562.

[39] A.H. Hutagalung, P.J. Novick, Role of Rab GTPases in membrane traffic and cell physiology, Physiol. Rev. 91 (1) (2011) 119–149.

[40] J.R. Goldenring, K.R. Shen, H.D. Vaughan, I.M. Modlin, Identification of a small GTP-binding protein, Rab25, expressed in the gastrointestinal mucosa, kidney and lung, J. Biol. Chem. 268 (25) (1993) 18419–18422.

[41] B.D. Grant, J.G. Donaldson, Athways and mechanisms of endocytic recycling, Nat. Rev. Mol. Cell Biol. 10 (2009) 597–608.

[42] S.C.D. van Ijzendoorn, Recycling endosomes, J. Cell Sci. 119 (2006) 1679–1681.

[43] E.A. Bruce, P. Digard, A.D. Stuart, The Rab11 pathway is required for influenza A virus budding and filament formation, J. Virol. 84 (2010) 5848–5859.

[44] K. Coller, N. Heaton, K. Berger, J. Cooper, J. Saunders, G. Randall, Molecular determinants and dynamics of hepatitis C virus secretion, PLoS Pathog. 8 (2012) e1002466.

[45] J. Robalino, T. Bartlett, E. Shepard, S. Prior, G. Jaramillo, E. Scura, R.W. Chapman, P.S. Gross, C.L. Browdy, G.W. Warr, Double-stranded RNA induces sequence-specific antiviral silencing in addition to nonspecific immunity in a marine shrimp: convergence of RNA interference and innate immunity in the invertebrate antiviral response? J. Virol. 79 (2005) 13561–13571.

[46] J. Robalino, C.L. Browdy, S. Prior, A. Metz, P. Parnell, P. Gross, G. Warr, Induction of antiviral immunity by double-stranded RNA in a marine invertebrate, J. Virol. 78 (2004) 10442–10448.

[47] C. Harak, V. Lohmann, Ultrastructure of the replication sites of positive-strand RNA viruses, Virology 497 (2015) 418–433.

[48] S. Mukhopadhyay, R.J. Kuhn, M.G. Rossmann, A structural perspective of the flavivirus life cycle, Nat. Rev. Microbiol. 3 (2005) 13–22.

[49] W. Chen, Y. Feng, D. Chen, A. Wandinger-Ness, Rab11 is required for trans-golgi network-to-plasma membrane transport and a preferential target for GDP dissociation inhibitor, Mol. Biol. Cell 9 (1998) 3241–3257.

[50] E.G. Acosta, V. Castilla, E.B. Damonte, Differential requirements in endocytic trafficking for penetration of dengue virus, PLoS One 7 (2012) e44835.

[51] T. Ye, W. Tang, X. Zhang, Involvement of Rab6 in the regulation of phagocytosis against virus infection in invertebrates, J. Proteome Res. 11 (2012a) 4834–4846.

[52] T. Ye, R. Zong, X. Zhang, The role of white spot syndrome virus (WSSV) VP466

protein in shrimp antiviral phagocytosis, Fish. Shellfish Immunol. 33 (2012b) 350–358.
[53] W. Wu, X. Zhang, Characterization of a Rab GTPase up-regulated in the shrimp *Peneaus japonicus* by virus infection, Fish Shellfish Immunol 23 (2007) 438–445.
[54] W. Wu, R. Zong, J. Xu, X. Zhang, Antiviral phagocytosis is regulated by a novel Rab-dependent complex in shrimp *Penaeus japonicus*, J. Proteome Res. 7 (2008) 424–431.
[55] R. Zong, W. Wu, J. Xu, X. Zhang, Regulation of phagocytosis against bacterium by Rab GTPase in shrimp *Marsupenaeus japonicus*, Fish. Shellfish Immunol. 25 (2008) 258–263.

BS-05

MOLECULAR CLONING OF THE FULL LENGTH CDNA OF RAB11 IN *Penaeus monodon*

Akechai Kongprajug[1,*], Sakol Panyim[2], Chalermporn Ongvarassopone[2,#]
[1]Master of Science Program in Molecular Genetics and Genetic Engineering (International Program), Institute of Molecular Biosciences, Mahidol University.
[2]Molecular Genetics and Genetic Engineering Program, Institute of Molecular Biosciences, Mahidol University. Phuttamonthon 4 Road, Salaya, Nakhon Pathom, 73170, Thailand.
*e-mail: akechai.kon@student.mahidol.ac.th, #e-mail: chalermporn.ong@mahidol.ac.th.

Abstract

Rab11 is a small GTPase protein belonged to a Ras superfamily which functions in the recycling endosome and plays a crucial role to transport cargo vesicles including some RNA viruses to plasma membrane. To understand whether Rab11 is required for transportation of shrimp viruses especially yellow head virus (YHV) out of the cell, the molecular cloning of the full length cDNA of Rab11 of *Penaeus monodon* was studied. A partial cDNA of PmRab11 (494 bp) was obtained from the hemocytes cDNA. In order to clone the full length cDNA of Rab11 of *Penaeus monodon*, 5'and 3' rapid amplification of cDNA ends (RACE) were performed. The results showed that the full length cDNA of PmRab11 was approximately 1253 bp and coding sequences was 642 bp encoding Rab11 protein of size 214 amino acids. Sequence analysis demonstrated that PmRab11 contained the conserved domains similar to the Rab11 in others species. The phylogenetic tree analysis showed that PmRab11 was closely related to Rab11 in vertebrate and arthropods.

Keywords: endocytosis, recycling endosome, 3'and 5' RACE, black tiger shrimp

BS-05

MOLECULAR CLONING OF THE FULL LENGTH cDNA OF RAB11 IN *Penaeus monodon*

Akechai Kongprajug[1,*], Sakol Panyim[2], Chalermporn Ongvarassopone[2,#]
[1]Master of Science Program in Molecular Genetics and Genetic Engineering (International Program), Institute of Molecular Biosciences, Mahidol University.
[2]Molecular Genetics and Genetic Engineering Program, Institute of Molecular Biosciences, Mahidol University, Phuttamonthon 4 Road, Salaya, Nakhon Pathom, 73170, Thailand.
*e-mail: akechai.kon@student.mahidol.ac.th, #e-mail: chalermporn.ong@mahidol.ac.th

Abstract

Rab11 is a small GTPase protein belonged to a Ras superfamily which functions in the recycling endosome and plays a crucial role to transport cargo vesicles including some RNA viruses to plasma membrane. To understand whether Rab11 is required for transportation of shrimp viruses especially yellow head virus (YHV) out of the cell, the molecular cloning of the full length cDNA of Rab11 of *Penaeus monodon* was studied. A partial cDNA of PmRab11 (494 bp) was obtained from the hemocytes cDNA. In order to clone the full length cDNA of Rab11 of *Penaeus monodon*, 5'and 3' rapid amplification of cDNA ends (RACE) were performed. The results showed that the full length cDNA of PmRab11 was approximately 1253 bp and coding sequences was 642 bp encoding Rab11 protein of size 214 amino acids. Sequence analysis demonstrated that PmRab11 contained the conserved domains similar to the Rab11 in others species. The phylogenetic tree analysis showed that PmRab11 was closely related to Rab11 in vertebrate and arthropods.

Keywords: endocytosis, recycling endosome, 3'and 5' RACE, black tiger shrimp

Introduction

Rab11 is a small GTPase protein belonged to a Ras superfamily that involved in the recycling endosome pathway which transports cargo vesicles through the trans-golgi network (Horgan and McCaffrey, 2009), apical recycling endosomes and perinuclear recycling endosome compartment before redirecting the vesicular cargo back to the apical plasma membrane (Bruce, et al. 2012). Rab11 associates with the membrane in a cyclical of GTP/GDP- bound form. After binding GTP, a conformational change allows the isoprenylated C-terminus of Rab11 to associate with a vesicular membrane (Joberty et al., 1993). Then, it will associate to Rab11 effectors that are various cytoskeletal components. In complex with Rab11, the Rab11 effectors then direct the vesicles trafficking throughout the recycling pathway, primarily by mediating associations with a specific motor protein. Interestingly, subtractive hybridization study found that Rab11 was upregulated after YHV infection (Prapavorarat, et al. 2010). In contrast, the Rab GDP-dissociation inhibitor that prevents the disassociation of GDP and Rab binding complex during the trafficking cycles is decrease (Bourchookarn et al., 2008).

Preliminary study to obtain the Rab11 of *Penaeus monodon* (PmRab11) was performed by designing the degenerate primers based on the invertebrate Rab11 sequences available in the GenBank database. The partial nucleotide sequence of PmRab11 of size about 494 bp was amplified from hemocytes cDNA. Sequence analysis in the nucleotides database showed 98% identity with Rab11 mRNA of *Litopenaeus vannamei* (Accession number; JN082706.1).

Therefore, based on this evidence, it is hypothesized that Rab11 protein is required for the transportation of YHV out of the cell. Thus, the objective of this study is to clone the full length cDNA of PmRab11.

Methodology

1. Molecular cloning of the full length cDNA of PmRab11

1.1 Primers design

The gene specific primers that used to amplify in 5' and 3' RACE were designed based on the partial sequences of PmRab11. The PRT oligo (dT) primer was designed to facilitate to bind at poly A of mRNA and PM-1 primer is an adaptor primer complementary to the adaptor sequences in the PRT oligo (dT) primer. The sequences and the position of primers were displayed in Table 1 and Figure 1, respectively.

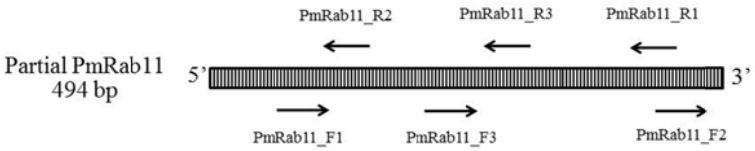

Figure 1. Primer position**.** The positions of gene specific primers of PmRab11 that used in 5' and 3' RACE-PCR are shown.

Table 1. Primers used in each experiment.

Experiments and Primers	**Sequences (5' → 3')**	**Size (bp)**	**Tm (ºC)**
Reverse transcription			
PRT oligo (dT)	CCGGAATTCAAGCTTCTAGAGGATCCTT TTTTTTTTTTTTT	42	70
Adaptor primer			
PM-1	CCGGAATTCAAGCTTCTAGAGGATCC	26	60.5
5' RACE			
PmRab11_R1	GCACACTCTCAGCATTTACAGTTGG	25	65.8
PmRab11_R2	ATTCTGATCTGCATGATCTCTGAGC	25	64.1
PmRab11_R3	GGCCGTCTCTACATTAGTGGAGCC	24	60.8
3' RACE			
PmRab11_F1	CACTTACACTAATGTAGAACGTTGGC	26	64.6
PmRab11_F2	GCTGATGTTAAGGCTATTCACGTGG	25	65.8
PmRab11_F3	AAGGCATTTGCAGAAAAGGAGGGAC	25	57.7

1.2 5' RACE

Total RNAs was extracted from ovary by TRIzol reagent according to the manufacture's protocol and the rapid amplification of cDNA ends (RACE) – PCR was performed to amplify the 5'ends of PmRab11. 5' RACE-PCR began by using mRNA as a template for a first round of cDNA synthesis (or reverse transcription) reaction using gene specific primer R1 (PmRab11_R1) and it copied the mRNA template in the 3' to the 5' direction to generate a specific single-stranded cDNA product by using SuperScript® III reverse transcriptase (Invitrogen™). Following cDNA synthesis, the enzyme terminal deoxynucleotidyl transferase (NEB) was used to add a string of identical nucleotides, known as a homopolymeric tail, to the 3' end of the cDNA. In this case, poly A was added. A 5'RACE PCR reaction was then carried out, which used gene specific primer R3 (PmRab11_R3) and PRT oligo (dT) primer that bound the poly A tail to amplify a cDNA product

from the 5' end. Thus, 5' end sequences will be obtained in this method. Confirmation of the 5'RACE PCR product was performed by the nested PCR using gene specific primer R2 (PmRab11_R2) and PM-1 primer. The PCR products of both RACE- PCR and nested PCR were run on the agarose gel electrophoresis and the expected bands was cloned to pGEM-T-easy vector and subjected to sequencing.

1.2 3'RACE

In the 3' RACE PCR, total RNAs from the previous experiment was used as templates for reverse transcription reaction. The natural poly A tail was existed at the 3' end of most mRNAs. So cDNA was generated using a PRT oligo (dT) primer according to the manufacturer's protocol of ImProm-II™ reverse transcriptase (Promega). Then, 3' RACE PCR was performed by using Taq DNA polymerase (NEB) with gene specific primers F1 (PmRab11_F1) and PM-1 primers. The 3'RACE PCR product was confirmed by nested PCR using gene specific primers; PmRab11_F2, PmRab11_F3 and PM-1 primer. The PCR products were run on the agarose gel electrophoresis and the expected bands was cloned to pGEM-T-easy vector and subjected to sequencing.

1.3 Amplification of the full length cDNA of PmRab11 and sequence analysis

The sequences of the 5' and 3' end that obtained from RACE-RCR were assembled to the partial sequences of PmRab11. Then, The PCR using Tag DNA polymerase (NEB) was performed to amplify the full length cDNA of PmRab11 using the primers designed based on the 5' and 3' ends sequences. The contig PmRab11 sequence was analysed by using nucleotides blast of NCBI database. Multiple alignments of Rab11amino acid sequences with other species were performed to identify the conserved domains of Rab11 protein. Then, the phylogenetic tree analysis was performed by MEGA 4.1 program based on the neighbor-joining methods.

Results

1. Amplification of the 5' and 3'end by RACE method

1.1 5' RACE-PCR product and sequence analysis

In order to identify the 5' end sequences of PmRab11, 5' RACE- PCR was performed in this step. The first PCR product was amplified by using PmRab11_R3 and PRT oligo (dT) primer. The result showed two bands size about 790 and 650 bp. Then, the first PCR product was used as a template for nested PCR by using PmRab11_R2 and PM-1 primer. The result showed two bands of PCR products size approximately 660 and 490 bp (Figure 2, a). The largest bands of both PCR reaction size 790 and 660 bp were selected to purify and clone to pGEM-T-easy vector. Two clones were subjected to sequencing. The result showed 99% nucleotide sequence identity with *Litopenaeus vannamei*'s Rab11 mRNA (Accession number: JN082706.1).

1.2 3' RACE-PCR product and sequence analysis

3'RACE-PCR was performed to amplify PmRab11 cDNA using PmRab11_F1 and PRT oligo (dT) primers. The PCR product has size about 820 bp. Then, the nested PCR using PmRab11_F3 and PM-1 primers was performed and has size about 650 bp (Figure 2, b). Two clones were subjected to sequencing. The sequencing results showed 99% nucleotide sequence identity with *Litopenaeus vannamei*'s Rab11 mRNA (Accession number: JN082706.1).

2. Amplification of the full length cDNA of PmRab11

The sequences from 5' and 3' RACR were assembled to the partial sequences of PmRab11 by using program ContigExpress of Vector NTI. The result showed that the full length cDNA of PmRab11 has size about 1253 bp. The initiation codon and poly A signal were analyzed by using program ATGpr and Poly(A) Signal Miner, respectively. The open reading frame has size about 642 bp encoding 214 amino acids. 5'UTR and 3'UTR have size about 246 bp and 362 bp. Then, the predicted full length cDNA of PmRab11 was confirmed by PCR using primers that designed from 5' and 3' end. The result showed that the expected band size about 1253 bp was obtained (Figure 2, c). In addition, the coding sequences were translated to amino acid and blasted to

NCBI conserved domain analysis. The result showed that PmRab11 protein shared the characteristics of Rab11 protein with others species (Figure 3).

3. Phylogenetic tree analysis

The phylogenetic tree showed that PmRab11 protein was closely related with Rab11 in vertebrate and arthropods and showed more than 80% amino sequence identity (Figure 4).

Discussion and Conclusion

The full length cDNA of PmRab11 was successfully cloned by 3' and 5' RACE methods. The amino sequences of PmRab11 was translated and subjected to identify Rab11 conserved domains. The PmRab11 protein contained 5 GTP binding sites (G), Rab family (RabF1-5) and Rab subfamily (RabSF1-4) domains which were the characteristics of Rab11 protein. In addition, the phylogenetic analysis revealed that PmRab11 protein is very closely related to Rab11 of *Litopenaeus vannamei* and shared 100% amino sequences identity. Furthermore, the PmRab11 protein was closely related to Rab11 in arthropods. Future study will be focused on characterization of the function of PmRab11 and its involvement during YHV infection by using RNAi technology.

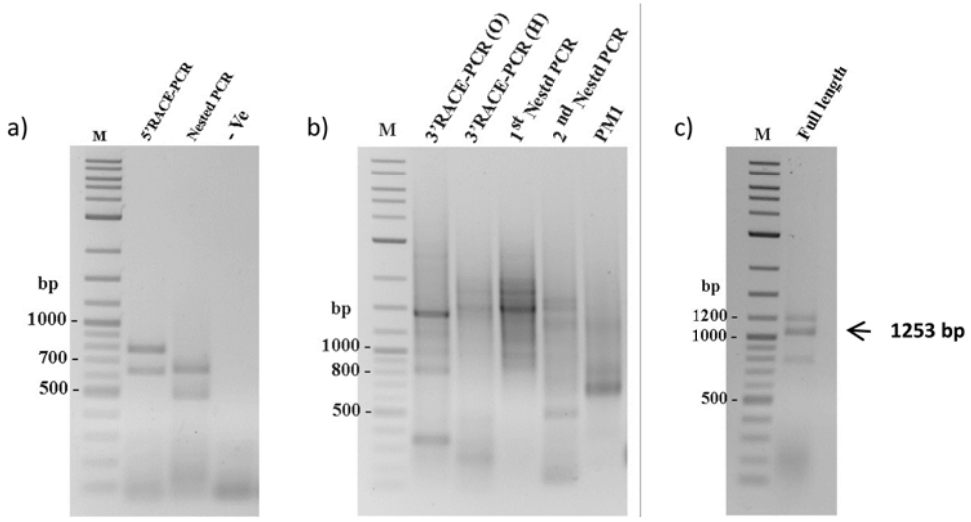

Figure 2. Representative gels showing 5' and 3' RACE-PCR products and the full length cDNA of PmRab11. a) 5'RACE-PCR products, the negative control (-Ve) was performed with distilled water. b) 3'RACE-PCR products, the templates were cDNA from ovary (O) and hemocytes (H). Lane M is 2-log DNA marker (200 ng).

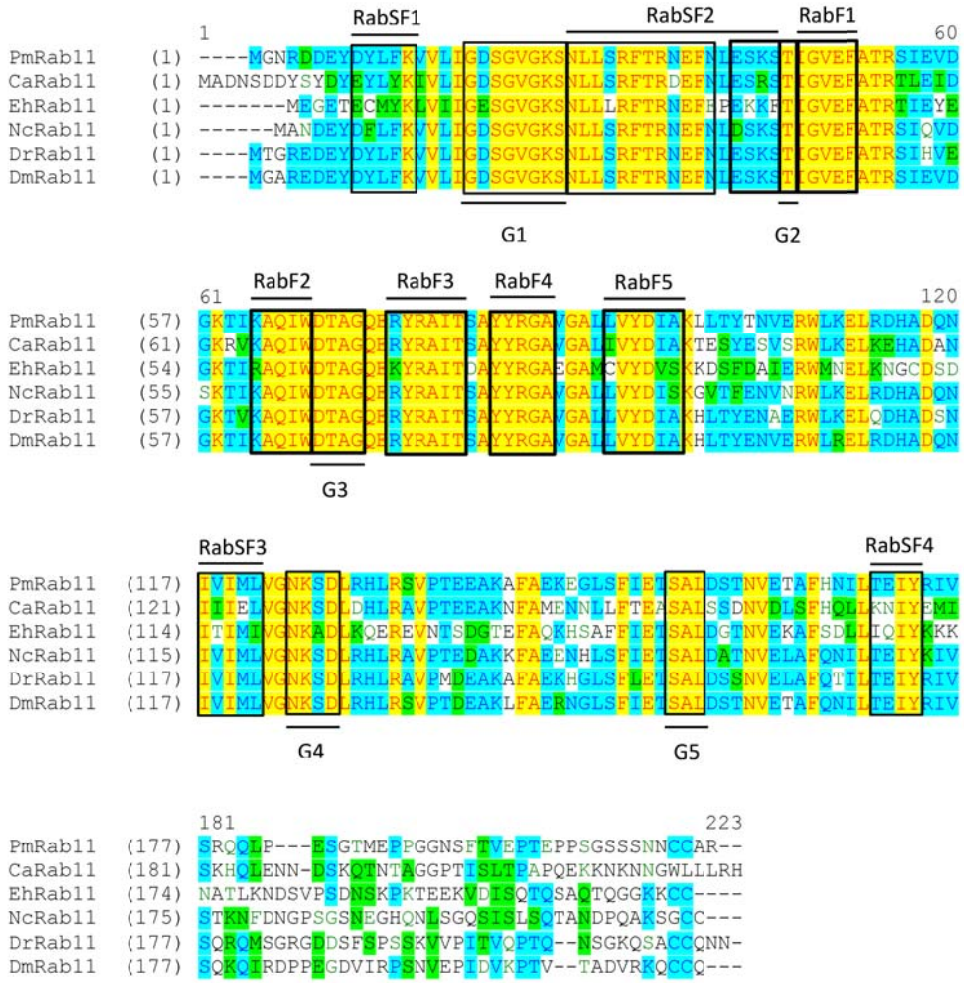

Figure 3. Multiple sequence alignment showing conserved domains of PmRab11 compared to Rab11 proteins from other species. The GTP binding sites are shown in boxes G1-5. The conserved domain of Rab family protein and Rab subfamily are shown in boxes, RabF1-5 and RabSF1-4, respectively.

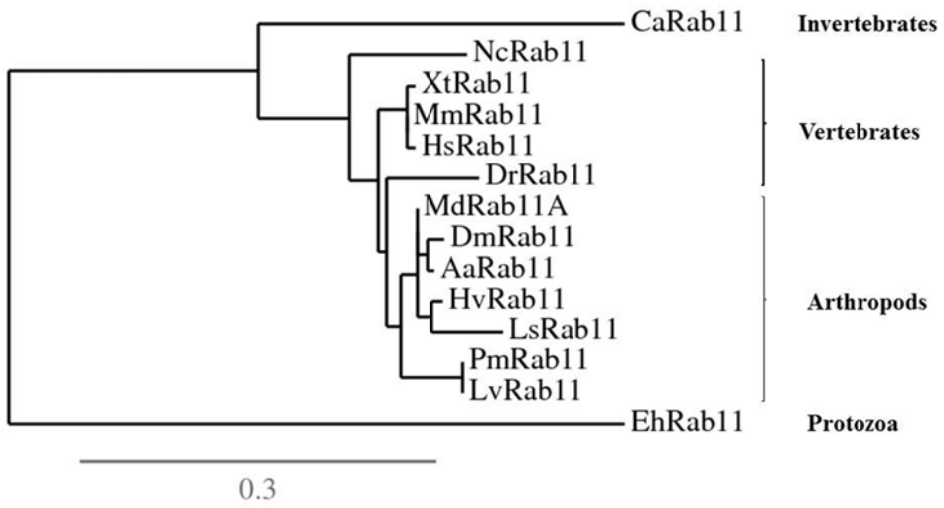

Figure 4. The phylogenetic analysis of Rab11 of *P. monodon* and other species. The amino acids of PmRab11 was used to analyze the genetic relationship with Rab11 proteins of *Neurospora crassa* (Nc) (accession number; CAD21237), *Lepeophtheirus salmonis* (Ls) (accession number; ACO11934.1), *Candida albicans* (Ca) (accession number; XP_710387), *Danio rerio* (Dr) (accession number; AAH55141), *Xenopus tropicalis* (Xt) (accession number; AAH41250), *Mus musculus* (Mm) (accession number; NP_033023.1), *Homo sapiens* (Hs) (accession number; CAG38733.1), *Homalodisca vitripennis* (Hv) (accession number; AAT01087.1), *Microplitis demolitor* (Md) (accession number; EZA45322.1), *Aedes aegypti* (Aa) (accession number; XP_001659918.1), *Drosophila melanogaster* (Dm) (accession number; NP_477170), *litopenaeus vannamei* (Lv) (Accession number; JN082706.1) and *Entamoeba histolytica* (Eh) (accession number; XP_649609).

Table 2. The percent amino acid sequence identity of Rab 11 compared between 2 species.

Species	Dm	Hv	Md	Hs	Mm	Xt	Dr	Ca	Eh	Nc	Ls	Lv	Pm
Aa	95	95	94	84	85	85	79	60	53	77	82	83	83
Dm		94	94	84	84	85	80	60	53	75	81	82	82
Hv			94	86	86	86	78	60	52	75	82	83	83
Md				86	86	86	81	60	52	76	82	82	82
Hs					99	97	80	60	51	73	80	79	79
Mm						97	80	60	52	74	80	80	80
Xt							80	60	51	73	80	81	81
Dr								60	51	71	77	78	78
Ca									44	59	61	62	62
Eh										51	51	52	52
Nc											74	72	72
Ls												80	80
Lv													100

References

1. Bourchookarn A, Havanapan P-O, Thongboonkerd V, Krittanai C. Proteomic analysis of altered proteins in lymphoid organ of yellow head virus infected *Penaeus monodon*. Biochimica et Biophysica Acta (BBA) - Proteins and Proteomics. 2008;1784(3):504-11.
2. Bruce EA, Stuart A, McCaffrey MW, Digard P. Role of the Rab11 pathway in negative-strand virus assembly. Biochemical Society Transactions. 2012;40(6):1409-15.
3. Horgan CP, McCaffrey MW. The dynamic Rab11-FIPs. Biochemical Society Transactions. 2009;37(5):1032-6.
4. Joberty G, Tavitian A, Zahraoui A. Isoprenylation of Rab proteins possessing a C-terminal CaaX motif. FEBS Letters. 1993;330(3):323-8.
5. Prapavorarat A, Pongsomboon S, Tassanakajon A. Identification of genes expressed in response to yellow head virus infection in the black tiger shrimp, *Penaeus monodon*, by suppression subtractive hybridization. Developmental and Comparative Immunology. 2010;34(6):611-7.

BMB 2016

The 5th International Biochemistry and Molecular Biology Conference

ABSTRACT BOOK

The 5th International Biochemistry and Molecular Biology Conference

SONGKHLA, THAILAND, MAY 26-27, 2016

Molecular cloning and sequence analysis of *Penaeus monodon* Rab9

Sudarat Thongsuksangcharoen[a] , Sakol Panyim[a,b], and Chalermporn Ongvarrasopone[a,*]

[a]*Institute of Molecular Biosciences, Mahidol University, Salaya, Nakhon Pathom 73170, Thailand*
[b]*Department of Biochemistry, Faculty of Science, Mahidol University, Rama VI Road, Bangkok 10400, Thailand*

Abstract

Rab proteins belong to a Ras superfamily of small GTPases, which play an important role in the regulation of vesicular transport in the cells. Previous studies found that Rab9 is important in regulation of the vesicle transport from late-endosomes to trans-Golgi network (TGN). In this study, the putative *Penaeus monodon* Rab9 (*PmRab9*) cDNA was cloned by 5' and 3' rapid amplification of cDNA ends (RACE). The results demonstrated that the full-length cDNA of *PmRab9* was approximately 958 bp containing 633 bp of the coding sequence, which encoded 210 amino acids. Sequence analysis demonstrated that PmRab9 contained the conserved domains similar to the Rab9 of other species. Phylogenetic tree analysis showed that PmRab9 was clustered in the group of *Marsupenaeus japonicus* (MjRab9) and *Macrobrachium rosenbergii* (MrRab9). In order to study the function of PmRab9 in the vesicle trafficking inside the cells, RNA interference technology using double-stranded RNA targeting to *PmRab9* (dsRNA-*PmRab9*) was performed. Injection of dsRNA-*PmRab9* at 0.63, 1.25, 2.5 and 5 µg/ g shrimp resulted in approximately 60% reduction of *Rab9* expression when compared to the NaCl injected group. In the future, knockdown effect of *PmRab9* during virus trafficking in *P. monodon* will be investigated.

Keywords: Endocytosis; Rapid amplification of cDNA ends; RNA interference; black tiger shrimp

1. Introduction

Rab proteins are members of the Ras superfamily of small GTPases, and are involved in several cellular processes relating to membrane trafficking and organelle mobility throughout the cell. They play important regulatory roles in motility by recruiting molecular motors to organelles and transport vesicles (Zeria *et al*., 2001). Rab protein acts as a molecular switch between an active, GTP bound and an inactive, GDP bound conformation. In the GTP-bound state, Rab interacts with various effector proteins that function in the regulation of many key steps in membrane trafficking including vesicle formation, vesicle motility, membrane remodeling, vesicle docking, membrane fusion, and multiple stages of intracellular transport processes. At present, more than 70 Rabs have been identified in mammals.

One of the Rab proteins that is found in late endosome and plays an essential role in the transportation of mannose-6-phosphate receptor (M6PR) from late endosomes to the trans-Golgi network (TGN) is Rab9. It is a key mediator of vesicular transport and is important for lysosomal enzyme delivery (Lombardi *et al*., 1993). Moreover, it is responsible for the maintenance of specific late endocytic compartments and endosome/lysosome localization (Barbero *et al*., 2002). In addition, Rab9 GTPase is a key component for the replication of several viruses including human immunodeficiency virus type 1 (HIV1), Ebola, Marburg, and measles virus (Murray *et al*., 2005). Silencing of Rab9 by lentiviral transduction during an enveloped, positive-sense single-stranded RNA virus, hepatitis C virus (HCV) infection resulted in prevention of the release of viral particles. This result suggested that loss of Rab9 impaired HCV replication (Ploen, D. *et al*. 2013). Therefore, to understand the endosomal trafficking pathway of the vesicle transport from late endosome to trans-Golgi network, silencing effect of Rab9 was studied.

2. Materials and Methods

2.1 Molecular cloning of the PmRab9 cDNA

2.1.1 Primer design

Cloning of the partial cDNA sequence of PmRab9 was performed by designing primers, MjRab9F and MjRab9R (Table 1) based on the coding sequence of Marsupenaeus japonicus Rab9 (kindly provided by Prof. Hidehiro Kondo from Tokyo University of Marine Science and Technology, Japan).

2.1.2 RNA extraction and RT-PCR analysis

Total RNA from ovary of P. monodon was isolated by TRI Reagent according to the manufacturer's protocol. Two microgram of total RNA was used to generate cDNA by Improm-II reverse transcriptase (Promega) and

* *Corresponding author. chalermporn.ong@mahidol.ac.th.*

PPD

PRT oligo-dT primer (Table 1). PCR reaction was performed by using specific primers (according to 1.1.). The RT-PCR product of PmRab9 was cloned into pGEM-T easy vector (Promega) and sequenced. The partial DNA sequence of PmRab9 was confirmed by blasted to the GenBank database.

2.1.3 5' and 3' rapid amplification of cDNA ends (RACE)

The 5' and 3' ends of PmRab9 were amplified by using rapid amplification of cDNA ends (RACE) approach. For 3' RACE, total RNA was extracted from ovary. First stranded cDNA was generated by Impromp II reverse transcriptase (Promega) with PRT-oligo dT primer (Table 1). Then, cDNA was used as a template for the first PCR with 3' RACE primer, 3F1 (Table 1) and PRT-oligo dT primer to amplify the 3' end. In order to perform 5' RACE, the first stranded cDNA was generated by a specific primer, 5R1 (Table 1) based on the partial sequence of PmRab9 by using Superscript III® reverse transcriptase (Invitrogen). Poly A tail was added at the 3' end by terminal deoxynucleotidyl transferase (TdT) (Promega). Then A-tailed cDNA was purified and used as a template to perform the first PCR with 5' RACE primer, 5R2N (Table 1) and PRT-oligo dT primer to amplify the 5' end. To increase the specificity of the PCR product, nested PCR using specific primer 3F2N (Table 1) for 3' end was performed. The PCR products from RACE- PCR and nested PCR were run on the agarose gel electrophoresis. The expected bands were excised, gel-purified and subjected for cloning into pGEM-T-easy vector. The positive clones were sequenced by First Base Co., Ltd. (Malaysia).

2.1.4 Amplification of the PmRab9 cDNA

Amplification of the available sequence of PmRab9 cDNA was performed by designing the specific primers, FLRab9-F and FLRab9-R (Table 1) based on the sequences of 5' and 3' RACE-PCR products. The PCR products were run on the agarose gel electrophoresis. The expected bands were cloned into pGEM-T-easy vector and sequenced.

2.1.5 Sequence analysis

The sequences of the full-length cDNA of PmRab9 were confirmed by using nucleotides blast to the GenBank database. Multiple alignments of Rab9 sequences among arthropods were performed to identify the conserved domains of Rab9 protein by using AlignX. The conserved domains of Rab9 protein were identified by NCBI database (http://www.ncbi.nlm.nih.gov/Structure/cdd/wrpsb.cgi). Then, a phylogenetic tree was constructed to analyse the relationship between PmRab9 and Rab9 of other species by using available program (http://www.phylogeny.fr/) based on the neighbor-joining method.

2.2 Functional analysis of PmRab9

2.2.1 Construction and expression of a plasmid for dsRNA-PmRab9 expression

The stem loop of dsRNA-PmRab9 in length 489 bp and antisense in length 408 bp (Table 1) was constructed and ligated into pET17b plasmid. The recombinant plasmid of PmRab9 was transformed into E.coli HT115, which is a ribonuclease III (RNaseIII) mutant strain. The expression of dsRNA-PmRab9 in bacteria was induced by 0.1 mM isopropyl-β-D thiogalactopyranoside (IPTG). The bacterial cells were harvested and dsRNA-PmRab9 was extracted by an ethanol method (Posiri, 2013). The quality of dsRNA-PmRab9 was determined by ribonuclease digestion assay using RNase III which cleaved dsRNA and RNase A, which cleaved only single-stranded RNA (ssRNA).

2.2.2 Silencing of PmRab9 by dsRNA-PmRab9

In order to optimize the amount of dsRNA-PmRab9 that can specifically inhibit PmRab9 expression, shrimp size about 3 g was injected with 0.63, 1.25, 2.5 and 5 µg/g shrimp of dsRNA-PmRab9. Injection of NaCl was used as a control group. Then gill tissues were collected at 24 hours after injection. Total RNAs were extracted by TRI Reagent according to the manufacturer's protocol. RT-PCR was performed to generate cDNA by Impromp II reverse transcriptase (Promega) with PRT-oligo dT primer. The level of PmRab9 expression was monitored by semi-quantitative PCR using PmRab9 specific primers, detRab9-F and detRab9-R (Table 1) and PmActin (Table 1) was used as an internal control.

Table1. List of primers that used in this study.

Primers	Sequences (5'→3')	Experiments
PRT-oligo dT	CCG GAA TTC AAG CTT CTA GAG GAT CC(T)16	Reverse transcription
MjRab9-F MjRab9-R	ATG AGY AAT ARY CAC AGA AGA C TTA CGA CGA ACA TGC ACA G	Partial PmRab9 cDNA region
3F1 3F2N	TCT CGT GGT TGG GAA CAA GGT GG GGC AGG AGA GAA TGC CAA TGC C	3' RACE 3' RACE (nested PCR)
5R1 5R2N	AAC CAC GGT AGA ATG GGG TTC GC TTT AAG ACT GTC GAC CGG CCA CG	5' RACE 5' RACE (nested PCR)
FLRab9-F FLRab9-R	GGT TGC AGA GGT GAG GG AAC ATT TAT CCA GAC TTT ATG AC	Full length of PmRab9

StRab9F1- *XbaI* StRab9R1-*KpnI*	GCT CTA GAA GGT TGT GAT CCT AGG GGA TGG GGG GTA CCT GTT AGC CCA TCG TCT TAA GC	Construction of dsRNA-PmRab9
AsRab9F1- *EcoRI/XhoI* AsRab9R1- *KpnI*	GGA ATT CCT CGA GAG GTT GTG ATC CTA GGG GAT GG GGG GTA CCG ATC TCC ATT TTC CTT ACA CCA GGC	Construction of dsRNA-PmRab9
detRab9-F detRab9-R	ATT CAA GAG CCT GCG AAC CC TGC ACA GAG ACG ATG GTG GG	Detection of PmRab9 mRNA
PmActin-F PmActin-R	GAC TCG TAC GTG GGC GAC GAG G AGC AGC GGT GGT CAT CTC CTG ACTC	Detection of PmActin mRNA

The underlined sequences showed restriction site.

Abbreviations: R represents A, G and Y represents C, T.

3. Results and Discussion

3.1 Molecular cloning of the *PmRab9* cDNA

PmRab9 cDNA had 958 nucleotides containing 156 nucleotides for 5'UTR, 169 nucleotides for 3'UTR and 633 nucleotides for the coding region, which could be translated into 210 amino acids. The nucleotide sequences of the cDNA of *PmRab9* was blasted to the GenBank database. The multiple alignments of *Rab9* sequences among arthropods was performed to identify the conserved domains of Rab9 protein by using AlignX (Figure 1). The conserved domains of PmRab9 consisted of 5 GTP binding sites (G1-G5), Rab family (RabF1-5) and Rab subfamily (RabSF1-4) domains. The phylogenetic tree analysis of PmRab9 using online program demonstrated that PmRab9 was closely related to *Marsupenaeus japonicus* Rab9 (Figure 2). The result shows that PmRab9 is closely related to the invertebrate Rab9.

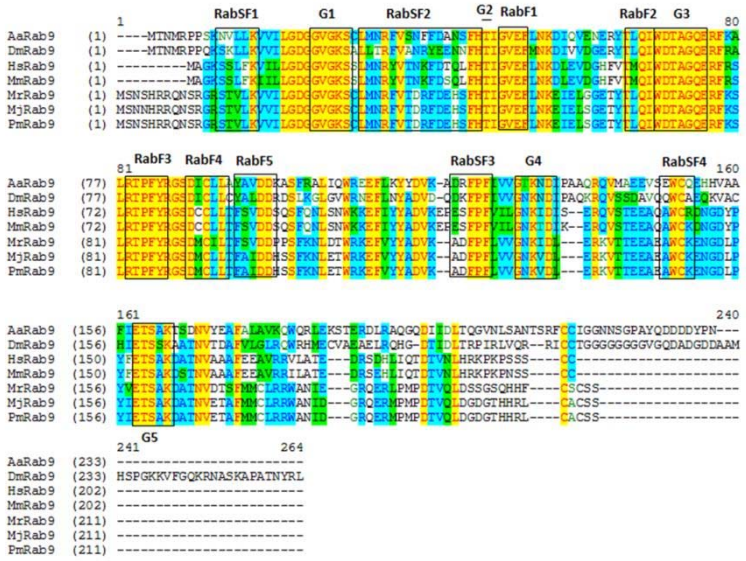

Figure 1. Multiple sequence alignment of Pm Rab9 with Rab9 from other species. Rab9 in *aedes aegypti* (aaRab9), *Drosophila melanogaster* (DmRab9), *Homo sapiens* (HsRab9), *Mus musculus* (MmRab9), *Macrobrachium rosenbergii* (MrRab9), *Marsupenaeus japonicus* (MjRab9), and *Penaeus monodon* (PmRab9). The conserved domains were shown in block; G1-G5 are GTP binding sites, RabF1-5 are Rab family, and RabSF1-4 are Rab subfamily domains.

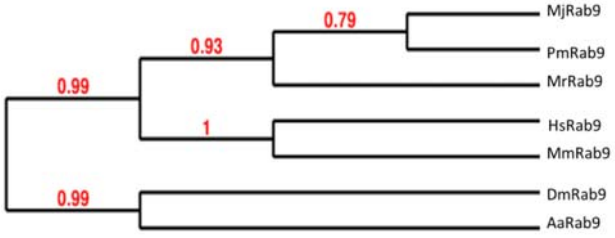

Figure 2. Phylogenetic tree analysis of PmRab9 compared to other Rab9 proteins. Rab9 proteins of *Aedes aegypti* (aaRab9), *Drosophila melanogaster* (DmRab9), *Homo sapiens* (HsRab9), *Mus musculus* (MmRab9), *Macrobrachium rosenbergii* (MrRab9), *Marsupenaeus japonicus* (MjRab9), and *Penaeus monodon* (PmRab9).

3.2 Suppression of PmRab9 by dsRNA-PmRab9

The stem loop of dsRNA-PmRab9 in length 489 bp and antisense in length 408 bp was constructed. Double-stranded RNA-*PmRab9* was produced by *in vivo* bacterial expression. Then the dsRNA-*PmRab9* were extracted by ethanol method. The quality of dsRNA was determined by ribonuclease digestion assay using RNase III which digested dsRNA and RNase A which digested only single-stranded RNA (ssRNA) compared with undigested dsRNA (Figure 3a). The dsRNAs could be digested by RNase III, but not RNase A, indicating that these were good quality of dsRNA-*PmRab9*.

Shrimp injected with dsRNA-PmRab9 at 0.63, 1.25, 2.5 and 5 µg/g shrimp showed significant reduction of *PmRab9* expression approximately 60% after 24 hours dsRNA injection when compared to the NaCl injected control group. (Figure 3b)

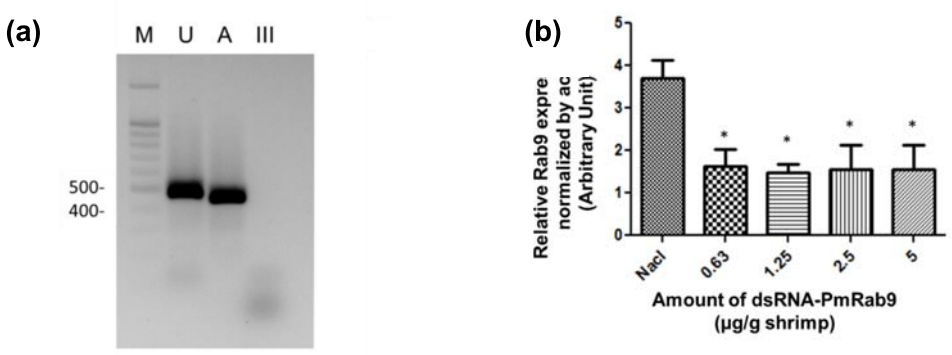

Figure 3. Silencing of PmRab9 in *Penaeus monodon*. The quality of dsRNA-PmRab9 was analysed by using RNase digestion assay: M is 100 bp. DNA ladder, U is undigested dsRNA, A and III are the dsRNAs that were digested by RNase A and III, respectively (a). Relative PmRab9 mRNA levels normalized with actin (mean ± SEM) in shrimp injected with various amounts of dsRNA (b). (*) Statistically significant difference of PmRab9 expression between shrimp injected with various amounts of dsRNA-PmRab9 and the NaCl group ($P < 0.05$).

4. Conclusions

The full length cDNA of *PmRab9* is 958 bp, encoding for 210 animo acid. Its conserved domains showed 5 GTP binding sites (G1-G5), Rab family (RabF1-5) and Rab subfamily (RabSF1-4) domains. The phylogenetic tree analysis of PmRab9 is closely related to the invertebrate Rab9.

Suppression of *PmRab9* by dsRNA-*PmRab9* that were produced by *in vivo* bacterial expression showed the silencing effect of PmRab9 expression approximately 60% in 24 hours post dsRNA injection.

5. Acknowledgements

This work was supported by the Thailand Research Fund (BRG5780006 to C.O.) and Mahidol University. Student scholarship is supported from the 60th Year Supreme Reign of His Majesty King Bhumibol Adulyadej Scholarship.

6. Conflict of interest: none.

7. References

Barbero P, Bittova L, Pfeffer SR. 2002. Visualization of Rab9-mediated vesicle transport from endosomes to the trans-Golgi in living cells. Journal of Cell Biology. 156, 511-518.

Lombardi, D., T. Soldati, M. A. Riederer, Y. Coda, M. Zerial, and S. R. Pfeffer. 1993. Rab9 functions in transport between late endosomes and the trans Golgi network. EMBO Journal. 12, 677-682.

Murray JL, Mavrakis M, McDonald NJ, Yilla M, Sheng J, Bellini WJ, Zhao L, Le Doux JM, Shaw MW, Luo CC, et al. 2005. Rab9 GTPase is required for replication of human immunodeficiency virus type 1, filoviruses, and measles virus. Journal of Virology. 79, 11742-11751.

Ploen D, Hafirassou ML, Himmelsbach K, Sauter D, Biniossek ML, Weiss TS, Baumert TF,Schuster C, Hildt E. 2013. TIP47 is associated with the hepatitis C virus and its interaction with Rab9 is required for release of viral particles. European Journal of Cell Biology. 92, 374–382.

Posiri P, Ongvarrasopone C, Panyim S. 2013. A simple one-step method for producing dsRNA from *E. coli* to inhibit shrimp virus replication. Journal Virological Methods. 188, 64-69.

Zerial M, McBride H. 2001. Rab proteins as membrane organizers. Nature Reviews Molecular Cell Biology. 2, 107-117.